DIPOLE MOMENTS AND KERR EFFECT OF POLY(N-VINYLCARBAZOLE) AND ITS COMPLEXES WITH TRINITROFLUORENONE

MOHAMMED FIAZ

A thesis submitted for the degree of

DOCTOR OF PHILOSOPHY

THE UNIVERSITY OF ASTON IN BIRMINGHAM

MARCH 1994

Dipole moments and Kerr effect of Poly(N-vinylcarbazole) and its complexes with Trinitrofluorenone

A thesis presented for the degree of
Doctor of philosophy
to
The University of Aston In Birmingham
by
Mohammed Fiaz, BSc, GRSC
1994

Summary

N-vinylcarbazole was polymerised using the free radical catalyst (azo-bisisobutyronitrile) and cationic catalysts (boron-trifluoride etherate and aluminium chloride). The polymers produced were characterised by molecular weight measurements and powder x-ray diffraction. The tacticity of the polymer samples was determined using proton and carbon-13 nuclear magnetic resonanace spectroscopy.

Measurements of their static dielectric permittivity and electro-optical birefringence (Kerr effect) in solution in 1,4-dioxane were carried out over a range of temperatures. The magnitudes of the dipole moments and Kerr constants were found to vary with changes in the tacticity of poly(N-vinylcarbazole). The results of these measurements support the view that the stereostructure of poly(N-vinylcarbazole) is sensitive to the mechanism of polymerisation. These results, together with proton and carbon-13 N.M.R. data, are discussed in terms of the possible conformations of the polymer chains and the relative orientation of the bulky carbazole side groups.

The dielectric and molecular Kerr effect studies have also been carried out on complexes formed between 2,4,7-trinitro-9-fluorenone (TNF) and different stereoregular forms of poly(N-vinylcarbazole) in solution in 1,4-dioxane. The differences in the molar Kerr constants between pure (uncomplexed) and complexed poly(N-vinylcarbazole) samples were attributed to changes in optical anisotropy and dipole moments.

A molecular modelling computer program Desktop Molecular Modeller was used to examine the 3/1 helical isotactic and 2/1 helical syndiotactic forms of poly(N-vinylcarbazole). These models were used to calculate the pitch distances of helices and the results were interpreted in terms of van der Waal's radii of TNF. This study indicated that the pitch distance in 3/1 isotactic helices was large enough to accommodate the bulky TNF molecules to form sandwich type charge transfer complexes whereas the pitch distance in syndiotactic poly(N-vinylcarbazole) was smaller and would not allow a similar type of complex formation.

Keywords:

Dielectric permittivity, Electro-optical birefringence, Charge transfer, Stereoregular, Temperature coefficient.

To my family

ACKNOWLEDGEMENTS

I would like to thank my supervisor, Dr. Martin S. Beevers most sincerely for his constant help, patience and encouragement which proved to be of such inspiration throughout the course of this work and made this period of research so fulfilling.

My thanks are also extended to the academic and technical staff of the department, in particular to Dr M. Yasin and DR J. Robson for their valuable advice concerning certain experimental aspects of the work.

Thanks to my fellow postgraduate friends and colleagues at Aston for their companionship and cooperation throughout my stay.

I am indebted to Dr. M. Perry who gave a good deal of his time to obtain the high quality proton and carbon-13 nuclear magnetic resonance spectra of poly(N-vinylcarbazole) presented in Chapter 3.

Finally, I am grateful to the University of Aston for provision of facilities and to the Science and Engineering Research Council for their financial support during the period 1990-1993.

ABBREVIATIONS

$AlCl_3$	aluminium trichloride
Å	Ångstrom
AZBN	azo-bisisobutyronitrile
BF_3OEt_2	boron trifluoride etherate
^oC	Degrees Celcius
cm	Centimetres
C-13-NMR	Carbon-13 nuclear magnetic resonance
DMSO	dimethyl sulphoxide
EtOH	ethanol
g	Grammes
gpc	Gel permeation chromatography
h	Hours
Hz	Hertz
1H-NMR	Proton nuclear magnetic resonance
KHz	Kilohertz
K	Kelvin
KV	Kilovolts
ln	Natural logarithm
mg	Milligrammes
min	Minutes
ml	Millilitres
mM	Millimolar
mmol	Millimoles
MeOH	methanol
MHz	Megahertz
nm	Nanometres
NEK	N-ethylcarbazole

PVK	poly(N-vinylcarbazole)
SLD	Static light diffraction
Sec	Seconds
TCNQ	tetracyanoquinone dimethane
TNF	2,4,7-trinitro-9-fluorenone
UV	Ultra-violet
V	Volts
v / v	Volume per volume
w / v	Weight per volumes (g/100 ml)
µg	Micrograms
µl	Microlitres
µm	Micrometres
XRD	Powder x-ray diffraction
%	Percentage

List Of Contents

CHAPTER 3 SYNTHESIS AND CHARACTERISATION OF POLY(N-VINYLCARBAZOLE)

CHAPTER 4 THE TEMPERATURE DEPENDENCE OF STATIC DIELECTRIC PERMITTIVITY AND DIPOLE MOMENTS OF POLY(N-VINYL-CARBAZOLE) IN SOLUTION IN 1,4-DIOXANE AND TOLUENE

List Of Figures

List Of Tables

CHAPTER ONE

Introduction

1.1 Introduction to electrically conducting polymers and the importance of poly(N-Vinylcarbazole) as an electro-optic polymer

Polymeric materials in recent years have been rapidly replacing conventional materials such as metals, glass and natural fibres. Their increased use is due to their ease of fabrication and cost compared to metallic or glassy materials used for the same purpose. During the last decade the research effort has focussed on the development of speciality polymers for high-performance applications.

The emergence of the polymer industry as an important segment in the country's economy occurred shortly after World War II. Prior to this, production of plastics was limited due to shortages of raw materials caused by the war effort, as well as the newness of the materials themselves. About the only polymers available for production in the early 1950's were nylons, polyesters, polyethylene, polystyrene, phenolics and polyvinylchloride. Today there are approximately forty major classes of polymeric materials produced in commercial quantities.

During the past twenty five year period, research in new monomers and polymerisation techniques has led to the production of already important polymers as well as new ways of utilizing these materials. These past twenty-five years of polymer history can be subdivided into three periods. The first period between 1940's and 1950's saw the major research thrust in the synthesis of new polymers. The physics of polymerics materials was

vigorously studied in the next period with such areas as crystallization, rheology, thermal analysis, and configurational statistics receiving attention. Some of the most important materials developed and used in large amounts during this time period were epoxys, fluoropolymers, polycarbonates and polyurethanes. The areas of free-radical, cationic and anionic polymerization grew concurrently. The two most important developments in the area of synthesis were those of heterogeneous and stereoregular polymerization.

The second period between 1960's and 1970's appears to be a decade of polymeric materials for engineering applications. Areas receiving considerable support at this time were composites and materials for medical applications.

During the third and current period, efforts have been geared towards developing electrically conducting polymeric materials. Many polymers which show considerable electrical conductivity have now been synthesized successfully and are potentially important for electrical applications. Many new and important developments in the field of electricity and electronics would not have been possible without these continuing developments. The wide use of plastics in electrical applications is based primarily on their excellence as insulating matrials[1,2,3]. Polymers, and in general most organic compounds in the pure state, are known principally more for their insulating properties than their ability to conduct an electric current. It was this former attribute of non-electrical conduction, inherent in most polymers, which was first exploited commercially. In the area concerned with high frequency, high voltage insulation, if the frequencies employed correspond to the natural orientational frequency of the dipolar units of the polymers, then there will be absorption of energy, which may lead to heating and subsequent breakdown of the material. For this reason it is important that the temperature of application does not exceed, or approach, the glass transition temperature of the polymer (temperature where polymer changes from its glassy state to rubbery form). However, the phenomenon of dielectric

heating has found widespread use, an important application of which concerns the pre-heating of plastic preforms prior to moulding. The heating of food in a microwave oven, by causing the water molecules to rotate under the influence of an intense electric field, oscillating at approximately 22GHz, is another well known example of dielectric heating. Electrical insulators must have good physical properties to function satisfactorily since their role in the system is often mechanical as well as electrical. In addition to withstanding the mechanical forces during the manufacturing process, the insulators are designed to meet a specific mechanical performance. For example, high tensile strengths are required for filament-wound rings that are used to support and restrain the end turns of turbine generators during short-circuit conditions. Where insulation systems are used in air environments, oxidation reactions become important and must be considered in determining the life of the insulating polymer.

Prior to World War II, the only insulating elastomer available to the wire and cable industry was natural rubber which, being a unsaturated polymer, limited the useful temperature and voltage rating of solid dielectric cables. During and subsequent to World War II, styrene-butadiene rubber, isobutylene-isoprene rubber, polyethylene and ethylene-propylene copolymer were developed as alternative wire and cable insulation compounds. Insulation compounds based on the polyolefin elastomers, such as, polyethylene and ethylene-propylene, because of their moisture and heat resistance, predominate in cable installations requiring the highest degree of reliability and long life. Compounds based on isobutylene-isoprene rubber and styrene-butadiene rubber achieved their peak usage when they were either the only elastomer available or offered the best properties. These polymers are now used in limited cases either because they offer economic advantage for non-critical cables or because the manufacturer, having developed specific recipes and processing, does not wish to change to new materials until forced to do so by economics or non competitive performance characteristics. Natural rubber insulation compounds are

no longer used. However, because natural-rubber is non petroleum based and a renewable natural resource, a combination of economic and availability conditions may occur that could lead to a resumption of its use for wire and cable insulation.

Currently, one of the most widely used polymers for wire and cable applications is poly(vinyl chloride), (PVC). The main factor which makes PVC a extremely successful commercial polymer lies in the ability to use this polymer both as plasticized and unplasticized forms. For example in the cable and wire covering applications, PVC is used in the plasticized form which extends it useful life time by preventing it from air oxidation and thermal degradation as well as providing flexibility to polymer, whereas in double glazing, PVC is used in the unplasticized form where the toughness is an important requirement.

A notable advance in purely insulating polymer materials has been the synthesis of low permittivity polyimide resins enabling the manufacture of smaller and faster microelectronic circuits[4]. Heat resistant polymers are more and more needed for structural applications in aerospace and for electrical applications in electronics. Thermostable dielectric coatings are used as intermetallic layers in wafer fabrication or for interconnection processes[5] and dielectric films find their main applications in the production of flexible circuits. On the other hand, for the development of surface mount technology, heat resistant films are required, due to the severe thermal stresses encountered by the components during the soldering[6]. Among the heat resistant polymers, polyimides are the most popular[7,8]. In spite of all the work performed on polyimides, these materials still exhibit certain short comings such as a lack of good processability. An approach to improve the processability involves the synthesis of fully cyclized linear polyimides with a good solubility, as shown by Korshak et al[9] who introduced lateral groups with large steric hinderance or polar groups in the main chain giving strong interactions with solvent.

Although there still remain enormous potential areas for the application of conducting polymers, these have been employed successfully in low current circuitry systems, electromagnetic and electrostatic shieldings, batteries, semiconductor devices and in solar cells. Perhaps the most important application of a conducting polymer system to date is the use of poly(N-vinylcarbazole), (PVK) in the electroreprographic industry. N-vinylcarbazole was first prepared by Reppe in 1924[10]. This involved direct vinylation of carbazole, which is readily available as a by-product from coal-tar distillation and is the most important synthetic method for the preparation of the monomer. The reaction was originally conducted at 190°C with the actylene pressure of 10-20 atm using a catalyst comprised of an alkali metal hydroxide together with an alkaline earth or zinc oxide activator. Low reaction temperatures were later found to be favourable. Thus, the yield of N-vinylcarbazole was improved to 95-99% for the vinylation at 145°C and 170 psi with cyclohexane as the diluent[11]. Unfortunately, carbazole, the starting material for the synthesis of vinylcarbazole, often contains a high level of sulphur compounds and complete elimination of these impurties is difficult but possible by repeated recrystallisation of N-vinylcarbazole, by sacrificing yield. The purified monomer is thermally stable at room temperature but should be kept in dark since it easily polymerises in light, especially with light of ultra-violet wavelength.

The commercialisation of Reppe's development did not start until 1935. In the Second World War there was a severe shortage of mica in Germany and the United States. A need therefore arose for a material with good electrical insulation characteristics coupled with good heat resistance. In an attempt to meet this requirement, PVK was produced in both Germany (Luvican-IG Farben) and the United States (Polectron-General Aniline and Film Corporation). In addition to the homopolymer, IG Farben also produced copolymers of Styrene and PVK. At one time production of vinylcarbazole polymers reached a level of

five tons a month, but due to its brittleness and its tendancy to cause an eczema type of rash on people handling the material, the production of these polymers was reduced to small quantities. Earlier scientific investigations concentrated upon its dielectric properties, however, recent research is mainly devoted to its electrical, photoconductive and optical properties. Indeed, PVK found a widespread use in the electrophotographic industry as a replacement for selenium. Since PVK is also an excellent electrical insulator it may also be used in many applications where dielectric heating technology is involved.

A practical application, known as xerography, has been developed by Xerox in the United States, in which the photoconductive property of this polymer is exploited commercially. In xerography the surface of a drum, coated with a photoconductive material, is first uniformly charged by a corona and then exposed to a bright image of the item to be copied. Where the light falls, the charge leaks away to the underlying earthed, metal drum. The remaining charged, originally dark areas are able to attract the dry ink or toner for transfer to the copy paper. Amorphous selenium used to be the photoconductive material on the drum, but now PVK is also used extensively. It has an added advantage in its toughness and ease of fabrication.

Hoegl, Sus, and Negebauer[12] in 1957 reported the use of polymeric N-vinylcarbazole films as photoconductors. The discovery that PVK, when sensitized with dyes and pigments, exhibited high enough levels of photoconductivity to be useful in electrophotography has lead to the growth of research into many other photoconductive polymers. The open and patent literature presents many examples of photoconductive polymers, but detailed research has not been carried out on any of them. However, the polymers containing the carbazole moity[13] have been studied in detail. The lack of detailed studies on photoconductive polymers, other than those containing carbazole moity, is noteworthy in view of the commercial importance of organic photoconductors which are

essential in the multibillion-dollar, xerographic-copier, laser printer, and duplicator industry.

The practical polymeric photoconductors are based on two types of systems which are structurally and conceptually different, but the mechanism of charge-carrier generation and transport is similar. In one class the activity is built into the polymer structure itself such that the pendent groups, the in-chain groups or chain itself, absorb light and support charge migration. The second class consists of polymers which contain inactive binder additives. These are widely used in xerographic photoreceptor because of ability to dope the polymer molecularly and ease of fabrication. Froix et al[14] suggested that the photo-generation process is controlled by impurities or defects. Solvents and oxidised carbazole units were believed to assist in the process. The addition of suitable electron acceptors, which form coloured, charge-transfer complexes is a proven way of increasing photo-generation efficiency; 2,4,7-trinitro-9-fluorenone (TNF) is so effective with PVK that the combination is used in xerography. TNF resolves the problem of trapped electrons since it is itself an electron-transporting material. Another efficient way of enhancing photo-generation efficiency and overcoming the trapped electrons is a physical separation of charge-carrier generation and charge transport into two different, adjacent materials. Organic pigments and dyes dispersed in PVK initiate photoconductivity in the visible or even near infra-red range, where PVK alone does not absorb. The electronic transitions involved in the generation process proceed within the dye molecules that absorb the light.

There has been a quest for conducting polymers for a long time, because there is an undisputed commercial prize for the development of a plastics material which combines high electrical conductivity with typical plastics properties such as low density, toughness and ease of fabrication. Conducting polymers have been around since the latter half of the last century. Indeed many of the "new" conducting polymers are prepared by synthetic

routes which are decades old but which were discarded at the time of their original discovery because they only produced black, interactable powders. The first step on the route to scientific respectability came in the 1950s when Natta polymerised acetylene using a catalyst. He too obtained a black, intractable powder, but it was sufficiently pure to be properly characterised. It was at this point that chemistry entered the field of conducting polymers.

Twenty years earlier it had been postulated that an infinitely long chain of carbon atoms, joined by alternating single and double bonds, would be electrically conducting. Each carbon atom in the chain possesses four electrons in its outer shell. Two of these electrons are used to form the s bonds which make up the polymer chain, the third electron is used to bond to the hydrogen atom which is attached to each carbon atom and the final electron occupies a p_z orbital which forms the p double bond. These p orbitals were envisaged as being delocalised along the chain to form a one-dimentional band. Since each orbital possessed only one electron this band would be half-filled, and thus metallic. The material would be a metal along the chain, and an insulator across it.

Alternative theories suggested that the energy required to effect this structural reorganisation was prohibitive, and that some bond alternation would remain. This residual bond alternation causes a defect to be formed in the middle of the band and the material would be a semiconductor. The polyacetylene Natta produced was a semi conductor. If it had been a thermoplastic this would have been an exciting discovery, but the lack of any form of processibility meant that the polymer was of little interest to anyone.

The real breakthrough came in 1971 with the technique of making thin polymer films of the polymer. These films were grown on surfaces wetted by a very concentrated solution of

the same catalyst used by Natta. Films are far better than powders both for the investigation in fundamental properties and for applications. Even though it turned out that these films were in fact fibrillar materials made of 20 nm fibres and two-thirds void space, a critical advance had been made. Conducting polymers became a hot scientific field of research. The final part of their elevation to scientific respectibility came in 1976 with the discovery that oxidation and reduction could increase the conductivity of these films up to metallic levels, with conductivities of $1000\Omega^{-1}cm^{-1}$ being reported. Since the conductivity of the pristine material was around $10^{-9}\Omega^{-1}cm^{-1}$, the conductivity of polyacetylene could be varied over 12 orders of magnitude, from insulator, through semiconductor, to metal.

Organic materials can be divided into two classes - crystalline solids (charge-transfer complexes and ion radical salts), and conjugated polymers.

1.1.1 Crystalline solids

Charge-transfer complexes and ion radical salts are typically highly crystalline solids comprising two component molecules (binary systems). Charge transfer complexes are formed by the interaction of electron donor and electron acceptor molecules which have neutral ground state, while radical ion salts are formed from component molecules with ionic ground states. In 1973 Ferraris et.al.[15] developed a complex of the donor tetrathiafulvalene (TTF) and the acceptor 7,7,8,8-tetracyano-*p* - quinodimethane (TCNQ) and found it to be metallic, with room temperature conductivity. Subsequently, a galaxy of conducting complexes from analogues of TTF and TCNQ were developed. As a general guideline, a prerequisite for conductivity in this class of organic metals is that one or both of the components is a planar molecule with a delocalised p electron system. In the crystal lattice the component molecules must segregate into two types of stack; one composed of donor molecules, the other of acceptor molecules. Close face-to-face stacking within these columns favours extensive *p* orbital overlap and the formation of an energy band along the

stacking axis. When this structural feature is combined with a band that is less than half filled, high conductivity can result and is highly anisotropic. The more diffuse *p* and *d* orbitals centred on selenium and tellurium give larger intrachain bandwidths, relative to TTF (and hence increased metallic conductivity) and also favour increased interchain interactions. A large number of selenium containing donors are known, but tetratellurafulvalenes are harder to synthesise and the parent system, tetratellurafulvalene, has only recently become available(16).

1.1.2 Conjugated polymers

No polymers based on carbon atom backbones are intrinsically conducting; in the virgin state they are insulators. Subtle chemical manipulations are needed to coax the polymers into a conducting state. Polyacetylene is the prototype conducting organic polymer. *Cis* - polyacetylene can be prepared at low temperatures, but at room temperature or above, the *cis* forms isomerises to the thermodynamically more stable *trans* form. In the pure state conductivity is approximately 10^{-7} - 10^{-9} Ωcm^{-1}, but on doping the conductivity increases spectacularly to 1000 Ωcm^{-1} This effect was first observed in 1977.

The oxidation and reduction processes are termed *p* and *n* type doping, respectively. Initially, the high conductivity increase was explained by an energy band picture. It was assumed that upon doping, oxidants removed electrons from the filled valence band and reductants added electrons into the vacant conduction bands, by analogy with the doping of inorganic semiconductors. However, it quickly became apparent that this was an oversimplified picture because experiments showed that the conductivity in polyacetylene and other conducting polymers is not associated with unpaired electrons but with charge carriers that do not have free spins.

Polyacetylene is unique among conducting polymers in having a degenerate ground state. The two ground states are related by interchange of double and single bonds. However, because a ground state with alternating single and double bonds is favoured over a fully delocalised ground state this has the effect of opening a semiconductor energy gap. An important factor for the conduction properties is that the chain can accommodate stable defects in the bond alternation sequence (scheme 1). These defects move along the chain under the influence of an electric field as charge carriers called solitons. Doping produces more solitons; for oxidatively doped polyacetylene the soliton is essentially a delocalised carbocation.

Polyacetylene is an inconvenient material for fabrication for several reasons: it is insoluble, it cannot be melt processed below its degradation temperature and oxidises on contact with air. Moreover, the polymer has all to frequently been studied in an impure form, contaminated with residues from the polymerisation catalyst. However, this problem can be overcome by the use of soluble precursor polymers, developed by Feast and co-workers at Durham, that yield *trans* -polyacetylene of high purity[17]. Doped polyacetylene is now, essentially as conducting as copper. Prepared as stretch-orientated films, initially by Naarman at BASF in Germany, these films have the highest room temperature conductivity of any organic materials and have been successfully reproduced[18].

1.1.3 Other polymers

Numerous other conjugated polymers are conducting, for example poly-p-phenylene, polyaniline, polypyrrole and polythiophene. The search for improved mechanical properties and processibility without sacrificing high conductivity has directed research activities towards the polyheterocyclic systems. For these materials polymerisation is usually done electrochemically by subjecting the monomer to the appropriate voltage in the electrochemical cell. This method produces the polymer in the doped (conducting) state;

the charge on the polymer is neutralised by counter ions from the electrolyte solution. These polymer films are typically very dark in colour and, with care they can be peeled off the electrode and characterised as free standing films.

Soliton defects in these cyclic systems are not stable unlike those in polyacetylene because the different phases forming bond alteration are not degenerate: the thiophene units are aromatic in phase A and hence lower in energy than in the non-aromatic (quinoid) units in phase B (Scheme 2). Consequently, for these systems there is an additional contribution to the semiconductor gap, which is increased relative to polyacetylene.

Scheme 1

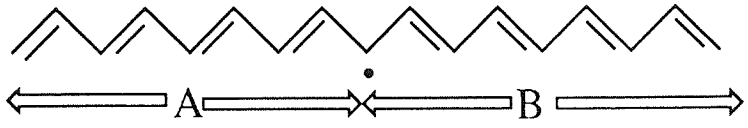

Soliton defect in a trans-polyacetylene chains separating the degenerate phases A and B.

Scheme 2

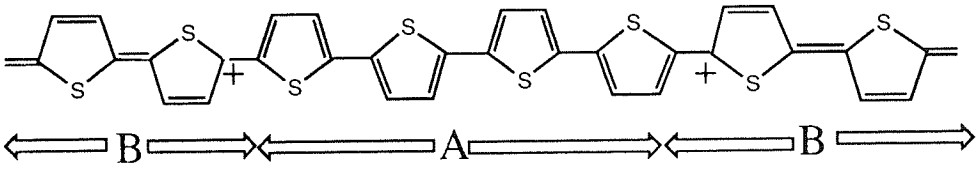

Positively charged bipolaron in thiophene chain. The phases A and B are not degenerate. The thiophene rings are aromatic in phase A and quinonoid in phase B.

Figure 1.1 Electronic defects in polyacetylene and polythiophene

The past two years have seen some exciting advances in the development of conducting polymers that are solution processible. This would allow polymer films which could be dissolved and then recast into films that retain conductivity. Solubility in organic solvents has been achieved by attaching flexible, long chain substituents onto the thiophene ring. Research groups in Japan and the United States have reported that poly(3-alkyl)thiophenes are conducting and soluble. Polyaniline has attracted considerable attention since MacDiarmid et.al.[19] investigated this material as a conducting polymer. Polyaniline is unique among conducting polymers in that its electrical properties can be reversibly controlled both by charge-transfer doping and by protonation. The wide range of associated electrical, electrochemical and optical properties, coupled with good thermal stability, make polyaniline potentially attractive for application as an electronic material. Throughout the extensive literature, polyaniline has been generally categorized as an intractable material. Recently, however, two groups[20,21] have reported methods to dissolve and process polyaniline without changing the structure of the polymer in N-methylpyrrolidinone or in concentrated sulphuric acid. In contrast to alternative methods for achieving solubility through preparation of substituted polyaniline[22] or through the synthesis of graft or block copolymers[23], the resulting films[20,21] and fibers[20] are highly conductive after processing. The use of concentrated acids[20] has specific advantages in that both the salt and the base form of polyaniline can be completely dissolved at room temperature. The solubility of this conducting polymer opens the way to processing pure, partially crystalline polyaniline or composites of polyaniline with the other commercial polymers into fibers and films. In addition, this solubility enables extensive characterization of polyaniline as a macromolecular system and of polyaniline as a conductive polymer. Polyanilines have reached commercial application as the anode in lithium rechargeable batteries. Considerable success has been achieved with derivatives of poly(p-phenylene vinylene) such as poly(dimethoxy p-phenylene vinylene) made by a precursor route, where the material is cast into a film before coversion to the conductive,

conjugated structure. By a combined coversion/drawing process, Smith[24] has made highly oriented material combining exceptional conductivity, (1000S/cm), with exceptional mechanical tensile modulus, (250 GPa). Similarly highly conductive, strong fibres have also been made from poly(2,5-thienylenevinylene) by Tokito, Smith and Heeger[24].

The photo-induced and bulk electrical conductivity of poly(N-vinylcarbazole), PVK, as mentioned earlier, has been the subject of intensive investigation. The system is particularly interesting because the intrinsic semiconductivity (approximately 10^{-14} $\Omega^{-1}cm^{-1}$) of the polymer may be greatly enhanced by treatment with various dopant molecules such as tetracyanoquinodimethane (TCNQ) and iodine (I_2). The dopants also influence the photoconductivity of the polymer by shifting the absorption spectrum into the visible region. In the pure PVK, conduction is dominated by holes which are long-lived and photo injected from metal electrodes. The unusual performance of this photoconductive polymer has been connected with its tendancy to take up a helical conformation with successive aromatic side chains lying parallel to each other in a stack along which electron transfer is relatively easy[25]. The addition of equimolar amounts of electron acceptor such as tetracyanoquinodimethane (TCNQ) and 2,4,7-trinitrofluorenone (TNF) leads to increased photoconduction and is particularly useful in the generation of significant conductance under visible radiation. This is achieved by the formation of charge transfer complexes (which strongly absorb in the visible region) between pendant carbazole residues acting as donor groups and acceptor dopant molecules. The conductance is then dominated by electrons rather than holes. In PVK: TCNQ complexes, the carbazole side group acts as the donor and TCNQ is the electron acceptor. As a direct result of the PVK : TCNQ complex formation, there is a charge transfer band in the absorption spectrum at 600 nm[26,27].

Poly(N-vinylcarbazole), exists in various stereoregular forms because of the presence of an asymmetrical carbon in the repeat unit of the polymer. Proton and ^{13}C n.m.r. studies have indicated that synthetic routes used to prepare the polymer have a marked effect on its stereostructure[28-31]. The various stereoregular forms of PVK therefore provide an interesting opportunity to study the effects of tacticity on the electrical and photo-electrical properties of the pure polymer and when complexed with various dopants. Although some work has been done on the dielectric properties of PVK, Beevers and Mumby[32] were the first to present a detailed study in which the dielectric and electro-optical data were correlated with proton ^{13}C n.m.r. spectra for well characterised fractions of different stereostructural forms of PVK. Although the exact nature of these various structures has been the subject of much interesting discussion, broadly speaking there appear to be three main types of stereostructures as judged by n.m.r. spectroscopy[28,33-35], x-ray diffraction[36-38] and measurements of glass transition temperature[39].

High molecular weight chains can present an almost unlimited number of conformations in space and this conformational wealth governs the physical properties of polymers. Among the most important conformation-dependent properties, the mean-square end-to-end distance, the mean-square dipole moment, the optical anisotropy and the molar Kerr constant stand out. Usually, skeletal bonds vary much more in polarity and polarizability than they do in length, and, consequently, the dielectric and optical conformational properties are more sensitive to structure than more traditional properties such as the molecular dimensions.

For many years, the measurement of [40,41] dipole moments has been used as a means of investigating the conformational characteristics of polymeric materials. Since the dipole moments of molecules in solution may be readily determined over the entire range of chain length from monomer through to high molecular weight polymer, this has proved to be a

convenient and valuable technique. Also there is both theoretical[42-46] and experimental[47] evidence that dipole moments of many chain molecules are unaffected by excluding volume interactions[48]. The chain molecules most extensively studied with regard to the dependence of the dipole moment on chain length, temperature and the nature of the solvent medium are the dimethyl siloxanes[49-51], and a vast amount of information about the conformations of these interesting materials has been deduced as a consequences of these studies.

Le Fevre and coworkers[52-58] have paid considerable attention to the Kerr effect studies of synthetic polymers. Recently, there has been a great deal of interest in studying the tacticities of vinyl polymers through the measurement[59-61] and theoretical calculation[59-61] of the Kerr effect and optical anisotropy. Poly(vinyl chloride)[60,61] and poly(p-chlorostyrene)[60,61] are the two polymers that appear to have received most attention. Mark[49] has presented extensive calculations of dipole moments of these polymers and their dependence on composition and stereoregularity. From Mark's investigations it transpires that the dipole moments are often nearly constant over a substantial range of tacticity. Tonelli[60] has calculated Kerr constants for a wide variety of vinyl copolymers and considered variations of both stereoregularity and composition. In general, the Kerr constants appear to show greater sensitivity to both sequence and stereostructure. However, very little literature is published that indicates the work that has been carried out on behaviour of dipole moments with temperature and the effects of tacticities of poly(N-vinylcarbazole) polymers. Hence, one of the aims of this research has been to investigate this behaviour and thus understand the molecular and conformational behaviour of these polymers using dielectric and electro-optic methods.

Dielectric and electro-optical techniques may also be used to study a variety of other molecular systems. Generally, the measurements are made on dilute solutions and the

results extrapolated to infinite dilution. Thus, the solute molecules are assumed to be unperturbed by intermolecular interactions from solute molecules[62]. When considering the conformations adopted by the solute molecules this affords considerable simplification. However, in certain circumstances, electro-optical and dielectric techniques may in fact be employed in the study of molecular interactions and many studies of this kind have been reported[63]. The measurement of dielectric permittivity and the Kerr effect have also been used to study the effect of pH and ionic strength on the overall shape and related properties of a variety of macromolecules and suspended particles (protein molecules, viruses, bacteriophages and clays) in aqueous media[64-66].

Dynamic electro-optical Kerr effect and dielectric relaxation techniques may be used to study the rate of orientation of macromolecules in solution. These techniques have become an important tool of studying the size and shapes of rigid or semi-rigid macromolecules. Since rigid molecules often have well defined geometries, and rotate relatively slowly in solution, their rates of rotational diffusion can be accurately measured, thus permitting useful analyses to be performed concerning the dependence of hydrodynamic behaviour on there molecular structure. Molecular mobility and long-range order in liquid crystals[67-71] have been determined by applying a number of closely related relaxation techniques. These rod-like molecules often have large molecular dipole moments and are usually highly optically anisotropic, as is their pure liquid phase, due to the extensive geometrical correlations between the molecules in the liquid-crystalline phase.

A detailed kowledge of molecular structure is an important prerequisite for deeper understanding of the macroscopic properties of any material. In addition the ability to correlate desirable physical properties with molecular structure provides a powerful method of testing molecular models. In this thesis the principal experimental techniques used to study the conformational depended properties of various stereostructural forms of

poly(N-vinylcarbazole), in the pure state (undoped) and in doped forms in solution, are based on the measurement of dielectric permittivity and electrically-induced optical birefringence. It is generally accepted that it is valuable to employ techniques which rely upon different aspects of the conformational structure and behaviour of molecules. The parameters so obtained may then be interpreted in parallel, to see if, when considered together, they support, or refute, the conformational possibilities. This use of complementary methods helps to eliminate ambiguities which may arise if reliance is placed upon a single experimental technique. Thus, wherever possible, dielectric and electro-optic data were obtained for the same molecular system. The following chapter describes in detail the theory of dielectric and electro-optic techniques used in the experimental determination of dielectric and optical properties of poly(N-vinylcarbazole) with special emphasis on dipole moments, the molecular Kerr constant, and the optical configurational parameter.

1.2 Applications

The possibility of using PVK as a large general-purpose plastic is very limited because of two main reasons. Firstly, the monomer, N-vinylcarbazole is too expensive, in comparison with starting materials for general-purpose polymers, and secondly the PVK is too brittle. On the other hand, PVK has many properties such as high thermal stability, unique dielectric properties, and photoconductivity which are hardly rivalled.

PVK and copolymers with styrene and its derivatives have been most extensively investigated. Incorporation of 0.1-2% of styrene with PVK is sufficient to improve the workability of PVK while retaining the electrical properties of the base polymer. Besides the direct impregnation or film making, PVK can be compounded with other polymeric materials, for example poly(tetrafluoroethylene), and can then be used as dielectric spacer.

The high softening temperature of PVK makes its foam useful as a thermal insulator at temperatures up to 150 °C.

There are two important applications of N-vinylcarbazole for imaging systems. The extreme sensitivity of N-vinylcarbazole to charge transfer photopolymerisation permits its application to photopolymer systems. Although the mechanism of the polymerisation has not yet been clarified, there seems to be no oxygen effect on this polymerisation. By contrast, coventional photopolymerisation, via free radical intermediates, is generally retarded or inhibited by air during the initial period. The oxygen effect is particularly troublesome for imaging systems which are used as a thin layer having a large area exposed to air. An additional advantage of N-vinylcarbazole as an imaging material is in the use of the color reaction of tertiary amines with halogenated hydrocarbons.

Another application of PVK is as a photoconductive material for electrophotography. At present, this field of application is probably much more important than the photopolymerisation systems. The advantages of organic photoconductors are transparency, high resolution, flexibility (film forming property) and light weight . As has been described in section 1.1, the photoconductivity of the polymer can be enhanced by the addition of electron acceptors.

1.3 Aims

(i) To synthesise various stereoregular samples of poly(N-vinylcarbazole) using different catalyst systems.

(ii) To determine the isotactic levels of different poly(N-vinylcarbazole) samples using ^{1}H and ^{13}C NMR spectroscopy.

(iii) To measure the dielectric permittivity and calculate the temperature coefficients of dipole moments of various stereoregular poly(N-vinylcarbazole) samples.

(iv) To measure the experimental Kerr constant and calculate the molecular Kerr constants of various stereoregular samples of poly(N-vinylcarbazole).

(v) To prepare charge transfer complexes between samples of poly(N-vinylcarbazole) and 2,4,7-trinitrofluorenone and determine their dipole moments and molecular Kerr constants.

(vi) To use Desktop Molecular Modeller to construct molecular models of isotactic and syndiotactic forms of poly(N-vinylcarbazole) and to use these models to calculate the interatomic distances between carbazole groups seperated by one pitch of the helix. Compare the distances to the Van der Waal's dimensions of 2,4,7-trinitro-9-fluorenone.

CHAPTER TWO

Experimental Techniques - theoretical background

2.1 Nuclear magnetic resonance studies of poly(N-vinylcarbazole)

High resolution nuclear magnetic resonance (NMR) spectroscopy has been used extensively for many years to obtain information on the structure of polymers. Much attention has been directed towards the elucidation of the microstructure of polymers and copolymers. The affects of tacticity on NMR chemical shifts have been studied extensively[72]. The effects of copolymer sequence distributions on NMR chemical shifts have also been the subject of considerable attention[73]. The problem of polymer conformation has been considered and has generally taken the form of reconciling the spectrum of the polymer with spectra of low molecular weight model compounds. This approach has provided an understanding of the conformation of polymers in solution, for example, polystyrene[74].

Poly(N-vinylcarbazole) (PVK) appears to offer a system for study by NMR where the conformations are dominated by hindered rotation about backbone bonds. The proton NMR spectrum of PVK was first reported by Heller et al[75]. The polymer obtained with a stereospecific Ziegler-type catalyst possessed an NMR spectrum similar to those obtained by free radical and cationic systems. Heller et al concluded that non-crystalline, atactic polymers were obtained either because of the bulkiness of the carbazole side group, or because of the non-stereospecific nature of the polymerisation process.

Yoshimoto et al[76] reported the assignment of proton NMR peaks without showing the spectrum. They reported that the relative intensities of the methine peaks at 2.7 and 3.6 ppm differed between samples produced by the thermal polymerisation and cationic polymerisation, respectively. It was concluded that the difference in the chemical shifts for the two methine protons peaks seemed too large to attribute it to different tacticities. These observations were explained in terms of interactions associated with the neighbouring carbazole groups belonging to a chain molecule with restricted internal rotation.

Williams[77] suggested that the spectra of PVK indicated the presence of hindered rotation with temperature dependent populations of conformers. Williams concluded that the tacticity of PVK appeared to be fairly insensitive to the method of polymerisation.

Okamoto et al[28] clarified the situation by demonstrating that the stereoregularity of PVK depended on the polymerisation method. When examined by proton NMR,both methylene and methine type protons of PVK showed 'doublet' signals. They assigned the higher field peaks to the isotactic sequences and the lower field peaks to the syndiotactic sequences. Using this analysis Okamoto et al[28] estimated that the polymers prepared by cationic catalysts had the largest degree of the isotacticity (50%), and that the free radical polymers had the smallest (25%).

Tsuchihashi et al[78] published one of the earliest carbon-13 NMR spectra of PVK. By comparing the the absorption spectrum of the polymer, they assigned the majority of peaks with those obtained for the model compond N-ethylcarbazole. The shape and intensities of methine and methylene carbon absorptions of carbon-13 of PVK observed by Kawamura and Matsuzaki[30] was related to the method of polymerisation. Only peak resolution changed between 298K and 363K and no temperature dependent conformation effect was observed between. The absorptions of the methine carbon of PVK prepared by free radical routes were observed to be split into a 'triplet', whilst those for PVK obtained by cationic methods were split into a 'doublet'. The relative intensities of the 'doublets' or

PVK prepared by free radical routes were observed to be split into a 'triplet', whilst those for PVK obtained by cationic methods were split into a 'doublet'. The relative intensities of the 'doublets' or 'triplets' of both the methylene and methine carbons may be seen to vary with the synthesis route. From the measurements of the relative intensities of methine and methylene, it is apparent that the polymers of N-vinylcarbazole obtained via radical polymerisation, possessed a high portion of syndiotactic sequences whilst PVK prepared by using boron-trifluoride etherate was predominantly isotactic and that synthesised using aluminium trichloride was composed of stereoblock structures.

The carbon-13 NMR studies of PVK has also been studied by Williams and Froix[29]. These workers reported that carbon-13 spectra of AZBN initiated sample compared well with the corresponding spectrum reported by Kawamura and Matsuzaki[30]. However, the spectrum reported by Williams and Froix for the boron-trifluoride etherate initiated samples resembles much more closely the spectrum of the aluminium trichloride initiated samples published by Kawamura and Matsuzaki[30]. Williams and Froix[29] deduced that the methine peak was comprised of absorption due to meso and racemic dyads and that the methylene carbon-13 peak was the sum of absorptions associated with the meso and racemic tetrad stereostructures. By measuring relative intensities of these various contributions the authors were able to refuted the notion that PVK molecules consist of long blocks of either isotactic or syndiotactic sequences. Their results, however, note that there is an increase in the racemic content for cationically prepared PVK whereas the corresponding NMR data apparently indicate a decrease in the racemic content, in agreement with the observations of Okamato et al[28]. Williams and Froix disagree with the notion that PVK consists of either long chains of isotactic or syndiotactic sequences.

Therefore, in summary, it would seem that the synthetic route does affect the tacticity of the polymers produced and this may be detected by either proton or carbon-13

NMR. However, there appears to be some doubt as to how the bulky carbazole side groups are ordered in these different structures.

2.2 Dielectric theory

The total dielectric polarization, P_T, of a material is comprised of three main terms. These are the electronic, P_e, atomic, P_a, and rotational, P_o, polarizations, which are usually assumed to be additive. The total polarization is given by,

$$P_T = P_e + P_a + P_o \qquad (2.1)$$

If the dipole moment of a molecule is to be calculated from the total measured polarization then P_o must be isolated from this expression, since it is the orientation of the dipole moment in an electric field which gives rise to P_o. A method often employed to evaluate P_o is to measure P_T at different frequencies. The typical frequency dependence of P_T is illustrated in figure 2.1. The total polarization (P_T) can be obtained from measurements at radio frequencies, from which may be subtracted the electronic polarization calculated from refractive indices measured at optical frequencies. A value for the atomic polarization cannot be determined directly since a simple molecule in the gaseous state requires about 10^{-12} seconds to rotate and the complex orientation polarizability for a gas will generally not be detected at frequencies above 10^{12} Hz. At higher frequencies, the contribution to the polarization of the medium will come from the induced polarization. For small molecules in liquids of low viscosity, the time required for the orientation polarization process is 10^{-10} to 10^{-11} seconds, whereas for large molecules in dilute solutions and for viscous liquids, the time is of the order of 10^{-6} seconds.

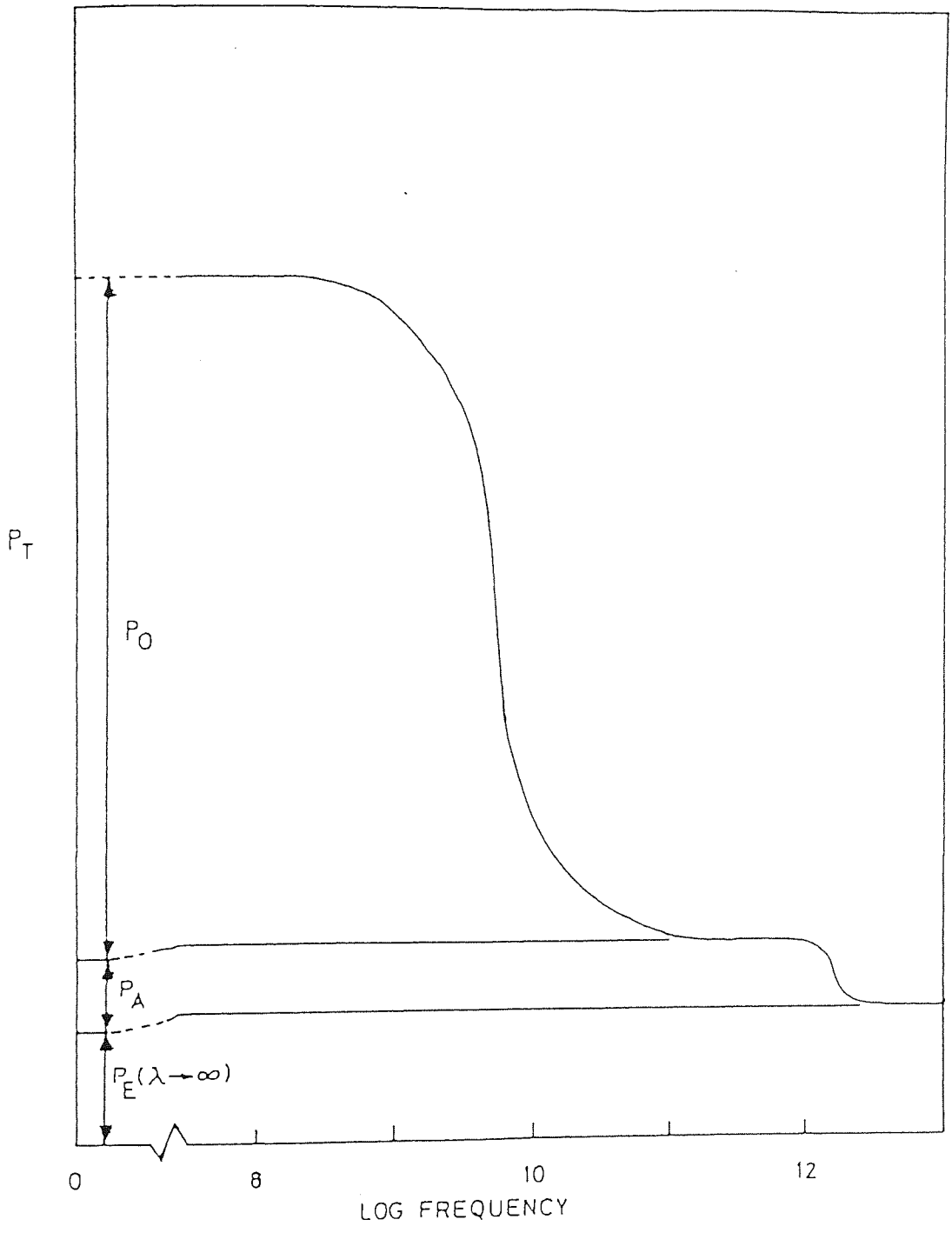

Figure 2.1 Typical frequency dependence of the total polarization, P_T

However, the atomic polarizability lies in the range 10^{-12} to 10^{-14} seconds. As can be seen from figure 2.1, resonance absorption will appear at the frequency of the infrared in the matter. For a polar dielectric medium, n^2 is equal to the dielectric constant ε measured at a frequency so high that the permanant dipoles cannot contribute to the polarization of the medium. Therefore, ε_∞ is defined by the equation

$$M(n^2 - 1) / (n^2 + 2)\rho \cong P_e + P_a = (M/\rho)(\varepsilon_\infty - 1) / (\varepsilon_\infty + 2) \qquad (2.2)$$

Where P_e and P_a are respectively, the electronic and atomic molar polarizations.The quantities ρ and M represent the density and the relative molar mass of the polar gas, respectively.

Often, many investigators have simply estimated P_a to be a fixed value somewhere in the region of 5 - 15% of P_e, or have neglected P_a completely. Since P_e is usually quite small, compared to P_o, this approach has normally been adequate.

The presently accepted interpretation of the dielectric constant, in terms of molecular dipole moments for electrically neutral materials is based upon the theory of Debye[79], who formed the equation : -

$$\mu_o^2 = \frac{9kT\varepsilon}{N} \frac{M}{\rho} \frac{[\varepsilon_o - 1]}{[\varepsilon_o + 2]} - \frac{[\varepsilon_\infty - 1]}{[\varepsilon_\infty + 2]} \qquad (2.3)$$

where,

μ_0 = dipole moment,

k = Boltzmann Constant,

N = Avagadro's number,

M = molecular mass,

ρ = density,

ε = static dielectric permittivity of free space, (8.854×10^{-12} $C^2kg^1m^{-3}sec^2$)

ε_0 = static dielectric permittivity of the medium,

and ε_∞ = dielectric permittivity measured at infinite frequency (optical wavelengths used)

Note that no allowance for atomic polarization is made in this equation.

Onsager[80] took account of the internal reaction field developed in a liquid, by effectively introduced a premultiplying term into Debye's equation : -

$$\mu_0^2 = \frac{9kT\varepsilon}{N}\,\frac{M}{\rho}\,\frac{[2\varepsilon_0 + \varepsilon_\infty]\,[\varepsilon_0 + 2]}{3\varepsilon_0[\varepsilon_\infty + 2]}\,\frac{[\varepsilon_\infty - 1]}{[\varepsilon_0 + 2]} - \frac{[\varepsilon_\infty - 1]}{[\varepsilon_\infty + 2]} \qquad (2.4)$$

Again, no allowance for atomic polarization is made.

Many subsequent refinements to this theory and equation have since been published, but only the Guggenheim-Debye rearrangement will be mentioned here. In this adaptation of the Debye equation, Guggenheim[81] defines and applies a 'fictitious' atomic polarization,

$$P_a = \frac{3\varepsilon}{N} \frac{[\varepsilon_\infty - 1]}{[\varepsilon_o + 2]} - \frac{[n_o^2 - 1]}{[n_o^2 + 2]} \qquad (2.5)$$

where n_o is the refractive index of solute.

Although this is only a disguised percentage estimate of P_a based on the value of P_e, if its presence is realised and understood it affords an improved description of the dielectric properties of 'typical' molecules, provided that P_a is relatively small compared to the total polarization.

The major difficulty arising in the determination of dipole moments from permittivity measurements lies in how to deal with the internal field problem. It is believed that, as a consequence of the condensed nature of the liquid state, each dipole experiences not the actual applied field, but a field modified by neighbouring dipoles. Among the approaches used to remedy this situation, the evaluation of dipole moments from permittivity measurements of solution stands out. In this approach, use is made of solvents of such low permittivity that the sample dipole effectively experiences the external field. In this case, the method based on the Debye equation[79] outlined by Guggenheim[81] becomes operative. A shortcoming of the Debye-based equations is that although progressive dilution eliminates intermolecular dipole-dipole interactions, intramolecuar dipole-dipole interactions, that may be important in polymers, are not considered. Models such as those developed by Kirkwood and Frolich, which allow

for the interaction of the surrounding dipoles via a correlation factor, would be more appropriate. However, their application introduces difficult computations that are often rather arbitrary. On the other hand, the Onsager theory, which is frequently favoured to obtain the dipole moment of polymer chains, is strictly applicable to situations possesing spherical symmetry and may be unappropriate for many polymers.

A large number of dipole moments obtained for oligomers and polymers by using treatments based on the Debye equation (e.g. Guggenheim[81a] and Smith[81b]) show consistency among them, possibly because intramolecular dipole-dipole interactions in flexible chains are rapidly attenuated for dipoles separated by four or more skeletal bonds. As a consequence, the Guggenheim and Smith equation is still one of the most reliable methods that can be used to evaluate the dipole moments of isolated molecular chains.

2.3 Electric birefringence

The phenomenon of electrical double-refraction discovered by John Kerr[82] whilst studying glasses is known as the electro-optical Kerr effect. If a transparent isotropic substance is placed in a uniform static electric field it becomes optically anisotropic and doubly-refracting. In liquids this is due to the orientation and polarisation of the molecules brought about by coupling of the electric field with their induced and permanant dipole moments. Although the tendency to orientate in the applied electric field is opposed by thermal motions, a steady state will exist for a given temperature and electrical field strength. If the molecules are not perfectly symmetrical, a difference in the velocity of light and hence refractive index in the directions parallel and perpendicular to the electric field will be observed. Thus, if a molecule is electrically anisotropic at low frequencies, then it usually follows that the molecules will exhibit optical anisotropy.

refractive indices produces a retardation δ between the two components of the incident-plane polarized light, which is given by the following equation:

$$\delta = 2\pi\upsilon \qquad (2.6)$$

where υ = number of waves.

During the twenty years that Kerr studied many substances, both solids and liquids, he was able to perform quantitative measurements and obtain the following empirical law relating the electric field applied to the sample E to the induced birefringence δ:

$$\delta = 2\pi l \ / \lambda = 2\pi l \ BE^2 \qquad (2.7)$$

where B represents a Kerr constant that is a characteristic of a particular sample. Thus, some substances such as benzene, toluene, chlorobenzene, etc., have a positive birefrigence (i.e., $B > 0$ or $n_p > n_v$) whereas some others like chloroform or olive oil exhibit negative values of B. The dimensions of B are [length x (electric field)^2]$^{-1}$, so that its SI units are mV^{-2}. The induction of birefringence in an isotropic sample by application of an electric field is known as the Kerr effect. Equation (2.7) is Kerr's law, and B is usually called the Kerr constant.

For solutions, the magnitude of B contains contributions from both solvent and solute. Although molar fractions were first used as a unit of concentration in equations relating

Kerr constants of solute and solvent, nowadays volume fraction ϕ are commonly used[83]. Thus, representing magnitudes of physical properties of solvent and solute by subscripts 1 and 2, respectively,

$$B = B_1\phi_1 + B_2\phi_2 = B_1 - B_1\phi_2 + B_2\phi_2 \qquad (2.8)$$

$$B_2 = (\Delta B / \phi_2) + B_1 \qquad (2.9)$$

Where ΔB represents the difference between the Kerr constant of solution and that of the pure solvent. Usually, an extapolation to zero concentration is taken in order to avoid intermolecular interactions between the molecules of solute.

The use of sinusoidal and pulsed electric fields opened two interesting perspectives. In the first place, conducting substances such as water solutions could be measured; in this regard, the pioneering work on Kerr constants of polymers carried out around 1950, was performed mainly in solutions of biopolymers, such as the tobacco mosaic virus, using this kind of technique. However, on the other hand, if a fast-response recording device such as an oscilloscope or a computer is used to store the signal from the detector, the dynamic birefringence (i.e., the variation of birefringence with time) of the sample can also be studied. Thus, information of magnitudes such as dipole moment and the rotational diffusion coefficient can also be obtained. Therefore, electric birefringence became a valuable tool for the determination of the size and shape of macromolecules and it is commonly used in the analysis of their hydrodynamic properties.

The most significant improvement in the instrumentation of electric birefringence is the use of intense beams of light to provide the electric field required to perform a Kerr-

constant measurement. The possibility of carrying out such an experiment was suggested by Buckingham[84] more than thirty years ago. However, the experimental measurements on pure liquids[85-87] and mixtures[88-89] were not performed for more than ten years afterwards, and only in the mid-1970s was it possible to measure polymer solutions[90-91]. In a typical experiment, pulses of a high-power laser beam are used to produce the electric field that orientates the molecules of the samples; the width of the pulse is smaller than 1μs, and the power may be as high as 20MW, producing electric fields up to 4×10^7 V/m.

Modern theories of electric birefringence use different treatments depending on the strength of the electric field. Under very strong fields, equation 2.7 does not hold; instead, a more complicated dependence of Δn with E is found. The results can then be expressed by a power series of field strength[92].

Theoretical analysis of polymer conformation is not simple since the flexibility of the macromolecules allows the chains to attain various conformations. The rigid polymers move inside the solution in order to orientate by the effect of the electric field, whereas flexible molecules not only move, but also can change their shape. Consequently, the treatment becomes more complicated as the flexibility of the polymers increases. A complete treatment of rigid polymers has been published by Wegener and co-workers[93-94]. Moderately flexible molecules such as bent rods requires the use of either approximate[95-96] or simulation procedures[97]. The realistic treatment of flexible polymers was started by Nagai and Ishikawa[98] to the point that all calculations carried out previously were of simplified models such as freely jointed or freely rotating chains.

The application of the Kerr constant to conformational analysis arises from the great sensitivity of this property to the variations of molecular geometry and environment[99]. The standard procedure used in these studies consists of a critical comparison between theoretical and experimental values of the molar Kerr constants, ($_mK$). In many cases, this comparison is done with the assistance of a similar analysis of some other conformation-dependent property[100] such as dipole moments. Experimental values of ($_mK$) are determined from measurements of the electrical birefringence of several solutions having different molar concentration of molecule to be studied in a suitable solvent.

Measurements performed on pure liquids are needed to evaluate the experimental Kerr constant (B) of the solvent which is required to calculate the molar Kerr constant of solute, ($_mK$). On the other hand, pure liquids of known Kerr constant are often used either for calibration or for testing the performance of experimental setups. The combination of these two factors makes it almost impossible to find an experimental determination of ($_mK$) in which no measurements of B for some pure liquid is also performed. Some interesting publications containing values of B for several pure liquids are due to Aroney and co-worker[101], who measured B at 20°C using a He-Ne laser, (λ = 632.8nm), and Lewis and Orttung[102], who determined B as a function of λ, mostly in the ultra violet region.

Determination of molar Kerr constants ($_mK$) of small molecules allows evaluation of optical properties, (mainly polarizability tensors), and energetic parameters of those molecules. This kind of analysis can be aimed to study the small molecules themselves; for instance, to determine the relative incidence of each allowed conformation. However, in most cases, the small molecules are oligomers of model compounds for the repeating unit of a polymer and the results of their analysis are used to study properties of the whole chain.

The synthesis of PVK polymers with different isotacticity and the measurement of dielectric permittivity and electrically induced optical birefringence (Kerr effect) for the undoped and doped forms of polymers forms the main basis of this work. The apparatus and techniques employed to facilitate these measurements are described in the following chapters.

CHAPTER THREE

Synthesis and Characterisation of Poly(N-vinylcarbazole)

3.1 Introduction

In Chapter 1 it was emphasised that the synthesis and evaluation of photoconductivity and photo-sensitivity of poly(N-vinylcarbazole) (PVK) have received considerable attention during recent years because of the increased demand for such materials in electrophotography and related processes. It was also shown that the photoconductivity of PVK depends on the stereostructures and tacticity of the polymers. In pure (undoped) PVK the photoconduction is dominated by holes that are long lived and are readily photoinjected from metal electrodes. PVK's unusual photoconductive behaviour is connected to its tendency to form helical structures, that is sterically hindered, with successive aromatic side chains lying parallel to each other in the stack. Electron transfer is therefore relatively easy along the side groups which are close together. The charge migration in PVK based materials is controlled by a hopping mechanism between traps. This suggests that the polymers that are high in isotactic structures would produce larger photoconduction than those which are random or syndiotactic. X-ray studies have shown that isotactic PVK consist of 3/1 helixes whereas syndiostructures are 2/1 helixes. As a result the trap distances between the adjacent pendent groups in 3/1 helixes are smaller than those in 2/1 helixes. It was also indicated in the first chapter that the photoconductive sensitivity of PVK could be increased by doping the polymer with small amounts of electron acceptors or dyes. The dyes, or electron acceptors which form charge transfer complexes with the polymers donor, increase the absorption in the visible region of the spectrum. This results in an increase in the sensitivity of the photoconductor.

In summary, therefore, the extent of photoconductivity could be controlled by carefully selecting the synthetic routes of the polymers and also by choosing complexing agents for the polymers. In this chapter details of the synthetic routes and characterisation methods are described. The polymers were prepared using cationic and free radical catalysts since these methods produce polymers with different tacticity and stereostructures. The cationically synthesised polymers produce polymers that are high in isotacticity whereas free radically prepared polymers are relatively lower in isotacticity. The characterisation of the polymers was carried out using a variety of techniques. Where possible efforts were made to obtain and compare the results derived from more than one technique. For example, the tacicity of the polymers were determined using proton and carbon-13 nuclear magnetic resonance spectroscopy. The molecular weights were determined using gel permeation chromatography and light scattering techniques.

3.2 Free radical addition polymerisation

The polymerisation involves the addition of free radicals to the double bond of the monomer. The first step in the propogation reaction is the addition of the initiator radical to the monomer followed by the addition of monomer units. In each step the consumption of a free radical is accompanied by the production of a free radical. The chain reaction is terminated by steps that consume but do not form free radicals. The free radical polymerisation of PVK is the same as that of many other vinyl monomers. An effective initiator is a molecule which, when subjected to heat, electromagnetic radiation, or chemical reaction, will readily undergo homolytic fission into radicals of greater reactivity than the monomer radical. These radicals must also be stable long enough to react with a monomer and create an active centre.

There are three stages in free radical polymerisation:

(i) *Initiation*, when the active centre which acts as a chain carrier is created in the monomer.

(ii) *Propagation*, involving growth of the macromolecular chain by a kinetic chain mechanism and is characterised by a long sequence of identical events, namely the repeated addition of a monomer to the growth chain.

(iii) *Termination*, whereby the kinetic chain is brought to a halt by neutralization or transfer of the active centre.

Initiator

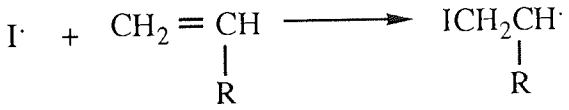

Where I· is initiator radical and R represents the carbazole group.

Propagation

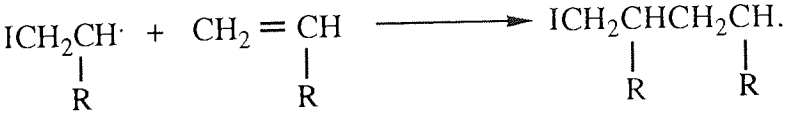

In theory, the chain could continue to propagate until all the monomer in the system has been consumed but, in fact the free radicals are paricularly reactive species and interact with each other as quickly as possible to form inactive covalent bonds. This means that short chains are produced when the radical concentration is high because the probability of radical interaction is correspondingly high. If long chains are required then the radical concentration should be kept small.

Termination of chains can take place in several ways:

(1) the interaction of two active chain ends;

(2) the reaction of an active chain end with an initiator radical ;

(3) termination by transfer of the active centre to another molecule which may be solvent, initiator, or monomer;

(4) interaction with impurities (e.g. oxygen) or inhibitors.

The most important termination reaction for this type of polymerisation is the first, bimolecular interaction between two chain ends. Two routes for this are possible :

(a) *Combination* , where two chain ends couple together to form one long chain.

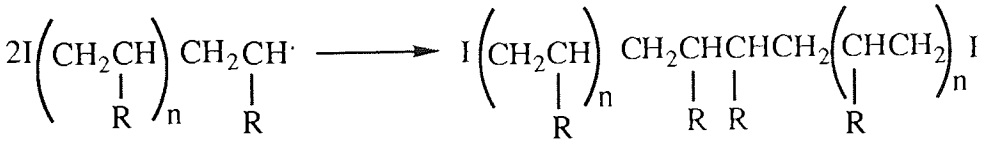

(b) *Disproportionation* , with hydrogen abstraction from one end to give an unsaturated group and two dead polymer chains.

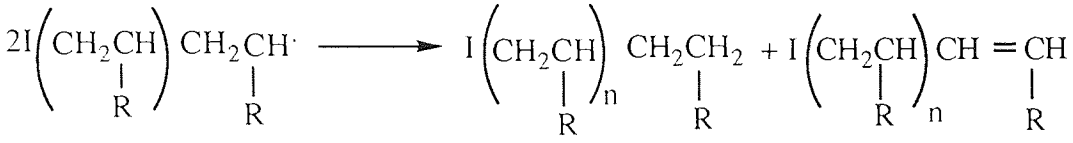

One or both processes may be active in any system depending on the monomer and polymerising conditions.

3.3 Cationic polymerisation

A common type of cationic initiation reaction is that represented as follows:

$$M + I^{+} \longrightarrow MI^{+}$$

Where I^{+} is typically a strong Lewis acid. These electrophilic initiators are classed in three groups:

(1) classical protonic acids or acid surfaces

(2) Lewis acids or Friedel-Craft catalyst (BF_3, $AlCl_3$)

(3) Carbonium ion salts.

The most important initiators are the Lewis acids (MX_n), but they are not particularly active alone and require a co-catalyst (SH) to act as a proton donor.

In general, the catalyst first forms an active species as shown below :

$$MX_n + SH \rightleftharpoons [SMX_n]^{-}H^{+}$$

(active species)

and a probable initiation mechanism is the two-step process.

Step one

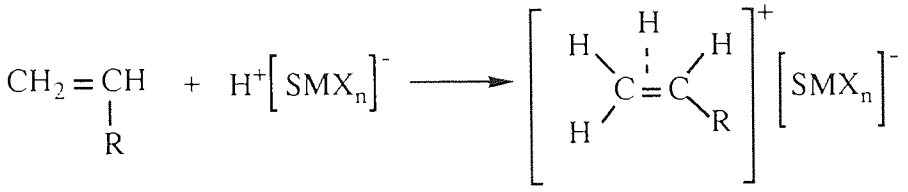

Step two

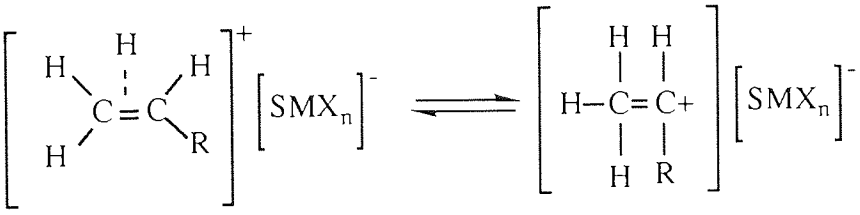

Where step one is the rapid formation of a p complex and step two is a slow intramolecular rearrangement. The active catalyst - cocatalyst species required to promote this reaction is $H^+[BF_3OH]^-$ which is formed by the following reaction:

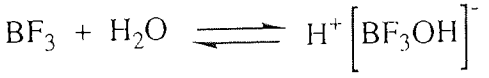

This complex reacts with the monomer to produce a carbonium ion chain carrier which exists as an ion pair with $[BF_3OH]^-$.

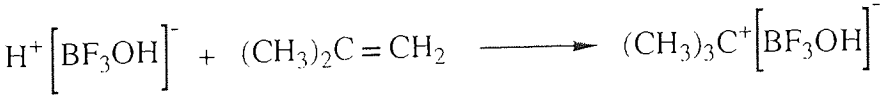

Chain growth takes place through the repeated addition of a monomer in a head-to-tail manner, to the carbonium ion, with the retention of the ionic character throughout.

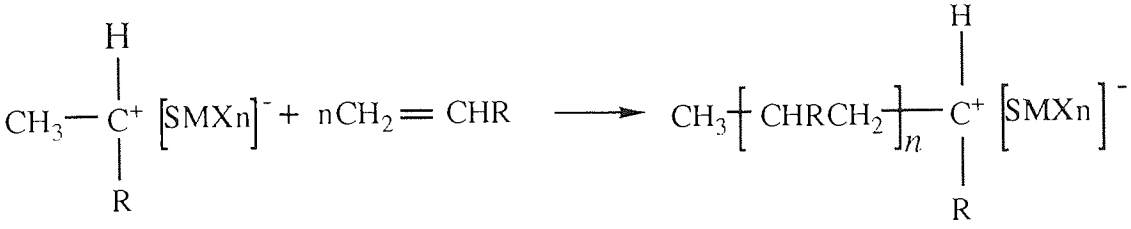

The mechanism depends on the counterion, the solvent, the temperature, and the type of monomer. Reactions of this type can be extremely rapid when strong acid initiators such as BF_3 are used, and long chain polymer are produced at low temperatures. The termination reaction in a cationic polymerisation is through to take place either by a unimolecular rearragement of the ion pair,

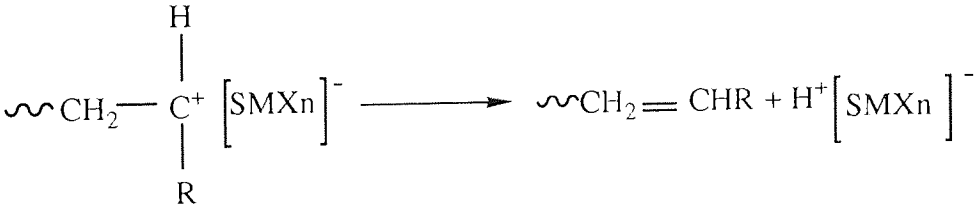

or through a bimolecular transfer reaction with a monomer :

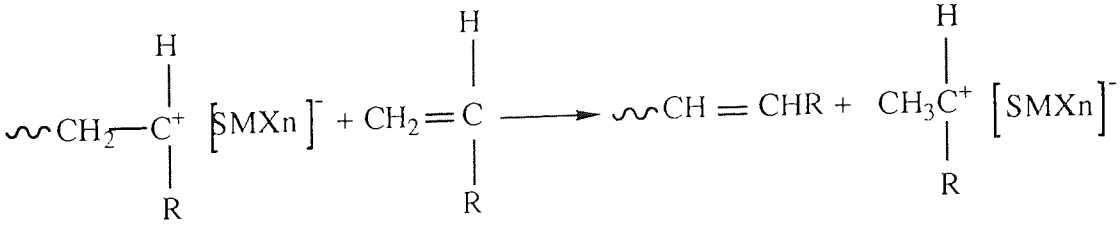

The first involves hydrogen abstraction from the growing chain to regenerate the catalyst - co-catalyst complex, while the second re-forms a monomer -initiator complex, thereby ensuring that the kinetic chain is not terminated by the reaction. In the unimolecular process, actual covalent combination of the active centre with the catalyst - co-catalyst complex fragment may occur giving two inactive species. This serves to terminate the kinetic chain and reduce the initiator complex and, as such, is a more effective route to reaction termination.

3.4 Reagents used

Chemicals	Source
N-vinylcarbazole	Aldrich
N-ethylcarbazole	Aldrich
Azo-bisisobutyronitrile	Fluka
Boron-trifluoride etherate	Aldrich
Aluminium trichloride	BDH
2,4,7-Trinitro-9-fluorenone	Aldrich
Dimethyl sulphoxide	Aldrich
Deuterated toluene	Aldrich
Toluene	Aldrich
Methanol	Aldrich
Ethanol	Aldrich
1,4-Dioxane	Aldrich

Table 3.1 Chemicals used and their suppliers

3.5 Synthesis of stereoregular poly(N-vinylcarbazole)

N-vinylcarbazole was polymerised in solution using three different types of initiators in order to produce samples of polymers with different stereostructures. The polymerisations were carried out in glass reaction vessels (250 cm^3) as shown in Figure 3.1. For all the polymerisation reactions the concentration of the monomer was approximately 0.5 M (14.49g in 150 cm^3 of solution). All of the polymerisations were terminated by pouring the reaction mixtures into methanol (500cm^3). The polymers were purified by dissolving them in toluene and then precipitation into methanol (500cm^3), while vigorously stirring the mixture. This polymers were reprecipitated three times in fresh methanol. The yields in all the polymerisations was over ninety percent.

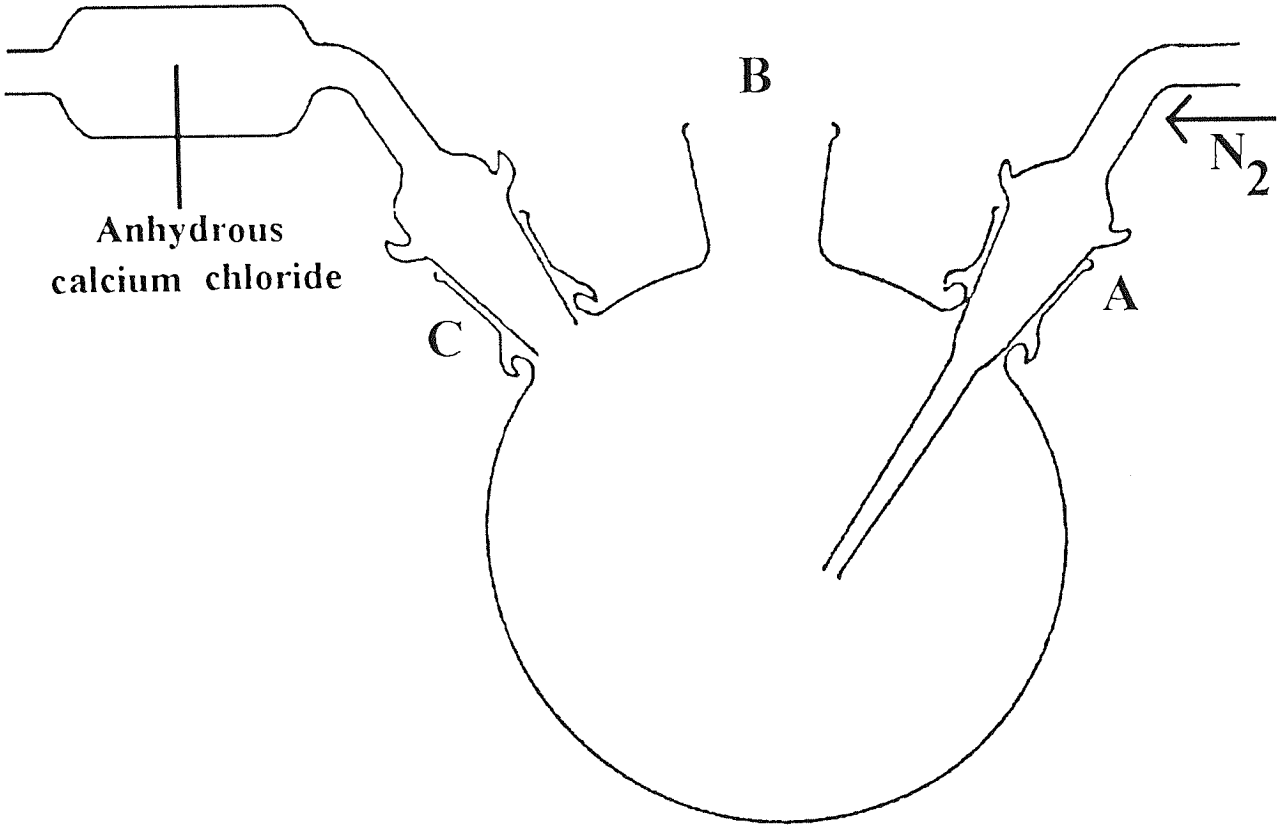

Figure 3.1 Reaction vessel

(a) Initiation with azobisisobutyronitrile:

A solution of the monomer in toluene ($140cm^3$) was evacuated and degassed several times. The initiator, azobisisobutyronitrile (0.123g) in toluene ($10cm^3$) was injected into the reaction vessel through a Suba seal. The concentration of the initiator was 1.0 mole percent of the monomer concentration (0.005M). The polymerisation reaction was allowed to proceed for 7 hours at 343K under the vapour pressure of the solution. Polymer obtained by this procedure will be referred to as F1.

(b) Initiation with boron trifluoride etherate:

The vinyl monomer and freshly distilled toluene ($150cm^3$) were placed in the reaction vessel. A small quantity ($0.17cm^3$) of the boron trifluoride etherate was injected into the reaction flask through a suba seal using a syringe. The concentration of the initiator was 0.5% (0.0025M) of the monomer concentration and the polymerisation time was 18.5 hours. All of these operations were conducted under an atmosphere of dry nitrogen. Polymers produced by this procedure will be referred to as F2.

(c) Initiation by aluminium chloride:

The vinyl monomer was placed in the reaction vessel and toluene ($140cm^3$) was then added. The solution was thermally equilibrated to 298K before adding a suspension of aluminium chloride (0.20g) in toluene ($10cm^3$). The concentration of the initiator was 0.5 mole percent of the monomer concentration (0.0025M). The polymerisation was allowed to proceed for 18.5 hours at 298 K under dry nitrogen gas. The polymer sample prepared in this manner will be referred to as sample F3.

The dielectric and electro-optic properties of N-ethylcarbazole were also investigated. This compound is regarded as a model compound in this study and represents a single repeat unit and is referred to as NEK.

3.6 Synthesis of low molecular weight PVK

Preliminary attempts were made to decrease the molecular weight of PVK. This was achieved by polymerising N-vinylcarbazole with $BF_3O(C_2H_5)_2$ in the presence of ethanol which acts as a chain transfer agent. The polymerisation was carried out with different concentrations of ethanol in order to obeserve its affect on the molecular weights of the polymers and this also provided a wider range of molecular weight for the analysis. Two polymers that were prepared in this way are referred to as samples F11 and F12. For the sample F11 the ethanol : catalyst ratio was 2:1, whereas in F12 this ratio was 3:1. The polymerisation and purification of the polymers was as described in section 3.5.

3.7 Characterisation of poly(N-vinylcarbazole) by gel permeation chromatography.

All gel permeation chromatography (gpc) work was carried out by the Rubber and Plastic Research Association (R.A.P.R.A.), Shawbury, Shrewsbury, Shropshire. The schematic diagram of a typical g.p.c. is shown in Figure 3.2. The principle of gpc is based on a type of liquid-solid elution column chromatography involving the permeation of solute molecules into rigid porous 'gel' particles (Figure 3.3).

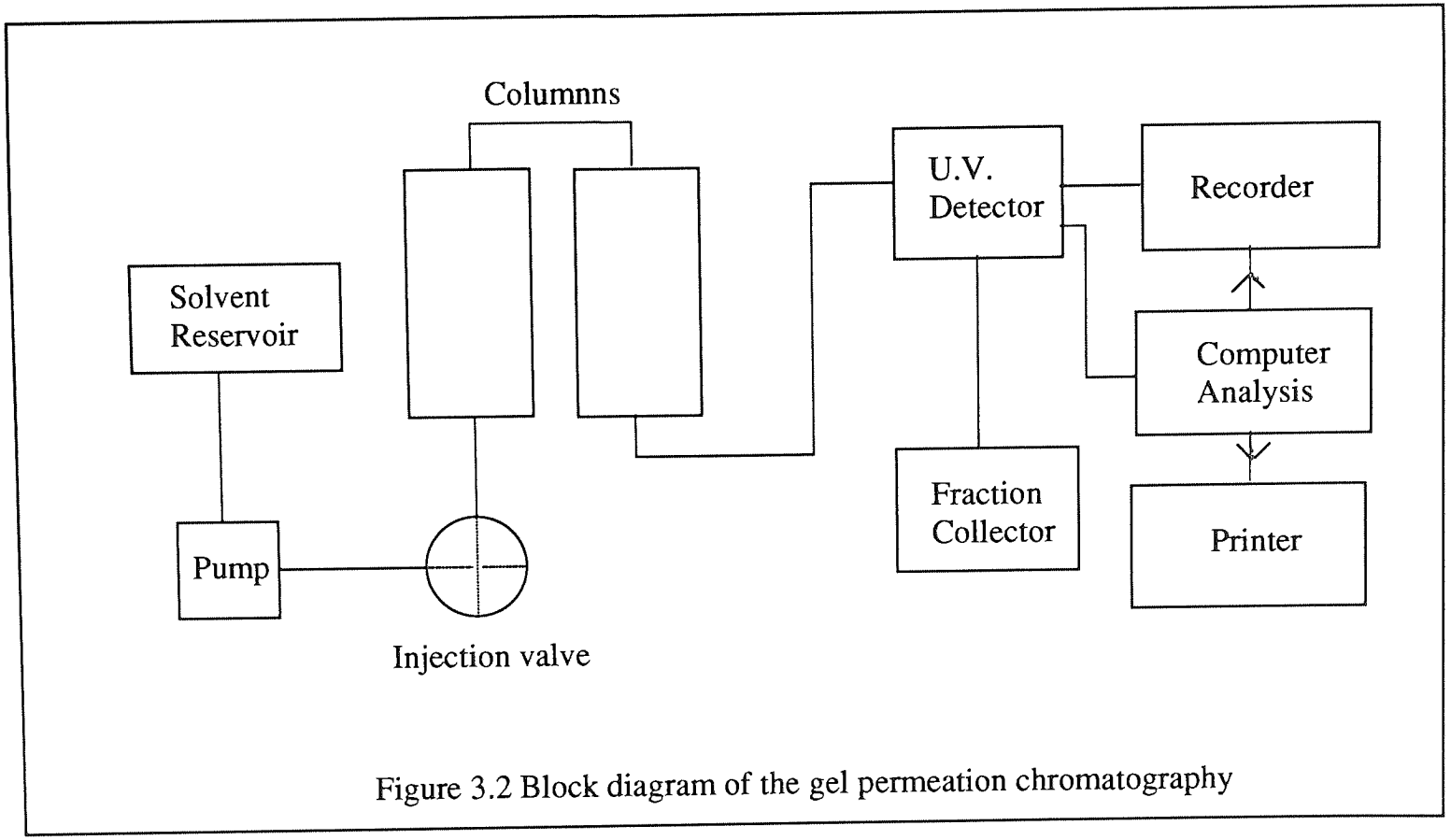

Figure 3.2 Block diagram of the gel permeation chromatography

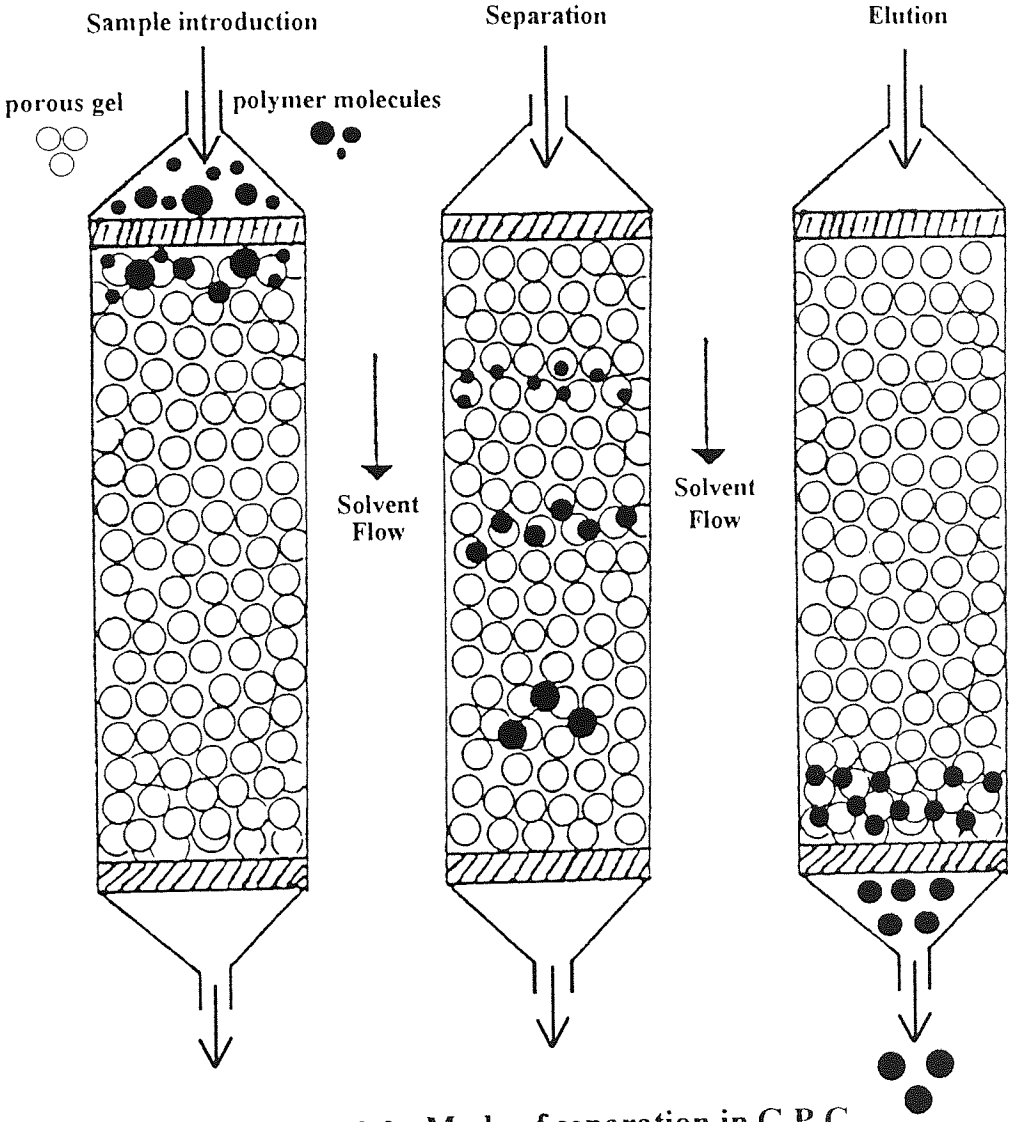

Figure 3.3 Mode of separation in G.P.C.

As the dissolved polymer molecules flow through the column they can diffuse into the internal pore structure of the gel to an extent depending on their size and pore-size distribution of the gel. Larger molecules can enter only a small fraction of the internal portion of the gel, or are completely exluded; small polymer molecules penetrate a larger fraction of the interior of the gel. The larger the molecule, therefore, the less time it spends inside the gel, and the faster it flows through the column. The different molecular species are eluted from the column in order of their molecular size as distinct from their molecular weight, the largest emerging first. Gel permeation chromatography provides the simultaneous measurement of molecular size and molecular weight distribution of polymers.

A specific column or set of columns with gel, of differing pore size (the most widely used being highly crossed-linked polystyrene), is calibrated empirically to give a relationship between retention times or volumes and molecular size of polymer. By means of this, a plot of the amount of solute versus retention volume can be converted into a molecular-size distribution curve.

Solutions of accurately known concentration of polymers were prepared and left overnight to dissolve. However, polymer F2 did not appear to be completely soluble and it was placed in an ultrasonic bath for about five minutes to assist maximum dissolution. R.A.P.R.A. ran the sample solutions using the following g.p.c. conditions:

Columns:	PL gel 2 x mixed gel, 10 microns, 30 cm,
Solvent:	Tetrahydrofuran, with anti-oxidant,
Flow-rate:	1.0 ml per minute
Temperature:	Ambient
Detector:	Refractive Index

The final product from gpc analysis is the recorded trace of the chromatogram in terms of polystyrene equivalent.. Figures 3.4 - 3.8, shows the chromatograms of PVK samples F1, F2, F3, F11, and F12 respectively, obtained from gpc analysis provided by R.A.P.R.A. Table 3.2 shows the average molecular weight values (M_n, M_w and M_z) and polydispersity ratios (M_w / M_n) of the polymers.

Sample	[Monomer]	[Initiator]	Reaction Temperature	M_n ($x10^3$)	M_w ($x10^3$)	M_w/M_n
F1	0.5M	AZBN (5mM)	343K	28.5	75.0	2.63
F2	0.5M	BF_3OEt_2 (2.5mM)	298K	30.9	630.2	20.37
F3	0.5M	$AlCl_3$ (2.5mM)	298K	23.7	134.0	5.65
F11	0.5M	BF_3OEt_2/EtOH (2.5mM : 5mM)	298K	1.17	13.7	11.65
F12	0.5M	BF_3OEt_2/EtOH (2.5mM:7.5mM)	298K	2.37	13.4	8.98

Table 3.2 Molecular weights of polymers prepared with various catalysts

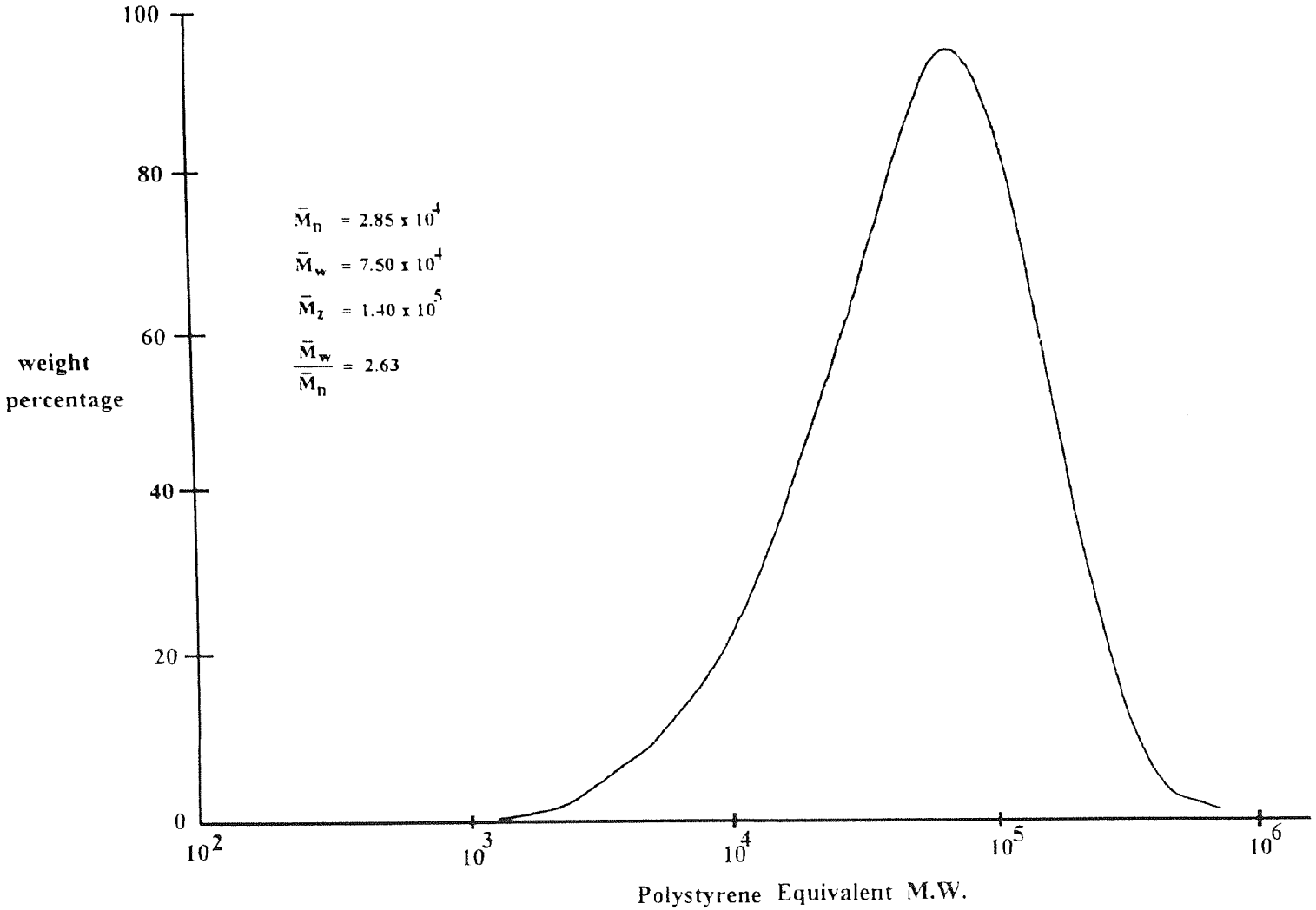

Figure 3.4 G.P.C trace of sample F1 . Poly(N-vinylcarbazole) prepared by initiation with AZBN

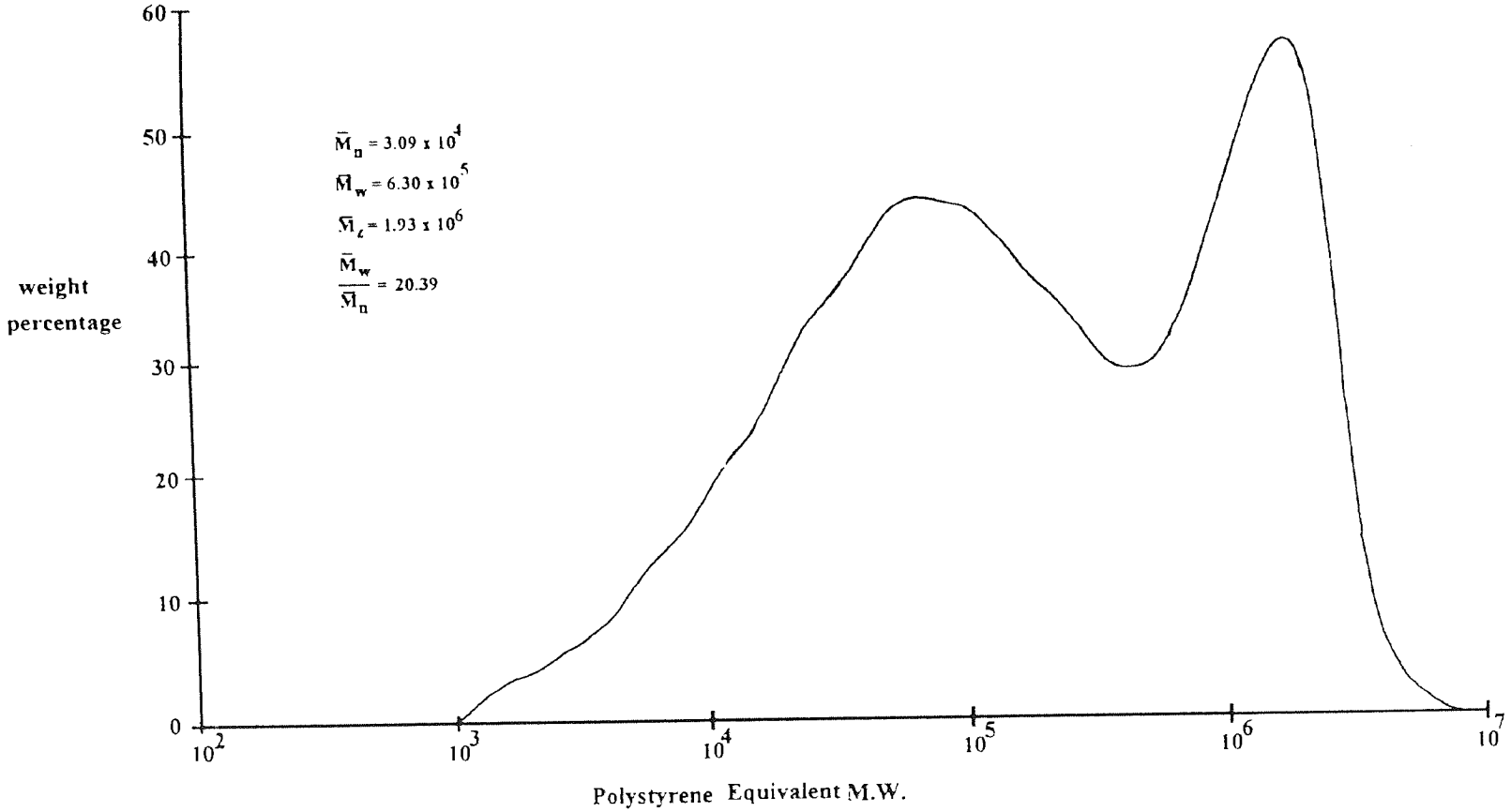

Figure 3.5 G.P.C trace of sample F2 · Poly(N-vinylcarbazole) prepared by initiation with $BF_3O(Et)_2$

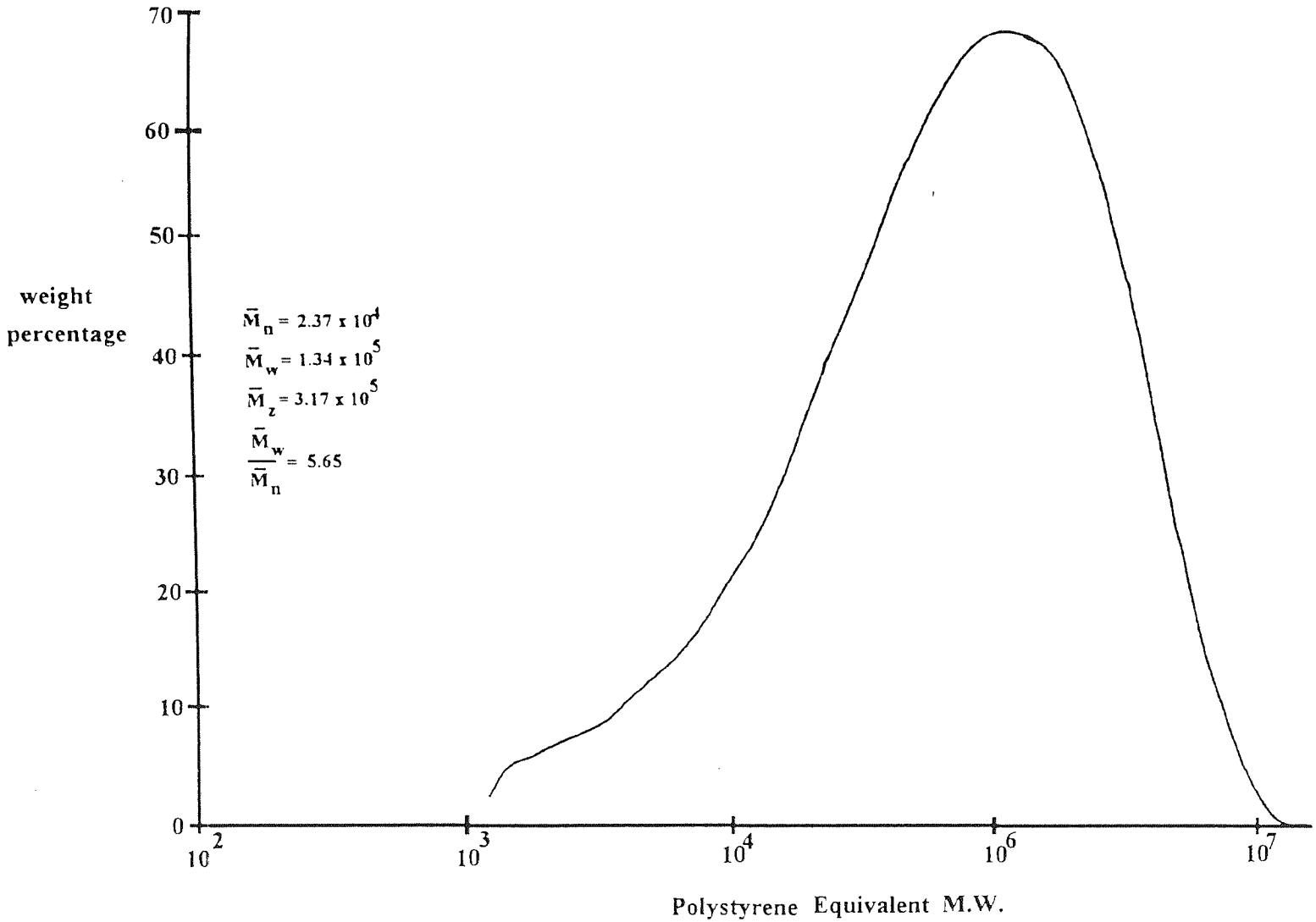

Figure 3.6 G.P.C. trace of sample F3. Poly(N-vinylcarbazole) prepared by initiation with $AlCl_3$

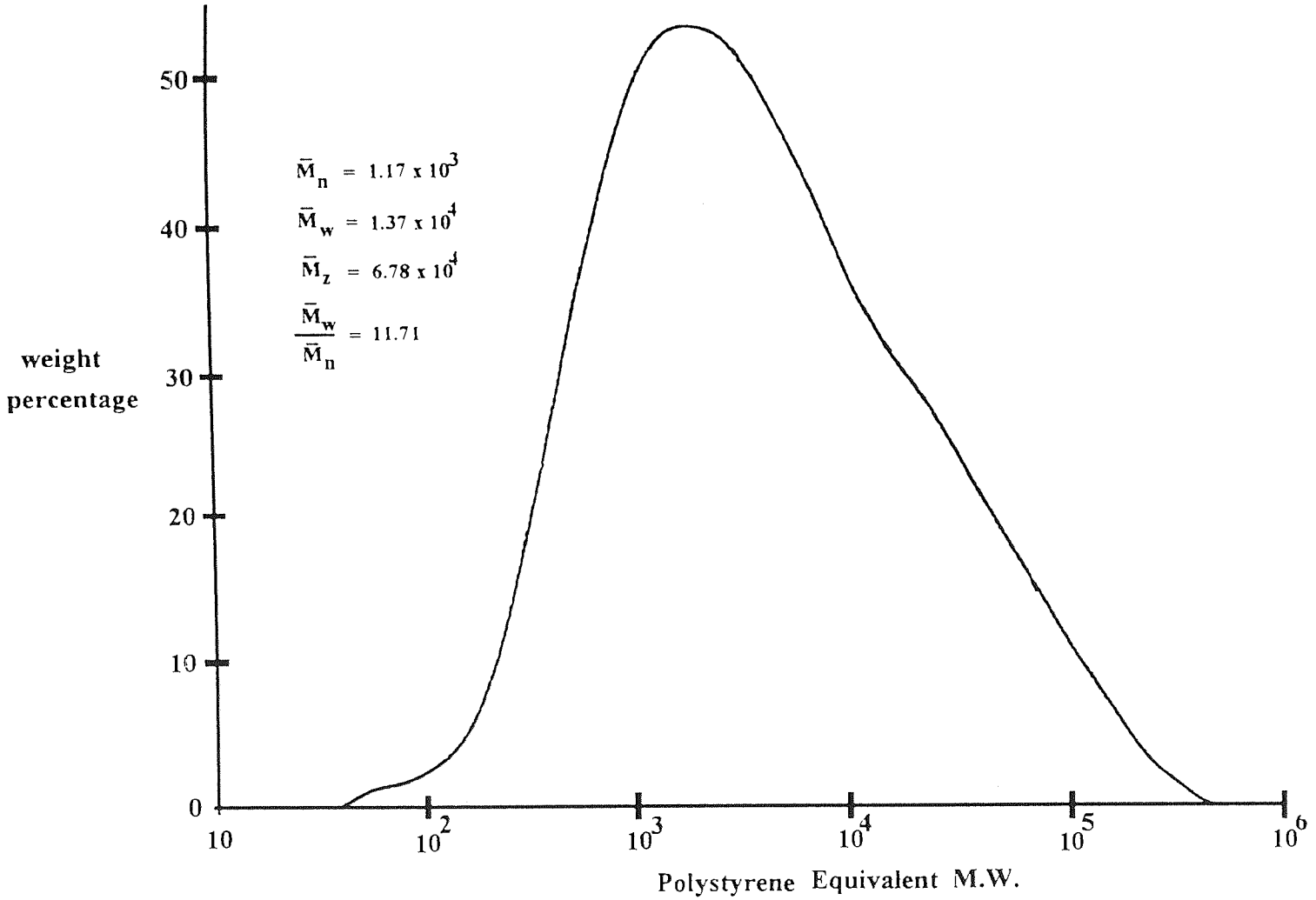

Figure 3.7 G.P.C. trace of sample F11· Poly(N-vinylcarbazole) prepared by initiation with $BF_3O(Et)_2$: EtOH (mole ratio 1:2)

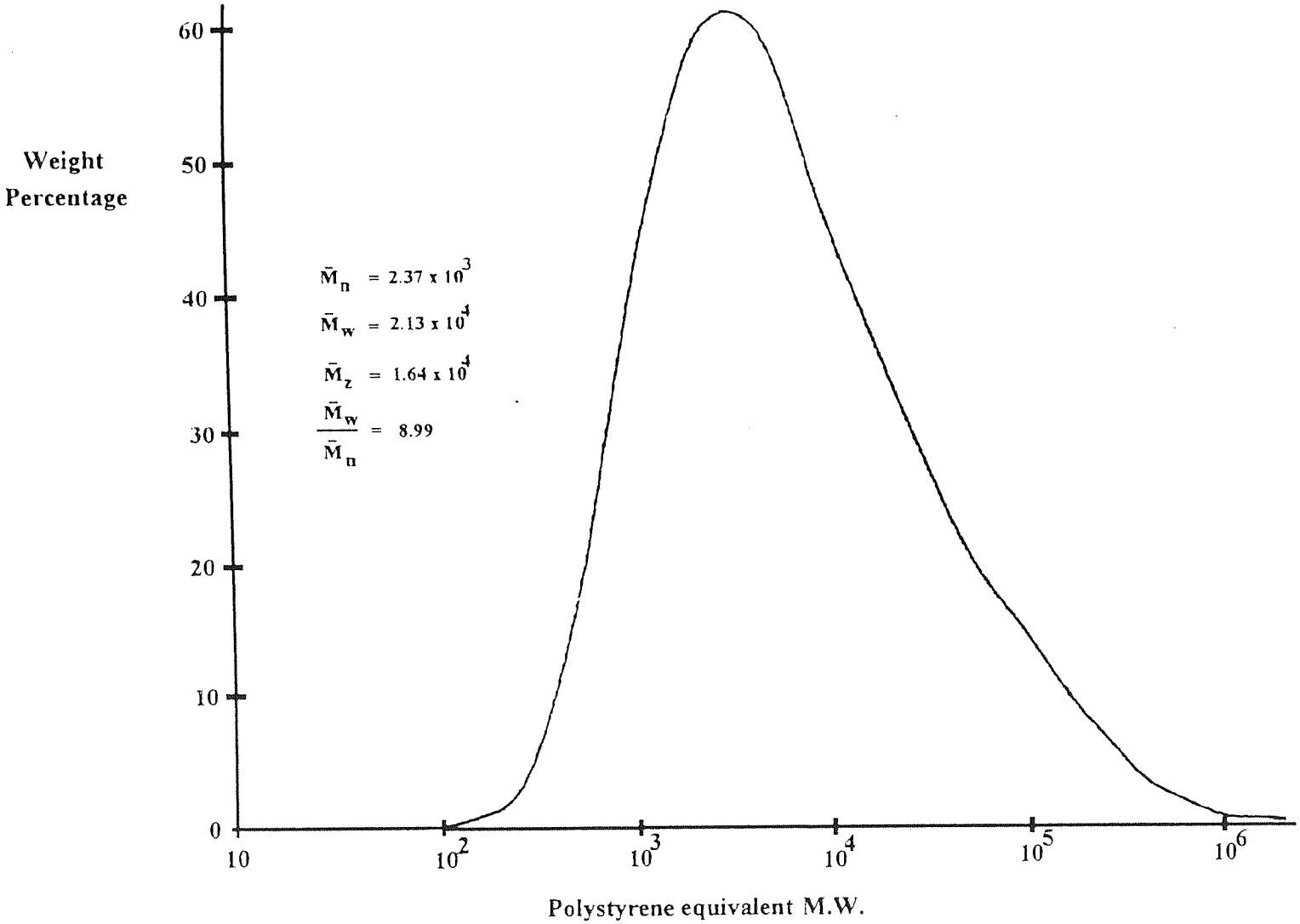

Figure 3.8 G.P.C. trace of sample F12. Poly(N-vinylcarbazole) prepared by initiation with $BF_3O(Et)_2$: EtOH (mole ratio 1:3)

Gel permeation chromatography results show that polymer samples F1, F2 and F3 have large molecular weights with a broad distribution of molecular weight. This was predictable since no steps were taken to control the molecular weights. However, F11 and F12 had much lower molecular weights (compared with F2). There is a twenty six fold decrease for F12. This indicates that when a small quantity of ethanol is introduced into the reaction a significant decrease in the molecular weight is obtained. These results indicate that the ethanol is acting as an efficient chain transfer agent in the polymerisation of N-vinylcarbazole since the accurate molecular weight control depends on the amount of ethanol present in the reaction. It was found that molecular weight was inversely propotional to the concentration of the chain transfer agent i.e. as the ethanol level increases, the molecular weight of the polymer decreases.

3.8 Light scattering

The first aim of this work was to compare the weight-average molecular weights of the polymers using light scattering and gel permeation chromatography. The second aim of this work was using light scattering, to investigate the solvent affect on the radius of gyrations of polymers. In this section, the operating procedure of light scattering is mentioned only briefly since the main aim is to highlight some of the difficulties involved in operating the equipment and to explain the results obtained from this instrument.

The light scatterer (Otsuka Electronic Co., Ltd., model number DL-700) is shown in Figure 3.9. The essential parts are:

(i) 5mW He-Ne laser.

(ii) glass cell, and

(iii) polariser and photomultiplier.

In order to find the radius of gyration of the polymers it is necessary to perform static light scattering (SLS) measurements. The SLS measurement uses angular scanning of the scattering intensity under the static light scattering method. This stored data is used to obtain the molecular weight and the radius of gyration of the polymer. Before a measurement can be made the sample has to be checked for dust using the intensity monitor, which monitors fluctuations in intensity of the sample. When the scattering intensity distribution fluctuates too much the warning, "DUSTY", appears to show that there is too much dust present in the sample solution. When this happens the solution has to be filtered again in an attempt to remove more of the dust.

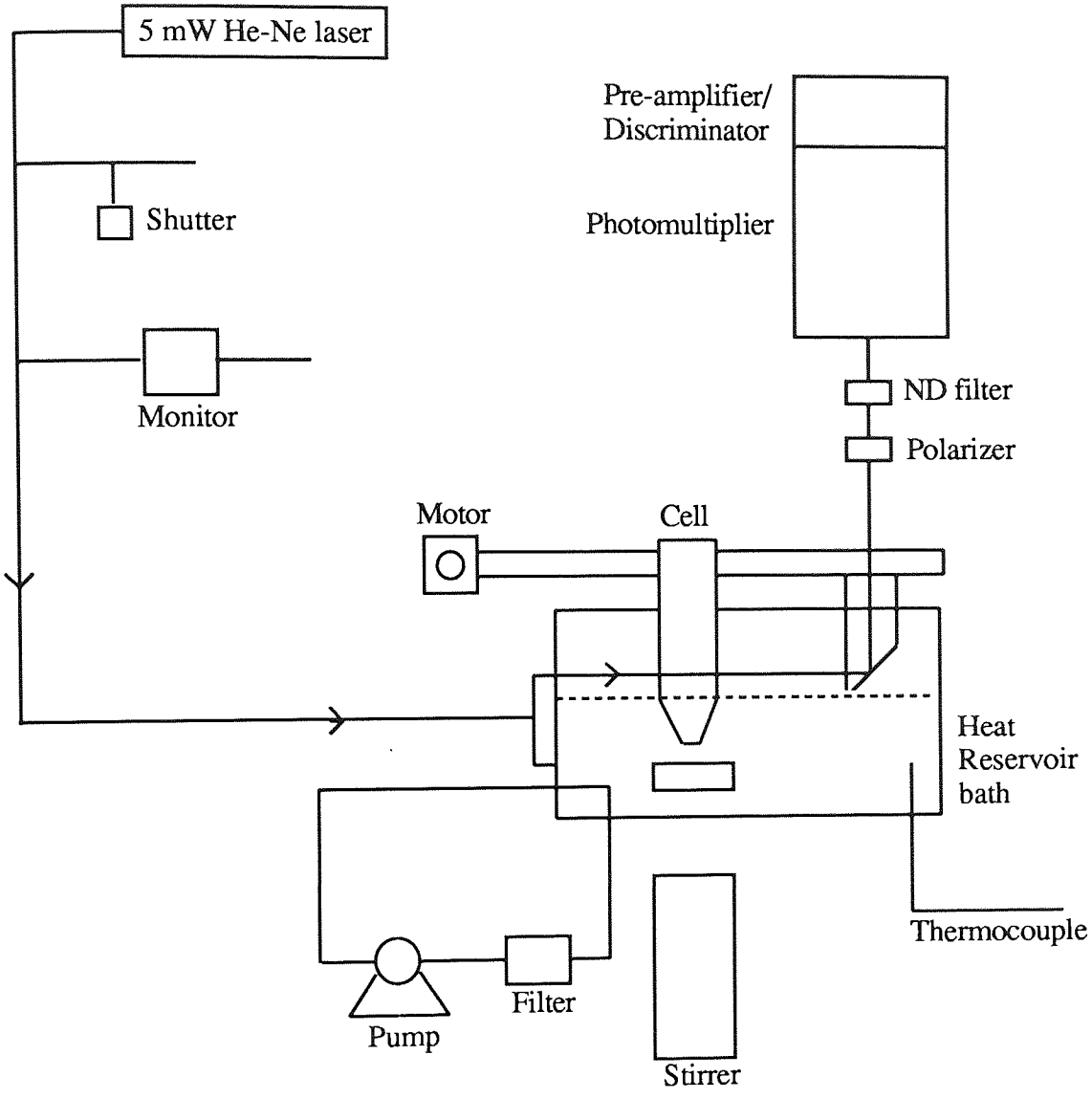

Figure 3.9 Schematic Diagram of Light Scattering (DSL 700)

Before sample measurements can be performed a solvent measurement has to be carried out first. A number of measurements were made for each polymer type in 1,4-dioxane (F1,F2, F3) and toluene (LS1, LS2, LS3) and the results were stored in the computer. For calculation purposes, the values of both the refractive index and the concentration of the sample solution need to be entered into the computer. The weight average molecular

weights and radius of gyrations of the polymers are then estimated by the computer by performing Zimm plots. The results are listed in table 3.3 (see also Appendix 1).

Sample	Molecular Weight (Weight average) $\langle M_w \rangle$	Radii of gyration $\langle S \rangle$ ($x10^2$ Å)
LS1	3.59×10^4	1.69
LS2	1.14×10^6	3.89
LS3	2.74×10^5	3.28
F1	9.59×10^4	3.57
F2	2.50×10^6	7.40
F3	2.10×10^5	4.50

Table 3.3 Light scattering data of molecular weights and radii of gyration of various samples of stereoregular PVK determined in toluene and 1,4-dioxane at 298K.

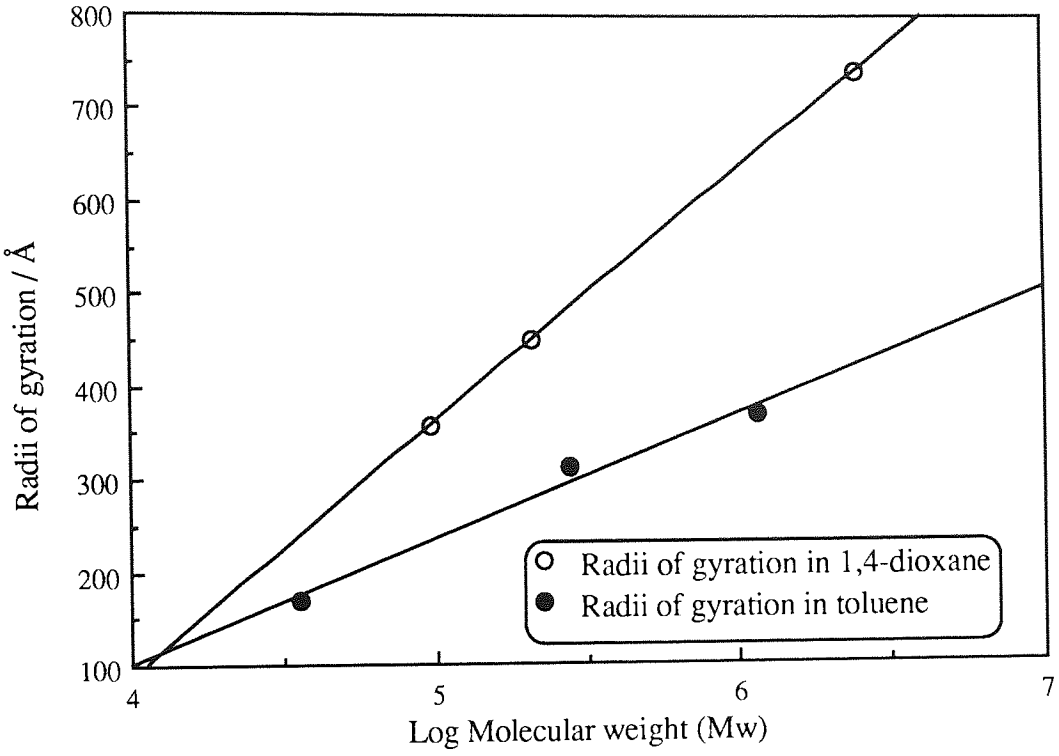

Figure 3.10 Radii of gyration of various samples of stereoregular PVK determined in toluene and 1,4-dioxane at 298K.

The molecular weight results from light scattering method are larger than those predicted by the gel permeation chromatography (gpc). The greatest difference was for the polymer sample F2 prepared with boron-trifluoride etherate. The light scattering provides an exact molecular weight measurement and not a polystyrene equivalent like the gpc method. Also some higher fractions of polymer sample F2 was excluded from the gpc column. This may well account for a large difference in the molecular weights predicted by these two methods.

In both solvents (toluene and 1,4-dioxane), polymer sample F1 (prepared with azo-bisisobutyronitrile), has the smallest radius of gyration, whilst polymer sample F2 synthesised using boron-trifluoride etherate, had the largest. It is clear from Figure 3.10 that the radii of gyration for all polymers are bigger when determined in 1,4-dioxane than

in toluene. This is surprising because as it was first thought that in what can be considered as a poor solvent, such as 1,4-dioxane, the PVK molecules "crumpled up" and there was very little interaction with the solvent. Toluene on the other hand, being considered a better solvent, was thought to have better interactions with the PVK molecules. In this case the polymer molecules were thought to be open and as the helices start to unwind, this would result in the polymer molecules having a larger radius of gyration than in 1,4-dioxane. These results show that this is not the case and that at room temperature toluene may in fact be encouraging the helical structure of PVK at room temperature. It is important to note that the value of dn/dc for PVK dissolved in toluene was determined to be 0.23ml/g. However, when determining the radii of gyration of PVK in 1,4-dioxane, dn/dc value was not measured but the value of 0.23ml/g was used. This produced radii of gyration that were larger than expected. It was then decided to repeat the measurements by using twenty percent larger and smaller values than 0.23ml/g (see Appendix 1) in order to test the dependence of radii of gyration (S) on the choice of dn/dc. The results, however, indicated that the change in dn/dc values did not significantly alter the radii of gyrations of PVK samples.

It is also important to consider how reliable and meaningful the estimate of the radius of gyration calculated by the computer. The computer calculation uses an assumption that the polymers behave in a Gaussian manner, (i.e. their configurations are imagined to be the result of random walk process) [79]. PVK is a stiff rod-like polymer, with a low-medium molecular weight, so it is not expected to behave in a Gaussian manner. For there to be a truely random chain configuration the polymer chain must be fairly long. In the measurements performed, the longest chain length calculated from the weight maverage molecular weight is approximately 13000 repeat units, with the smallest being approximately 500. Therefore, it is unlikely that these experiments have produced true Gaussian - type of radii of gyration (<S>). It should be noted, however that as all the

results produced are reproducible, it is the Gaussian assumption that is in doubt. The smaller molecular weight in toluene may also link in with the fact that no expansion of the dimensions of the polymer samples in the toluene system is seen. When the polymer goes into solution the radius of gyration is multiplied by an expansion factor:

$$\langle S \rangle = \alpha \langle S_0 \rangle$$

Where : $\langle S_0 \rangle$ is original radius of gyration for the unperturbed chains and
α is the expansion factor, which is a complex function of the molecular weight and solvent-solute interactions.

Therefore, in the case of these experiments where the molecular weights are small there will not be a large expansion factor. This means there will be very little difference between the expansion in good solvents and that in poorer solvents. The equipment and the conditions under which the experiments were performed may not have been sensitive enough to detect the small change between the radius of gyration in toluene and that in 1,4-dioxane.

It is obvious that any future work should include more extensive study of the solvent effects in PVK. Possibly at higher temperatures, and with a more reactive solvent such as xylene, for which there may be larger solvent effects on $\langle S \rangle$.

3.9 Characterisation of PVK using proton nuclear magnetic resonance spectroscopy

The level of polymer isotacticity was calculated from the ^1H nuclear magnetic resonance spectrometer (NMR) spectra (Figures 3.11-3.13) by comparing the ratios of the areas of methine and methylene peaks at 3.3 - 3.8 ppm. The spectra were obtained using a Bruker 300 MHz nuclear magnetic resonance spectrometer using tetramethylsilane as a standard. The methine and methylene peaks were not resolved sufficiently when the spectra were obtained at room temperature, but were fairly well resolved at higher temperatures. Therefore, the NMR was operated either at 125°C using dimethyl sulphoxide or deuterated toluene at 95°C. The results obtained are tabulated in table 3.4.

Sample	Catalyst	% isotacticity (from methine peaks)
F1	AZBN	24
F2	BF_3OEt_2	51
F3	$AlCl_3$	30
F11	BF_3OEt_2/EtOH 1 : 2	47
F12	BF_3OEt_2/EtOH 1 : 3	49

Table 3.4 Isotactic content of PVK samples determined from proton NMR spectra.

It is clear from table 3.4 that cationic catalysts, in general, yield polymers with higher isotacticity than those prepared using free radical initiators. A polymer sample with 51% isotactic level was obtained when the monomer was polymerised with boron trifluoride etherate whereas only 24% isotacticity was obtained using azobisisobutyronitrile. These figures were obtained by comparing the areas of methine and methylene peaks on ^1H NMR[103]. The aromatic region of the spectra ($\tau > 6.0$) vary only a little with the polymerisation method. The methylene and methine regions

of the spectra consists of two peaks, which vary appreciably with the polymerisation method. The intensity ratio of the higher field peaks to lower field peaks ($I_{H/L}$) is dependent on the polymerisation method. Polymers prepared cationically in a nonpolar solvent at room temperature have the largest $I_{H/L}$ values and the samples prepared using free radicals have the smallest values. The highly resolved spectra of methylene protons are composed of four peaks for both the samples prepared by cationic and free radical polymerisation. The differences in the $I_{H/L}$ values are attributable to some differences in the stereochemical configuration of the polymer chain. The splitting of both doublet signals of methylene and methine protons are too large to be attributable to some triad tacticity in the usual manner. Therefore, it may be necessary to assume the presence of two kinds of methylene and methine protons that have quite different environments, that is, stereoblock arrangements of isotactic 3/1 and syndiotactic 2/1 helixes, as has been proposed by Mikawa et.al. [104].

Heller et.al.[105] investigated the NMR spectra of polystyrene and poly(-1-vinylnaphthalene) in connection with the stereoregularity, and found that the aliphatic protons of poly-1-vinylnaphthalene has the following unusual behaviour, probably owing to the bulkiness of the pendent group [105] :

(1) Both the methylene and methine signals of the isotactic samples are remarkably upfield with respect to signals of the atactic polymer.

(2) The methine signals of both the samples are shifted appreciable downfield compared with those obtained for polystyrene.

In the present case, the aliphatic protons have chemical shifts similar to those obtained for poly(-1-vinylnaphthalene). Therefore, the higher peaks of both methylene methine protons may be tentatively assigned to the isotactic sequence, and the lower field peaks to syndiotactic sequences. According to this assignment, the $I_{H/L}$ value is a measure of the relative amount of the isotactic and syndiotactic sequences in the polymer. In the present study, polymers prepared with BF_3OEt_2 have the largest amount of the isotactic sequences (51%), whilst those prepared with free radicals have the smallest amount (24%).

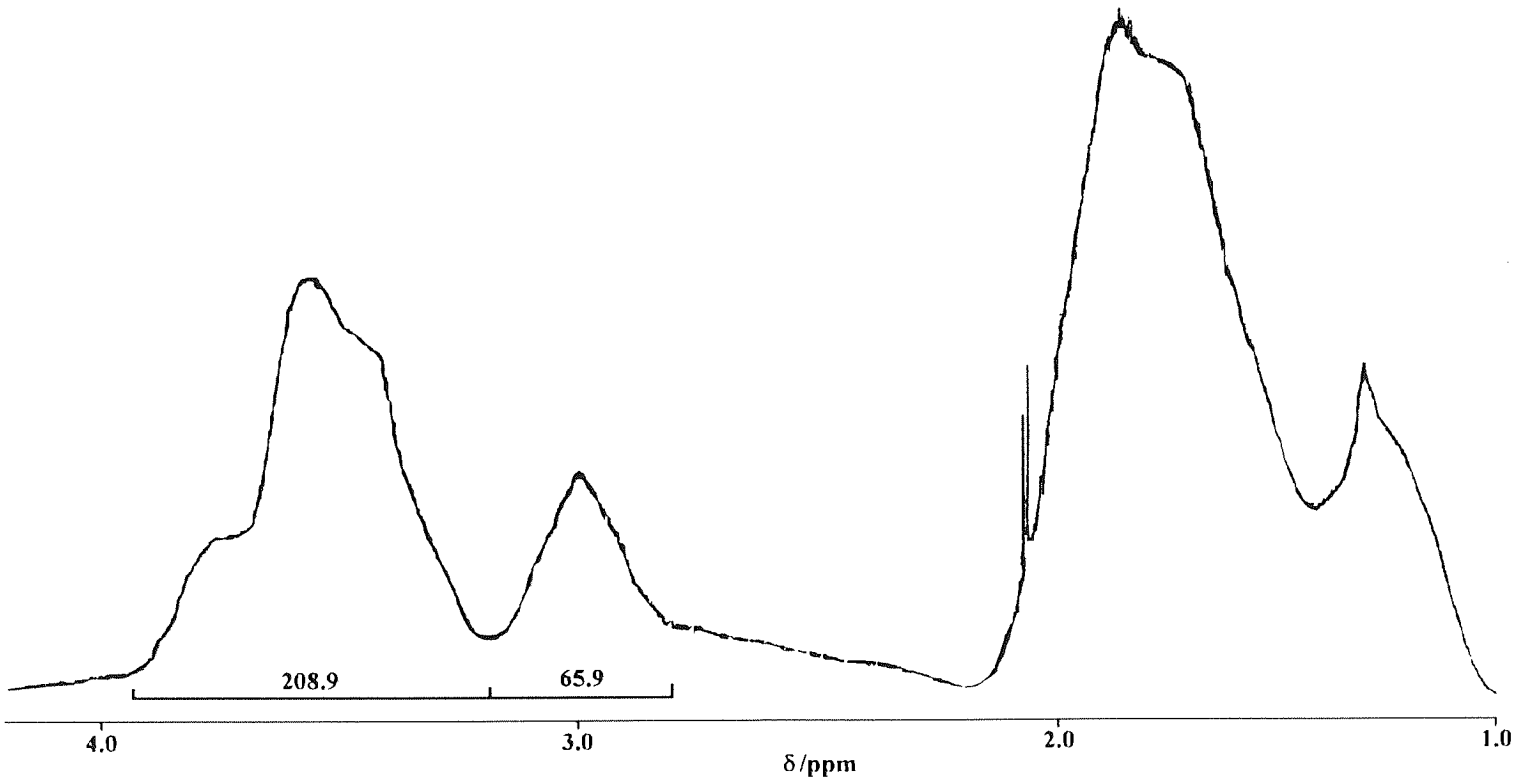

Figure 3.11 Methine and methylene peaks from H-1 N.M.R in $DMSOD_6$ at 398K spectrum of sample F1 (initiated with AZBN at 343K)

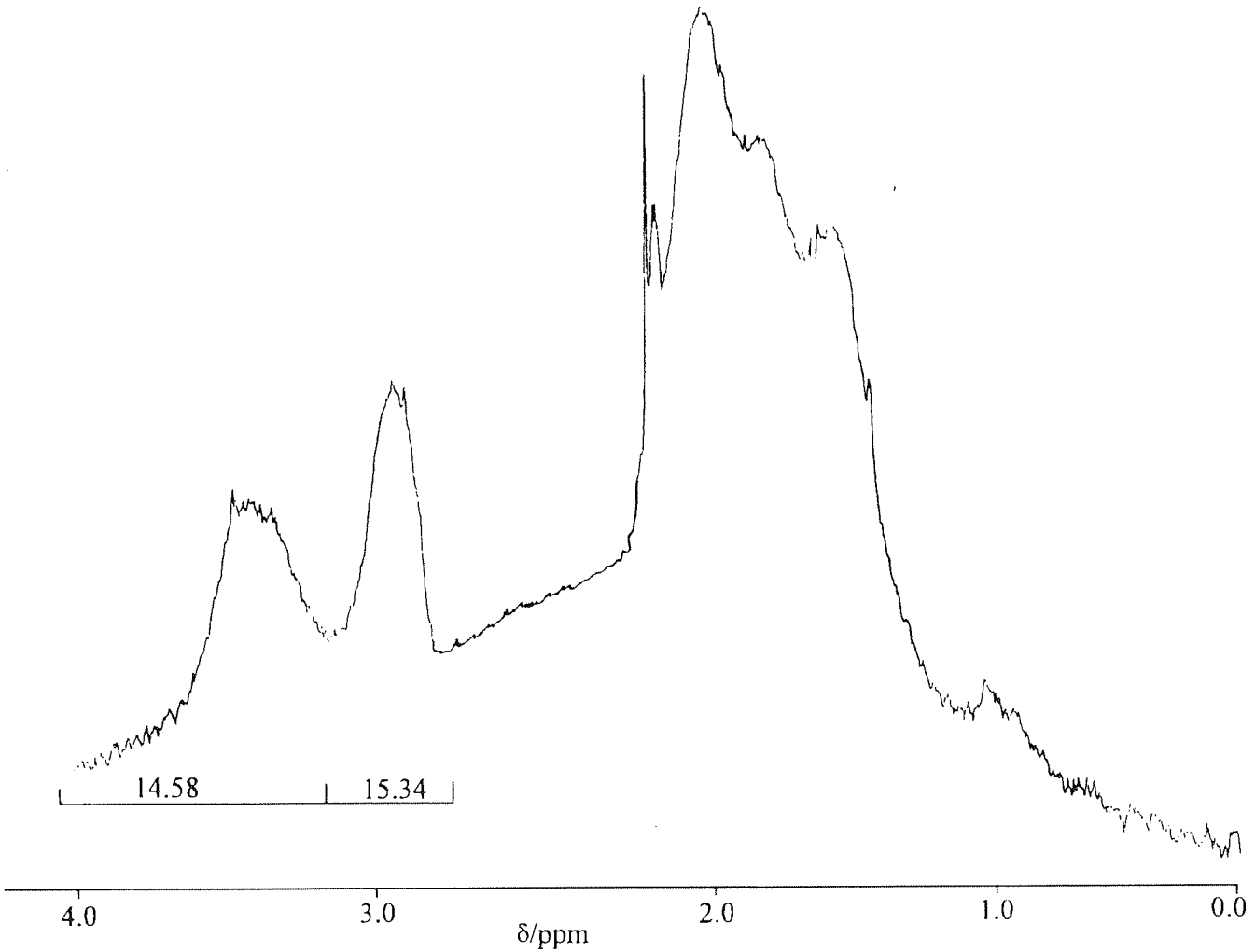

Figure 3.12 Methine and methylene peaks from H-1 N.M.R. spectrum in $DMSO_6$ at 398 K of sample F2 (initiated by BF_3OEt_2 at 298 K)

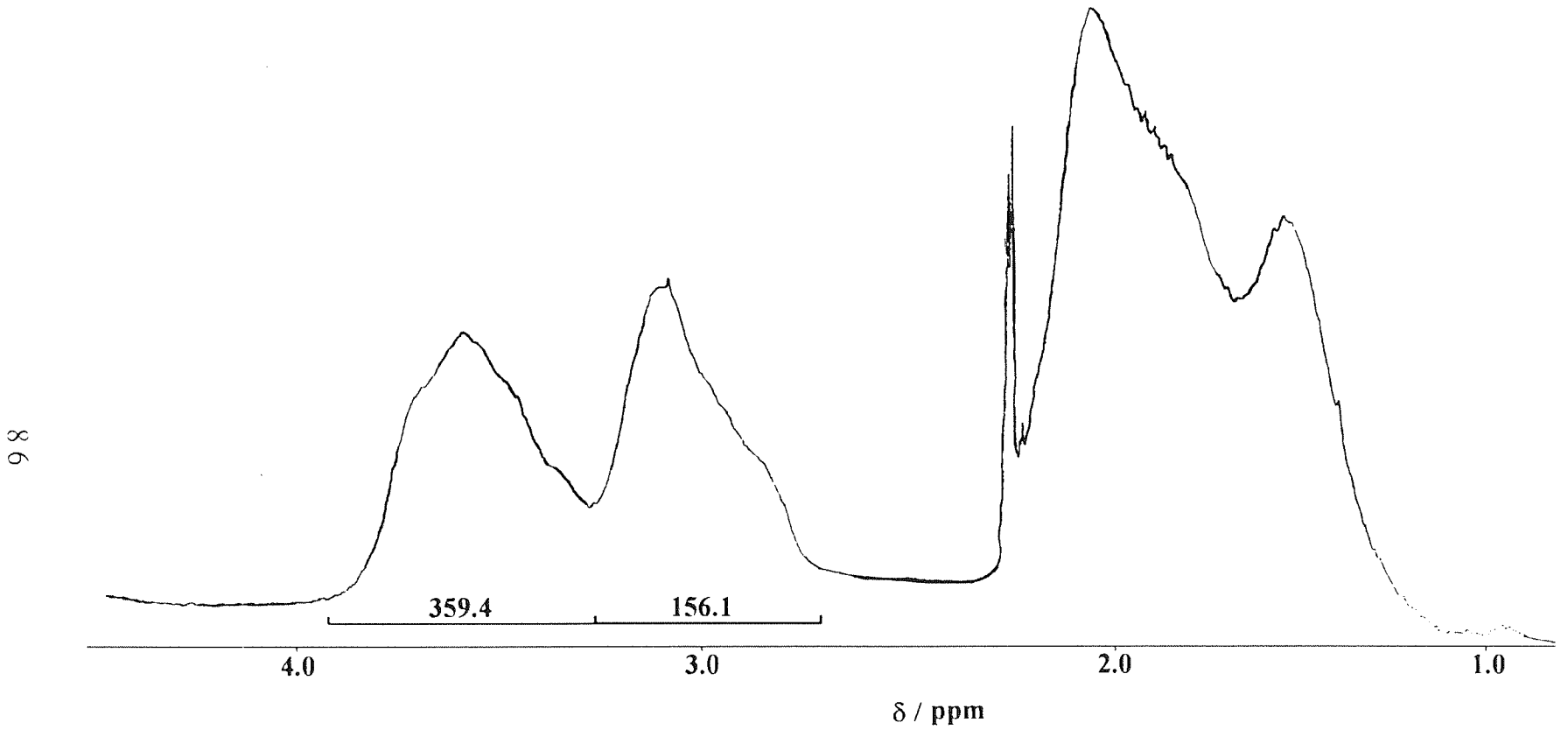

Figure 3.13 Methine and methylene peaks from H-1 N.M.R. spectrum in $DMSOD_6$ at 398K of sample F3 (initiated by $AlCl_3$ at 298K)

3.10 Characterisation of PVK using carbon-13 nuclear magnetic resonance spectroscopy

Paralleling other developments in carbon-13 nuclear magnetic resonance (NMR) spectroscopy, interest in carbon-13 spin relaxation data has increased greatly since the advent of Fourier Transform methods. This interest arises for two reasons. Firstly, it is necessary to have information about relaxation behaviour in order to achieve sensitivity advantages approaching those theoretically inherent in Fourier transform NMR experiments. Secondly, relaxation data can yield new kinds of chemical and molecular structural data that are either difficult or impossible to obtain from other kinds of studies. Carbon-13 spectra are primarily observed under proton-decoupled conditions, where each carbon in the molecule is generally represented by a single spectral line whose spin-lattice (T_1) and spin-spin (T_2) relaxation times are governed by single exponential time constants.

To date there is no evidence in the published literature of any worker of reporting fully relaxed NMR spectrums of poly(N-vinylcarbazole). Most workers have avoided measuring relaxation times (T_1) of PVK and nuclear Overhauser effects have also been ignored. The main reasons for this are that fully relaxed spectrum normally requires large amounts of instrument time. Also, some older nmr spectrometers are not equipped to carry out this complicated work. In this study, an attempt was made to obtain fully relaxed spectra of poly(N-vinylcarbazole) samples F1 and F2. The isotactic levels of these polymers was then calculated from the areas corressponding to the methine and methylene peaks. The techniques used to measuring spin-lattice (T_1) relaxation time and Nuclear Overhauser effect are described below.

A pulse technique was used for determining T_1 because this technique has two main advantages:

(i) all resonant nuclei (of the type of magnetic nucleus being observed) can be sampled simultaneously, and

(ii) pulsed methods are more amenable to repetition of the experiment (data accumulation) - an important aspect for the low natural-abundance carbon-13 isotope.

Furthermore, once initiated, the entire experiment can be performed under computer control and as such does not require the presence of the investigator.

The most widely applied puse sequence to determine T_1 is the 180-t-90 or inversion-recovery method. An intense radio-frequency field in the form of square-wave pulse rotates Mz through 180° (inverts the spin population), after which a time delay t is imposed. This is followed by a 90° monitor pulse that turns the recovered magnetization into the xy plane where its free induction decay (FID) is observed. The experiment is repeated as a function of t with a long delay, T, between 90° and 180° pulses (to allow recovery to the equilibrium situation before repetition of the sequences). The pulse sequence is represented as

$$—(180\text{-}t\text{-}90\text{-}T)_{-n} \qquad (3.1)$$

where the delay time T is 3-5 times the longest T1 to be determined in the experiment. The Fourier transformation of the FID yields the time-dependent intensity of each line in the spectrum. T_1 may be calculated from the following equation 3.2 by using the results at a series of t values.

$$St = S_x(1\text{-}2e^{-t/T1}) \qquad (3.2)$$

where S_x is the signal intensity at equilibrium and is propotional to the equilibrium magnetization, T_1 is the relaxation time, and S_t is the signal intensity.

Carbon-13 Overhauser effects (NOE's) for all carbons in a molecule may be determined directly from wide-band proton-decoupled carbon-13 spectra. First, a spectrum is obtained with continuous wide-band proton decoupling. Then a second spectrum is obtained by using pulse-modulated wide-band proton decoupling. The on duty cycle is kept low to prevent buildup of appreciable NOE. In these experiments wide-band decoupled carbon-13 spectra are obtained without nuclear Overhauser effects. NOE's are caculated simply by dividing each individual peak integration in the continuously decoupled spectrum by the analogous peak integration in the spectrum taken with interrupted decoupling.

In this work the tacticities of the polymer samples F1 and F2 were also estimated from carbon-13 inversely gated decoupled spectra recorded using a Bruker AC 300 MHz Fourier transform spectrometer. When recording the peaks due to the methylene and methine carbon absorptions, all other peaks were allowed to off-scale (overflow). All measurements were carried out in glass NMR tubes at 383K in deuterated xylene and the concentration of solution was approximately 5% w/v. The chemical shifts are reported on the δ-scale in ppm with respect to tetramethylsilane. The spin lattice relaxation time (T_1) was found to be 11 seconds. The total number of scans taken were 6256 for polymer sample F1 and 3686 for F2.

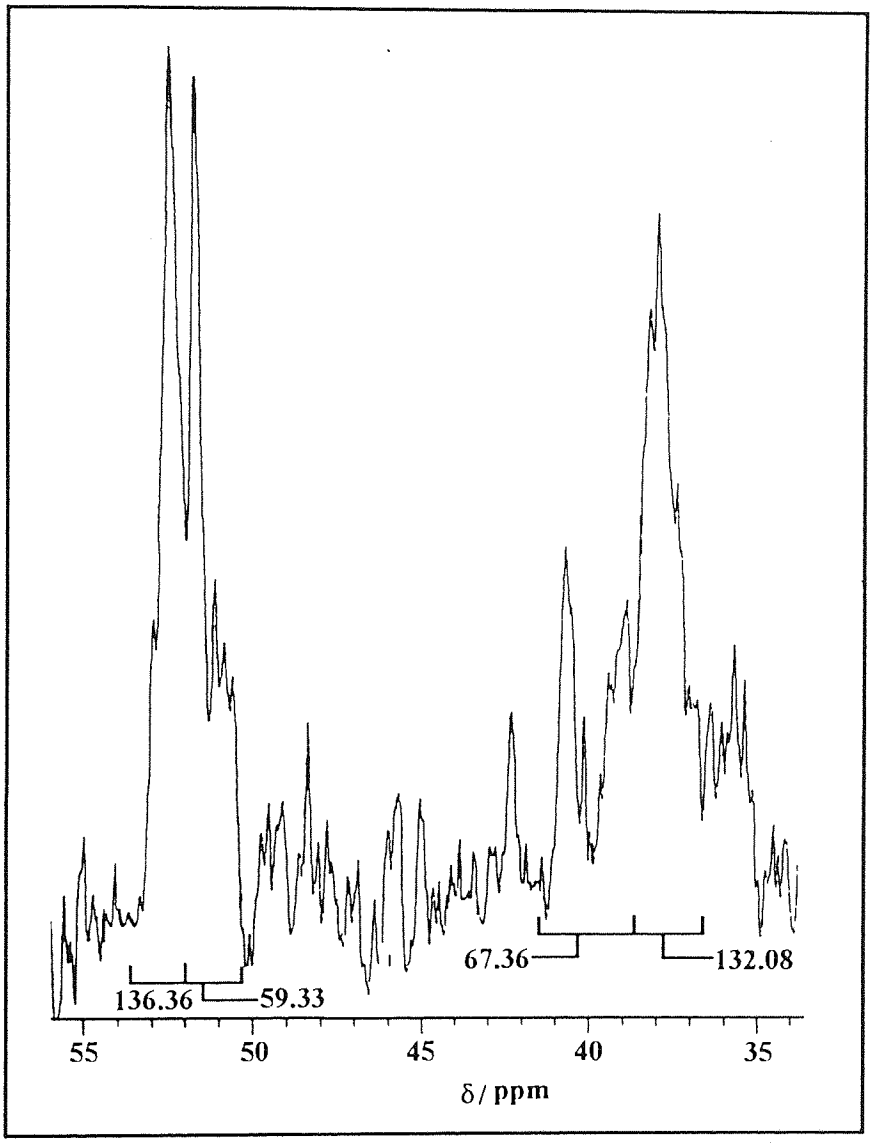

Figure 3.14 Methine and methylene peaks from C-13 inversely gated decoupled N.M.R. spectrum of sample F1 (initiated by AZBN at 343K) in D_{10}-ortho-xylene at 303K. For details of N.M.R. spectrometer settings see Appendix 2.

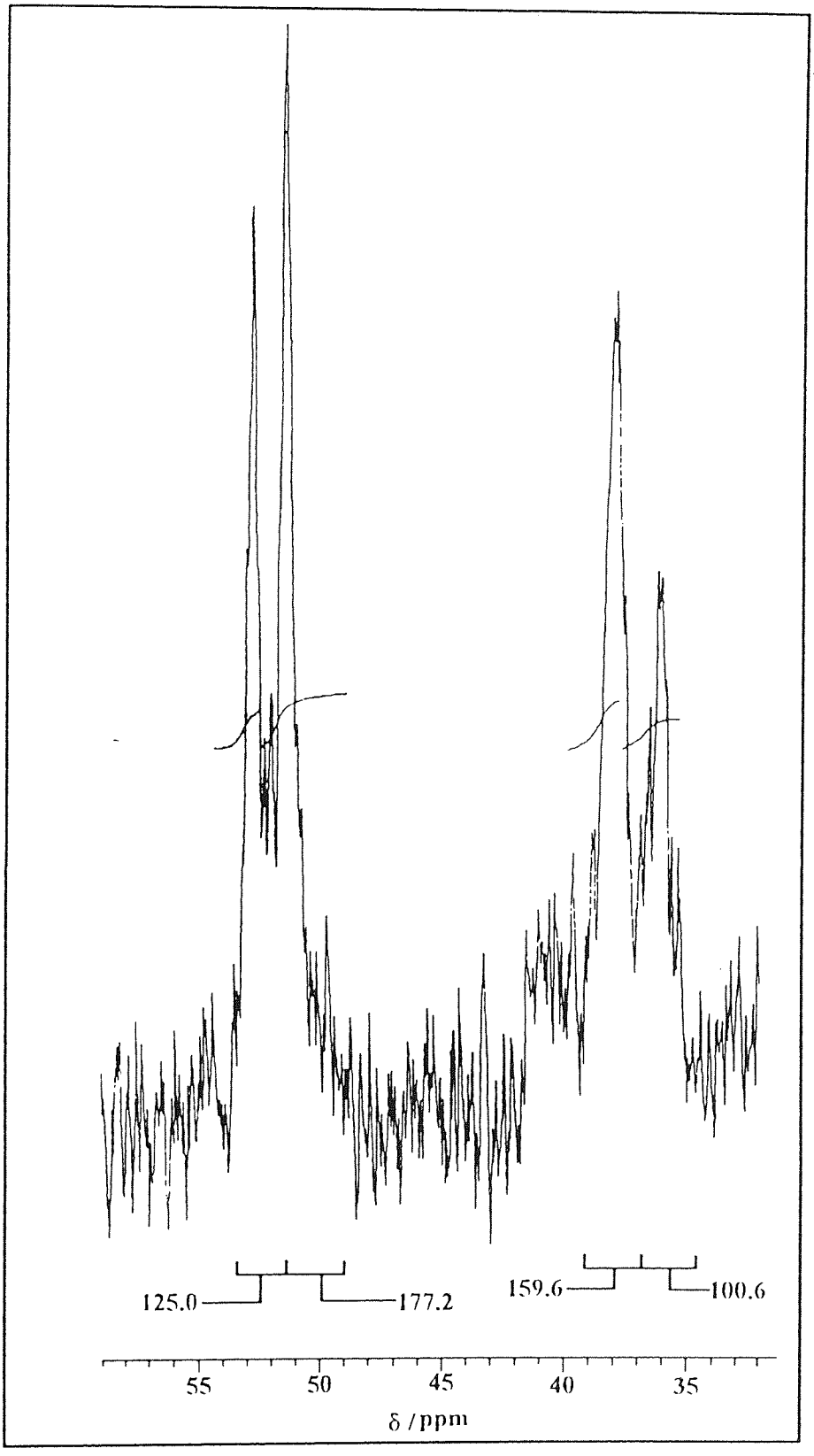

Figure 3.15 Methine and methylene peaks from C-13 inversly gated decoupled N.M.R. spectrum of sample F2 (initiated by BF_3OEt_2 at 298K) in D_{10}-ortho-xylene at 383K. For details of N.M.R. spectrometer settings see Appendix 2.

Figures 3.14 - 3.15 show the methine and methylene peaks from the carbon-13 NMR spectra of polymer samples F1 and F2, respectively. Carbon-13 signals of methine and methylene splits into doublets the one at the higher field is due to methylene whereas low field peaks corresponds to methine. The areas under the peaks are then used to calculate the isotactic content of the polymer samples. The results are listed in the table 3.5.

Sample	Catalyst	% isotacticity (from methine peaks)	% isotacticity (from methylene peaks)
F1	AZBN	30	66
F2	BF_3OEt_2	59	39

Table 3.5 Isotactic content of PVK samples determined by using carbon-13 NMR

The results of proton and carbon-13 NMR yield some interesting results. The isotactic contents determined from the methylene and methine peaks are surprisingly not in agreement with each other. The values obtained from the methylene peaks are rather ambigious because the methylene peak is not sufficiently resolved. However, isotacticity determined from methine peaks are in good agreement with those obtained from proton NMR spectra. For example, for polymer F2, 51% isotactic content was calculated from proton NMR whereas it is 59% from carbon-13. Therefore, it is clear that the polymer prepared using a free radical catalyst (azobisisobutyronitrile) produces highly syndiotactic polymer whereas, a cationic catalyst (boron-trifluoride etherate) produces an isotactic rich polymer.

The characterisation of poly(N-vinylcarbazole) samples by carbon-13 and proton NMR spectroscopy will be correlated later with the dielectric and electro-optical data obtained for these samples.

3.11 Powder X-Ray diffraction

The influence of crystallinity on the electrical properties of polymers has been studied by many workers. Studies by Hatano et al[106] conclude that the higher electrical conductivity in polyacetylene is associated with its crystallinity. The electrical conductivity of polyacrylonitrile pyrolyzate is increased when the polymer is oriented by stretching prior to pyrolysis[107].

An understanding of the photoconductivity properties of PVK and PVK-based material depends upon a knowledge of interactions occuring between the π electron systems of the large pendant groups. The intra and intermolecular π system interactions are in turn dependent on chain tacticity and conformation and on the degree of ordering of the chains. There is, therefore, an interest in the structure of PVK and in the production of crystalline material in which the active groups are in well-defined positions in a three dimensional lattice. Crystallizability is also a tool for determining the degree of stereoregularity in PVK.

Reference to crystallinity in the PVK appeared primarily in the patent literature as early as 1940. Beck and Dorrer[108] in their patent disclosure on a fabrication process for PVK, referred to a pear-like fibrous structure that, while not specified at the time, was apparently the crystalline form. Kimura[109] reported that drawn and thermally treated material exhibited a single crystalline diffraction peak at $2\theta = 8.15'$ or 10.7Å. This was interpreted as the (1010) reflection of a pseudohexagonal lattice with rigid hexagonally packed chains. The chains were said to be composed of stereoblock arrangements of isotactic 3/1 and syndiotactic 2/1 helixes (Figures 3.16 -3.17). Griffiths[104,110] has discussed the influence of molecular weight and temperature on crystallinity. The physical properties of amorphous PVK, other than glass transition, showed little

dependence on the molecular weight. The glass transition was linearly dependent on the reciprocal of the molecular weight, but density measurements indicated no measureable excess free volume associated with the chain ends as pridicted by the Fox-Flory[111] chain and free volume model. The degree of crystallinity decreases with molecular weight in the thermally crystallised polymer. PVK heated above its glass transition temperature crystallizes in the form of folded-chain lamellae. In the case of films on aluminium substrates these lamellae nucleated at the substrate interface and grew normal to this interface. Similar behaviour at polymer interfaces with high energy surfaces has been described by Schonhorn[112].

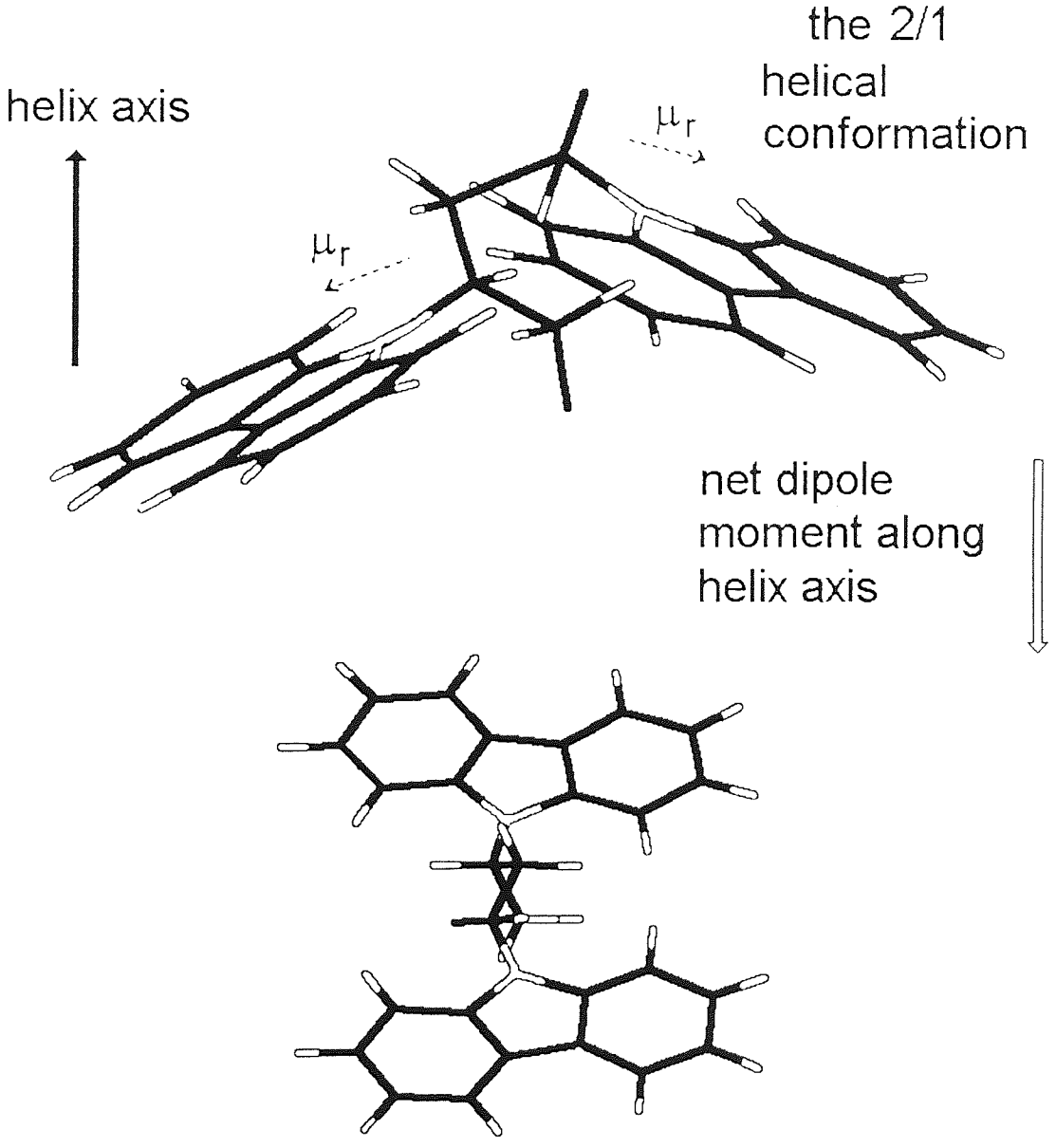

Figure 3.16 Syndiotactic poly(N-vinylcarbazole)

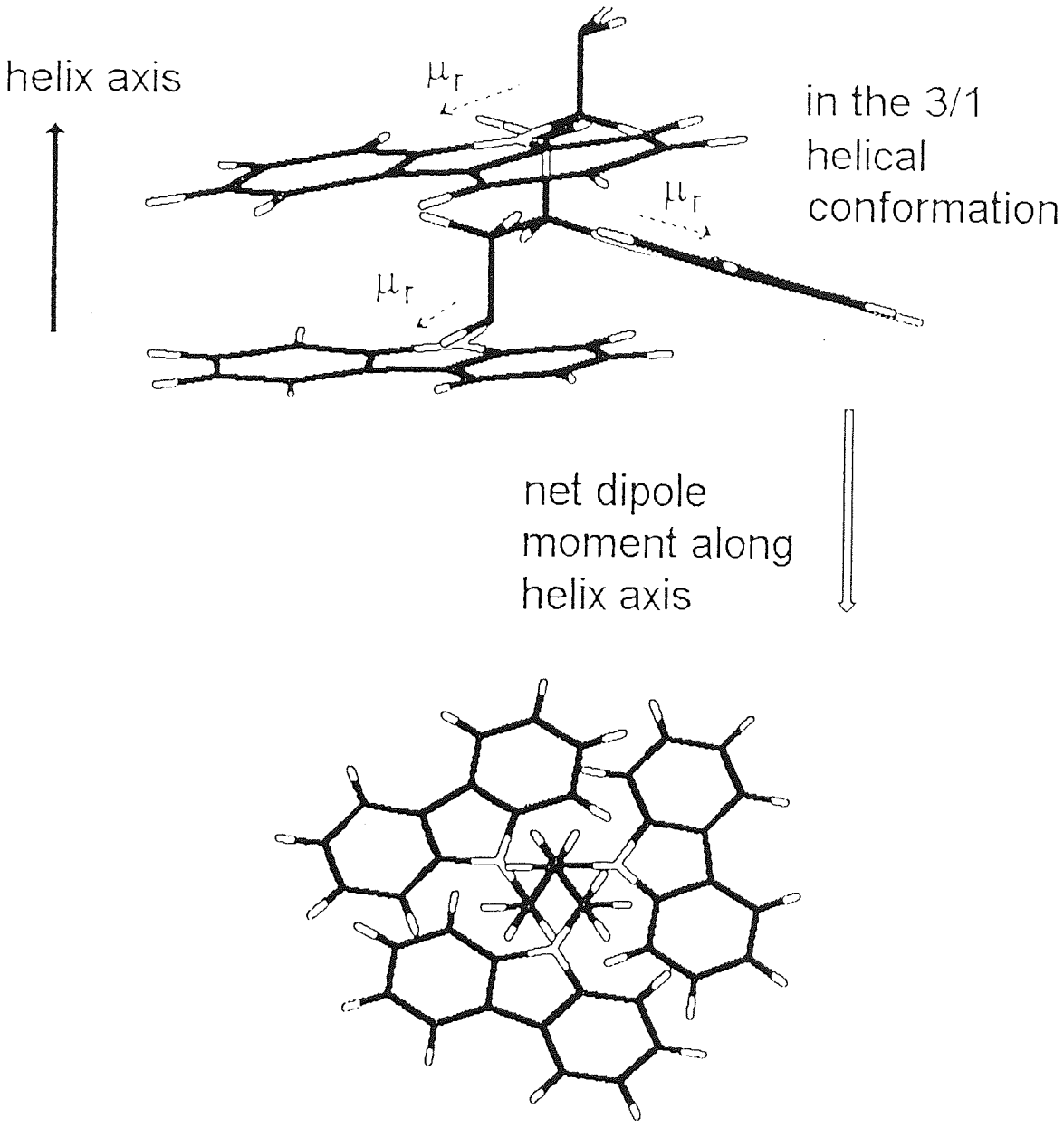

Figure 3.17 Isotactic poly(N-vinylcarbazole)

Powder x-ray diffraction was obtained for polymers F1 - F3 immediately after their preparation and after heat treatment (300°C for 30 minutes under argon) using Philips X-Ray diffractometer model PW 1120. The operating condition of the instrument was 40kV and 20mA, with nickel-filtered copper K_α (λ = 0.1542nm) radiation. The affect of annealing on polymer crystallinity was studied by comparing the intensity of the peaks, before and following heat treatment. The powder x-ray diffraction patterns are shown in Appendix 3. The crystallinity was calculated from the areas of diffracted intensity data in the range 2θ = 4 - 60°, using the method of Fredericks et al [113]. A baseline was drawn on the x-ray diffraction curve. The areas associated with the amorphous and crystalline regions were determined from the trace. The percentage crystallinity was calculated using the following equation :

$$\% \text{ crystallinity} = \frac{A_c}{A_c + A_a} \times 100 \qquad (3.3)$$

Where A_c is the area of the crystalline reflections and A_a is the area of the amorphous scattering.

Polymer sample	2θ (degree)	Intensity (arbitrary units)	d-spacing (Å)	Crystallinity (%)
F1 (pre-anneling)	9.50 15.0 24.0	9 20 24	10.802 6.853 4.302	45
F1 (after annealing)	9.50 17.0 24.0	22 26 28	10.802 6.050 4.302	61
F2 (pre-annealing)	9.50 17.0 24.0	10 18 20	10.802 6.052 4.302	43
F2 (after annealing)	9.50 17.0 24.0	18 20 22	10.802 6.052 4.302	46
F3 (pre-annealing)	9.50 17.0 24.0	9 20 22	10.802 6.050 4.302	43
F3 (after annealing)	9.50 17.0 24.0	22 24 24	10.802 6.052 4.302	50

Table 3.6 Crystallinity of polymer samples prepared using different catalysts

From table 3.6 and Appendix 4, it is clear that PVK shows three peaks which are located at 2θ = 9.5, 17.0 and 24.0 degrees. The crystallinity of untreated samples were surprisingly quite high (approximately 40%) compared with amorphous polystyrene. Increase of crystallinity after heated treatment at 300 °C for 30 minutes, is the greatest for sample F2 i.e. polymer prepared by BF_3OEt_2. The crystallinity of the untreated and

treated samples can be compared easily by measuring the changes in the areas under the peaks, and indeed the largest increase occurs for polymer F2. This result is in good agreement with that reported by Fox-Flory[111]. Thus, from X-ray diffraction studies, it can be concluded that polymers prepared using cationic catalysts have high crystallinity, whereas those prepared using free radical catalysts have lower crystallinity. This appears to support the results from the proton and Carbon-13 nmr spectroscopy that sample F2 (prepared with cationic catalyst), has the greatest isotactic content.

3.12 Conclusions

The polymerisation of polymers proved to be fairly easy and no major problem was encountered in their synthesis and the yields obtained were over ninety percent in every case. Low molecular weight PVK was also successfully prepared by using boron-trifluoride etherate catalyst and ethanol as a chain transfer agent. The analysis of gel permeation chromatographs of these polymers showed that the molecular weights of the polymers are directly related to the concentration of the chain transfer agent. As the level of ethanol in the reaction increases the molecular weight of the polymer also increases. This is because more active species i.e. $H^+[BF_3OH]^-$ are produced as the concentration of the chain transfer increases.

The results obtained from ^1H and ^{13}C nuclear magnetic resonance spectroscopy of polymers indicate that the cationically catalysed polymerisation produces polymer that has a higher isotactic level than polymers prepared by the free radical polymerisation. A polymer with an average isotacticity of 55% was produced with boron-trifluoride etherate as a catalyst, whereas, only 27% isotacticity was obtained using the catalyst azo-bisisobutyronitrile.

The X-ray diffraction trace of Poly(N-vinylcarbazole) shows three peaks which are located at $2\theta = 9.5$, 17.0 and 24.0 degrees. The increase in crystallinity, when PVK is heated at 300°C for 30 minutes, is greatest for sample F2, i.e. polymer prepared by BF_3OEt_2. This result is in good agreement with that reported by Fox and Flory[111]. Thus, from X-ray diffraction studies, it can be concluded that polymers prepared using cationic catalysts have high crystallinity, whereas those prepared using free radical catalysts have lower crystallinity. This appears to support the results from the ^1H and ^{13}C NMR which indicate that the sample F2 has the greatest percentage isotacticity.

The comparative study of the molecular weights of the polymers using gel permeation chromatography (gpc) and static light scattering techniques (SLS) clearly indicates that the results are very different. The molecular weights obtained from the light scattering are much larger than those obtained from gel permeation technique. The SLS technique gives an absolute molecular weight measurement and not a polystyrene equivalent. Also, in the gpc method some high molecular weight fractions were excluded from the gpc columns. This may well account for a large difference in the molecular weights determined by these two methods. The SLS data show two important features. The first concerns the differences in the radii of gyration of polymers prepared using different catalysts. PVK polymer that is prepared cationically has a bigger radius of gyration (relative to its radically produced counterpart), indicating a more extended and perhaps more rigid polymer. This observation is in line with the results obtained from the ^1H NMR and X-ray diffraction. Secondly, the preliminary results of the effect of solvents on conformations appear to indicate that the solvent has very little effect on the radii of gyration when the same polymer is in solution in either a good or a poor solvent. However, it was indicated above that the method used to analyse SLS data may be ambigious since it makes an assumption that the polymer behaves in a Gaussian manner (see above) and it was concluded that it was unlikely that PVK was following Gaussian statistics.

CHAPTER FOUR

The Temperature Dependence of Static Dielectric Permittivity and Dipole Moments of Poly(N-vinylcarbazole)

4.1 Introduction

A great deal of interest has been shown in the photo-induced electrical conductivity of bulk poly(N-vinylcarbazole) (PVK) and PVK systems doped with a variety of electron accepter molecules, such as 2,4,7-trinitro-9-flourenon (TNF) (see chapter 1). Since PVK possesses a chiral centre in its repeat unit an important question arises concerning the effect of tacticity on its various electrical and photo-conductive properties. In the previous chapter it was shown that the synthetic route used to prepare poly(N-vinylcarbazole) has a marked effect on its stereoregularity and crystallinity. Thus, radical based polymerisations are believed to lead to an increased racemic content while cationic systems result in the production of polymers possessing higher isotactic contents. However, it is recognised that the interpretation of proton and carbon-13 NMR spectra is not completely unambiguous. Thus, additional complementary experimental data on these materials, using techniques sensitive to their conformations, are essential if meaningful correlations are to be made between their physical properties and the tacticity of polymer samples.

The dielectric permittivity and dipole moment is a popular method, for characterising the conformations of polymer molecules since the experimentation is not too demanding (cf Kerr effect) and the interpretation of the results is often straight-forward. Debye and Bueche[114] have shown that a comparison of the dipole moment of a polymeric molecule to that of one of its structural units can yield information concerning the average chain

configuration. A variety of polymer types have been successfully studied using this technique. Therefore, along with the Kerr effect (Chapter 6) the determination of dipole moments makes an ideal complementary tool for the study of the average configurational structures of PVK in this investigation.

The Debye-Guggenheim equation (see Chapter 2) can only be used to determine the dipole moment of polar molecules in the vapour phase. However, if the molecules are sufficiently seperated from one another by nonpolar molecules that reduce the interaction among their permanant dipole moments, it can be argued that much a system would resemble the dielectric behaviour of a gaseous phase. This approach is used to determine the dipole moments of long molecular chains. It should be stressed that whereas simple molecules have permanent dipole moments similar for all of them, long flexible molecules are continuously changing their spatial conformation, and because the dipole moment associated with each conformation is generally different, the dipole moments that are measured are necessarily average values. For very dilute solutions, the intermolecular interactions between solute molecules can be assumed to be negligble. Hence, all the dipole moments are calculated by using dielectric data obtained from dilute polymer solutions, generally in the concentration range 0.25% - 2.0% w/v.

The measurement of static dielectric permittivity and the electro-optic Kerr effect form an important part of this thesis. The apparatus and techniques employed to facilitate the measurement of dielectric permittivity are described in this chapter. Previous studies of the dielectic properties of PVK have focused either on dielectric relaxation or have been performed on poorly characterised polymer samples[115-120]. Mumby and Beevers[121] have correlated dipole moment and electro-optic Kerr effect with the tacticity of PVK polymers. They concluded that as the isotacticity of the polymer increases the dipole moment and Kerr effect both increase. It was also shown that the dipole moment and Kerr

effect is independent of the molecular weight of the polymers. In this work an attempt is made to further extend this area of research by studying the influence of temperature on the dielectric permittivity, dipole moment and molecular Kerr effect of PVK produced using various catalyst systems (for the synthesis of PVK refer to section 3.5). The results will be interpreted in terms of tacticity and conformations of these polymers. The Debye-Guggenheim equation (see section 4.2) is very useful for calculating approximate values of molecular dipole moment from the dielectric constants and densities of dilute solutions of polar molecules in nonpolar solvents. The solvent 1,4-dioxane was chosen as an acceptable medium in which all the dielectric permittivity measurements on various streostructural forms of PVK were carried out. The dipole moments were also measured in toluene which is believed to be a "good" solvent for PVK. It is believed that PVK consists of rigid rod-like structures consisting of 2/1 and 3/1 helixes[104,110].Therefore, toluene would be expected to unwind and open up the helices, more than 1,4-dioxane. This provides an opportunity to measure and compare the temperature coefficients of dipole moments with those obtained in 1,4-dioxane (poor solvent for PVK). This approach would help to avoid any ambiguities arising from solvent affects at higher temperatures.

4.2 Dielectric measurements

All dielectric measurements were performed using a Genrad 1689 RCL Bridge operating at a chosen, fixed frequency of 1kHz. The dielectric cell (manufacturer unknown) comprised two cylindrical blocks of brass (figure 4.1). The external surfaces were nickel plated and the internal surfaces in contact with the sample were gold plated. The outer cylinder (A) was hollow to allow passage of a coolant liquid. The cell was fitted with an external screw-top lid (B) through which the cell could be filled. An inner chamber (C) ensured that the effective sample volume of the dielectric cell was reproducibly constant and independent of actual volume (approximately $20cm^3$) provided that the liquid level was

above the internal lid. The height and diameter of the inner cylindrical electrode (D) were 35mm and 33mm respectively. The electrode gap was approximately 1.5mm. The temperature of the cell could be controlled to better than +/- 0.1 ^{o}C. The instrument was calibrated at every working temperature with air (ε_o=1.000) and using liquids with well-known dielectric constants (toluene and cyclohexane). Capacitances of the solutions of F1, F2, F3 and the model compound N-ethylcarbazole were measured at temperatures in range of 288K to 338K and dielectric increments of the solutions were calculated using equation 4.1.

$$\varepsilon_{solution} = \frac{(C_{solution}(1-\varepsilon_{solvent})) - (C_{solvent} - (\varepsilon_{solvent} \times C_{air}))}{C_{air}(1-\varepsilon_{solvent}) - (C_{solvent} - (\varepsilon_{solvent} \times C_{air}))} \qquad (4.1)$$

Where C = capacitance and ε = dielectric permittivity of the materials shown.

Mean-square dipole moments (in Debyes) per repeat unit of the polymer chain were calculated using an appropriate form of the Guggenheim-Debye Equation. viz,

$$\langle\mu^2\rangle = \frac{27kT}{4\pi N_L(\varepsilon_1 + 2)(n_1^2 + 2)} (\Delta/C)_{c->o} \qquad (4.2)$$

where ε_1 is the dielectric permittivity of solvent, ε_{12} is the dielectric permittivity of polymer solution, n_1 is the refractive index of solvent, $\Delta = [\varepsilon_{12}-(n_{12})^2] - [\varepsilon_1 - (n_1)^2]$, and $(\Delta/C)_{c->o}$ is the limiting gradient of the plot of Δ versus concentration.

The refractive index of 1,4-dioxane was measured at 632.8nm over the temperature range 288K - 338K. Since the polymers were dissolved in this solvent at very low concentration (0.25% - 2.0% w/v) it was assumed that the solution refractive index would be equal to that of the solvent.

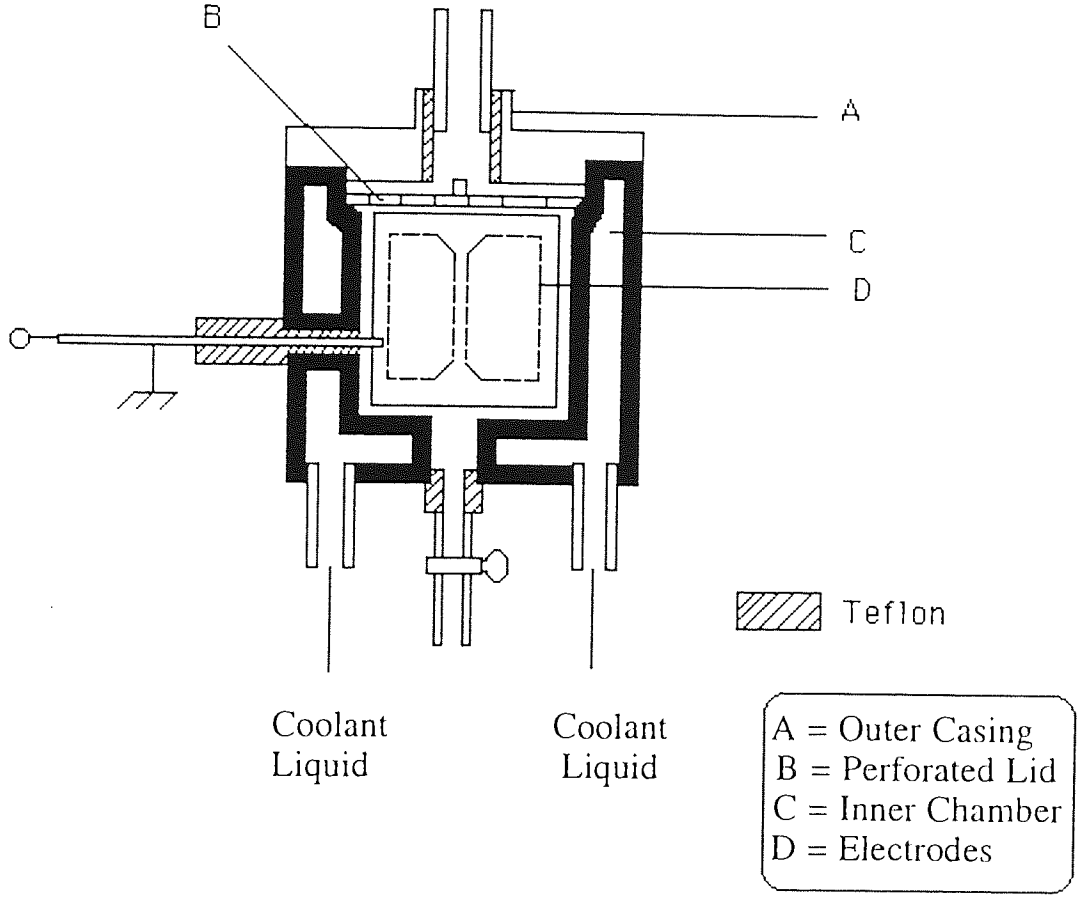

Figure 4.1 Dielectric Cell

4.3 Measurement of the temperature dependence of the dielectric permittivity of 1,4-dioxane and toluene

From an examination of equation 4.2, it can be seen that it is essential to know the dielectric permittivity and refractive index of of solvents used to prepare solutions of the polymers. Therefore, these parameters were determined by using the Genrad 1689 RCL Bridge, dielectric cell and refractometer (ABBE '60'), respectively. The solvents used were HPLC grade and were used as supplied. The results obtained are tabulated in tables 4.1 and 4.2. Graphical representations of these results are shown in figures 4.2 and 4.3. It is clear from the graphs that the plots are linear and that their slopes may be used to calculate the temperature coefficients for dielectric permittivity and for refractive index.

Temperature / K	Dielectric Permittivity of 1,4-dioxane *frequency* = 1kHz	Dielectric Permittivity of toluene *frequency* = 1kHz
288	2.229 +/- 0.011	2.409 +/- 0.012
298	2.226 +/- 0.011	2.379 +/- 0.012
308	2.219 +/- 0.011	2.367 +/- 0.012
318	2.188 +/- 0.011	2.330 +/- 0.012
328	2.170 +/- 0.011	2.306 +/- 0.012
338	2.150 +/- 0.011	2.282 +/- 0.011

Table 4.1 The Static Dielectric Permittivity of 1,4-dioxane and toluene

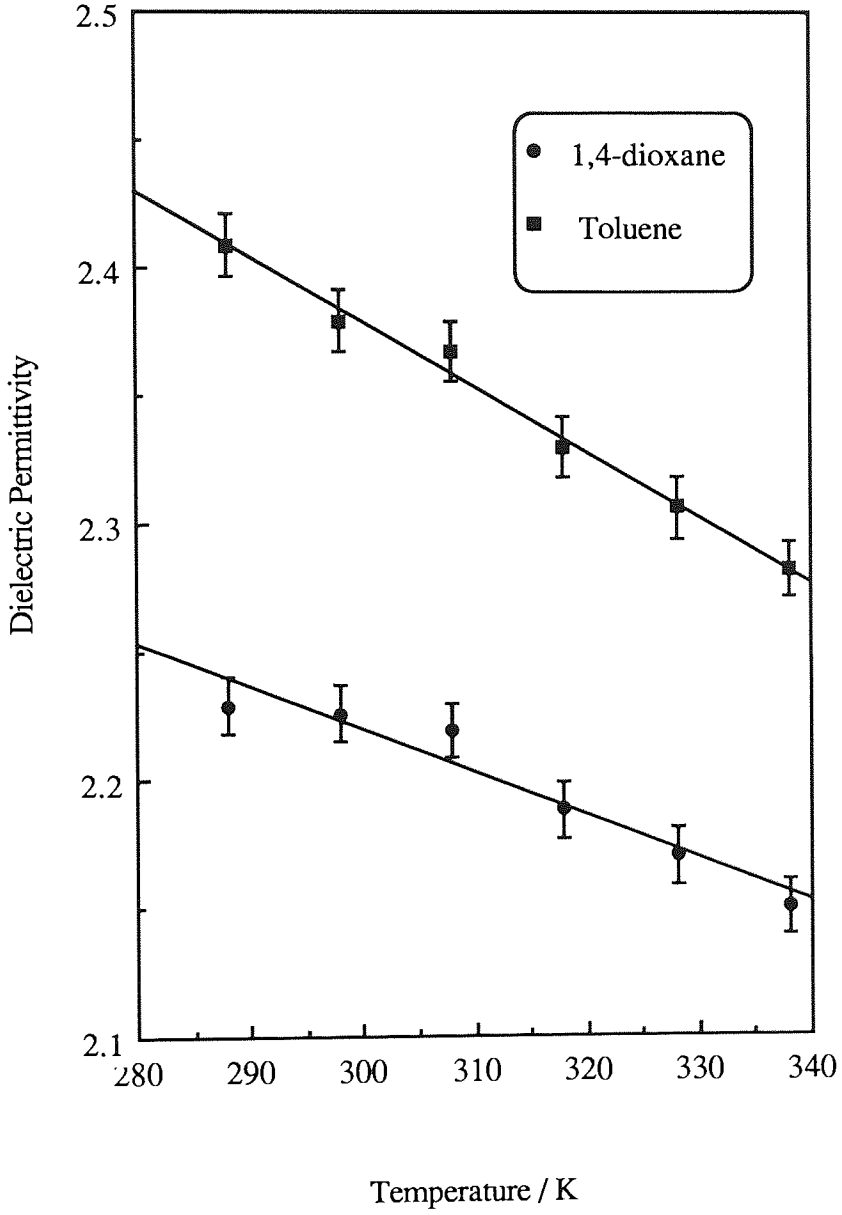

Figure 4.2 The Static Dielectric Permittivity of 1,4-dioxane and toluene

4.4 The temperature coefficients of the refractive index of 1,4-dioxane and toluene

The refractive indices of 1,4-dioxane and toluene were measured over the temperature range of 298 - 338K using an ABBE '60' Refractometer. The instrument employs the critical angle effect marked by a demarcation line between light and dark portions of the telescope field, this demarcation line generally being known as the borderline. A few drops of sample under test are placed on the prism. The laser beam (wavelength = 632.8nm) strikes the prism and then falls on a mirror where it is reflected into the field telescope of the instrument. The position of the mirror required to bring the borderline into coincidence with the telescope cross-wires is indicated by a moving scale observed in the scale telescope. This scale is a direct function of the refractive index.

Temperature (K)	Refractive Index of 1,4-dioxane (λ = 632.8nm)	Refractive Index of toluene (λ = 632.8nm)
288	1.443 +/- 0.001	1.493 +/- 0.001
298	1.420 +/- 0.001	1.488 +/- 0.001
308	1.416 +/- 0.001	1.483 +/- 0.001
318	1.412 +/- 0.001	1.478 +/- 0.001
328	1.408 +/- 0.001	1.472 +/- 0.001
338	1.403 +/- 0.001	1.467 +/- 0.001

Table 4.2 Refractive Index of 1,4-dioxane and toluene

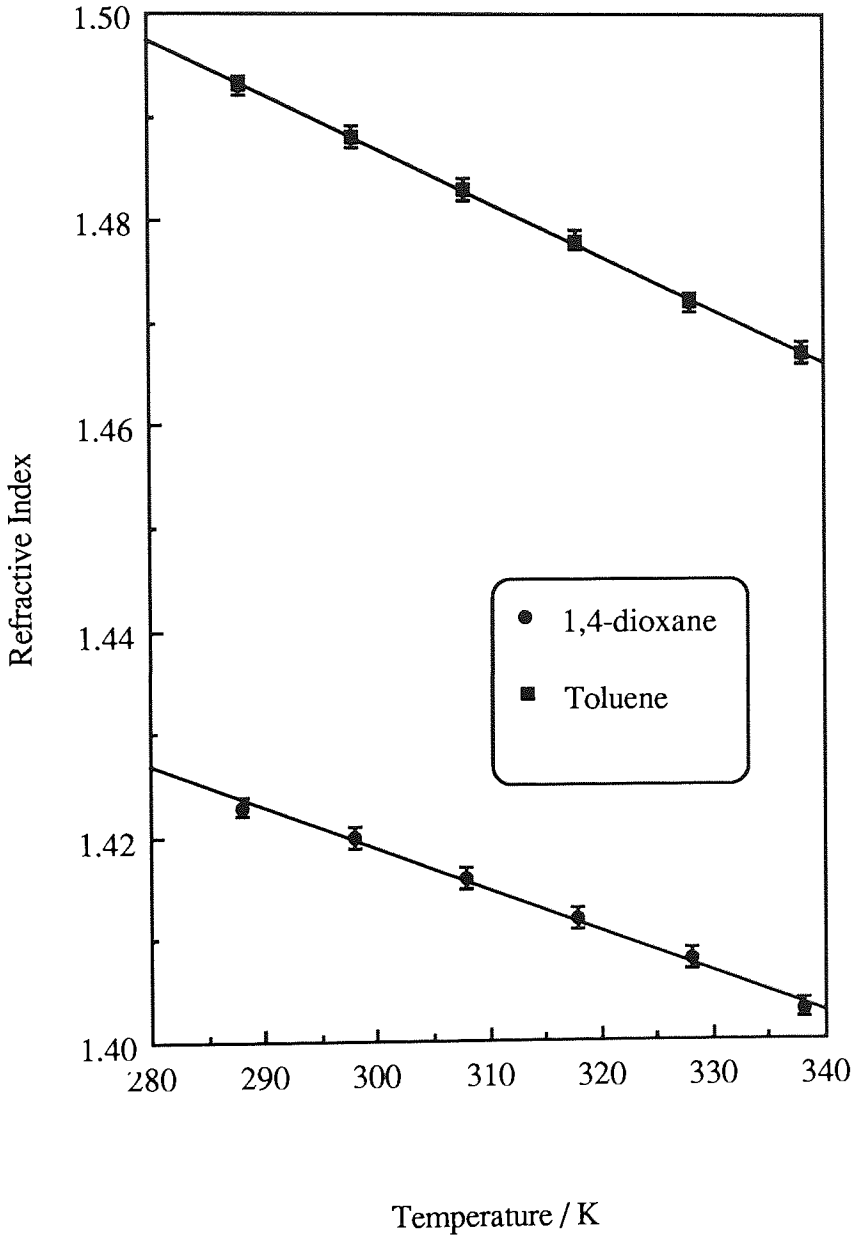

Figure 4.3 Refractive Index of 1,4-dioxane and toluene

4.5 Measurement of the static dielectric permittivity and determination of the dipole moments of PVK and N-ethylcarbazole in 1,4-dioxane

A major objective was to determine the dipole moments of the PVK samples F1, F2, F3 and the model compound N-ethylcarbazole in solutions of 1,4-dioxane in order to investigate the conformations and tacticities of the polymers. In addition, the tacticities were also measured using proton and carbon-13 NMR (see Chapter 3). It is believed that PVK consists of rigid rod-like structure consisting of 2/1 and 3/1 helixes[104,110], the dipole moments were also measured in toluene which is a "good" solvent for PVK. Therefore, toluene would be expected to unwind and open up the helices, more than 1,4-dioxane. This provides an opportunity to measure and compare the temperature coefficients of dipole moments with those obtained in 1,4-dioxane (poor solvent for PVK). This approach would help to avoid any ambiguities arising from the solvent affects at higher temperatures. In order to study this fully, it was decided to carry out temperature studies by measuring the static dielectric permittivities at several different temperatures between 288 and 338 K.

The electrical capacitance of a dielectric cell was measured when empty and when filled with polymer solutions at five different concentration levels (0.25%, 0.5%, 1.0%, 1.5%, 2.0% w/v). The static dielectric permittivities and refractive indices of 1,4-dioxane and toluene at 288, 298, 308, 318, 328, 338K were determined (section 4.3 and 4.4, respectively). The graphs of dielectric permittivities ($\varepsilon_{12} - \varepsilon_1$) against concentration (c) of repeat units per cm^3 i.e weight of polymer per cm^3 divided by 194 (the relative molecular mass of the repeat unit) yielded a straight line, and the gradients were substituted into the Guggenheim rearrangement[81] (equation 4.2) of the Debye equation, in order to calculate the average repeat unit dipole moments of the polymers.

Conc. x (10^{-4}) mol cm^{-3}	ε_{12}					
	288K	298K	308K	318K	328K	338K
F1						
0.13	2.248	2.243	2.235	2.022	2.184	2.163
0.26	2.255	2.252	2.243	2.212	2.193	2.172
0.52	2.259	2.255	2.247	2.215	2.192	2.173
0.78	2.272	2.265	2.257	2.225	2.203	2.184
1.04	2.284	2.279	2.271	2.237	2.218	2.196
F2						
0.13	2.259	2.255	2.248	2.215	2.194	2.174
0.26	2.275	2.274	2.265	2.230	2.210	2.188
0.52	2.321	2.316	2.307	2.269	2.249	2.226
0.78	2.358	2.350	2.338	2.300	2.278	2.253
1.04	2.366	2.357	2.348	2.310	2.288	2.262
F3						
0.13	2.220	2.218	2.211	2.181	2.162	2.143
0.26	2.227	2.225	2.217	2.186	2.167	2.147
0.52	2.249	2.245	2.237	2.205	2.186	2.165
0.78	2.274	2.272	2.263	2.230	2.210	2.189
1.04	2.295	2.292	2.284	2.252	2.232	2.209
NEK						
0.13	2.250	2.245	2.236	2.199	2.179	2.158
0.26	2.285	2.276	2.266	2.227	2.205	2.181
0.52	2.314	2.302	2.294	2.253	2.228	2.206
0.78	2.348	2.336	2.325	2.283	2.257	2.233
1.04	2.373	2.360	2.349	2.305	2.282	2.256

NEK = N-ethylcarbazole

Table 4.3 The static dielectric permittivities of the PVK polymers and the model compound all determined in solution in 1,4-dioxane.

At first glance these results look fairly similar in magnitude. The differences due to tacticity and polymer conformations are easier to observe when $(\Delta/C)_{->0}$ is plotted against polymer concentration (mol cm^{-3}). Table 4.4 lists the gradients determined from graphs of ε_{12} versus concentration. Plots of $(\Delta/C)_{->0}$ against temperature are presented in figure 4.4.

Temperature /K	(Δ/C) / cm^3 mol^{-1}			
	F1	F2	F3	NEK
288	374	1260	844	601
298	362	1184	839	561
308	365	1153	822	554
318	356	1099	802	518
328	333	1082	787	499
338	335	1022	753	484

Table 4.4 Gradients (Δ/C) (see equation 4.2) of dielectric permittivity ($\varepsilon_{12} - \varepsilon_1$) against concentration for PVK and NEK in solution in 1,4-dioxane.

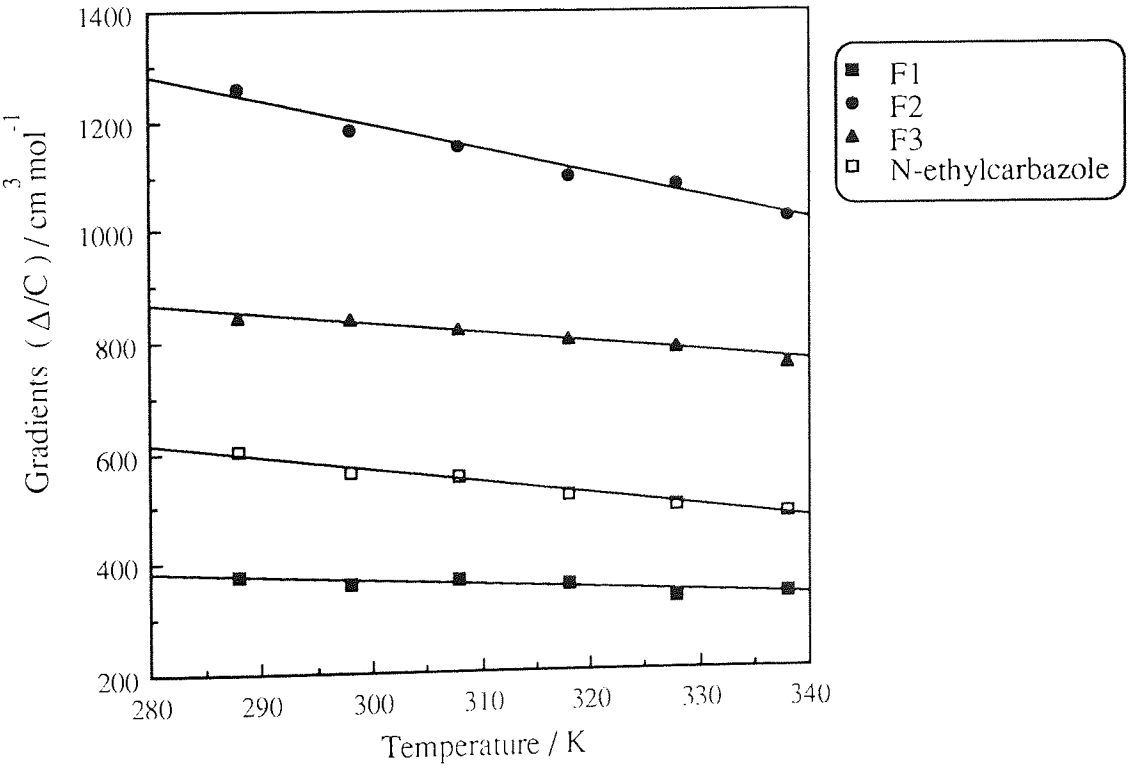

Figure 4.4 Temperature dependence of dielectric permittivity of various stereostructural forms of PVK in solution in 1,4-dioxane

From table 4.4 and figure 4.4 it is evident that all polymers have negative temperature coefficients, that is, as the temperature rises the dielectric permittivity drops. Thus, it is concluded that the dielectric permittivity is significantly affected by the temperature and that this is related to the degree of tacticity of the polymers. The dielectric permittivity of solutions of the polymers increases with an increase of the isotactic content of polymer. The higher static dielectric permittivities of polymer F2 are correlated to the higher % isotacticity of this polymer (as deduced by proton and carbon-13 NMR spectroscopy). Therefore, F3 with an isotactic content lower than that of F2, would be expected to exhibit gradients lower than those of F2, but higher than F1, and this is found to be the case.

By subsituting values of $(\Delta/C)_{c->0}$ into the Guggenheim-Debye equation (equation 4.2) the average dipole moment per repeat unit of the polymers and that of N-ethylcarbazole can be found. The results of these calculations are presented in Table 4.5 and figure 4.5.

Temperature /K	$10^{18} <\mu>$ / **esu**			
	F1	**F2**	**F3**	**NEK**
288	1.764	3.236	2.644	2.235
298	1.768	3.200	2.694	2.202
308	1.810	3.216	2.716	2.230
318	1.825	3.208	2.741	2.202
328	1.799	3.245	2.766	2.203
338	1.840	3.214	2.758	2.212

esu = electrostatic units

Table 4.5 The temperature dependence of dipole moments of various stereoregular forms of PVK in 1,4-dioxane

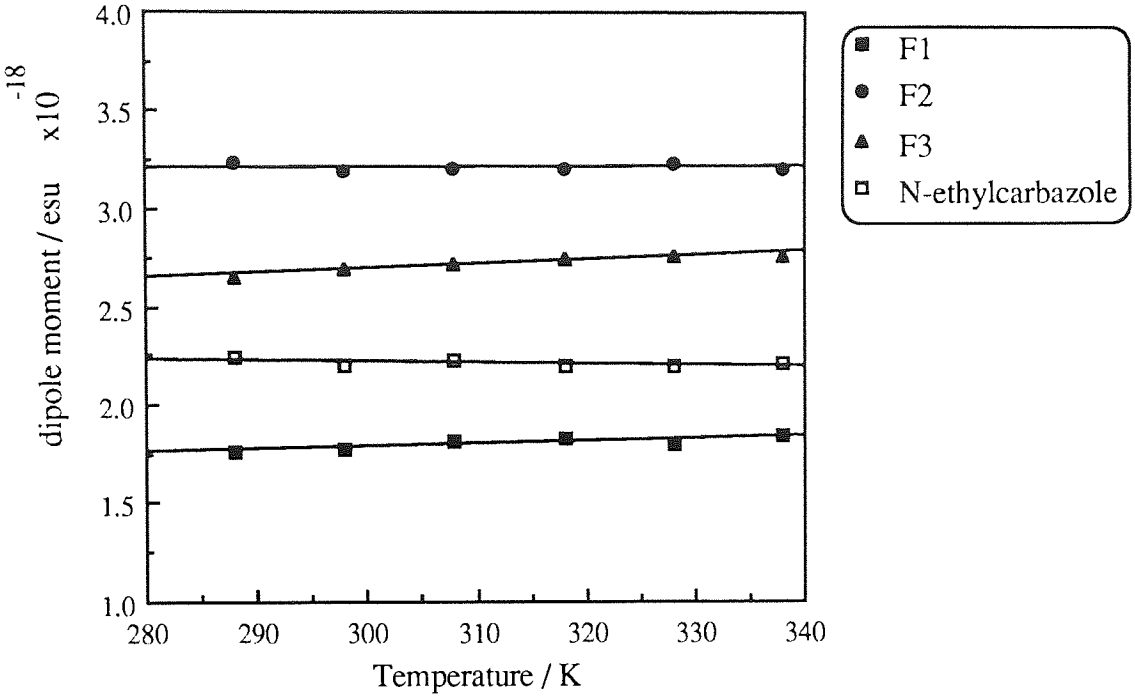

Figure 4.5 Variation with temperature of the dipole moment of samples F1, F2, F3 and N-ethylcarbazole determined in 1,4-dioxane.

The temperature coefficient of the dipole moments is defined experimentally as the quantity

$$\frac{d(\ln\langle\mu^2\rangle)}{dT} \qquad (4.3)$$

Temperature /K	ln ($\langle\mu^2/10^{-36}\rangle$)			
	F1	F2	F3	NEK
288	1.135+/-0.017	2.348+/-0.035	1.948+/-0.029	1.608+/-0.024
298	1.140+/-0.017	2.326+/-0.035	1.982+/-0.030	1.579+/-0.024
308	1.186+/-0.017	2.336+/-0.035	1.998+/-0.030	1.604+/-0.024
318	1.203+/-0.018	2.331+/-0.035	2.017+/-0.030	1.579+/-0.024
328	1.174+/-0.018	2.354+/-0.035	2.035+/-0.031	1.579+/-0.024
338	1.219+/-0.018	2.335+/-0.035	2.029+/-0.031	1.588+/-0.024

Table 4.6 The temperature dependence of dipole moments of various stereoregular forms of PVK in 1,4-dioxane.

Graphs of ln μ^2 versus temperature are presented in Figure 4.6. Calculations were carried out using a linear regression program to provide the gradients of the plots and associated errors.

Samples in 1,4-dioxane	$10^3(\ln\langle\mu^2\rangle)/dT)$ /K	Error (10^{-3})
F1	1.7	+/- 0.5
F2	0.2	+/- 0.2
F3	1.8	+/- 0.4
NEK	-0.2	+/- 0.3

Table 4.7 Temperature coefficients of dipole moments of various PVK polymers and the model compound NEK measured in solution in 1,4-dioxane

The plots in figure 4.6 reflect the temperature dependence of the conformations of the polymer samples and the temperature independent behaviour of the model compound. The plots show three interesting features, which are:

(i) Sample F1 with the least isotactic content shows smallest average dipole moment per repeat unit but the largest positive temperature coefficient.

(ii) The polymer with the most largest isotactic content, F2, has the largest average dipole moment per repeat unit but the lowest temperature coefficient.

(iii) The model compound, N-ethylcarbazole has a temperature coefficient close to zero.

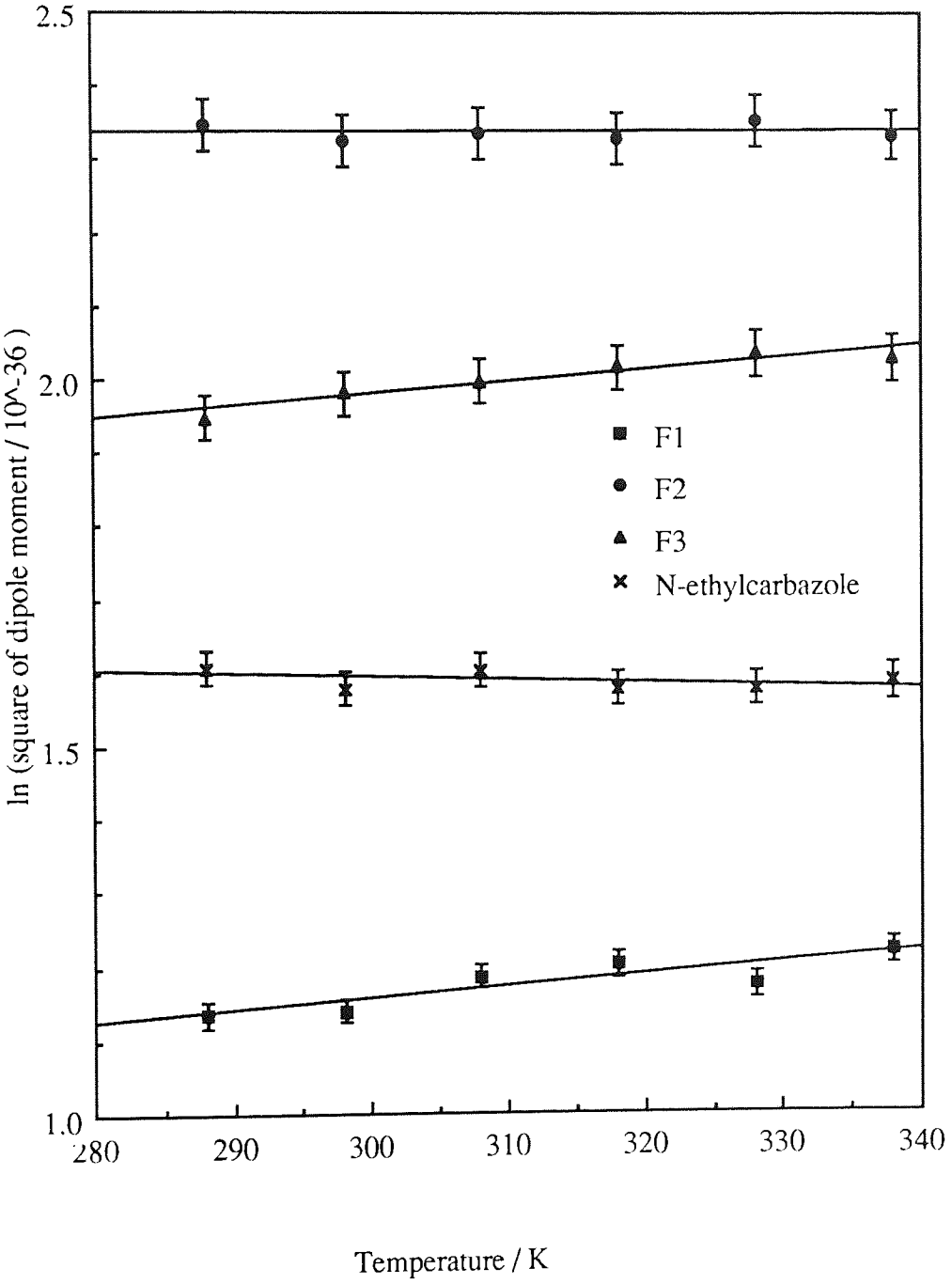

Figure 4.6 Temperature coefficients of dipole moment in 1,4-dioxane of stereoregular PVK prepared with different catalysts

These observations are discussed in detail below:

(i) The polymers F1 and F3 (synthesised by using AZBN and $AlCl_3$ catalysts respectively), possess mainly syndiotactic stereostructures with the possibility of forming 2/1 helixes (see Chapter 3) that are not as sterically hindered as the 3/1 helixes believed to be formed in isotactic rich F2. At low temperatures, the chains are very much restricted in their movement, and hence tend to occupy a helical conformation. This conformation results in the cancellation of dipole moments. As the temperature increases, there is more thermal energy and hence a greater degree of freedom of the pendent groups and as a consequence this results in the formation of non helical structures. This change in the proportion of helical structures leads to decrease in the cancellation of their dipole moments of the repeat units.

(ii) It is clear that polymer type F2, prepared by using boron-trifluoride etherate catalysts, shows the largest degree of isotacticity, has the smallest positive temperature coefficient and the largest dipole moment per repeat unit compared to types F1 and F3. From the literature survey it is believed that the isotactic PVK consist of 3/1 helixes and that the polymer chains are fairly rigid. At low temperatures, the chains are very much restricted in their movement, and hence maintain their basic helical conformation. Generally, in a 3/1 helical conformation the cancellation of dipole moments is not as complete as that occuring in 2/1 helixes (where the pendent groups are almost trans to each other). As a result, the average dipole moment per repeat unit is higher than that observed for the 2/1 helixes. In addition, polymers with 3/1 helical chains are so sterically hindered that they are less affected by the heat and tend to retain their configurations and as a consequence the temperature coefficient of the dipole moment is lower than that found for syndiotactic rich samples of PVK.

(iii) N-ethylcarbazole, the model compound, may be regarded approximately as a single rigid repeat unit of PVK. There will of course be no increase in the dipole moment of the N-ethylcarbazole as the temperature increases. The slightly negative temperature coefficient found for the dipole moment is possibly due to the thermal expansion of the polymer solution in the dielectric cell over the experimental temperature range. A further discussion of this effect is found in section 4.6.

It is interesting to note that sample F2 has a average dipole moment per repeat unit that is larger than that of 9-ethylcarbazole, whereas samples F1 and F3 have smaller values. This is because it is impossible to measure dipole moments directly. The equipment used in the experiment measures the sum of the squares of the dipole moments and when the square root is taken it is not the same as summing up of all the dipole moment values and averaging them. The square root turns out to be either higher or lower then the average value depending on how much one repeat unit cancels the dipole moment of another intramolecular repeat unit. Consequently, in this study, it was found that the highly isotactic polymers had higher dipole moments than the syndiotactic polymers. The temperature coefficient for polymer F1 ($0.0017K^{-1}$) compares well with the results obtained by Riande et al [122] ($0.0021K^{-1}$) measured under similar conditions and procedures. As far as the auther is aware the temperature coefficients of the dipole moments of PVK polymers with different tacticities have not been published by these or any other workers. Therefore, it is impossible to compare the temperature coefficients with those of other PVK samples. However, from the information available, the values of temperature coefficients of polymer F1 obtained in our work compare extremely well with those obtained by Riande et al, hence, it is fair to conclude that our method for the determination of dipole moments is reasonably reliable.

4.6 Measurement of the static dielectric permittivity and determination of dipole moments of poly(N-vinylcarbazole) and N-ethylcarbazole in toluene

In section 4.5 it was concluded that the average dipole moment per repeat unit of PVK polymers determined in 1,4-dioxane depends on the tacticity of the polymers, and that all polymers have positive temperature coefficients . There appears to be an increase in dipole moments as the isotacticity of the polymers increases, but temperature coefficients of dipole moments are smaller than those found for the less isotactic polymers. Hence, polymers prepared with a free-radical catalyst (producing the lowest percentage tacticity) have the highest temperature coefficient but the lowest dipole moments.

An interesting study can be carried out if the temperature coefficients of dipole moments were measured in a solvent that is considered to be better than 1,4-dioxane. Toluene was, therefore, chosen as a solvent to measure the dipole moments of PVK samples F1, F2, F3 and model compound, N-ethylcarbazole. The solutions (concentration 0.25% - 2.0% w/v) of different PVK samples and N-ethylcarbazole were prepared in toluene and dipole moments determined in the temperature range of 288 - 338K using the method described previously in section 4.5.

Conc. x(10^{-4}) mol cm^{-3}	ε_{12}					
	288K	298K	308K	318K	328K	338K
F1						
0.13	2.423	2.380	2.373	2.334	2.312	2.281
0.26	2.421	2.382	2.382	2.332	2.313	2.290
0.52	2.431	2.391	2.393	2.335	2.320	2.302
0.78	2.442	2.403	2.404	2.364	2.353	2.343
1.04	2.463	2.421	2.404	2.373	2.341	2.332
F2						
0.13	2.420	2.392	2.371	2.342	2.313	2.303
0.26	2.432	2.391	2.370	2.350	2.325	2.301
0.52	2.452	2.412	2.402	2.362	2.343	2.312
0.78	2.461	2.443	2.412	2.384	2.371	2.342
1.04	2.493	2.450	2.430	2.402	2.390	2.364
F3						
0.13	2.423	2.334	2.374	2.334	2.312	2.291
0.26	2.431	2.392	2.382	2.341	2.311	2.293
0.52	2.442	2.412	2.392	2.353	2.342	2.324
0.78	2.462	2.420	2.410	2.384	2.351	2.331
1.04	2.480	2.442	2.432	2.391	2.374	2.342
NEK*						
0.13	2.410	2.381	2.373	2.332	2.312	2.280
0.26	2.423	2.392	2.383	2.330	2.293	2.282
0.52	2.342	2.402	2.394	2.331	2.352	2.331
0.78	2.444	2.410	2.431	2.352	2.334	2.292
1.04	2.461	2.432	2.423	2.362	2.352	2.311

*NEK = N-ethylcarbazole

Table 4.8 The static dielectric permittivity increment of various forms of PVK and model compound in toluene

At first glance these results look fairly similar in magnitude. However, the differences due to the tacticity become more apparent when the dielectric permittivity increments of the solutions are plotted against their respective concentrations. Table 4.9 lists the values (Δ/C) i.e. slopes of the dielectric increments plotted against concentrations.

Temperature /K	(Δ/C) / cm^3mol^{-1}			
	F1	F2	F2	NEK
288	444	741	643	526
298	429	744	661	514
308	445	768	637	514
318	424	688	670	528
328	486	822	688	553
338	481	671	591	391

Table 4.9 Gradients of the graphs of dielectric permittivity of the solutions of PVK and model compound N-ethylcarbazole against concentration

From table 4.9, it is noted that the dielectric permittivity of the polymers and the model compound in toluene behaves in a very similar manner to that observed for these solutes in 1,4-dioxane. Again, the dielectric permittivity is related to the stereostructures of the polymers. The dielectric permittivity increases with an increase in the isotactic content of the polymers. Thus, polymer F2, prepared with a cationic catalyst, has the highest dielectric permittivity whereas F1 (synthesised with free radical catalyst) possesses the lowest dielectric permittivity.

It is interesting to note that the order of the dielectric permittivities of the polymers is not altered when measured in 1,4-dioxane and toluene. However, the dielectric permittivity increments of polymer samples are generally lower when determined in toluene than in 1,4-dioxane. The biggest change observed in the dielectric permittivity values are

considerably lower than those obtained for the case in which the polymer is dissolved in 1,4-dioxane. For the model compound, the dielectric permittivity increments are similar for both solvents systems.

The dipole moments of PVK and N-ethylcarbazole were calculated as described previously (section 4.5) and are tabulated in tables 4.10 and 4.11

Temperature /K	$10^{18} <\mu> / esu$			
	F1	F2	F3	NEK
288	1.841	3.271	2.211	2.002
298	1.850	3.352	2.253	2.020
308	1.922	3.480	2.220	2.060
318	1.921	3.371	2.291	2.121
328	2.090	3.773	2.333	2.231
338	2.050	3.483	2.171	1.912

Table 4.10 The temperature dependence of the dipole moments of various stereoregular PVK and N-ethylcarbazole in toluene.

Temperature /K	ln $(<\mu^2 / 10^{-36}>)$			
	F1	F2	F3	NEK
288	1.220+/-0.018	2.370+/-0.036	1.587+/-0.023	1.376+/-0.021
298	1.230+/-0.018	2.418+/-0.036	1.625+/-0.024	1.406+/-0.021
308	1.307+/-0.019	2.494+/-0.037	1.595+/-0.024	1.445+/-0.021
318	1.306+/-0.020	2.530+/-0.036	1.658+/-0.025	1.503+/-0.021
328	1.474+/-0.022	2.554+/-0.039	1.694+/-0.025	1.595+/-0.021
338	1.436+/-0.022	2.594+/-0.037	1.550+/-0.023	1.608+/-0.019

Table 4.11 The temperature dependence of dipole moments of various stereoregular forms of PVK in solution in toluene.

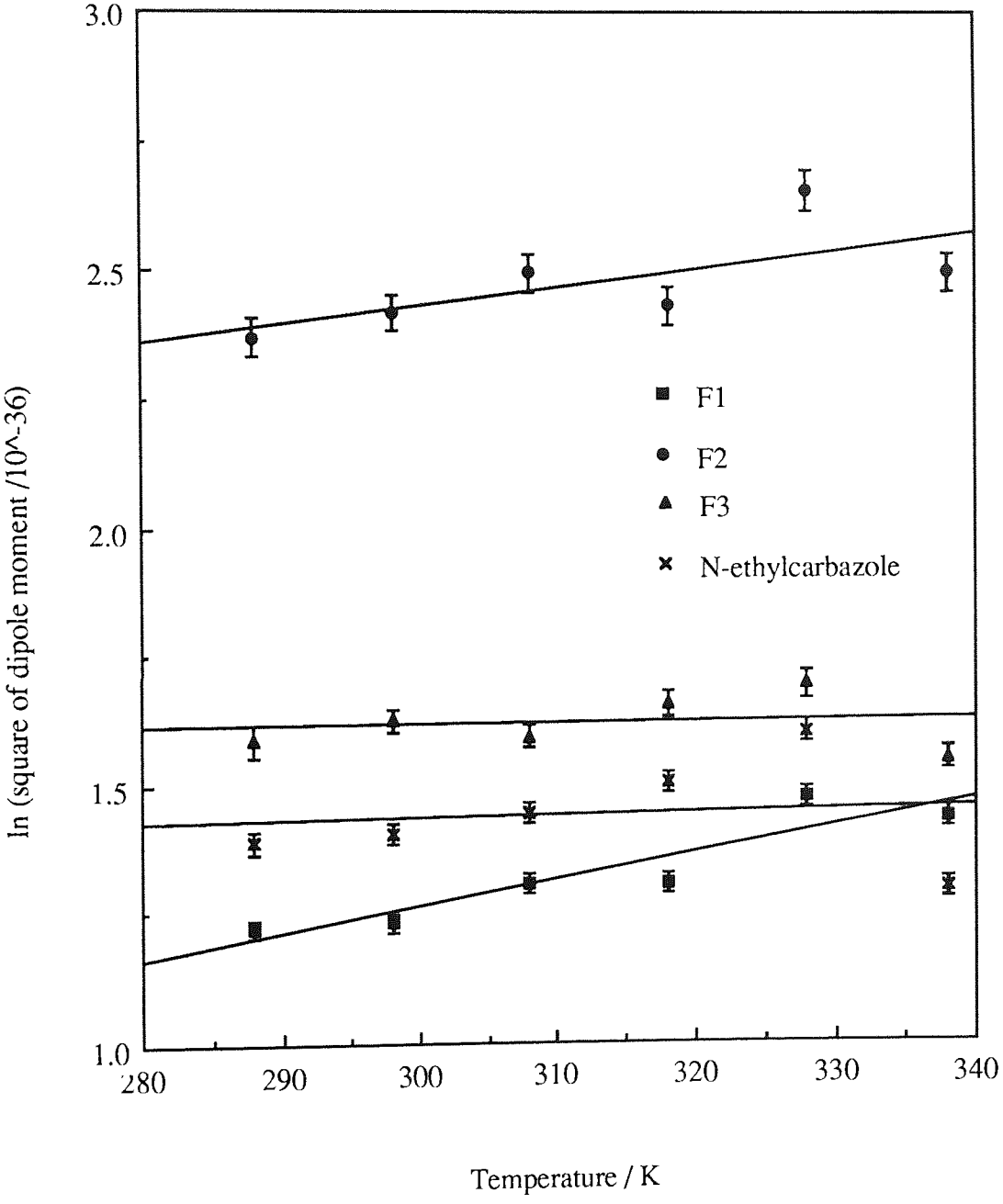

Figure 4.7 Temperature coefficients of dipole moment in toluene of stereoregular PVK prepared with different catalysts

The gradients of plots of ln μ^2 versus temperature were used to calculate the temperature coefficients of the dipole moments. These gradients are listed in table 4.11. A linear regression program was used calculate errors in these quantities.

Samples in toluene	$10^3(\ln\langle\mu^2\rangle)/dT)$ /K	Error (10^{-3})
F1	9.2	+/- 2.2
F2	3.6	+/- 2.5
F3	8.5	+/- 0.8
NEK	0.4	+/- 5.0

Table 4.11 The temperature coefficients of dipole moments of various PVK polymers and model compound N-ethylcarbazole measured in solution in toluene

It is interesting to note that the temperature coefficients of all the polymers are larger when measured in toluene when compared to the values measured in 1,4-dioxane. This is not surprising since 1,4-dioxane can be considered as a poor solvent, and the PVK molecules are "crumpled up" and there is minimized interaction between repeat units and solvent molecules. Toluene on the other hand, is believed to be a better solvent, was thought to have stronger Val der Waal interactions with the PVK molecules. In the latter case the polymer molecules are induced to expand and as a consequences it is possible that the the helices start to unwind i.e. tendency to form random coil configurations at increased temperatures.

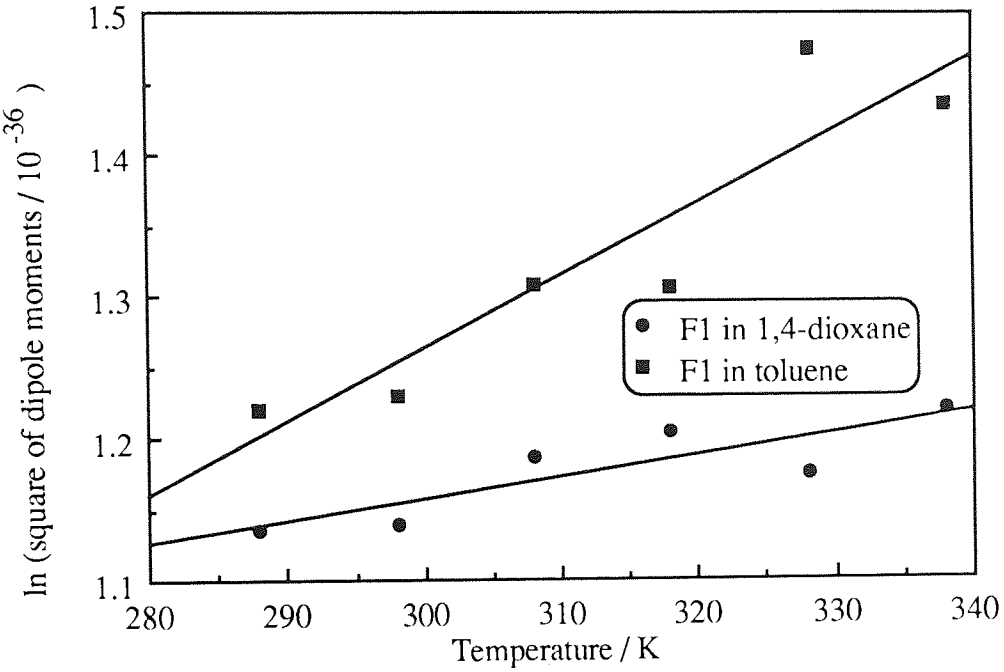

Figure 4.8 Variation of the average dipole moments per repeat unit with temperature of polymer sample F1 in 1,4-dioxane and toluene.

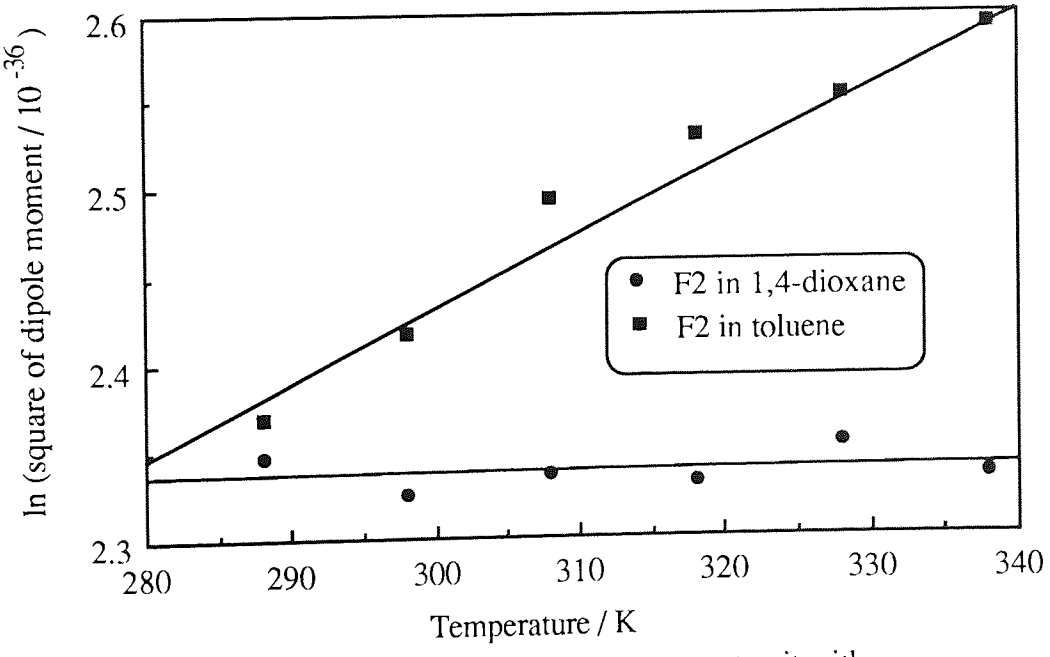

Figure 4.9 Variation of average dipole moments per repeat unit with temperature of polymer sample F2 in 1,4-dioxane and toluene.

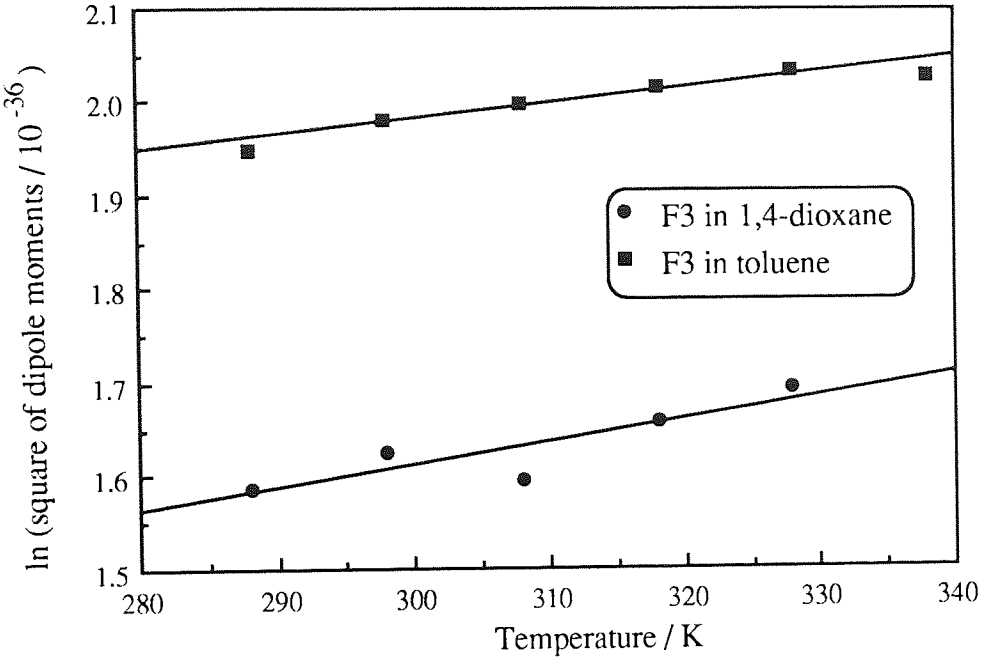

Figure 4.10 Variation of average dipole moment per repeat unit with temperature of polymer sample F3 in 1,4-dioxane and toluene

Figures 4.8 - 4.10 shows the comparison of average dipole moments per repeat unit. For the dielectric measurements made in toluene there seems to be a "fall off" in the magnitude of the dipole moment at the higher temperatures (see figure 4.7). It is possible that this may be the result of an apparent diluting effect caused by the expansion of the polymer solution at high temperatures. This would produce a decrease in the number of polymer molecules between the plates of the capacitor and a reduction in the capacitance value, which would in turn produce an apparent decrease in the dipole moment at high temperatures. It is therefore, important to investigate the thermal expansion of toluene over the temperature range used in the dielectric measurements.

For N-ethycarbazole, as the model compound, for the repeat unit of PVK it is reasonable to assume that there should be no increase in the dipole moment of N-ethylcarbazole as the temperature increases. In fact, as the temperature increases the dipole moment of N-ethycarbazole does increase slightly, but the dipole moment at 65 ^{o}C is noticeably lower than the previous values.

From an analysis of the dielectric data it is deduced that the temperature coefficient for N-ethylcarbazole is slightly negative, implying that the dipole moment is decreasing at higher temperatures. This supports the idea of that thermal expansion causes an apparent decrease in the concentration of the solute at the higher temperatures and that this produced an apparent a decrease in the dipole moment.

4.7 Conclusions

From the static dielectric studies it can be concluded that the temperature coefficients of dipole moments of the PVK samples are strongly related to the stereostructures and tacticity of the polymers. Sample F1 with the least isotactic content (prepared with a free radical catalyst) shows lowest dipole moments but the largest positive temperature coefficient. The polymer possesses mainly syndiotactic stereostructures with 2/1 helixes and are not as sterically hindered as 3/1 helixes of sample F2. At low temperatures, the chains are very much restricted in its movement, and hence maintains their basic helical conformation. This conformation enables the cancellation of dipole moments to some extent, resulting in lower dipole moments at low temperatures. As the temperature increases, there is more thermal energy and hence the rotation of the pendant groups and polymer chain movement also increases, resulting in the disturbance of the rigid helical structure. This change in the helical structure causes the decrease of the cancelling of the dipole moments. In addition, polymer F2 with 3/1 helical chains are so sterically hindered that they are less affected by the heat and they almost retain their basic helical configurations and thus the temperature coefficient is lower than those measured for polymers F1 and F3.

The model compound, N-ethylcarbazole shows no measureable temperature coefficient. This is because N-ethylcarbazole may be regarded approximately as a single rigid repeat of PVK. Therefore, there will be no cancellation effects present like those in the PVK

samples with helical structures. Therefore, no increase in the dipole moment of the N-ethylcarbazole was observed as the temperature increased.

The temperature coefficients of all the polymers are higher when measured in toluene than the values obtained when measured in 1,4-dioxane. This is not surprising since what can be considered as a poor solvent, such as 1,4-dioxane, the PVK molecules "crumpled up" and there was very little interaction with the solvent. Toluene on the other hand, being considered as a better solvent, was thought to have better interactions with the PVK molecules. In this case the structures of the polymer molecules were thought to expand and the helices start to unwind.

A "fall off" of the dipole moment at high temperatures in all of the dielectric measurement in toluene was observed. Experimental errors in the measurements of dielectric permittivities and apparent diluting of solution at higher temperatures were the two possible reasons for this fall off. The use of higher boiling point solvent, such as xylene would enable a more extensive investigation into the effects of solvents on PVK molecules and their structures.

CHAPTER FIVE

Temperature Coefficients of the Dipole Moment of Poly(N-vinylcarbazoles) Doped With 2,4,7-Trinitro-9-fluorenone

5.1 Introduction

Poly(N-vinylcarbazole) exhibits high photoelectric sensitivity within the ultra-violet spectrum, and in combination with suitable dopants as charge-transfer agents, the photoelectric sensitivity extends into the visible region. It is believed[123] that high photoconductivity in charge-transfer complexes is favored where orbitals of adjacent donor or acceptor molecules are reasonably overlapping each other. Kuczkowski et al[124] suggest that tetracyanoquinone dimethane (TCNQ) as an acceptor with poly(N-vinylcarbazole) would satisfy this condition because of the high electron affinity (2.8 eV) of TCNQ and its absorption in the visible region. The shape of the photoconductive spectrum changes with an increase of the concentration of the charge-transfer agent and is characterized by two maxima, one positioned at 370-390 nm, (for the PVK : TCNQ complex) and another at 490nm. The first maximum of photoconductivity, in PVK and in films of the charge-transfer complex, corresponds to the singlet absorption edge π-π^* transition of the carbazole chromophore; photoconductivity, here, depends slightly on the concentration of TCNQ. The other maximum for the photoconductivity lies in the long wavelength absorption region of the complexing agent at 490nm.

The photosensitivity of purified poly(N-vinylcarbazole)[125] is further enhanced by dye-sensitisation in the visible region. Doping of purified PVK with 2,4,7-trinitro-9-fluorenone (TNF) improves the spectral response. An improvement in the performance of the PVK : TNF photoreceptor film appears to be feasible in double layer structure[125] formed by dip-coating of the complex onto cast films of PVK. The shift of the spectral sensitivity maximum toward the visible region is a desirable aspect for electrophotographic applications, as white light illumination would be possible for exposure.

An inherent defect in the sensitization of PVK is that the sensitizing material is dispersed throughout the polymer matrix via solvent dissolution and subsequent casting, producing molecularly dispersed dyes or dye aggregates. In such systems the possibility of time-dependent phenomena exists if the dispersion of the dye aggregates causes the formation of a metastable solid solution. An alternative method involving, evaporation of the dye onto the polymer surface has disadvantage that the dye may readily be removed by abrasion. Pochan and Gibson[126] suggest a procedure in which the dye sensitizing molecules are chemically bound to PVK in a controlled manner, which remain prefentially attached to the surface layers of free-standing polymer films. Among the various charge-transfer agents used in combination with PVK and its derivatives the 1,4-naphthaquinones are claimed[127] to be very effective sensitizers. Also 2-Aryl-3-acetyl-1,4-naphthaquinone and its halogen derivatives are particularly effective with PVK.

The dye-sensitized photoconductivity of PVK has been examined with a number of dye systems including rhodamine 6zh[128], alizarin, chlorophyll, β-carotene, and flavone[129]. Stationary photoconduction and fluorescence studied with a PVK-rhodamine system have confirmed the participation of excited charge-transfer complexes in the generation of electric currents in the polymer. The dissociation of the charge-transfer complex with the formation of the electric current carriers occurs through a vibration relaxation state. Interestingly, an

external magnetic field causes the dissociation of the complex. The photocurrent reportedly[130] increases with the chemisorped amount of the dye, and is proportional to the square root of the illumination intensity[130].

As mentioned above, one of the important factors in charge transfer complexes is the overlap of molecular orbitals, the extent of which is affected indirectly by steric effects. In general, polymers can form three types of charge transfer complexes[131] :

(a) polymeric donor + monomeric acceptor,

(b) polymeric donor + polymeric acceptor, and

(c) polymeric acceptor + monomeric donor.

There is practically no information available in the literature on complexes involving type (c), for example with carbazole units in the polymeric chain. Only type (a) complexes will be discussed in detail since PVK : TNF complexes fall into this category.

Polymeric donor + monomeric acceptor system

Polymers containing pendant carbazole groups (donors) linked directly or through flexible side-chain units to the backbone, can combine with monomeric acceptors through three types of charge transfer interaction[132],viz.

(i) A 1:1 interaction involving a donor group and a single monomeric acceptor molecule,

(ii) a sandwich-like interaction in which an acceptor molecule is located between two donor groups, and

(iii) an interaction involving participation of more than two donor groups aggregated around a single acceptor molecule.

The relative effectiveness of these three modes of donor-acceptor interaction is governed by the nuclear substituent of the pendent system, the nature of the polymeric backbone and the side-chain structure. For correlating the structure of polymers with the different modes of charge transfer complex formation, various homopolymers and copolymers containing pendent carbazole units have been employed. In general, PVK, appears to be the most throughly studied homopolymeric[133] donor system, the charge transfer interaction of which, with various monomeric acceptors, has been examined and both electrical and photoconductive properties evaluated[133]. The mixture of PVK and TNF contains three structural components, i.e. a complex PVK : TNF, uncomplexed carbazole units of PVK and uncomplexed TNF molecules, which can make the interpretation of the electrical properties rather ambiguous in terms of a simple model.

In the previous chapter it was concluded that the temperature coefficients of dipole moments of the poly(N-vinylcarbazole) samples are strongly related to the stereostructures and tacticity of the polymers. Sample F1 with the least isotactic content (prepared with a free radical catalyst), had the smallest dipole moment per repeat unit but the largest positive temperature coefficient. Contrasting behaviour was shown by sample F2 (synthesised by cationic catalyst), which showed the largest dipole moment but the smallest temperature coefficient. The dipole moment of the model compound, N-ethylcarbazole had no measureable temperature coefficient. The trends of the results were explained in terms of polymer stereostructures, the conformations of the polymers and the intramolecular cancelling of dipole moments.

The various stereoregular forms of PVK, therefore provide an interesting opportunity to further extend this work by including PVK complexes. Useful information, concerning the structures of the donor / acceptor complex can be derived by measuring the dipole moment of the complex moiety. In principle, it should be possible to calculate, using measured dielectric permittivities, the molecular dipole moment of the complex formed between the carbazole side group and TNF. However, there are a number of difficulties associated with this exercise. Firstly, it is important to have an accurate estimate of the concentration of complex formed in solution. This is because it is essential that the dielectric increment is accurately apportioned to free (uncomplexed) carbazole, free TNF molecules and the amount of PVK and TNF that are complexed. Secondly, the experimentally determined dielectric increment must be very accurate. In practice this is a difficult constraint to satisfy mainly due to the rather poor solubility of the PVK : TNF complex. However, despite these drawbacks concerning the interpretation of the solution dielectric permittivities it is concluded that they are sufficiently accurate to be used in the determination of the dipole moments of the complexes.

In this chapter, calculations are presented of the dipole moments of PVK:TNF complexes. Also, a study is described of the influence of the temperature on the dipole moments of these complexes. A method by Weiser and Seki[133a] (see below) was employed to obtain the values of the equilibrium constants which were then used to calculate the concentration of the PVK:TNF complexes in solution in 1,4-dioxane. The equilibrium constant provides an indicator of the degree of charge transfer interaction. Perhaps, more importantly it enables the concentration of the complex to be accurately determined. This is essential if specific properties, for example, dipole moment and molecular Kerr constant, of the complex are to be studied. By relating these interactions to the molecular structures of PVK and TNF, specific characteristics of PVK:TNF complex, such as temperature coefficients of the dipole moment and molecular Kerr constant can be investigated.

5.2 Determination of the concentration of TNF : PVK complex in 1,4-dioxane using visible spectra

For measurements of equilibrium constants, solutions of the charge transfer complexes were prepared by dissolving the polymer samples in 20ml of 1,4-dioxane in a 25ml volumetric flask and then adding the TNF to the solution and diluting to volume. The polymers were left to dissolve completely for a week before the TNF was added. Deep red solutions were immediately formed when TNF was added to the polymer solutions. Using quartz cells (2mm path length) the samples were analysed on ultra-violet and visible spectrophotometer (wavelength 450 -700nm). The concentration of the polymer was maintained at 2% (w/v) but the TNF concentration was varied from 0.25 to 2% (w/v). Since the main aim of this part of the work was to study the temperature coefficients of dipole moment of PVK:TNF complexes via the analysis of uv-visible, spectra were obtained at temperatures over the range of 298 - 338K. The optical density at 500nm was read from the spectra and used to calculate the equilibrium constants at the various temperatures. The data were analyzed in the following manner: Charge transfer complex formation may be described by

$$D + A \rightleftharpoons DA \qquad (5.1)$$

Where D and A are the electron donor (PVK) and acceptor (TNF) and DA is the complex having a concentration characterized by the equilibrium constant K_e

$$K_e = \frac{[DA]}{[D][A]} \qquad (5.2)$$

If a_o and d_o are the initial concentration of the acceptor and donor and if c is the concentration of the complex then,

$$K_e = \frac{c}{(a_o - c)(d_o - c)} \qquad (5.3)$$

also $$\Delta G = -RT \ln(K_e) \qquad (5.4)$$

hence $$\ln(K_e) = \frac{-\Delta G}{RT} \qquad (5.5)$$

where $R = 8.3142\ JK^{-1}mol^{-1}$

Substituting for K_e gives

$$\ln(c) - \ln(ao - c) - \ln(do - c) = \frac{-\Delta G}{RT} \qquad (5.6)$$

Also,

$$\text{optical density absorbance (OD)} = \varepsilon cl \qquad (5.7)$$

Where, OD is the optical density reading for the absorption of the complex, ε is the extinction coefficient, and l is the pathlength of the cell

hence, $$c = \frac{OD}{\varepsilon l} \qquad (5.8)$$

and following substitution for c,

$$\ln \frac{OD}{\varepsilon l} - \ln(a_o) - \ln(d_o) = \frac{-\Delta G}{RT} \qquad (5.9)$$

It is important to note that the equation (5.9) is only valid for the case where $c << a_o$ and $c << d_o$. Equation 5.10 can be rearranged to give:

$$\ln(OD) = \frac{-\Delta G}{RT} + \ln(\varepsilon\, l\, a_o\, d_o) \qquad (5.10)$$

Expanding ΔG gives

$$\ln(OD) = \frac{-\Delta H}{RT} + [\Delta S/R + \ln(\varepsilon\, l\, a_o\, d_o)] \qquad (5.11)$$

Rewriting equation (5.10) as y = m.x.+ constant, then :

$$y = \ln(OD),\ x = 1/T \text{ and } m = \frac{-\Delta H}{R} \qquad (5.12)$$

Thus, a plot of $y = \ln(OD)$ against $x = 1/T$ should give a straight line plot that has a gradient of $\frac{-\Delta H}{R}$ and an intercept of $[\Delta S/R\ \ln(\varepsilon\, l\, a_o\, d_o)]$. For the case in which $\Delta G \approx \Delta H$ equation (5.5) allows the equilibrium constant K_e to be found which can be used in conjunction with equation 5.3 to calculate the concentration of complex (c). A computer program (Appendix 4) was written to facilitate the above calculations.

5.3 Results and Discussion

The procedure described in section 5.2 was used to calculate the equilibrium constants for PVK:TNF complexes. The results are presented in Table 5.1.

Temperature (K)	Sample	Initial acceptor : donor concentration (mol dm^{-3})			
		0.016:0.104	0.032:0.104	0.048:0.104	0.064:0.104
298	F1	2.9	2.6	2.5	2.6
	F2	2.8	2.6	2.4	2.3
	NEK*	18.2	15.5	11.6	9.5
308	F1	2.9	2.6	2.5	2.6
	F2	2.7	2.6	2.4	2.3
	NEK*	16.6	14.2	10.7	8.8
318	F1	2.8	2.5	2.4	2.5
	F2	2.6	2.5	2.3	2.2
	NEK*	15.2	13.0	9.9	8.2
328	F1	2.7	2.4	2.3	2.5
	F2	2.5	2.4	2.3	2.2
	NEK*	13.9	12.0	9.2	7.7
338	F1	2.6	2.4	2.3	2.4
	F2	2.4	2.4	2.2	2.1
	NEK*	12.9	11.2	8.7	7.3

*NEK = N-ethylcarbazole

Table 5.1 Equilibrium constants for complexes of 2,4,7-trinitro-9-fluorenone with polymer types F1, F2 and the model compound N-ethylcarbazole.

From Table 5.1, it is evident that the equilibrium constants for PVK : TNF complexes are fairly independent of temperature whereas for the model compound N-ethylcarbazole : TNF, the value of equilibrium constant tends to decrease considerably with temperature. For example, in the first solution of NEK : TNF sample shown in Table 5.1 (NEK = 0.016 mol dm^{-3} and TNF = 0.104 mol dm^{-3}) the equilibrium constant decreases from 18.2 at 298K to 12.9 at 338K. However, in the case of PVK : TNF samples the decrease in equilibrium constant with temperature is much smaller (see Table 5.1). This indicates that in the case of complex PVK : TNF the enthalpy (ΔH) is large compared to $T\Delta S$ where S is the entropy. However, in the case of NEK : TNF, the ΔH is comparable or smaller than $T\Delta S$ and therefore the effects of temperature are relatively large.

A computer program (Appendix 4) was used to calculate the concentration (c) of complexes which are listed in Tables 5.2 - 5.4. The concentations were used to calculate the appropriate dielectric permittivity of charge transfer complexes in solution ($\varepsilon_{complex} = \varepsilon_{solution} - \varepsilon_{freePVK} - \varepsilon_{free\ TNF}$). The dielectric data for solutions of the various PVK: TNF complexes are presented in tables 5.2 - 5.4. Dielectric data for solution of PVK in 1,4-dioxane and for solutions of TNF in 1,4-dioxane are listed in Appendix 5.

Intial concentration of TNF (mol cm^{-3}) (**F1=1.04x10^{-4}** mol cm-3)	**Temperature** (K)	**Derived concentration of complex** (mol cm^{-3})	**ε complex**
1.65 x10^{-5}	298	1.86 x10^{-6}	2.1826
3.20 x10^{-5}		6.26 x10^{-6}	2.1892
4.80 x10^{-5}		9.30 x10^{-6}	2.1900
6.35 x10^{-5}		2.15 x10^{-5}	2.2076
1.65 x10^{-5}	308	1.85 x10^{-6}	2.1636
3.20 x10^{-5}		6.13 x10^{-6}	2.1766
4.80 x10^{-5}		9.11 x10^{-6}	2.1830
6.35 x10^{-5}		2.07 x10^{-5}	2.1985
1.65 x10^{-5}	318	1.84 x10-6	2.1497
3.20 x10^{-5}		5.99 x10^{-6}	2.1556
4.80 x10^{-5}		8.92 x10^{-6}	2.1576
6.35 x10^{-5}		2.01 x10^{-5}	2.1713
1.65 x10^{-5}	328	1.83 x10^{-6}	2.1126
3.20 x10^{-5}		5.87 x10^{-6}	2.1229
4.80 x10^{-5}		8.72 x10^{-6}	2.1306
6.35 x10^{-5}		1.95 x10^{-5}	2.1532
1.65 x10^{-5}	338	1.81 x10^{-6}	2.0912
3.20 x10^{-5}		5.85 x10^{-6}	2.1045
4.80 x10^{-5}		8.58 x10^{-6}	2.1183
6.35 x10^{-5}		1.89 x10^{-5}	2.1358

Table 5.2 Concentration and dielectric permittivity of complexes of F1: TNF formed in solution in 1,4-dioxane at various temperatures.

Intial concentration of TNF (mol cm^{-3}) (**F2 =1.04x10^{-4}** mol cm^{-3})	**Temperature** (K)	**Derived concentration of complex** (mol cm^{-3})	**ε complex**
1.65 x10^{-5}	298	3.46 x10-6	2.1776
3.20 x10^{-5}		6.35 x10^{-6}	2.4586
4.80 x10^{-5}		8.97 x10^{-6}	2.6164
6.35 x10^{-5}		1.12 x10^{-5}	2.8628
1.65 x10^{-5}	308	3.38 x10^{-6}	2.1722
3.20 x10^{-5}		6.38 x10^{-6}	2.4309
4.80 x10^{-5}		8.78 x10^{-6}	2.5558
6.35 x10^{-5}		1.10 x10^{-5}	2.7467
1.65 x10^{-5}	318	3.30 x10^{-6}	2.1503
3.20 x10^{-5}		6.24 x10^{-6}	2.3931
4.80 x10^{-5}		8.61 x10^{-6}	2.5379
6.35 x10^{-5}		1.08 x10^{-5}	2.6767
1.65 x10^{-5}	328	3.23 x10^{-6}	2.1334
3.20 x10^{-5}		6.11 x10^{-6}	2.3839
4.80 x10^{-5}		8.43 x10^{-6}	2.5113
6.35 x10^{-5}		1.06 x10^{-5}	2.6275
1.65 x10^{-5}	338	3.16 x10^{-6}	2.1228
3.20 x10^{-5}		5.99 x10^{-6}	2.3824
4.80 x10^{-5}		8.29 x10^{-6}	2.4977
6.35 x10^{-5}		1.04 x10^{-5}	2.5934

Table 5.3 Concentration and dielectric permittivity of Complexes of F2 : TNF formed in solution in 1,4-dioxane at various temperature.

Initial concentration of TNF (mol cm^{-3}) (**NEK=1.04x10^{-4}** mol cm^{-3})	**Temperature** (K)	**Derived concentration of complex** (mol cm^{-3})	**ε complex**
1.65 x10^{-5}	298	1.01 x10-5	2.2334
3.20 x10^{-5}		1.82 x10^{-5}	2.2324
4.80 x10^{-5}		2.32 x10^{-5}	2.2442
6.35 x10^{-5}		2.68 x10^{-5}	2.2535
1.65 x10^{-5}	308	9.75 x10^{-6}	2.2276
3.20 x10^{-5}		1.76 x10^{-5}	2.2295
4.80 x10^{-5}		2.24 x10^{-5}	2.2357
6.35 x10^{-5}		2.59 x10^{-5}	2.2474
1.65 x10^{-5}	318	9.43 x10-6	2.2078
3.20 x10^{-5}		1.70 x10^{-5}	2.2068
4.80 x10^{-5}		2.16 x10^{-5}	2.2162
6.35 x10^{-5}		2.50 x10^{-5}	2.2241
1.65 x10^{-5}	328	9.11 x10^{-6}	2.1924
3.20 x10^{-5}		1.64 x10^{-5}	2.1910
4.80 x10^{-5}		2.09 x10^{-5}	2.2001
6.35 x10^{-5}		2.42 x10^{-5}	2.2065
1.65 x10^{-5}	338	8.82 x10^{-6}	2.1762
3.20 x10^{-5}		1.59 x10^{-5}	2.1750
4.80 x10^{-5}		2.02 x10^{-5}	2.1843
6.35 x10^{-5}		2.34 x10^{-5}	2.1898

NEK = N-ethylcarbazole

Table 5.4 Concentration and dielectric permittivity of complexes of N-ethylcarbazole : TNF formed in solution in 1,4-dioxane at various temperatures.

From Tables 5.2 - 5.4, the percentage of free donor and acceptor molecules can be calculated. It is worth noting that nearly all of the acceptor molecules (>85%) are in a complexed form, the rest remaining free in the solution. For the PVK : TNF and NEK : TNF complexes, the concentration of the complex decreases with temperature, due to expansion of the sample and also dissociation of the complexes and this leads to a small decrease in the dielectric permittivity of the complexes.

Using the method developed by Debye-Guggenheim (see Chapter 4), the dipole moments of the complexes were calculated by using the gradients $(\Delta/C)_{c->0}$ of plots of the dielectric permittivity against concentration (see Equation 4.2). The slopes at different temperatures for all samples of PVK : TNF and NEK : TNF are listed in the the table 5.5.

Temperature (K)	(Δ/C) / cm^3 mol^{-1}		
	F1: TNF	**F2 : TNF**	**NEK : TNF**
298	1261	86130	2448
308	1570	73351	2105
318	1166	69688	2156
328	2276	66467	1989
338	2547	64370	1984

NEK = N-ethylcarbazole

Table 5.5 Gradients of plots of dielectric increment (Δ) against concentration (C)

By subsituting values of (Δ/C) into the Guggenheim-Debye equation (equation 4.2) the dipole moment the PVK : TNF complex and that of the N-ethylcarbazole : TNF complex can be found. The results are shown in figure 5.1.

Temperature /K	$10^{18}\mu$ / esu		
	F1: TNF	F2 : TNF	NEK : TNF
298	0.739	6.089	1.031
308	0.841	5.741	0.980
318	0.739	5.713	1.014
328	1.050	5.694	0.993
338	1.131	5.716	1.012

NEK = N-ethylcarbazole, esu = electrostatic units

Table 5.6 The dipole moments (μ) of various types of stereoregular PVK in solution 1,4-dioxane at different temperatures.

The temperature coefficient of the dipole moments is conventionally defined by

$$\frac{d(\ln\langle\mu^2\rangle)}{dT} \qquad (5.13)$$

Temperature /K	$\ln(\langle\mu^2 / 10^{-36}\rangle)$		
	F1 : TNF	F2 : TNF	NEK : TNF
298	-0.605 +/-0.018	3.613 +/- 0.072	0.061+/- 0.002
308	-0.346 +/-0.010	3.495 +/- 0.070	-0.040+/- 0.001
318	-0.126 +/-0.004	3.485 +/- 0.069	0.028+/- 0.001
328	0.098 +/-0.003	3.479 +/- 0.069	-0.014+/- 0.001
338	0.246 +/-0.007	3.487 +/- 0.070	0.024+/- 0.001

Table 5.7 The temperature dependence of dipole moments (μ) of various stereoregular PVK in 1,4-dioxane

Plots of ln μ^2 versus temperature are shown in Figure 5.1.

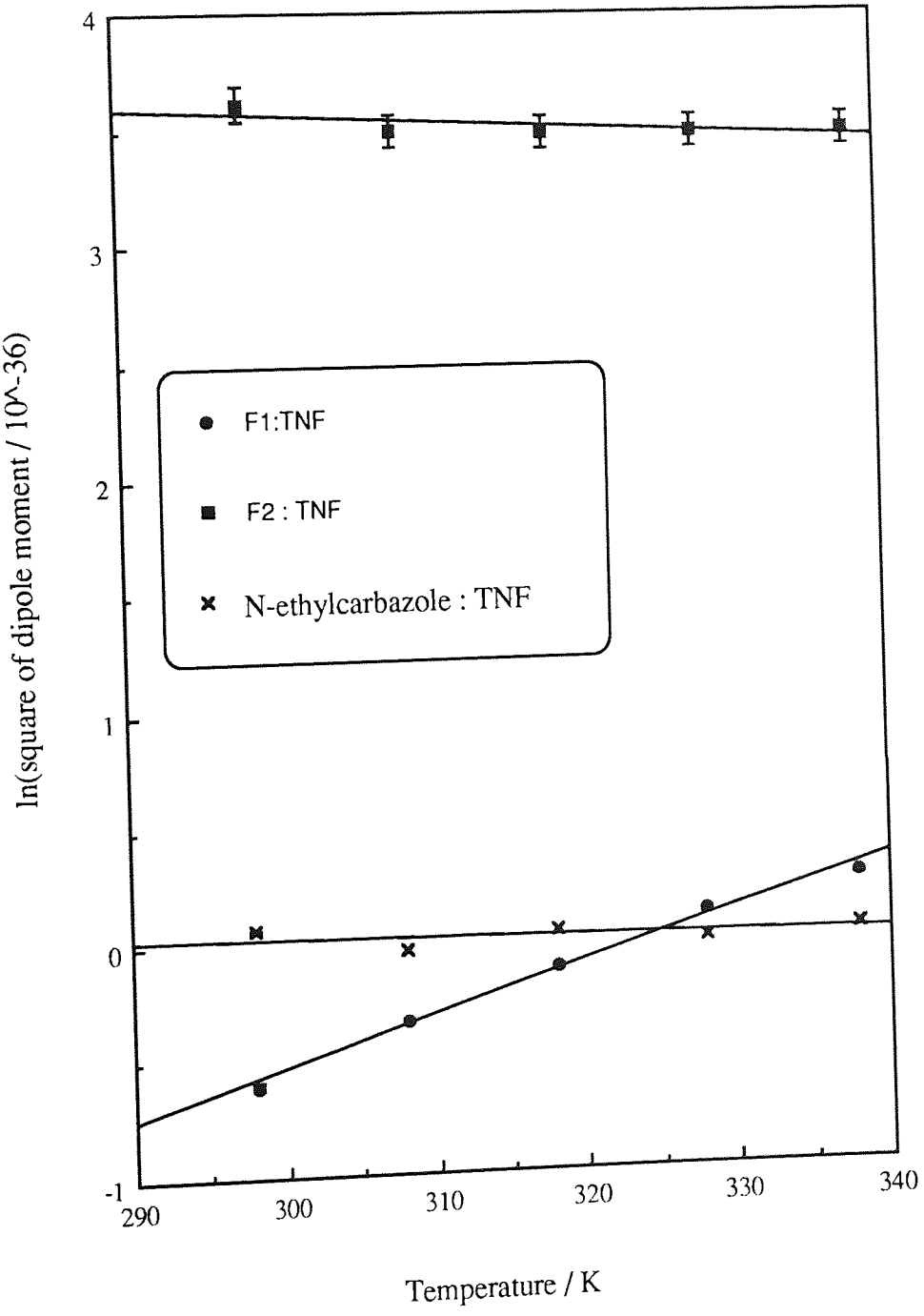

Figure 5.1 Solution temperature coefficients of N-ethylcarbazole and PVK prepared with different catalysts and doped with TNF. The solvent is 1,4-dioxane.

A linear regression program was used to provide the gradients of the plots and associated errors.

Polymer type (solvent = 1,4-dioxane	**$d\ln\mu^2 / dT$ (K^{-1})**	**Error**
F1 : TNF	0.0017	+/- 0.0005
F2 : TNF	0.0002	+/- 0.0002
NEK : TNF	-0.0002	+/- 0.0003

Table 5.8 Temperature coefficients of dipole moments of PVK:TNF and NEK:TNF complex determined in 1,4-dioxane over the temperature range 298 - 338K.

In figures 5.2 - 5.3 a comparison is made between the dipole moments of undoped poymer samples F1 and F2 and the dipole moment of the PVK:TNF complexes formed by doping with TNF. Figure 5.4 shows a similar comparison of the dipole moments determined for pure NEK and NEK:TNF complexes in 1,4-dioxane. For a more detailed discussion of the dipole moments of undoped PVK see Chapter 4.

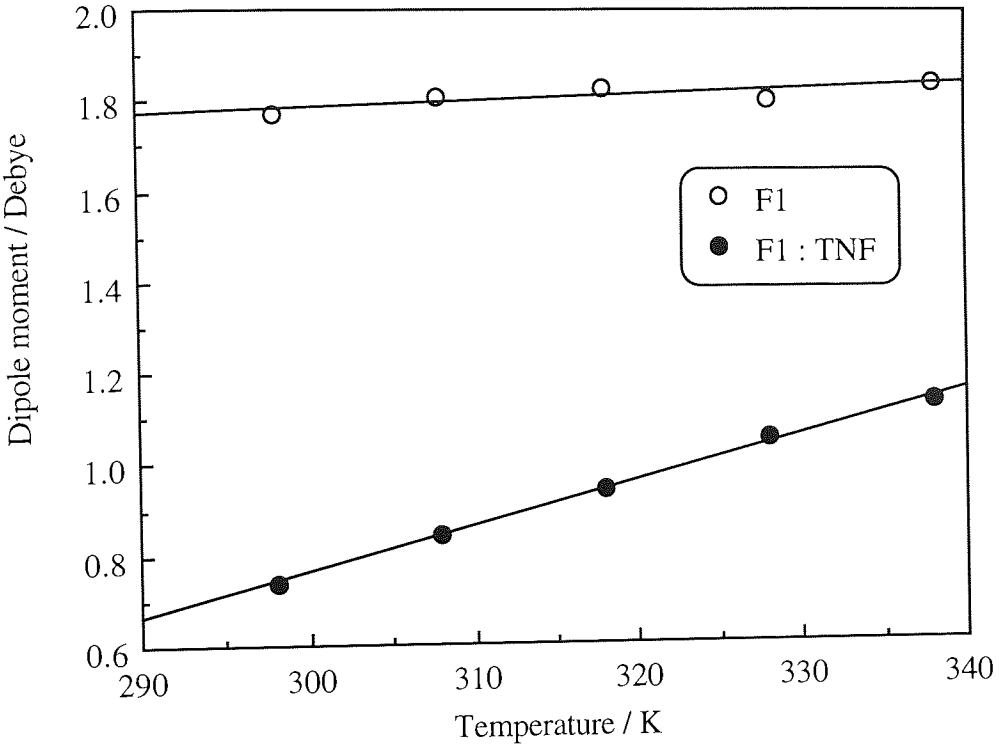

Figure 5.2 Dipole moments per repeat unit of polymer sample F1 and complexes F1 : TNF in 1,4-dioxane .

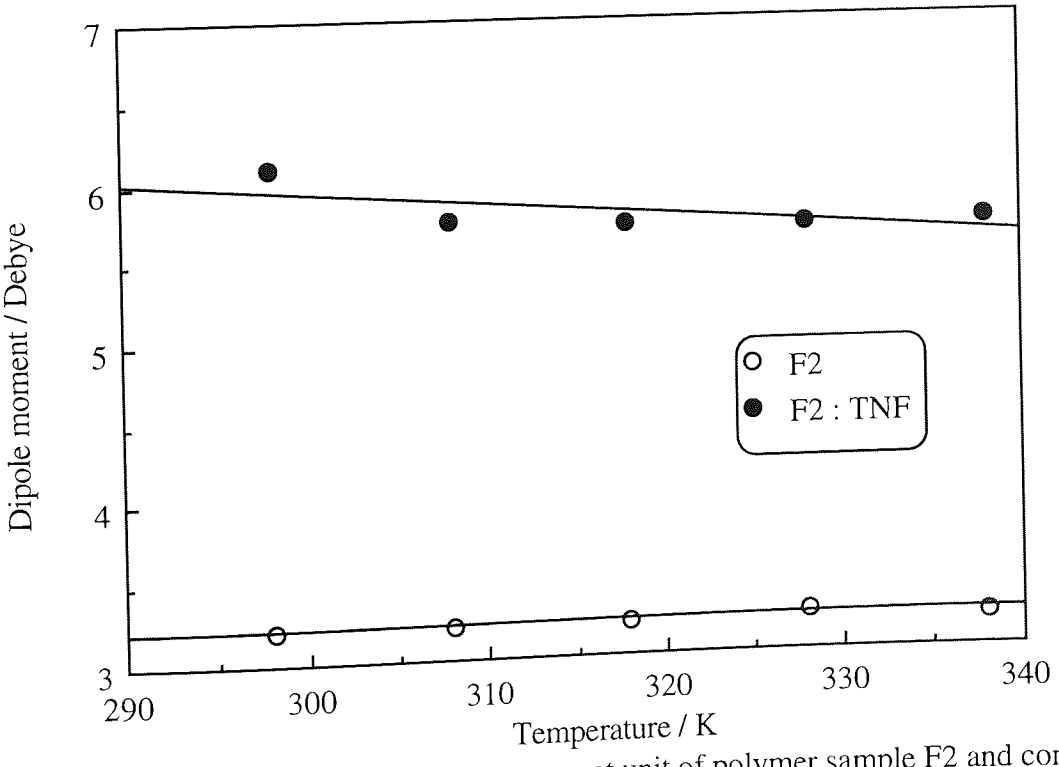

Figure 5.3 Dipole moments per repeat unit of polymer sample F2 and complexes F2 : TNF in 1,4-dioxane.

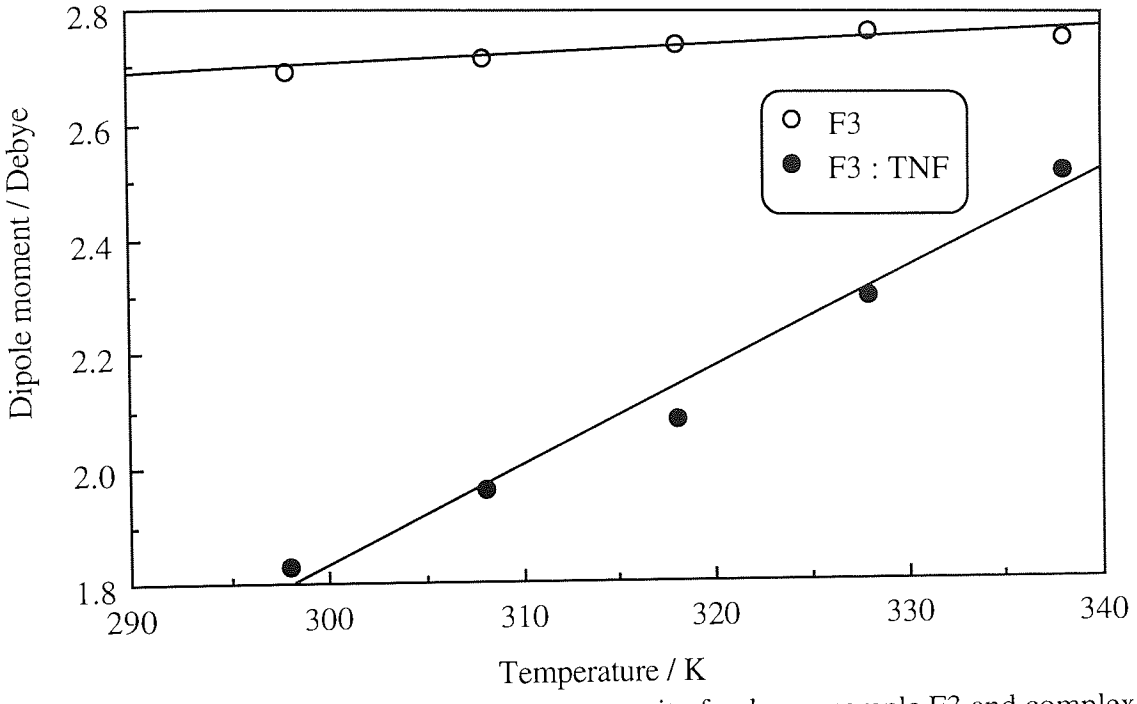

Figure 5.4 Dipole moments per repeat unit of polymer sample F3 and complexes F3 : TNF in 1,4-dioxane.

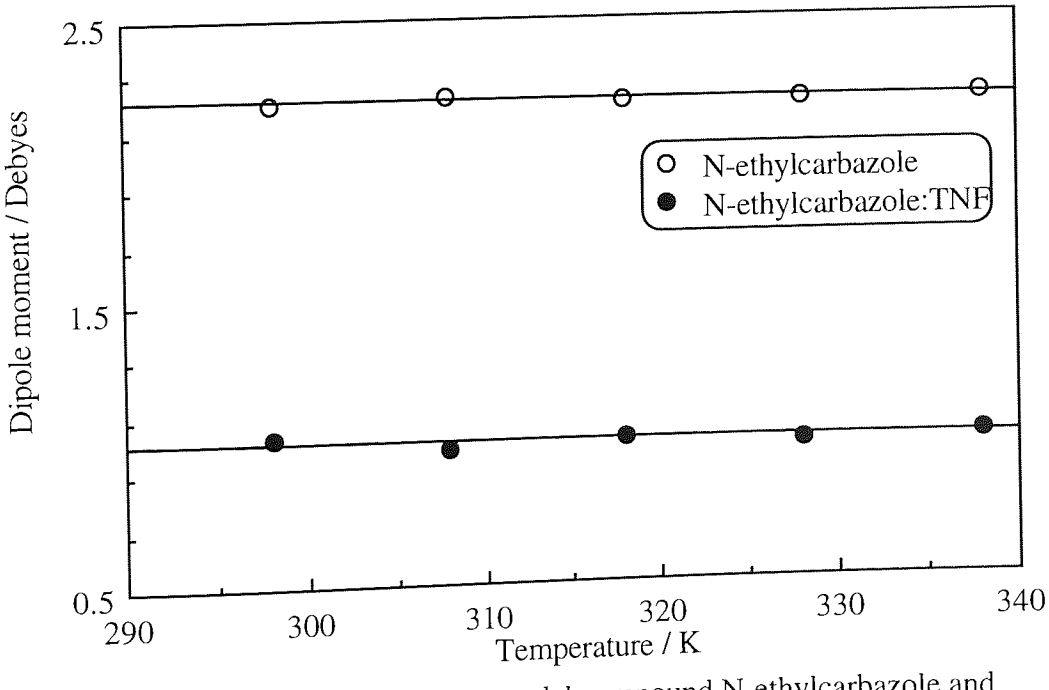

Figure 5.5 Dipole moment of the model compound N-ethylcarbazole and of the complexes N-ethylcarbazole : TNF in 1,4-dioxane.

From the dipole moment - temperature coefficient data (figure 5.1) the following observations can be made:

(i) The dipole moments of complexes formed between TNF and F1 (lowest isotacticity) have the lowest dipole moment of the various types of PVK but they exhibit the largest temperature coefficient.

(ii) The complexes formed between TNF and polymer F2 (largest isotacticity) have the highest dipole moment of the various types of PVK but they exhibit the smallest (almost zero) temperature coefficient .

(iii) The temperature coefficients of the dipole moment of NEK : TNF complexes is close to zero.

These observations are discussed in detail below:

The proton and carbon-13 NMR study (see Chapter 3) indicated that polymer F1 synthesised with AZBN catalyst possessed 30% isotacticity whereas for sample F2 prepared with cationic catalyst (boron trifluoride etherate) the isotacticity was estimated to be 55%. From the X-ray studies[104,110], it is evident that the polymer of type F1 would be expected to possess mainly syndiotactic stereostructures with the possibility of forming 2/1 helixes that are not as sterically hindered as the 3/1 helixes believed to be formed in isotactic rich polymer F2. The degree of complex formation and the strength of the charge transfer differs considerably and depends on the conformation and tacticity of the polymer chains. As the polymeric structures of 2/1 and 3/1 helices of PVK shown in figure 7.6 (Chapter 7) indicate, the distances between the adjacent pendant carbazole groups in a helix in the 2/1 helix differs considerably when compared to the same distance in helices composed largely of 3/1

helices. In the case of 2/1 helical chains this distance is (4.33Å) whereas in 3/1 type structures the distance is 6.10Å. As explained in section 5.1, the PVK and TNF form sandwich type charge transfer complexes[131,132] where the π orbital of the carbazole group would interact with the electron deficient TNF. However, for the 2/1 helical conformation (predominant in polymer F1) there is not sufficient room for the TNF molecule to adopt this conformation. However, it is important to emphasise that the charge transfer complexes are formed with all types of PVK polymers, it is only the amount of complexation and relative stability that differs. The higher dipole moments and virtually zero temperature coefficient observed for F2 : TNF complex provides evidence that the charge transfer complexes are relatively stronger then of F1:TNF and F3:TNF. The strength of the F2:TNF complexes seem to be little affected by an increase of temperature. As a result the dipole moment remains virtually constant. Positive temperature coefficients were obtained for F1: TNF complexes, suggesting that these complexes were thermally less stable compared to F2 : TNF. At low temperatures, the chains are very much restricted in movement, and also tend to occupy the more energetically favourable helical conformations. The adoption of helical conformations results in the cancellation of dipole moments. As the temperature increases, there is more thermal energy and hence a greater degree of freedom of the pendant groups and as a consequence this results in the formation of non helical structures. This change in the proportion of helical structures leads to decrease in the cancellation of the dipole moments of the repeat units.

For the model compound N-ethylcarbazole and TNF the dipole moments remain virtually unchanged since for N-ethylcarbazole, which may be regarded as representing a single repeat polymer unit, no intramolecular cancellation of dipole moments is possible.

Conclusions

A modified method of Weiser and Seki[125] was successfully used to estimate the equilibrium constants of charge transfer complexes of PVK and TNF and of model compound, N-ethylcarbazole and TNF. These values were then used to calculate the concentrations of the charge transfer complexes in solutions of 1,4-dioxane. The knowledge of the concentration levels of complexes facilitated calculation of the dielectric increments of charge transfer complexes. It was found that all PVK samples formed complexes with 2,4,7-trinitro-9-fluorenone. However, the amount of complexation and the thermal stability of the complexes differed significantly. The complex F2 : TNF was the most stable with the highest dipole moments and almost zero temperature coefficient for the dipole moments. The complexes formed between TNF and F1 (polymer with lowest isotacticity) were found to have lowest dipole moments but the largest dipole moment temperature coefficient .

CHAPTER SIX

Experimental Determination of the Electro-optic Kerr Effect of Poly(N-vinylcarbazole) and its Charge Transfer Complexes

6.1 Introduction

The applicability of the Kerr constant to conformational analysis arise from the great sensitivity of this property to variation of molecular geometry and environment[134], including aspects such as the geometry of solvation[135-137] and the aggregation of solutes[137]. The standard procedure used for these studies consists of the determination of the experimental values of the molar Kerr constant ${}_mK$, often together with measurement and similar analysis of some other conformationally dependent property[138] such as dipole moments, mean squared optical anisotropy, etc. The determination of the molar Kerr constant ${}_mK$ of small molecules allows the evaluation of either of the above mentioned optical properties via a description of their polarizability tensors. The small molecules may be oligomers or model compounds of the repeat unit of a polymer and the results of these analyses may be used to study the electro-optic properties of the polymer chain. In the measurement of ${}_mK$ it is necessary to use solvents having small dielectric permittivity and relatively low optical anisotropy; such as carbon tetracholoride, cyclohexane, 1,4-dioxane and benzene. Many examples of the conformational analysis of small molecules can be found in the reviews published by Aroney and other co-workers[134].

The Kerr effect has also been used quite widely to analyze the conformations of flexible polymers. Le Fevre's group has studied poly(ethylene glycol)[139] poly(methyl

methacrylate)[140] and poly(methyl acrylate)[141]. For the case of poly(ethylene glycol), Le Fevre measured dipole moments and molar Kerr constants at 25°C and λ = 589.3 nm for benzene solutions of HO-$(CH_2$-CH_2-$O)_x$-H with <x> = 4.1, 6.4, 18, 34, 78, and 153. They concluded that both properties can be reconciled with the supposition that gauche and trans conformations of groups O-CH_2-CH_2-O are equally probable for x not greater than about 5, but that for larger values of x then gauche or cis arrangements occur more frequently than trans, thus explaining the tendency for the larger molecular chains to contain helical portions.

Another typical example of the application of $_mK$ to conformational analysis is provided by the work of Tonelli[142] who performed calculations of molar Kerr conatants on five homopolymers: poly(propylene) (PP), poly(vinylchloride) (PVC), poly(styrene) (PS), poly(*p* - methylstyrene) (PPMS) and poly(*p* -chlorostyrene) (PPCS), and three copolymers (PP-PVC, PS-PPCS, and PPMS-PPCS) as functions of stereoregularities and sequence distribution. Among the five homopolymers studied, only the results obtained for the polar polymers poly(vinylchloride) and poly(*p* -chlorostyrene) exhibit marked sensitivities to stereosequences. The molar Kerr constant calculated for each of the three copolymers systems show high sensitivities to both stereosequences and monomer sequence distribution. Tonelli concluded that the molar Kerr constant may hold promise as an easily measured molecular property of copolymer chain that is sensitive to its sequence distribution. The sensitivity of $_mK$ to the stereosequence in the case of polar vinyl polymers is confirmed by the analysis of the mean-square optical anisotropy and Kerr constants of p-chloro- and p-bromostyrene performed by Flory and co-workers[143].

A typical Kerr constant measurement consists in applying an electrical field to a given sample and determining the birefringence produced by the field. For this purpose, a beam of monochromatic and plane polarized light is passed through the sample. When the

electrical field is on, the sample becomes birefringent and transforms the incoming plane polarized light into elliptically polarized light. The degree of ellipticity of this outcoming light is directly related to the birefringence of the sample. Thus, all that the experiment requires is to measure the state of polarization of a beam of light emerging from the sample when it is under a strong electric field.

As indicated in Chapter 4 the dipole moments could be used to differentiate the differences in the stereostructures of PVK chains. Since molecular Kerr constants also depend on the anisotropy, molecular geometry and polymer chain structures, the measurement of electrical birefringence provides an interesting opportunity to study PVK prepared with different catalysts. In this chapter a procedure to measure electrical birefringence (experimental Kerr constant, B) and calculations of the molecular Kerr constant, $_mK$ are described. It is generally accepted that it is valuable to employ several techniques that rely upon different aspects of the conformational structure and behaviour of molecules. The parameters so obtained may then be interpreted in parallel, to see if, when considered together, they support, or refute, the conformational possibilities. This use of complementary methods helps to eliminate ambiguities which may arise if reliance is placed upon a single experimental technique. Therefore, the interpretation of electrical birefringence data, is necessarily integrated with the dipole moment data as far as possible.

Much of the equipment required to measure the Kerr constant had previously been assembled by other researchers in this group, and was mostly suitable for the experiments carried out in this thesis. The preparation of the solutions used and the Kerr constant results obtained are also described.

6.2 The Kerr Effect Apparatus

The molar Kerr constant of a substance may be visualised as the difference in the molecular refraction along directions parallel to the major and minor axis of the polarizability ellipsoid of the molecule. An important quantity is the experimental Kerr constant (B), defined by the equation:

$$B = \frac{n_p - n_s}{E^2\lambda} = \frac{\delta}{2\pi l E^2} \qquad (6.1)$$

where n_p and n_s are the refractive indices for the component of the light in the medium parallel and perpendicular to the applied electric field E, λ is the wavelength of light, l is the optical pathlength and δ is the phase difference between components of light having electric vectors parallel and perpendicular to E.

The diagrammatic representation of the apparatus used to measure the electrically induced phase difference, is shown in figure 6.1. A parallel plane-polarised beam of monochromatic light is passed through the Kerr cell such that the plane of polarization of light is at an angle of 45° relative to the direction of the applied electric field, E. In the presence of this electric field the light leaving the cell is generally elliptically polarized. After passing through a quarter-wave retarder orientated with its principal optical axis at 45° to the direction of the applied electric field, the resultant plane-polarized light can be nulled by rotating the analyser. The angular difference, α, between the principal planes of the polarizer and the analyzer is equal to $\delta/4$ provided that the electric field is applied as a rectangular pulse.

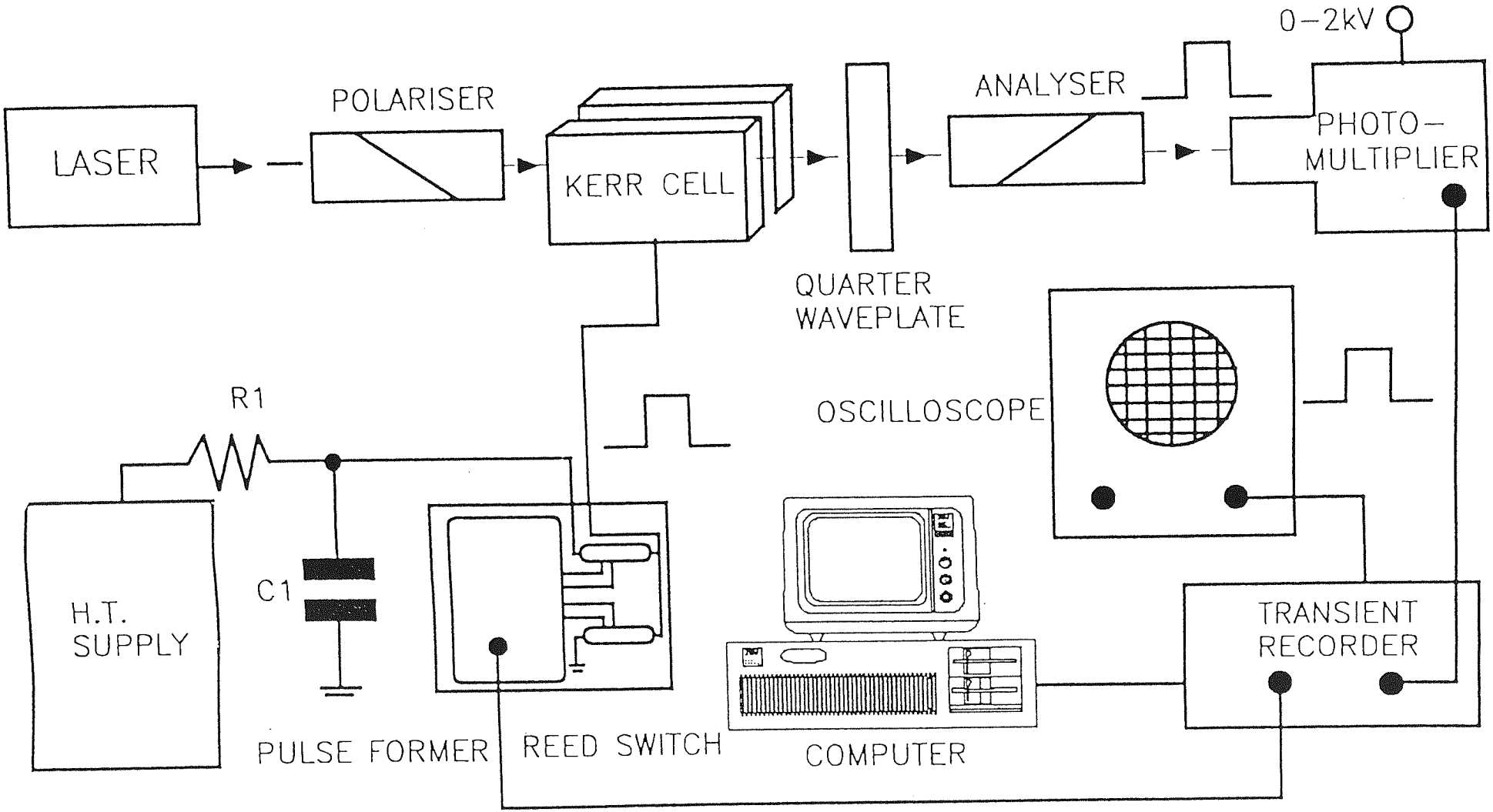

Figure 6.1 Apparatus used to measure the electrically induced phase difference

The light source was 5mW He/Ne laser (Scientific and Cook, model SLH/2) emitting at 632.8nm. The degree of polarization of the light entering the Kerr cell (15cm optical path length) was improved by passing the beam through a high quality polarizer. Both the polarizer and analyser were Glan - type prisms (Ealing Beck Ltd.) mounted in brass tubes. The analyser could be rotated by means of a series of gears allowing rotations as small as 0.005 degrees to be read with an accuracy of $\pm$ 0.002 degrees. The quarter wave retarder was of mica (F.Wiggins and Sons Ltd.), used at 632.8nm and mounted between glass discs.

A Wallis (Worthing) model S103/3 power pack was used to supply the high-tension voltage, which was continuously variable in the range 0-10kV. The voltage applied to Kerr cell was measured on a Thurlby digital multiplier (Model 1503-HA). The optical signal, is captured by the transient recorder and the signal can be diplayed continuously on an oscilloscope (Figure 6.2) or could be transferred to the computer. The signal is nulled when α becomes equal to $\delta/4$. The electrical configuration of the electrodes of the photomultipliers tube (E.M.I. 9816B) is shown in Figure 6.3 and is recommended by the manufacturer for high gain usage. Light impinging upon the semi-transparent caesium-antimony photocathode, K, causes the emission of electrons. After being focused and accelerated these electrons gives rise to an avalanche of electrons along the dynode chain, d1-d14. The extent of the gain and/or smoothing of the output from the photomultiplier tube may be adjusted by changing the values of R_L and/or C_L, respectively.

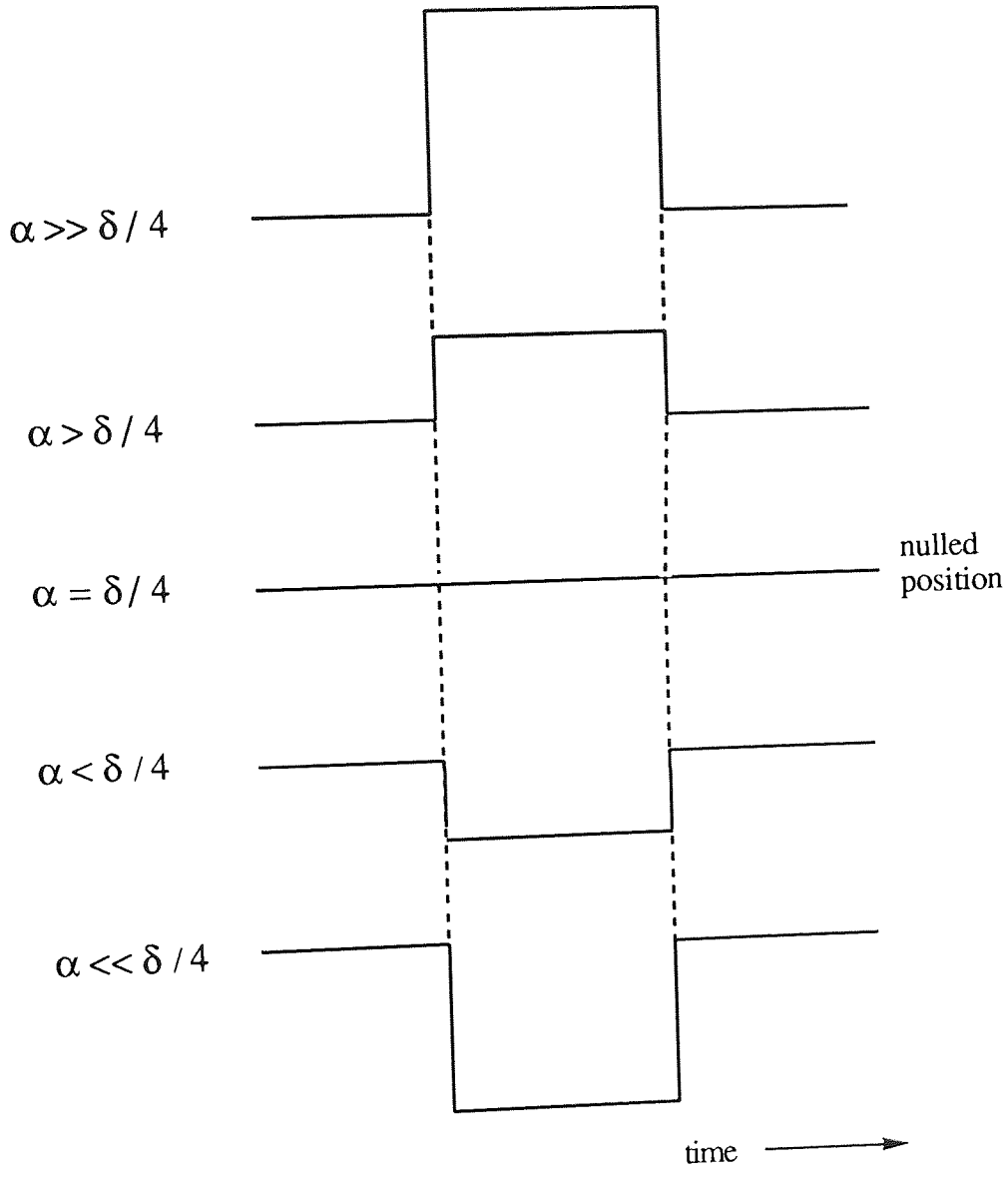

Figure 6.2 Rectangular-shaped pulsed as displayed on the oscilloscope

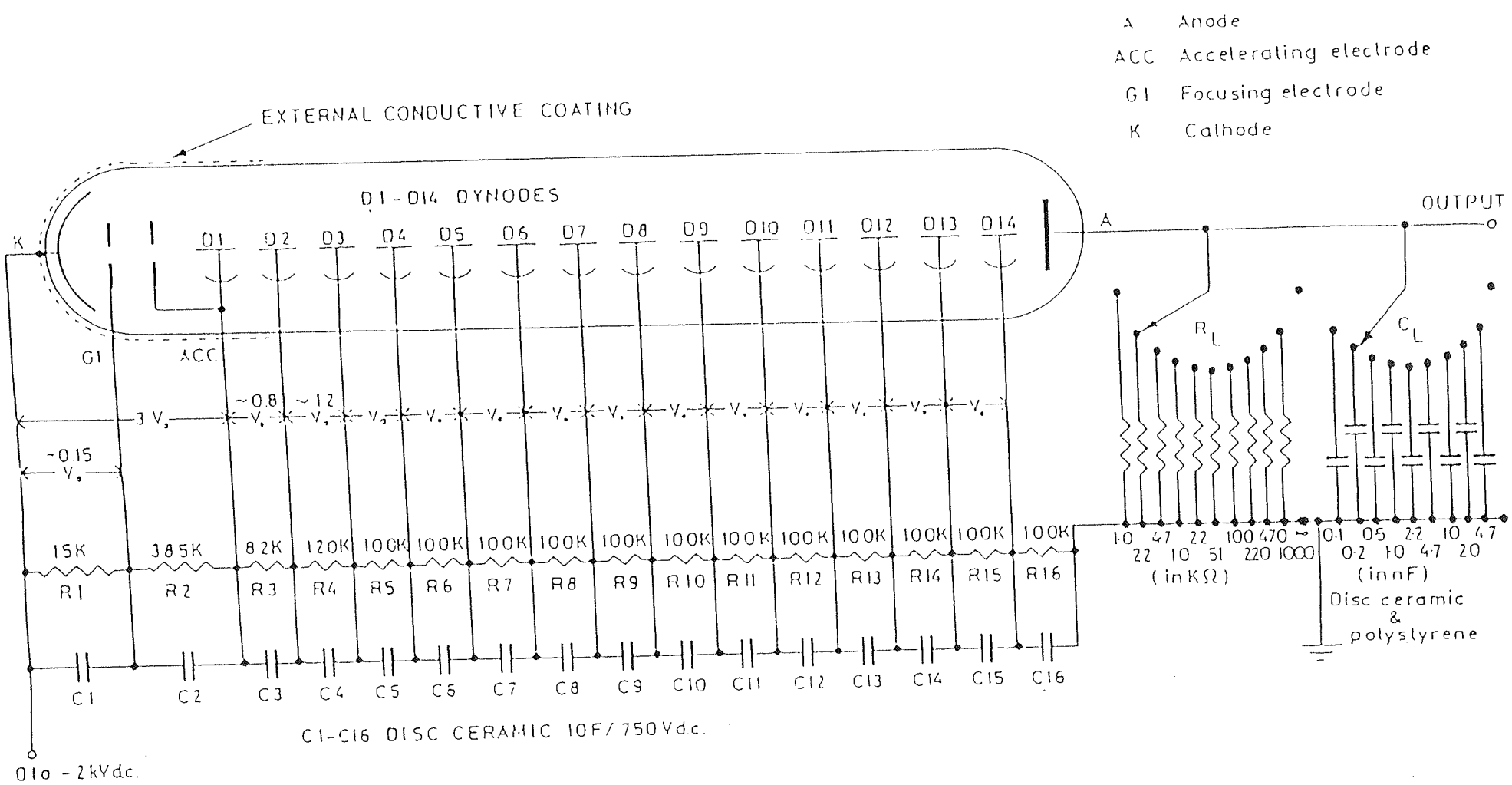

Figure 6.3 Electrical configuration of the electrodes of the photomultiplier tube

6.3 Kerr Cell

To date, there is no commercially available instrument for measuring Kerr constants. This means that every group working on the Kerr effect has built its own personalized equipment. Most instruments employ pulsed electric fields of different shape (square wave, bipolar, sawtooth, sinusoidal, etc.), and of variation duration, and frequency of repetition. These waveforms provide two major advantages over the previous dc field instruments because, in the first place, they minimizes the heating of the sample and reduce the problems arising from any electric conductivity, thus allowing measurements to be made on ionic solutions. Moreover, the evolution of birefringence with time can also be studied and valuable information about the dynamic properties of the polymer can be measured allowing valuable information about the conformation and shape of the polymer to be obtained.

Figures 6.4 - 6.7 are the diagrams for the Kerr cell used throughout this work. The Kerr cell consists of two tubes, one of glass and one of Perspex. The glass tube is placed inside the Perspex tube. Two Teflon end caps hold the tubes in place (refer to figure 6.6 and 6.7). A metal frame ensures a positive pressure between the glass tube and the Teflon by compressing the whole arrangement together. A silicon based sealant creates a seal between the Perspex tube and the Teflon. Each Teflon end cap has a hole drilled through its' centre and is fitted with a quality optical quartz disk that acts as a window. A hollow brass retaining ring, through which heated/cooled water is passed, and a rubber 'O' ring secure and seal the quartz windows to the Teflon end caps. A simple paper washer provides a seal between the quartz disk and the Teflon.

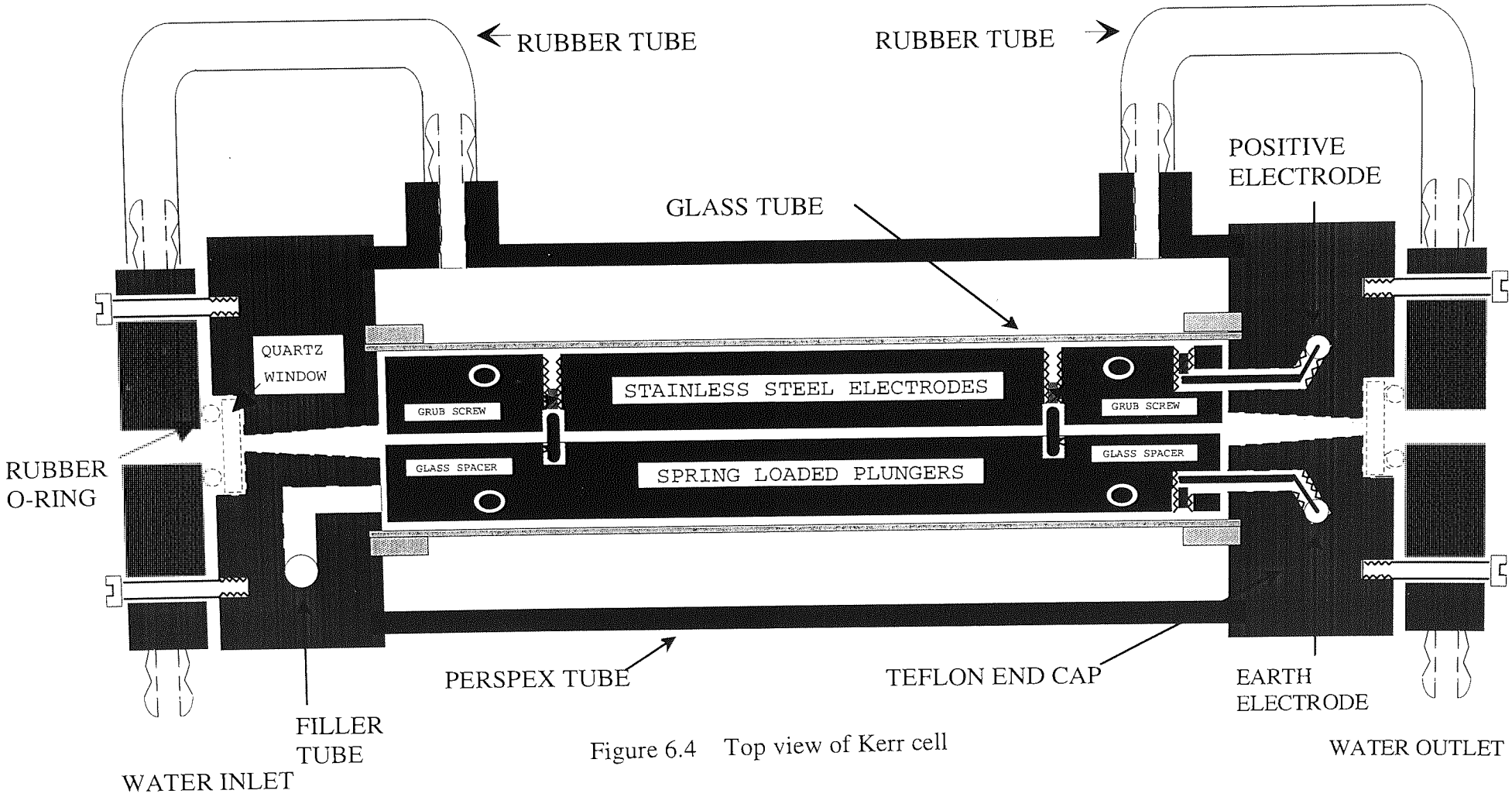

Figure 6.4 Top view of Kerr cell

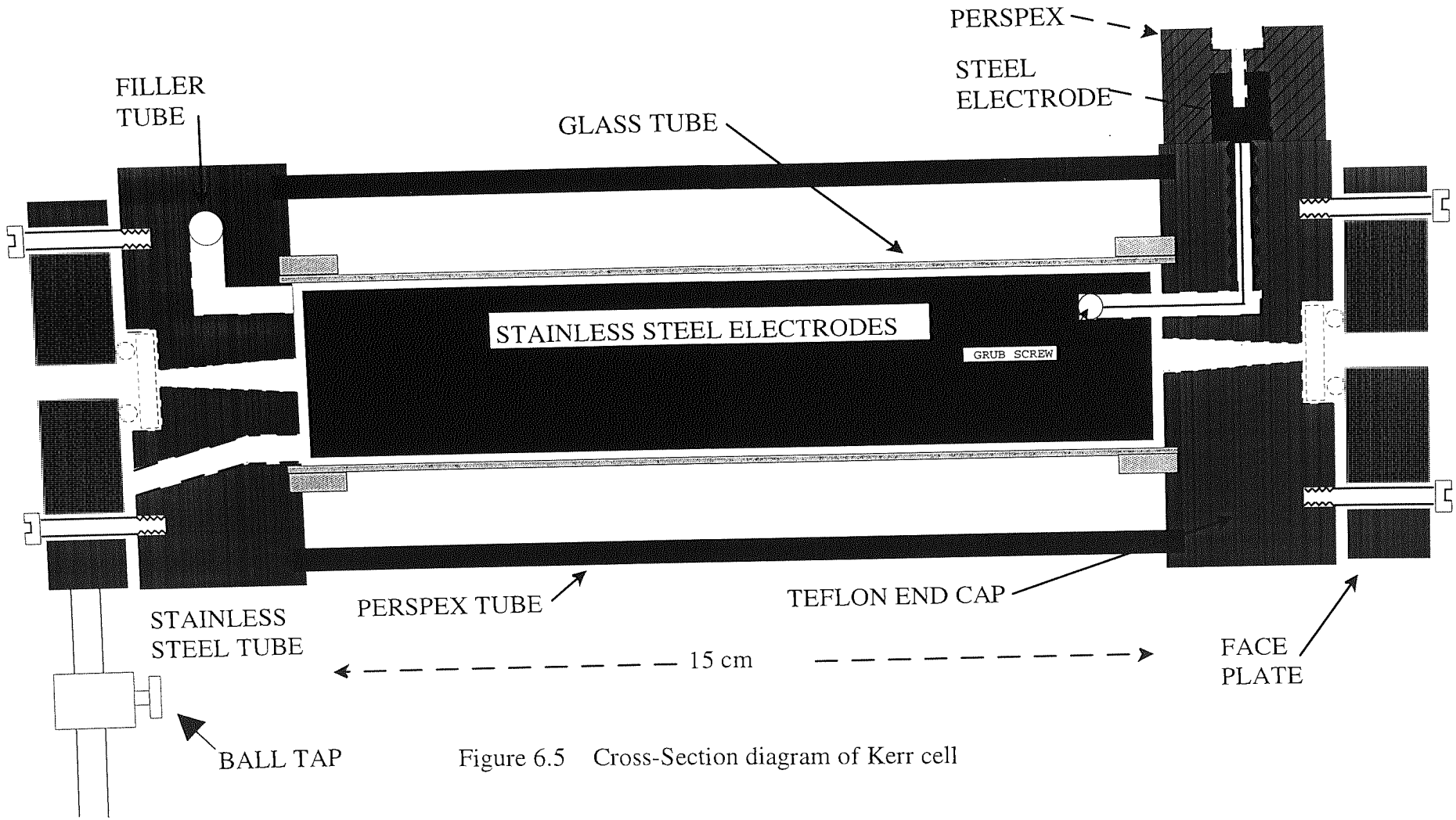

Figure 6.5 Cross-Section diagram of Kerr cell

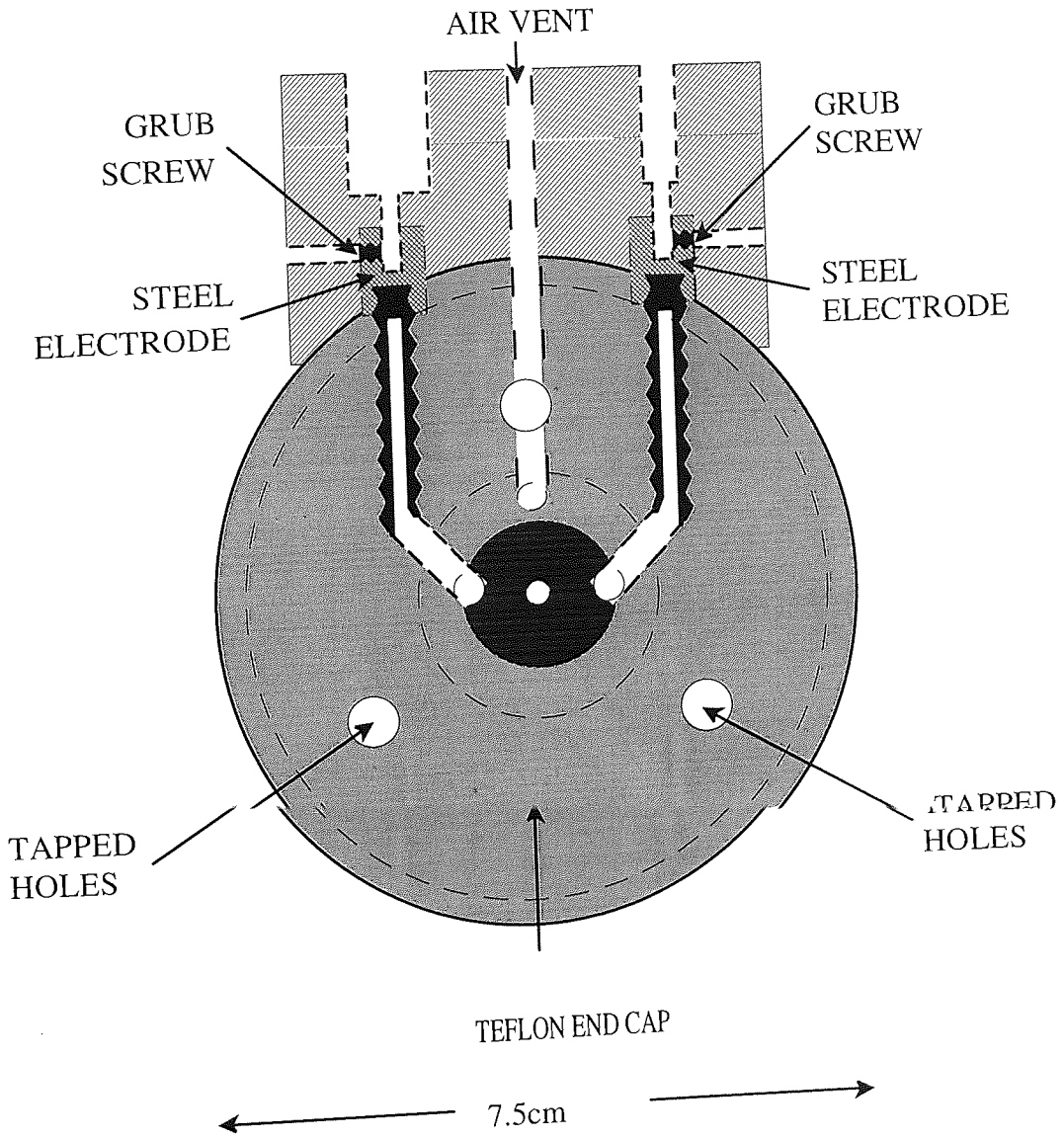

Figure 6.6 Front view of Kerr cell (side 1)

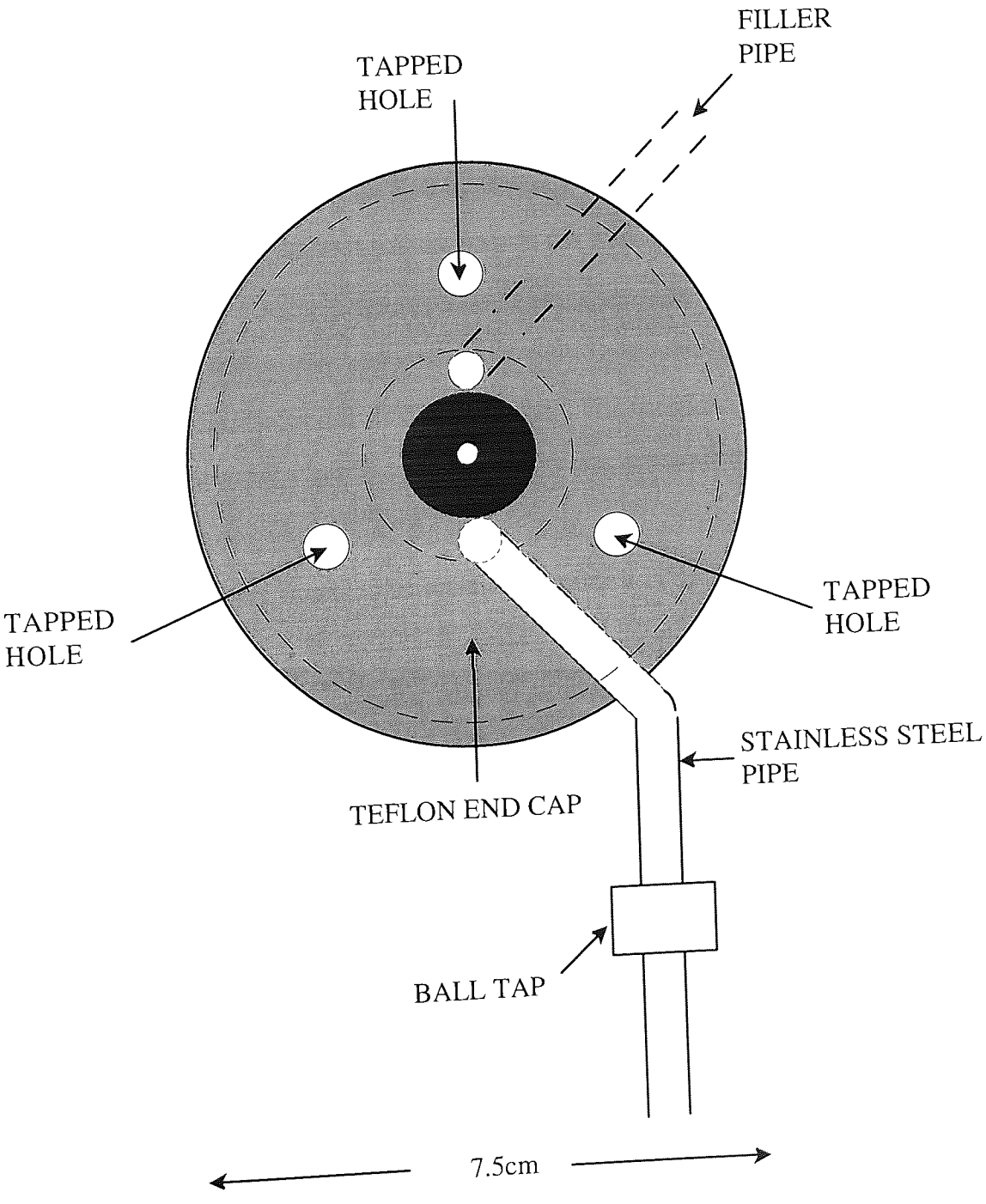

Figure 6.7 Front view of Kerr cell (side 2)

6.4 Optical Alignment

In optical systems, light is lost due to reflection and refractions from the optical components. Such loss of light increases with any misalignment of the optical components and would consequently reduce the signal/noise ratio. It is therefore important to properly align the optical components of the Kerr apparatus to minimise scattering and to prevent the hindrance of the light beam as it passed through the Kerr cell and other components prior to the photomultiplier tube. Deformations of the photocurrent pulses from the required rectangular shape are usually observed when there is an misalignment of the light beam with respect to the electrodes in the Kerr cell. The lateral position of the Kerr cell containing the electrodes and the liquid sample was achieved by fine adjustment of a transverse mechanism while observing the image of the light beam on a paper screen. The position of the cell was judged to be satisfactory when a single, uniform circular light was observed.

The screen was also placed between the analyser and the photomultiplier in order to observe the quality of the extinction of the image when the polarizers are crossed. Failure to achieve an extinction of the image would usually indicate the presence of a mechanically-induced optical strain due to overtightening of the securing screws of the windows of the cell. The light beam could also be moved vertically as desired by means of adjusting screws on the laser mounting.

6.5 Measurement of Experimental Kerr Constants (B)

The experimentally determined Kerr constant B, is defined by the equation:

$$B = \frac{\delta}{2\pi l E^2} \qquad (6.2)$$

where δ is the electrically induced phase difference between the components of plane polarized light possessing electric vectors parallel and perpendicular to the applied electric field E and l is the optical path length between the electrodes. E (=V/d) is the applied electric field and d and V are the electrode separation and applied voltage, respectively.

For the pulsed electric field method of measuring the Kerr effect the rotation of the plane of the plane of polarization , α , is related to the phase difference, δ, by

$$\alpha = \frac{\delta}{4} \qquad (6.3)$$

Eliminating δ from equation 6.2 and 6.3 and rearranging gives:

$$\alpha = \frac{\pi l (V/d)^2}{2} \qquad (6.4)$$

If the Kerr law is obeyed, then a plot of α versus V^2 should give a straight line graph passing through the origin with a gradient of $(\pi l B) / 2d^2$, from which the experimental Kerr constant B may be determined.

6.6 Measurement of Relative Kerr Constant

The Kerr effect of liquid samples was determined by comparing their electrically induced phase differences, δ , with that of a standard. The Kerr cell was first calibrated with a liquid of known Kerr constant, B_S. If the gradients of plots of α verses V^2 for the unknown and standard liquids are denoted by M_x and M_S respectively, then the experimental Kerr constant of the unknown material B_x can be readily calculated using the simple relationship:

$$B_x = \frac{M_x}{M_S} B_S \qquad (6.5)$$

Toluene is often used as the standard liquid.

6.7 Preparation of solutions of PVK and PVK : TNF complexes in 1,4-dioxane

Solutions of PVK samples F1 - F3 and model compound, N-ethylcarbazole (1% and 2% w/v) were prepared by dissolving accurately weighed quantities (approximately 0.5g and 1g) of polymer in $50cm^3$ of 1,4-dioxane. Granular forms of the polymers were first crushed into powders to aid the dissolution. In some cases, sonification was employed to aid the dissolution of the polymers. Generally, the solutions were allowed to stand for at least 24 hours to ensure that all the material has gone into solution. The solutions were transparent and viscous.

Similarly, solutions of the PVK : TNF complex were prepared by dissolving 1.0g (2% w/v) of polymer and 0.25g (0.5% w/v) of TNF in 50cm^3 of 1,4-dioxane. These solutions had an intense red colour. The solutions of N-ethylcarbazole and TNF were restricted to low concentrations (N-ethylcarbazole (1%) and TNF (0.25%)). This was due to the fact that the intense red colour strongly attenuated the laser light. All the solutions were filtered through paper filters type SS 3.0μm.

6.8 Experimental Kerr constants of Poly(N-vinylcarbazole) and its charge transfer complexes

Before the experimental Kerr contant of polymers and their complexes were measured, the Kerr cell had to be calibrated with a liquid of known experimental Kerr contant. In this work pure toluene (HPLC grade) was used for this purpose. The experimental Kerr constants at other temperatures (308K, 318K, 328K and 338K) were obtained by measuring the plane of the plane of polarization, α, and plotting them against the square of the applied voltage, V^2. The table 6.1 shows the experimental Kerr constants for toluene at different temperatures.

Temperature / K	Calibration constant for cell using toluene	Gradient (α/V^2) for toluene	Experimental Kerr constant (B_1) / 10^{-14} m V^{-2}
298	1389	0.05689	0.790
308	1389	0.05489	0.762
318	1389	0.05303	0.736
328	1389	0.05128	0.712
338	1389	0.04965	0.689

Table 6.1 Experimental Kerr constant of toluene

The solution experimental Kerr constants, B_{12}, of each polymer and that of the model compound, N-ethylcarbazole were determined at 298K, 308K, 318K, 328K and 338K in solution in 1,4-dioxane. These values of B_{12} were obtained by making measurements of analyser rotation, α, and plotting them against the square of the applied voltage, V^2. The gradient of such a plot was then compared to the gradient of a similar plot for pure toluene of known experimental Kerr constant (B_1) for one of the cited temperatures.

The molar Kerr constants ($_mK_2$) of the polymer samples and model compound were then calculated using:

$$_mK_2 = \frac{_mK_{12} - f_{1\,m}K_1}{f_2} \qquad (6.6)$$

where:

f_1 and f_2 are mole fractions of solvent and solute, respectively.

The molar Kerr constants of the solvent, ${}_mK$, is given by

$$ {}_mK_1 = \frac{6\lambda n_1 B_1 M_1}{((n_1)^2 + 2)^2(\varepsilon_1 + 2)^2 d_1} \qquad (6.7) $$

Where B_1, ε_1, M_1, n_1, and d_1 are the experimental Kerr constant, dielectric permittivity, relative molar mass, refractive index and density of the solvent, respectively.

The molar Kerr constant of the solution is given by

$$ {}_mK_{12} = \frac{6\lambda n_{12} B_{12} M_{12}}{((n_{12})^2 + 2)^2(\varepsilon_{12} + 2)^2 d_{12}} \qquad (6.8) $$

Where B_{12}, ε_{12}, M_{12}, n_{12}, and d_{12} are the experimental Kerr constant, dielectric permittivity, relative molar mass, refractive index and density of the solution, respectively.

In the calculation of the molar Kerr constants of the complexes, the quantity ε_{12} is replaced by the dielectric permittivity of the complex (i.e., $\varepsilon_{complex} = \varepsilon_{solution} - \varepsilon_{free\ polymer} - \varepsilon_{free\ TNF}$) (see Chapter 5).

The refractive index of the solutions was assumed to be approximately equal to the refractive index of the solvent since the concentrations of the polymer solutions were low

(1% - 2% w/v). The densities of the polymer solutions was also assumed to be approximately equal to that of the solvent.

Sample	Temperature (K)	Experimental Kerr Constant (B_1) / $10^{-16}(mV^{-2})$	Molar Kerr Constant ($_mK_1$) /$10^{-21}(m^5V^{-2}mol^{-1})$
1,4-dioxane	298	8.981 +/- 0.179	1.300 +/- 0.026
	308	7.943 +/- 0.159	1.169 +/- 0.023
	318	7.681 +/- 0.154	1.164 +/- 0.023
	328	7.481 +/- 0.150	1.159 +/- 0.023
	338	7.634 +/- 0.153	1.212 +/- 0.024

Table 6.2 Experimental and molar Kerr constants of 1,4-dioxane

Table 6.3 and 6.4 lists the solution experimental and Molar Kerr constants of polymer samples F1, F2, F3 and N-ethylcarbazole determined using solute concentrations of 1% and 2% w/v, respectively. The comparable results for charge transfer complexes are also shown in Table 6.5. The experimental Kerr constants can be reproduced within error limits of +/- 2%.

Sample	Temperature / K	Experimental Kerr Constant, B_{12} / 10^{-15} (mV^{-2})	Molar Kerr Constant, $_mK_{12}$ / 10^{-20}($m^5V^{-2}mol^{-1}$)
F1	298 308 318 328 338	-4.63 +/- 0.09 -4.52 +/- 0.09 -4.18 +/-0.08 -3.86 +/-0.07 -3.46 +/- 0.07	-0.73 +/- 0.01 -0.73 +/- 0.01 -0.69 +/- 0.01 -0.65 +/- 0.01 -0.60 +/- 0.01
F2	298 308 318 328 338	-16.91 +/- 0.34 -15.86 +/- 0.32 -13.98 +/- 0.28 -13.46 +/-0.27 -13.07 +/- 0.26	-2.60 +/- 0.05 -2.48 +/- 0.05 -2.26 +/- 0.05 -2.23 +/- 0.04 -2.22 +/- 0.04
F3	298 308 318 328 338	-14.19 +/- 0.28 -13.63 +/- 0.27 -12.83 +/- 0.26 -11.96 +/- 0.24 -11.17 +/- 0.22	-2.25 +/- 0.05 -2.20 +/- 0.04 -2.13 +/- 0.04 -2.04 +/- 0.04 -1.95 +/- 0.04
NEK	298 308 318 328 338	1.21 +/- 0.02 1.26 +/- 0.03 1.33 +/- 0.03 1.32 +/- 0.03 1.30 +/- 0.03	0.19 +/- 0.04 0.20 +/- 0.04 0.22 +/- 0.04 0.22 +/- 0.04 0.23 +/- 0.04

NEK = N-ethylcarbazole

Table 6.3 Experimental and Molar Kerr constants for 1% w/v solutions of various stereostructural forms of PVK in 1,4-dioxane at various temperatures.

Sample	Temperature / K	Experimental Kerr Constant, B_{12} / 10^{-15} (mV^{-2})	Molar Kerr Constant, ${}_mK_{12}$ / 10^{-20}($m^5V^{-2}mol^{-1}$)
F1	298 308 318 328 338	-8.83 +/- 0.18 -8.15 +/- 0.16 -8.05 +/- 0.16 -7.17 +/- 0.14 -6.69 +/- 0.13	-1.39 +/- 0.03 -1.30 +/- 0.03 -1.32 +/-0.03 -1.21 +/- 0.02 -1.16 +/-0.02
F2	298 308 318 328 338	-34.33 +/- 0.69 -30.67 +/- 0.61 -29.22 +/- 0.58 -26.07 +/- 0.52 -23.50 +/- 0.47	-5.20 +/- 0.10 -4.72 +/- 0.09 -4.65 +/- 0.09 -4.25 +/- 0.08 -3.94 +/- 0.08
F3	298 308 318 328 338	-20.18 +/- 0.40 -18.11 +/- 0.36 -17.36 +/- 0.35 -16.41 +/- 0.33 -15.89 +/- 0.32	-3.15 +/- 0.06 -2.87 +/-0.06 -2.84 +/-0.06 -2.74 +/-0.05 -2.73 +/-0.05
NEK	298 308 318 328 338	1.71 +/- 0.03 1.54 +/- 0.03 1.56 +/- 0.03 1.58 +/- 0.03 1.57 +/- 0.03	0.22 +/- 0.04 0.25 +/- 0.05 0.26 +/- 0.05 0.27 +/- 0.05 0.27 +/- 0.05

NEK = N-ethylcarbazole

Table 6.4 Experimental and Molar Kerr constants for 2% w/v solutions of various stereostructural form of PVK in 1,4-dioxane at various temperatures.

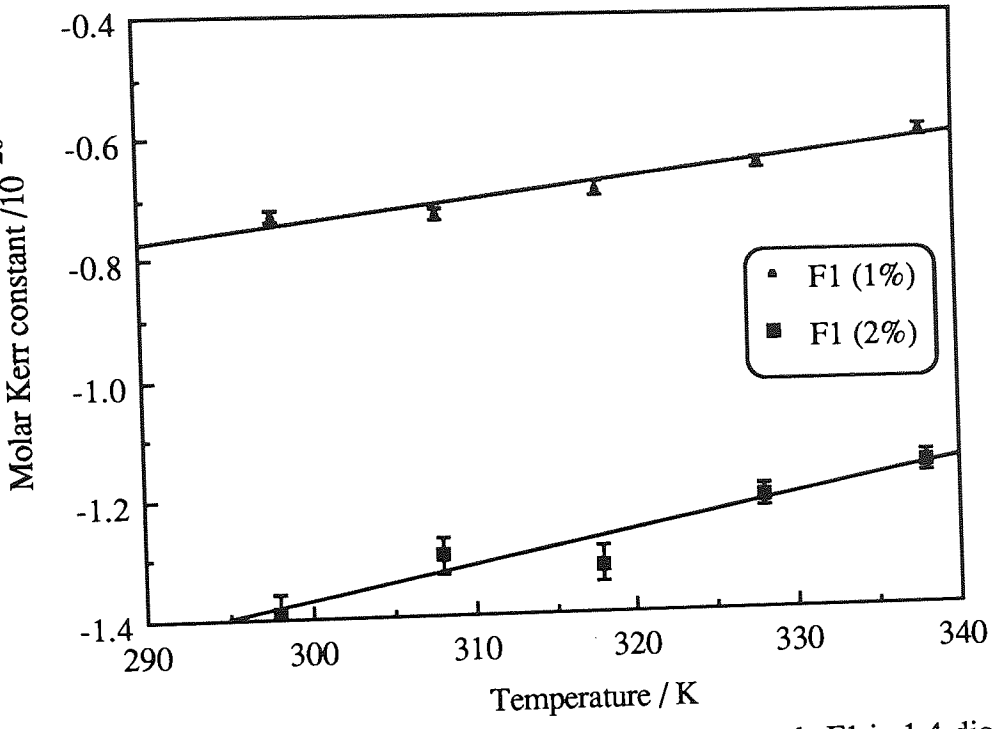

Figure 6.8 Solution molar Kerr constants of polymer sample F1 in 1,4-dioxane

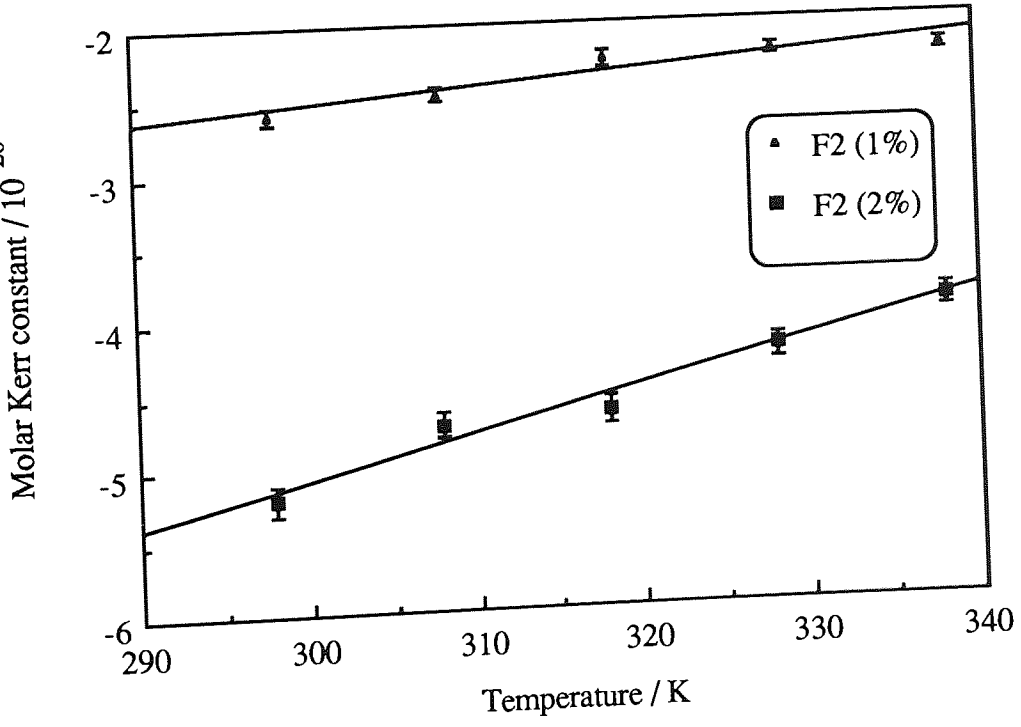

Figure 6.9 Solution molar Kerr constants of polymer sample F2 in 1,4-dioxane

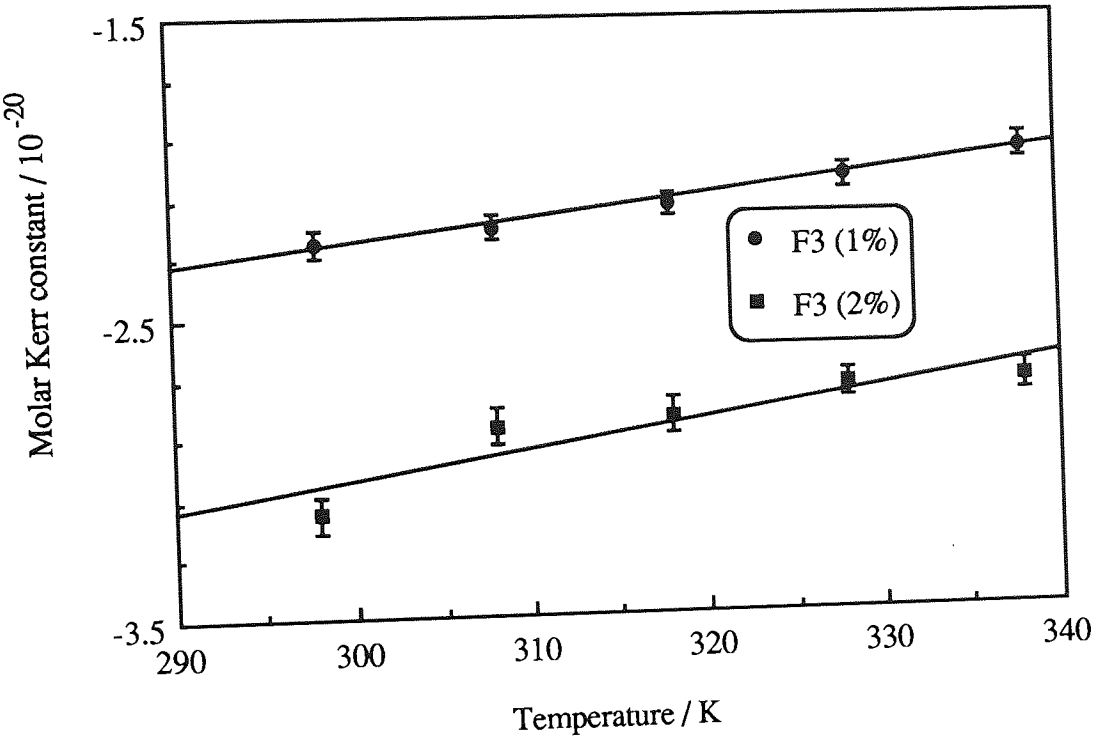

Figure 6.10 Solution molar Kerr constant of polymer sample F3 in 1,4-dioxane

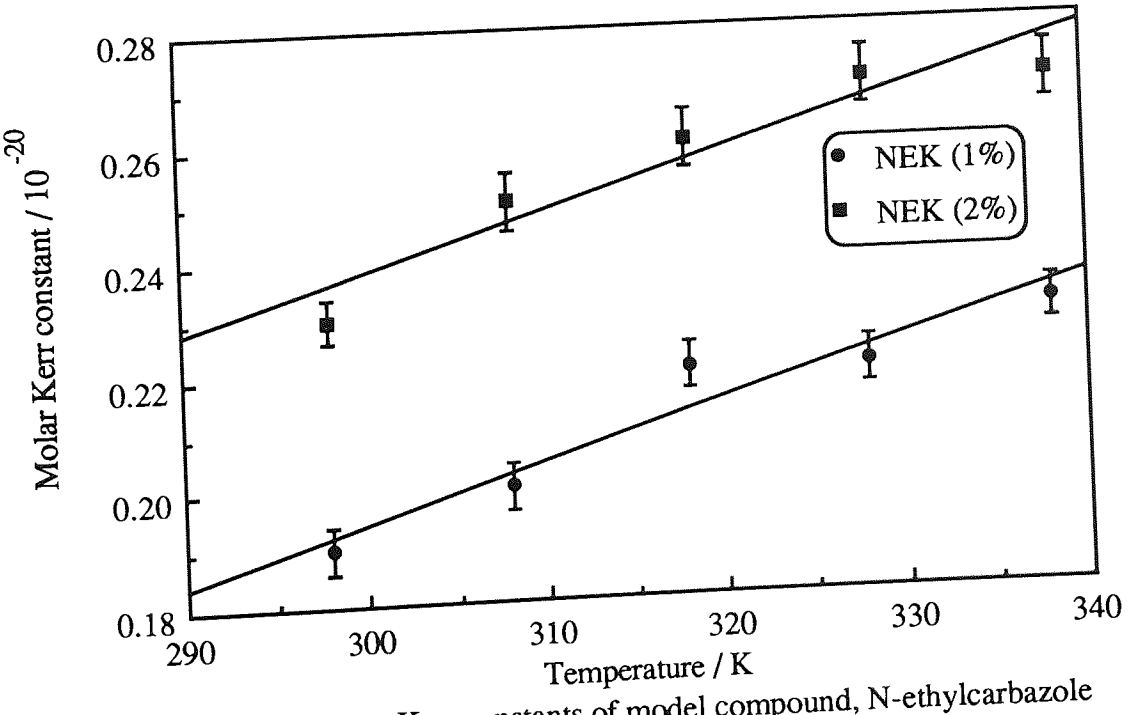

Figure 6.11 Solution molar Kerr constants of model compound, N-ethylcarbazole in 1,4-dioxane

Sample	Temperature / K	Experimental Kerr Constant of complexes, B_{12} / 10^{-15} (mV^{-2})	Molar Kerr Constant of complexes, ${}_mK_{12}$ /10^{-20} ($m^5V^{-2}mol^{-1}$)
F1 : TNF (2% : 0.5%)	298 308 318 328 338	-2.61 +/- 0.05 -2.39 +/- 0.05 -2.22 +/- 0.04 -1.95 +/- 0.04 -1.73 +/- 0.03	-0.45 +/- 0.009 -0.42 +/- 0.008 -0.39 +/- 0.008 -0.36 +/- 0.007 -0.33 +/- 0.007
F2 : TNF (2%: 0.5%)	298 308 318 328 338	-9.17 +/- 0.18 -8.79 +/- 0.18 -7.85 +/- 0.16 -7.62 +/- 0.15 -7.37 +/- 0.15	-1.57 +/- 0.03 -1.53 +/- 0.03 -1.40 +/- 0.03 -1.39 +/- 0.03 -1.37 +/- 0.03
F3 : TNF (2% : 0.5%)	298 308 318 328 338	-7.38 +/- 0.15 -6.96 +/- 0.14 -6.65 +/- 0.13 -6.51 +/- 0.13 -6.37 +/- 0.13	-1.24 +/- 0.02 -1.19 +/- 0.02 -1.17 +/- 0.02 -1.17 +/- 0.02 -1.17 +/- 0.02
NEK : TNF (1% : 0.25%)	298 308 318 328 338	0.67 +/- 0.01 0.62 +/- 0.01 0.55 +/- 0.01 0.46 +/- 0.009 0.40 +/- 0.008	0.11 +/- 0.004 0.11 +/- 0.005 0.10 +/- 0.005 0.08 +/- 0.005 0.07 +/- 0.005
TNF (2%)	298 308 318 328 338	1.91 +/- 0.04 1.66 +/- 0.03 1.59 +/-0.03 1.50 +/- 0.03 1.44 +/- 0.03	0.30 +/- 0.006 0.26 +/- 0.005 0.26 +/- 0.005 0.25 +/- 0.005 0.25 +/- 0.005

NEK = N-ethylcarbazole

Table 6.5 Experimental and molar Kerr constants for 2% : 0.5% w/v solution of various stereostructural forms of PVK : TNF complexes in 1,4-dioxane at various temperatures.

Figures 6.8 - 6.11 indicate a variation of molar Kerr constant per repeat unit of polymer with temperature. The plots shows the following interesting features:

(i) The molar Kerr constant of N-ethylcarbazole is positive whereas a negative molar Kerr constant is obtained for the polymer samples.

(ii) The molar Kerr constants of the polymers increases in magnitude as the isotactic content increases. Thus, polymer F2 (prepared by boron trifluoride etherate) shows the largest negative Kerr constant, whereas, sample F1, synthesised with azo-bisisobutyronitrile, shows the smallest negative molar Kerr constant. This trend is consistent with the dipole moment data (Chapter 4) where the largest dipole moment per repeat unit was were obtained for polymer F2 whereas polymer F1 showed the smallest dipole moment per repeat unit.

(iii) As the isotactic content in the polymer increases the temperature coefficient increases.

These results are discussed in detail below.

The molar Kerr constant of the solute in dilute solution may be resolved into a term θ_2 involving the permanent dipole moment, μ, and a term θ_1 involving only to induced dipole moments. The anisotropy term, θ_1, is expanded as

$$\theta_1 = [\ (a_1 - a_2)\ (b_1 - b_2) + (a_2 - a_3)\ (b_2 - b_3) + (a_3 - a_1)\ (b_3 - b_1)\ ]\ /\ 45kT \qquad (6.9)$$

and the dipolar term, θ_2, is expanded as

$$\theta_2 = [\ \{(\mu_1)^2 - (\mu_2)^2\}\ (b_1 - b_2) + \{(\mu_2)^2 - (\mu_3)^2\}\ (b_2 - b_3) + \{(\mu_3)^2 - (\mu_1)^2\}(b_3 - b_1)\ ]\ /\ 45kT^2 \qquad (6.10)$$

The parameters in Equation (6.9 and 6.10) are the electrostatic polarizabilities, a_1, a_2, and a_3, electro-optical polarizabilities, b_1, b_2 and b_3 and the dipole moment components μ_1, μ_2, μ_3 along the principle axes of the molecular polarizability ellipsoid.

The algebraic sign of the Kerr constant gives information concerning the disposition within the molecular framework of the resultant molecular dipole moment with respect to the principal axes of polarizability. This may be illustrated by a simple case. Assume that the resultant dipole moment μ of the molecule lies in the plane made by the axes b_1 and b_2 and makes an angle β with the former. Then, in equation 6.10, μ_3 is zero, $\mu_1 = \mu\cos\beta$ and $\mu_2 = \mu\sin\beta$. The part of equation 6.10 in square brackets then becomes

$$\mu^2[\, 3(b_1 - b_2)\cos^2 \beta + 2b_2 - b_1 - b_3] \qquad (6.12)$$

When $\beta = 0^o$, $\cos\beta = 1$ and the sign of θ_2 is controlled by $(b_1 - b_2)$. If b_1 is the axis of maximum polarizability, then θ_2 is positive. If on the other hand, β is 90^o, then $\cos\beta = 0$ and θ_2 is negative. The algerbraic sign of θ_2 changes from positive to negative when $3\cos^2\beta = 1$, i.e. when the angle β is 54.7^o. It is interesting to note that whilst the molecular Kerr constant of N-ethylcarbazole is positive the values for all the polymer samples are negative. These facts may be discussed in simplistic terms. The positive Kerr constants of the N-ethylcarbazole indicate that any angular displacement of the resultant molecular dipole moment vector from the principal axis of maximum polarizability is less than 54.7^o. However, it is believed that there is a strong tendency for the polymer to exist as a series of straight rigid helical sections[104, 101], because the rotations about bonds in PVK are severely sterically restricted. This places the planes of the carbazole units approximately normal to the axis of the helix. This means that the axis of maximum polarizability will be along a direction perpendicular to the helix axis, where the tendency for the individual group polarizabilities to be additive is greatest. However, the overall

repeat unit dipole moments of the carbazole groups are approximately perpendicular to the chain axis for PVK, and will cancel in along any direction taken perpendicular to the long axis of the rod yielding a resultant parallel to the helix axis. The nett effect, therefore, is that the resultant dipole moment of the molecule tends to be approximate perpendicular to the principal axis of polarizabilty, thus resulting in a negative Kerr constant.

The results obtained for the temperature coefficients are difficult to interpret quantitatively, because as the temperature rises the polymer chains are no longer rigid and rod-like but, instead, have some tendency to becoming more flexible. Rigid polymers rotate in solution in order to orientate in response to the application of electric field, whereas flexible polymers can also can change their shapes. Consequently, the treatment of results becomes more complicated as the flexibility of the polymer increases. In simplistic terms, supported by X-ray and NMR data it is suggested that polymer F2 consists largely of 3/1 helices and that sample F1, contains mostly 2/1 helices (see Chapter 3 and 7). As the temperature increases it is proposed that the helices tend to "unwind" and adopt a structure more closer to that of a random coil. The nett effect, in terms of polarizabilty is that the direction of the resultant dipole moment of the polymer molecule tends to deviate from being approximately perpendicular to the principal axis of polarizabilty, thus resulting in positive increase in the molar Kerr constant. This change is smallest in polymer F1, since it contains less 3/1 helical content, and consequently the molar Kerr constant is less sensitive to changes in temperature.

Sample	Temperature / K	Dipole Moment (μ) / 10^{-18}(esu)	Molar Kerr Constant (mK_{12}) / $10^{-20}(m^5V^{-2}mol^{-1})$
F1 (2%)	298	1.768	-1.39
	308	1.810	-1.30
	318	1.825	-1.32
	328	1.799	-1.21
	338	1.840	-1.16
F1 (2%): TNF (0.5%)	298	0.739	-0.45
	308	0.841	-0.42
	318	0.739	-0.40
	328	1.050	-0.36
	338	1.131	-0.33
F2 (2%)	298	3.236	-5.20
	308	3.216	-4.72
	318	2.208	-4.65
	328	2.245	-4.25
	338	2.214	-3.94
F2 (2%): TNF (0.5%)	298	6.089	-1.57
	308	5.741	-1.53
	318	5.713	-1.40
	328	5.694	-1.39
	338	5.716	-1.37
F3 (2%)	298	2.694	-3.15
	308	2.716	-2.87
	318	2.741	-2.84
	328	2.766	-2.74
	338	2.758	-2.73
F3 (2%): TNF (0.5%)	298	1.828	-1.24
	308	1.963	-1.19
	318	2.084	-1.17
	328	2.302	-1.17
	338	2.523	-1.17
NEK (2%)	298	2.202	0.22
	308	2.230	0.25
	318	2.202	0.26
	328	2.203	0.27
	338	2.212	0.27
NEK (1%): TNF (0.25%)	298	1.031	0.11
	308	0.980	0.11
	318	1.014	0.10
	328	0.993	0.08
	338	1.012	0.07

Table 6.6 The dipole moments and molar Kerr constants of pure polymer samples and of their corresponding TNF complexes in solution in 1,4-dioxane.

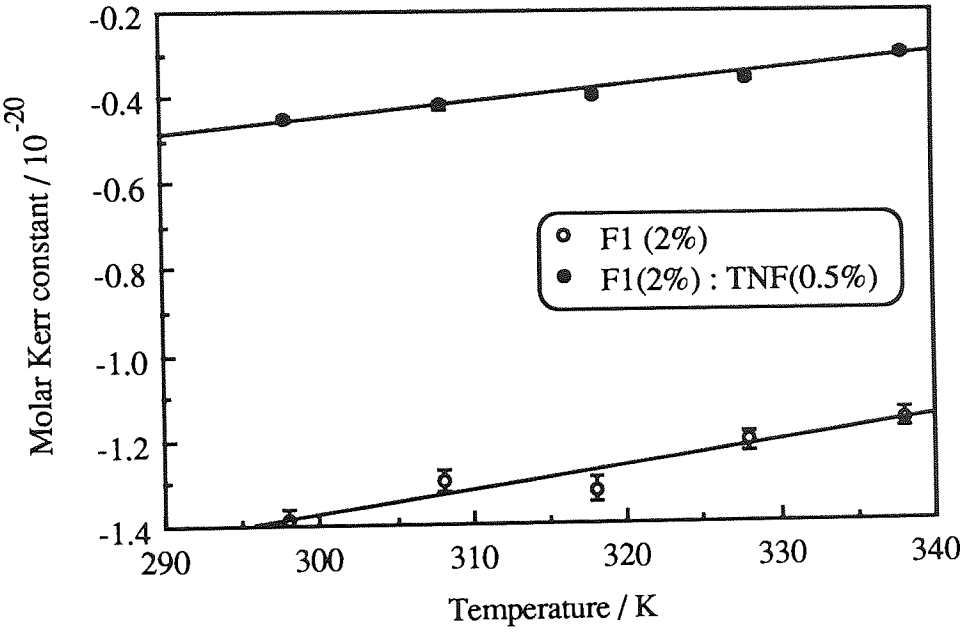

Figure 6.12 Solution molar Kerr constant of undoped polymer sample F1 and of the complexes of F1 : TNF in 1,4-dioxane

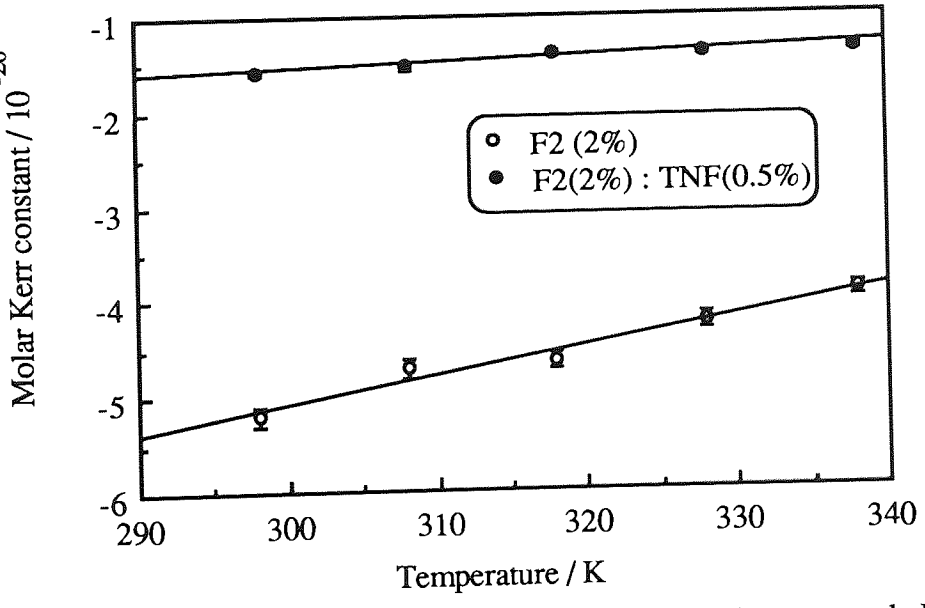

Figure 6.13 Solution molar Kerr constant of undoped polymer sample F2 and of the complexes of F2 : TNF in 1,4-dioxane

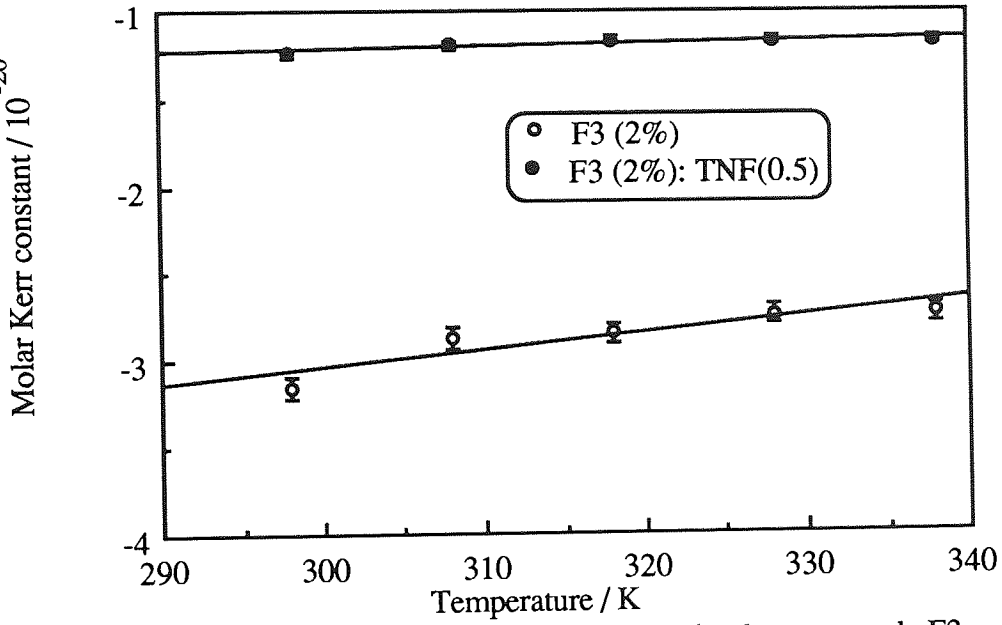

Figure 6.14 Solution molar Kerr constant of undoped polymer sample F3 and of the complexes of F3 : TNF in 1,4-dioxane

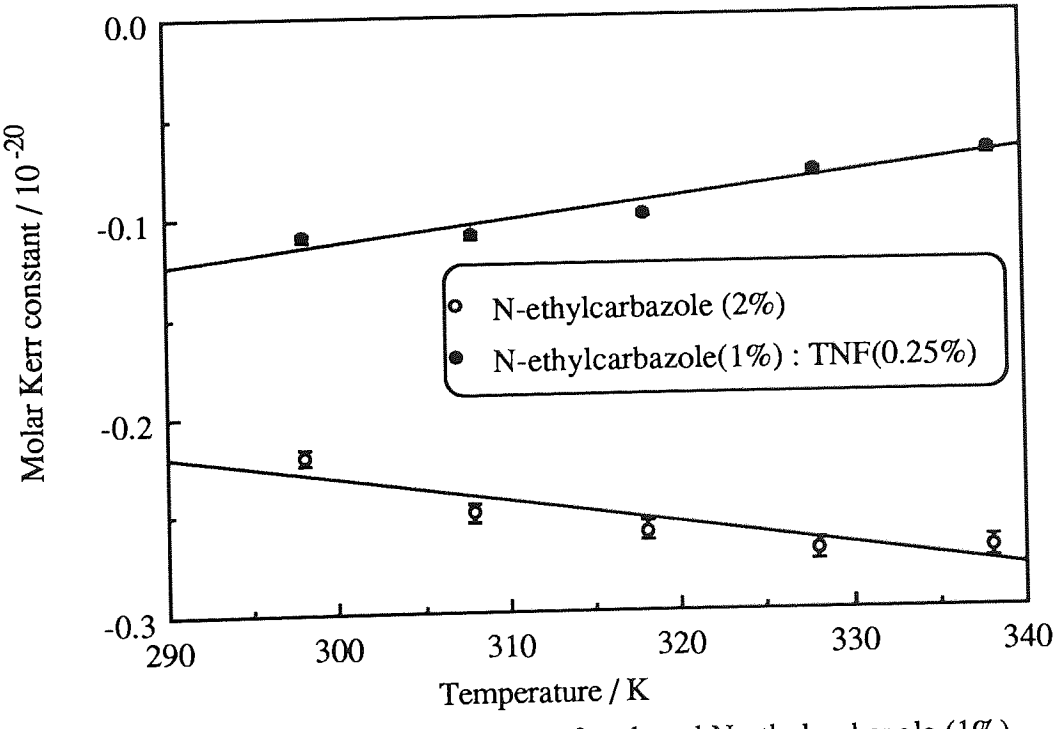

Figure 6.15 Solution molar Kerr constant of undoped N-ethylcarbazole (1%) and of the complexes of N-ethylcarbazole(1%) : TNF(0.25%)

Table 6.6 and Figures 6.12 - 6.15 compares the molar Kerr constants of charge transfer complexes formed between PVK and TNF to the Kerr constants of the corresponding undoped polymers. It is interesting to note that each PVK type (F1, F2, F3) formed TNF complexes and had solution molar Kerr constants that were smaller than solution Kerr constant of the corresponding pure polymer. This difference denoted by $\Delta({}_mK_{12})$, becomes smaller with an increase in the isotactic level of the polymer. Thus, PVK sample F1 (lowest isotactic) $\Delta({}_mK_{12}) = 0.11$ and for PVK (F2) (highest isotactic) $\Delta({}_mK_{12}) = 1.06$. These observations may be explained by concluding that complex formation is accompanied by a decrease in the optical anisotropy compared to that of the pure polymer. These changes could be due, in part, to a smaller dipole moment associated with the complex relative to that of the repeat unit of the pure polymer. However, the dipole moment data (see Table 6.6) indicates that the resultant dipole moment of the complex for polymer sample F2 is greater than that of the pure polymer, whereas a reduction in dipole moments per complex moiety is observed for polymer samples F1 and F3. Therefore, it appears that the dipole moments contributions to the Kerr constants, in this instance, are insignificant when compared to change to the optical anisotropy contribution.

6.9 Conclusions

The experimental Kerr constants of undoped poly(N-vinylcarbazole) and when complexed with electron acceptor (2,4,7-trinitroflurenone) were determined in 1,4-dioxane and molar Kerr contants per repeat unit of polymer was calculated. The influence of tacticity influence on the Kerr effect was investigated by studying three different PVK polymers (F1, F2 and F3) and the model compound (N-ethylcarbazole). The latter may be taken to represent a single repeat unit of PVK. From the results it can be concluded that the Kerr constant for PVK systems shows a high sensitivity to stereostructure. All of the polymers had a negative Kerr constant in contrast to N-ethylcarbazole which was positive. The

positive Kerr constant of the N-ethylcarbazole suggest that angular displacement of the resultant molecular dipole moment vector from the principal axis of maximum polarizability is small. However, since PVK exist as a series of straight rigid helical sections, the axis of maximum polarizability will be perpendicular to the chain axis, where the tendency for the individual group polarizabilities to be additive is greatest. However, the overall repeat unit dipole moment is approximately perpendicular to the chain axis for PVK, and will cancel along any direction taken perpendicular to the long axis of the rod. The resultant dipole moment of the molecule tends to be parallel to the principle axis of polarizability, thus resulting in a negative Kerr constant.

As the isotactic content of polymer increased, the molar Kerr constant per repeat unit was also observed to rise. Polymer F2 which was prepared with boron trifluoride etherate catalyst which had 55% isotactic content, showed the highest molar Kerr constant (-5.20 x $10^{-20}mV^{-2}$ at 298K for 2% w/v in 1,4-dioxane) whereas polymer F1 (prepared with aluminium chloride) had 30% isotacticity, -1.39 x $10^{-20}mV^{-2}$ was obtained under the similar experimental conditions. Dipole moment trends for PVK were also similar where they increase with an increase of isotactic content of polymer. Thus, the molar Kerr constants could be used alongside dipole moments to differentiate the stereostructures of PVK chains.

Positive temperature coefficients of Kerr constant were obtained for each of the types of PVK and were largest for polymer sample F2. This could be due to either a large change in the dipole moment or anisotropy. However, the dielectric data indicates that the temperature coefficient of dipole moments for polymer sample F2 is very small (see Chapter 4). Therefore, it appears that the dipole moment contributions to Kerr constants are rather insignificant and that changes in optical anisotropy mainly account for the differences in the Kerr constants of the undoped and complexed polymers.

All PVK samples produced TNF complexes with solution molar Kerr constants that were smaller than the solution Kerr constants of the pure (undoped) polymers. The magnitude of this difference becomes smaller with an increase of isotactic level of the polymer. This is only possible if the complex formation is accompanied by a decreased in the optical anisotropy compared to that of the pure polymer. It could also be due to a smaller dipole moment associated with the complex compared to the repeat unit of the pure polymer. However, the dipole moment indicates that the resultant dipole moment of the complex for polymer sample F2 is greater than that of the pure polymer, whereas reduced dipole moments are obtained for polymer samples F1 and F3. Therefore, for PVK polymers doped with TNF, the dipole moment contributions to the Kerr constants are rather insignificant with respect to the anisotropy contribution.

Chapter Seven

Molecular Modelling of Poly(N-vinylcarbazole) : Calculation of Interatomic Distances and Dipole Moments

7.1 Introduction

The various physical methods of structure determination such as, for example, dipole moments and electrical birefringence, may also be used to test molecular models. The general approach employed normally involves the calculation of some physical property of interest which is then compared with an experimentally determined value. Volkenstein[145] demonstrated that rotational isomeric state models could be very successfully used in the analysis of conformational-dependent properties of many types of polymer chain. Such models are now well established and are very successful when compared with the more simple freely-rotating or freely-jointed models[48].

Sundararajan[146] carried out the conformational analysis of PVK in terms of pairwise rotations around the skeletal bonds. As occurs with other vinyl chains bearing bulky planar substituents, the side group imposes severe restrictions on the available conformations so that the rotational isomeric states (RIS) scheme is suitable for the study of the configurational properties of PVK. By using this approach, the rather large unperturbed dimensions of the polymer were successfully explained.

Extensive calculations of end-to end distances and dipole moments, and their dependence upon composition and stereoregularity, have been presented for several polymers by

Mark[41]. The possibility of extending measurements into the region of very short chain length and the absence of any exluded volume effect on the dipole moments of most chain molecules were noted as being major advantages associated with the use of dipole moments, as opposed to end-to-end distances, for the characterisation of linear polymers. However, although mean-square dipole moments were found[41] to vary by up to factors of approximately 4 or 5 for different stereostructures of vinyl polymers, they were often either multivalued or nearly constant over a substantial range of tacticity, for polymers containing varying proportions of isotactic and syndiotactic blocks.

Kimura et al[36] showed that models of PVK reveals a rod like structure with reasonable intercarbazole group distances which seem to be confined to the isotactic 3/1 helix with TGTG conformation and the syndiotactic 2/1 helix consisting of TGTG' sequences. They concluded that the rodlike chains with a 4/1 helix and other higher order helices are improbable in PVK, because of the bulkiness of the carbazole groups.

In this chapter Desk Top Molecular Modeller (DTMM) by Polyhedron Software Ltd. was used to construct molecular models of syndiotactic and isotactic forms of poly(N-vinylcarbazole) by using the information on chain conformations of Kimura et al[36]. The interatomic distances between carbazole groups seperated by one pitch of the helix were calculated. The distances were compared to the Van der Waal's dimensions of 2,4,7-trinitro-9-fluorenone. This information forms a basis for understanding the nature of charge-transfer complexation between poly(N-vinycarbazole) and 2,4,7-trinitro-9-fluorenone and has been used to support the reasons for varying degree of complexation with isotactic and syndiotactic forms of PVK. The models were also used to calculate the dipole moments for comparison with the experimental values of syndiotactic and isotactic forms of PVK.

7.2 Overview of Desk Top Molecular Modelling Program

Desk Top Molecular Modeller (DTMM) by M.J.C. Crabbe (University of Reading) and J.R. Appleyard (Polyhedron Software Ltd.) is a simple-to-use molecular modellng, editing, and display package that offers some powerful and sophisticated facilities. The package is designed to run on all suitably equipped IBM PC, PS/2 microcomputers and PC compatibles. The software is operated using pull-down menus either directly from the keyboard or with the help of a mouse-driven pointer interface.

Desk Top Molecular Modeller operates by manipulating data loaded from structure files (see section 7.3). The software can display molecules comprising up to 1500 atoms and bonds, and subject to this overall limit, any number of molecules or fragments of molecules can be displayed immediately. The program allows manipulations that includes rotation of structures around any axis, translation in space, magnification and reduction of displays. When more than one molecule or fragment is to be displayed, it is possible to 'fix' one or more of these in orientation and space relative to the remaining structures, which are free to be manipulated. It is also possible to monitor the distances between up to three pairs of atoms in different molecules or fragments during any manipulation of the displayed structures.

The following six display styles are available:

(i) monochrome line (useful for fast response to changes)

(ii) coloured line (according to atom type),

(iii) stereo line pairs,

(iv) quick fill (elementary hidden-surface display),

(v) space fill (rigorous hidden-surface display), and

(vi) ball-and-stick

Additional options include superimposition of bonds on solid display; toggles for display of shading, highlights, atom outlines, perspective, bond thickness and removal of hydrogen atoms. Desktop Molecular Modeller offers calculation facilities to check and monitor bond lengths and angles and proximity of atoms. An energy minimization routine optimizes the geometry of molecules with up to 200 atoms and bonds. The parameters used in the calculations may be modified, and the routine produces a report on the progress of the minimization. The software also provides the facility to override the automatic assignments made by the minimization routine.

Screen images can be stored as compressed files on disk which can be redisplayed as full images through a seperate program DTMM*show*. The format used for storing the files is compatible with many paint packages. This offers the possibility of producing high-quality hard-copy ouput.

7.3 Data files

Desk Top Molecular Modeller stores atomic co-ordinate and connectivity data in files. Two types of data file with exactly the same structure are available for use with DTMM, and they are distinguished by their extensions. Files with the extension.MOL are intended to contain co-ordinate and connectivity data for whole molecules, whereas those with the extension.FRG are intended to contain information on molecular fragments. The files are standard ASCII text files which can be created or edited using a text editor or word processor.

The first four lines of the files contain header information and the remaining records specify the atoms comprising the molecules, their positions and connectivities. Each connection is expressed as an integer representing the number of the atom which is bonded. For atoms with fewer than 6 bonds the unused bonds are assigned the value zero or can be left blank.

The example below shows the molecular structure of benzene as defined in the DTMM data file BENZENE.MOL.

1C	1.69863	0.69201	0.00000	2	10	12	0	0	0
2C	0.50006	1.38401	0.00000	1	3	4	0	0	0
3C	0.69853	0.69203	0.00000	2	6	5	0	0	0
4H	0.50004	2.43401	0.00000	2	0	0	0	0	0
5H	1.60786	1.21703	0.00000	3	0	0	0	0	0
6C	0.69857	0.69196	0.00000	3	8	7	0	0	0
7H	1.60790	1.21695	0.00000	6	0	0	0	0	0
8C	0.49999	1.38401	0.00000	6	10	9	0	0	0
9H	0.49996	2.43401	0.00000	8	0	0	0	0	0
10C	1.69859	0.69207	0.00000	1	8	11	0	0	0
11C	2.60790	1.21710	0.00000	10	0	0	0	0	0
12H	2.56466	1.19200	0.00000	1	0	0	0	0	0

The format of the .FRG files is identical. The example given is that of the methyl group CH3, with only four atoms, all the hydrogen being connected to the single carbon atom.

1C	-0.77045	-0.32078	-0.03289	2	3	4	0	0	0
2H	-1.08538	0.14520	-0.95278	1	0	0	0	0	0
3H	-1.15977	-1.32150	0.03515	1	0	0	0	0	0
4H	-1.10370	0.27019	0.80836	1	0	0	0	0	0

7.4 Results and discussion

In this study the molecular models of helical forms (2/1 and 3/1) of PVK were drawn using Desk Top Molecular Modeller described above. Initially, in both isotactic and syndiotactic forms of PVK, all trans conformations ($\phi = 0^o$ bond angles) were assumed. The resultant planar backbone zig-zag structures of iso- and syndio- forms are represented in figure 7.1.

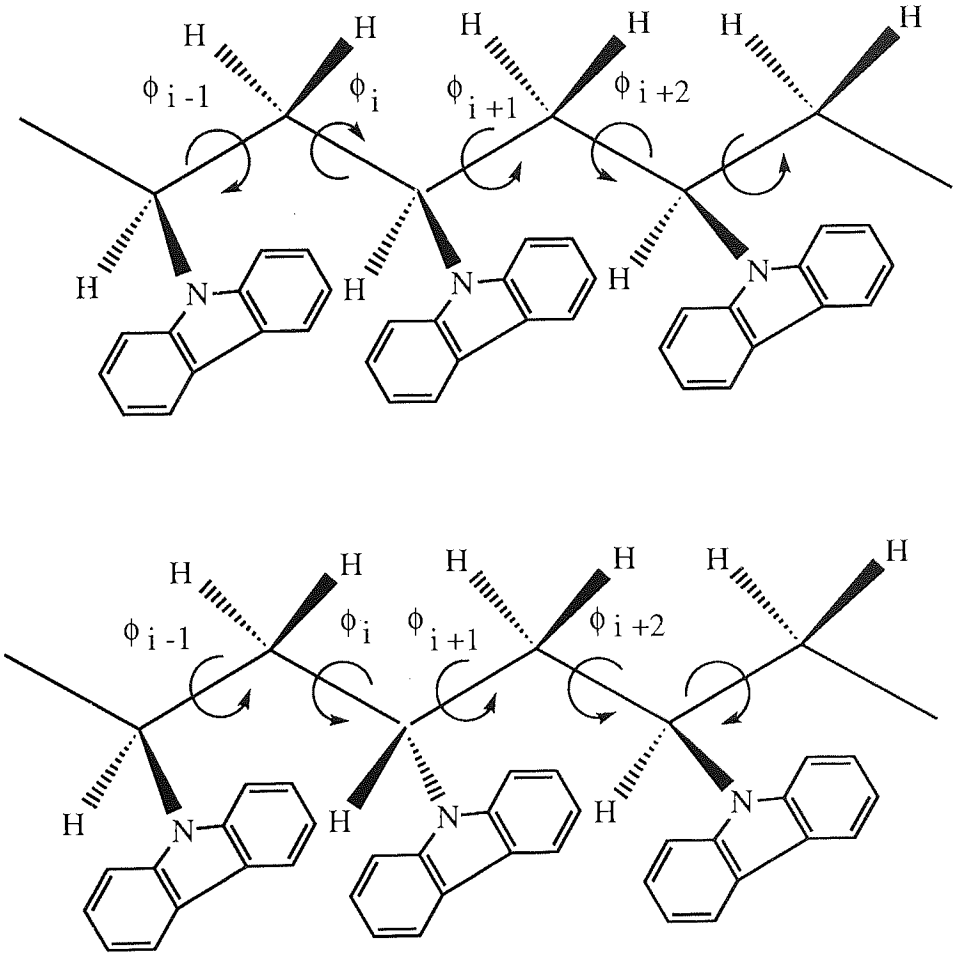

Figure 7.1 Isotactic and syndiotactic forms of poly(N-vinylcarbazole)

Table 7.1 and 7.2 list the DTMM data files for the 2/1 syndiotactic and 3/1 isotactic helices of PVK.

Poly(N-vinylcarbazole) Syndiotactic 2/1 Helix (109 atoms)

atom	x	y	z	atom connections
1 C	0.17723	2.73170	1.14874	2 3 4 5 0 0
2 C	-0.05356	1.29724	1.59926	1 6 7 88 0 0
3 H	0.82107	3.24374	1.87933	1 0 0 0 0 0
4 H	0.67020	2.72886	0.16516	1 0 0 0 0 0
5 C	-1.15357	3.46179	1.04694	1 18 19 46 0 0
6 H	-0.54430	1.29736	2.58375	2 0 0 0 0 0
7 C	-0.94072	0.58258	0.59157	2 8 9 10 0 0
8 H	-0.44931	0.58498	-0.39276	7 0 0 0 0 0
9 H	-1.90599	1.10558	0.51950	7 0 0 0 0 0
10 C	-1.17763	-0.85327	1.03372	7 11 12 67 0 0
11 H	-1.67071	-0.85711	2.01693	10 0 0 0 0 0
12 C	0.15386	-1.58203	1.13217	10 13 14 15 0 0
13 H	0.79445	-1.07003	1.86574	12 0 0 0 0 0
14 H	0.64658	-1.57524	0.14836	12 0 0 0 0 0
15 C	-0.07448	-3.01978	1.57419	12 16 17 109 0 0
16 H	-0.56614	-3.02665	2.55854	15 0 0 0 0 0
17 C	-0.95893	-3.73513	0.56592	15 20 21 25 0 0
18 H	-1.64611	3.46427	2.03070	5 0 0 0 0 0
19 C	-0.92176	4.89496	0.59675	5 22 23 24 0 0
20 H	-0.47372	-3.73127	-0.41012	17 0 0 0 0 0
21 H	-1.91861	-3.22297	0.49667	17 0 0 0 0 0
22 H	-0.43517	4.89519	-0.37862	19 0 0 0 0 0
23 H	-0.28558	5.40468	1.32034	19 0 0 0 0 0
24 H	-1.87832	5.41266	0.52572	19 0 0 0 0 0
25 H	-1.11624	-4.75451	0.88624	17 0 0 0 0 0
26 C	-1.42465	2.19009	-3.72027	27 33 35 0 0 0
27 C	-0.37050	2.85489	-3.07793	26 28 29 0 0 0
28 C	-0.42713	3.15338	-1.71144	27 31 30 0 0 0
29 H	0.50437	3.14234	-3.64938	27 0 0 0 0 0
30 H	0.38749	3.66581	-1.21314	28 0 0 0 0 0
31 C	-1.57107	2.76407	-1.01533	28 32 46 0 0 0
32 C	-2.61496	2.10512	-1.65552	31 33 36 0 0 0
33 C	-2.57025	1.80270	-3.01572	26 32 34 0 0 0
34 H	-3.38775	1.28730	-3.50581	33 0 0 0 0 0
35 H	-1.35140	1.97225	-4.77918	26 0 0 0 0 0
36 C	-3.57212	1.86946	-0.67101	32 37 42 0 0 0
37 C	-3.04263	2.40214	0.50135	32 38 46 0 0 0
38 C	-3.77605	2.34493	1.83537	37 39 44 0 0 0
39 C	-5.13272	1.64839	1.65839	38 40 45 0 0 0
40 C	-5.57853	1.14477	0.42978	39 42 41 0 0 0

Table 7.1 Atom coordinates and their connectivity data for four repeating carbazole groups in a 2/1 syndiotactic conformation.

Table 7.1 continued....

Poly(N-vinylcarbazole) Syndiotactic 2/1 Helix (109 atoms)

atom	x	y	z	atom connections
41 H	-6.54759	0.66197	0.38209	40 0 0 0 0 0
42 C	-4.81568	1.24443	-0.73748	36 40 43 0 0 0
43 H	-5.18387	0.84508	-1.67525	42 0 0 0 0 0
44 H	-3.44790	2.71907	2.78967	38 0 0 0 0 0
45 H	-5.77442	1.53968	2.52484	39 0 0 0 0 0
46 N	-1.82761	2.94562	0.29342	31 37 5 0 0 0
47 C	-1.41649	-2.12753	-3.73803	48 54 56 0 0 0
48 C	-0.36234	-1.46274	-3.09568	47 49 50 0 0 0
49 C	-0.41896	-1.16426	-1.72920	48 52 51 0 0 0
50 H	0.51253	-1.17530	-3.66713	48 0 0 0 0 0
51 H	0.39566	-0.65182	-1.23089	49 0 0 0 0 0
52 C	-1.56289	-1.55357	-1.03310	49 53 67 0 0 0
53 C	-2.60679	-2.21252	-1.67327	52 54 57 0 0 0
54 C	-2.56206	-2.51495	-3.03347	47 53 55 0 0 0
55 H	-3.37957	-3.03034	-3.52357	54 0 0 0 0 0
56 H	-1.34324	-2.34538	-4.79693	47 0 0 0 0 0
57 C	-3.56394	-2.44817	-0.68877	53 58 63 0 0 0
58 C	-3.03444	-1.91551	0.48360	57 59 67 0 0 0
59 C	-3.76788	-1.97270	1.81761	58 60 65 0 0 0
60 C	-5.12456	-2.66925	1.64063	59 61 66 0 0 0
61 C	-5.57036	-3.17286	0.41202	60 63 62 0 0 0
62 H	-6.53943	-3.65566	0.36434	61 0 0 0 0 0
63 C	-4.80751	-3.07320	-0.75524	57 61 64 0 0 0
64 H	-5.17570	-3.47257	-1.69301	63 0 0 0 0 0
65 H	-3.43973	-1.59857	2.77193	59 0 0 0 0 0
66 H	-5.76625	-2.77795	2.50709	60 0 0 0 0 0
67 N	-1.81944	-1.37202	0.27566	52 58 10 0 0 0
68 C	3.88605	-0.05969	-1.04830	69 75 77 0 0 0
69 C	2.75498	0.63058	-1.50657	68 70 71 0 0 0
70 C	1.70356	0.95485	-0.64112	69 73 72 0 0 0
71 H	2.69372	0.91900	-2.54945	69 0 0 0 0 0
72 H	0.82930	1.48970	-0.99343	70 0 0 0 0 0
73 C	1.82518	0.56523	0.69233	70 74 88 0 0 0
74 C	2.94823	-0.11958	1.14352	73 75 78 0 0 0
75 C	4.00141	-0.44832	0.29127	68 74 76 0 0 0
76 H	4.87352	-0.98064	0.65214	75 0 0 0 0 0
77 H	4.68411	-0.29593	-1.74215	68 0 0 0 0 0
78 C	2.73523	-0.33879	2.50274	74 79 84 0 0 0
79 C	1.49553	0.22919	2.78403	78 80 88 0 0 0
80 C	0.88348	0.21862	4.17904	79 81 86 0 0 0
81 C	1.82031	-0.50433	5.15717	80 82 87 0 0 0

Table 7.1 Atom coordinates and their connectivity data for four repeating carbazole groups in a 2/1 syndiotactic conformation.

Table 7.1 continued...

Poly(N-vinylcarbazole) Syndiotactic 2/1 Helix (109 atoms)

atom	x	y	z	atom connections
82 C	3.05392	-1.04616	4.77446	81 84 83 0 0 0
83 H	3.66368	-1.54012	5.52192	82 0 0 0 0 0
84 C	3.52506	-0.97180	3.46036	78 82 85 0 0 0
85 H	4.48418	-1.39849	3.19111	84 0 0 0 0 0
86 H	-0.05778	0.63483	4.49393	80 0 0 0 0 0
87 H	1.51361	-0.59808	6.19228	81 0 0 0 0 0
88 N	0.94205	0.77838	1.68544	73 79 2 0 0 0
89 C	3.83066	-4.39785	-1.08643	90 96 98 0 0 0
90 C	2.69960	-3.70758	-1.54468	89 91 92 0 0 0
91 C	1.64817	-3.38331	-0.67925	90 94 93 0 0 0
92 H	2.63834	-3.41916	-2.58758	90 0 0 0 0 0
93 H	0.77392	-2.84846	-1.03156	91 0 0 0 0 0
94 C	1.76980	-3.77294	0.65420	91 95 109 0 0 0
95 C	2.89285	-4.45774	1.10539	94 96 99 0 0 0
96 C	3.94603	-4.78649	0.25316	89 95 97 0 0 0
97 H	4.81814	-5.31880	0.61402	96 0 0 0 0 0
98 H	4.62872	-4.63408	-1.78027	89 0 0 0 0 0
99 C	2.67985	-4.67695	2.46463	95 100 105 0 0 0
100 C	1.44015	-4.10897	2.74590	99 101 109 0 0 0
101 C	0.82810	-4.11955	4.14091	100 102 107 0 0 0
102 C	1.76493	-4.84249	5.11906	101 103 108 0 0 0
103 C	2.99854	-5.38433	4.73633	102 105 104 0 0 0
104 H	3.60828	-5.87828	5.48379	103 0 0 0 0 0
105 C	3.46967	-5.30996	3.42223	99 103 106 0 0 0
106 H	4.42880	-5.73665	3.15300	105 0 0 0 0 0
107 H	-0.11316	-3.70333	4.45581	101 0 0 0 0 0
108 H	1.45823	-4.93624	6.15417	102 0 0 0 0 0
109 N	0.88666	-3.55979	1.64732	94 100 15 0 0 0

Table 7.1 Atom coordinates and their connectivity data for four repeating carbazole groups in a 2/1 syndiotactic conformation.

Poly(N-vinylcarbazole) Isotactic 3/1 Helix (83 atoms)

atom	x	y	z	atom connections
1 H	0.45025	-0.33804	-0.99832	2 0 0 0 0 0
2 C	0.45363	0.74189	-0.98718	1 3 4 5 0 0
3 H	-0.54326	1.10496	-0.69566	2 0 0 0 0 0
4 H	0.69972	1.11590	-1.99229	2 0 0 0 0 0
5 C	1.48812	1.24598	0.00797	2 6 7 83 0 0
6 H	1.24268	0.87219	1.01299	5 0 0 0 0 0
7 C	1.49182	2.76591	0.02278	5 8 9 14 0 0
8 H	1.73750	3.13832	-0.97172	7 0 0 0 0 0
9 H	2.23467	3.12045	0.73731	7 0 0 0 0 0
10 C	0.08990	4.79547	0.45178	11 12 13 14 0 0
11 C	0.42587	5.33434	-0.93051	10 15 16 41 0 0
12 H	0.83440	5.15955	1.17536	10 0 0 0 0 0
13 H	-0.90968	5.14835	0.74629	10 0 0 0 0 0
14 C	0.10509	3.27440	0.43120	7 10 20 62 0 0
15 H	1.42580	4.98467	-1.22710	11 0 0 0 0 0
16 C	0.40909	6.85489	-0.90318	11 17 18 19 0 0
17 H	-0.59223	7.20303	-0.60896	16 0 0 0 0 0
18 H	0.65049	7.24071	-1.90485	16 0 0 0 0 0
19 H	1.13777	7.21948	-0.19431	16 0 0 0 0 0
20 H	-0.64029	2.91047	-0.29154	14 0 0 0 0 0
21 C	-4.37603	5.42246	-1.93601	22 28 30 0 0 0
22 C	-3.73705	6.03202	-0.84701	21 23 24 0 0 0
23 C	-2.35256	5.92834	-0.66797	22 26 25 0 0 0
24 H	-4.32536	6.59423	-0.13121	22 0 0 0 0 0
25 H	-1.85693	6.40018	0.17241	23 0 0 0 0 0
26 C	-1.63513	5.19645	-1.61367	23 27 41 0 0 0
27 C	-2.27205	4.59286	-2.69245	26 28 31 0 0 0
28 C	-3.64998	4.68880	-2.88124	21 27 29 0 0 0
29 H	-4.13752	4.21657	-3.72591	28 0 0 0 0 0
30 H	-5.44926	5.52110	-2.04816	21 0 0 0 0 0
31 C	-1.26498	3.96310	-3.42055	27 32 37 0 0 0
32 C	-0.08374	4.22827	-2.73284	31 33 41 0 0 0
33 C	1.27393	3.72396	-3.20524	32 34 39 0 0 0
34 C	1.10977	2.90455	-4.49312	33 35 40 0 0 0
35 C	-0.12920	2.69225	-5.11096	34 37 36 0 0 0
36 H	-0.16699	2.10500	-6.02102	35 0 0 0 0 0
37 C	-1.31910	3.21193	-4.59286	31 35 38 0 0 0
38 H	-2.26458	3.03362	-5.09163	37 0 0 0 0 0
39 H	2.23594	3.88204	-2.74927	33 0 0 0 0 0
40 H	1.99399	2.47186	-4.94623	34 0 0 0 0 0

Table 7.2 Atom coordinates and their connectivity data for three repeating carbazole groups in a 3/1 isotactic conformation.

Table 7.2 continued...

Poly(N-vinylcarbazole) Isotactic 3/1 Helix (83 atoms)

atom	x	y	z	atom connections
41 N	-0.30735	4.97706	-1.63552	11 26 32 0 0 0
42 C	-3.08744	0.55806	3.06595	43 49 51 0 0 0
43 C	-3.14982	0.80708	1.68759	42 44 45 0 0 0
44 C	-2.18592	1.59630	1.04912	43 47 46 0 0 0
45 H	-3.95842	0.38036	1.10566	43 0 0 0 0 0
46 H	-2.23186	1.78847	-0.01646	44 0 0 0 0 0
47 C	-1.16297	2.12398	1.83641	44 48 62 0 0 0
48 C	-1.10422	1.87530	3.20333	47 49 52 0 0 0
49 C	-2.05829	1.09131	3.85036	42 48 50 0 0 0
50 H	-2.00347	0.90142	4.91576	49 0 0 0 0 0
51 H	-3.84795	-0.05745	3.53166	42 0 0 0 0 0
52 C	0.03049	2.54261	3.65943	48 53 58 0 0 0
53 C	0.58387	3.15141	2.53618	52 54 62 0 0 0
54 C	1.85878	3.98317	2.59561	53 55 60 0 0 0
55 C	2.38229	4.03802	4.03782	54 56 61 0 0 0
56 C	1.74944	3.38904	5.10558	55 58 57 0 0 0
57 H	2.17953	3.47017	6.09698	56 0 0 0 0 0
58 C	0.58107	2.64044	4.93567	52 56 59 0 0 0
59 H	0.11211	2.14711	5.77897	58 0 0 0 0 0
60 H	2.36344	4.48288	1.78693	54 0 0 0 0 0
61 H	3.28452	4.60369	4.23860	55 0 0 0 0 0
62 N	-0.14002	2.89789	1.42869	14 47 53 0 0 0
63 C	5.26104	-1.41426	1.68252	64 70 72 0 0 0
64 C	4.04783	-1.15848	2.33710	63 65 66 0 0 0
65 C	3.05146	-0.37843	1.73844	64 68 67 0 0 0
66 H	3.87789	-1.57263	3.32409	64 0 0 0 0 0
67 H	2.11256	-0.18105	2.24244	65 0 0 0 0 0
68 C	3.31242	0.13315	0.46767	65 69 83 0 0 0
69 C	4.51692	-0.12220	-0.17866	68 70 73 0 0 0
70 C	5.51670	-0.89718	0.40734	63 69 71 0 0 0
71 H	6.45155	-1.09238	-0.10460	70 0 0 0 0 0
72 H	6.01293	-2.02237	2.17136	63 0 0 0 0 0
73 C	4.43091	0.52907	-1.40723	69 74 79 0 0 0
74 C	3.17789	1.13589	-1.42261	73 75 83 0 0 0
75 C	2.67357	1.95160	-2.60626	74 76 81 0 0 0
76 C	3.74247	1.99370	-3.70752	75 77 82 0 0 0
77 C	4.98034	1.3479	-3.59589	76 79 78 0 0 0
78 H	5.68441	1.41939	-4.41665	77 0 0 0 0 0
79 C	5.33863	0.61452	-2.46092	73 77 80 0 0 0
80 H	6.30277	0.12333	-2.40077	79 0 0 0 0 0
81 H	1.72498	2.44857	-2.71372	75 0 0 0 0 0
82 H	3.52841	2.54731	-4.61417	76 0 0 0 0 0
83 N	2.49790	0.89616	-0.28465	5 68 74 0 0 0

Table 7.2 Atom coordinates and their connectivity data for three repeating carbazole groups in a 3/1 isotactic conformation.

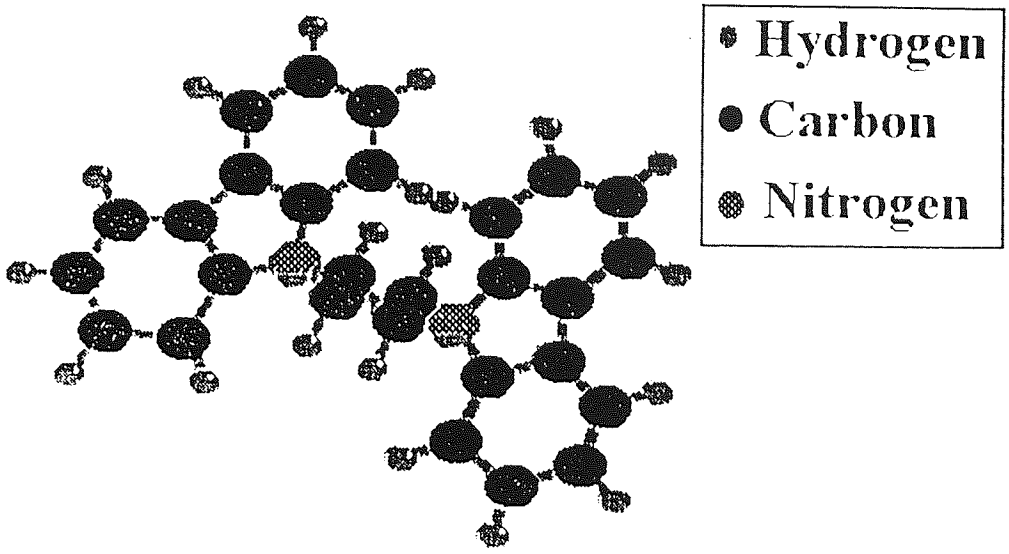

Transverse view of 2/1 helix of PVK

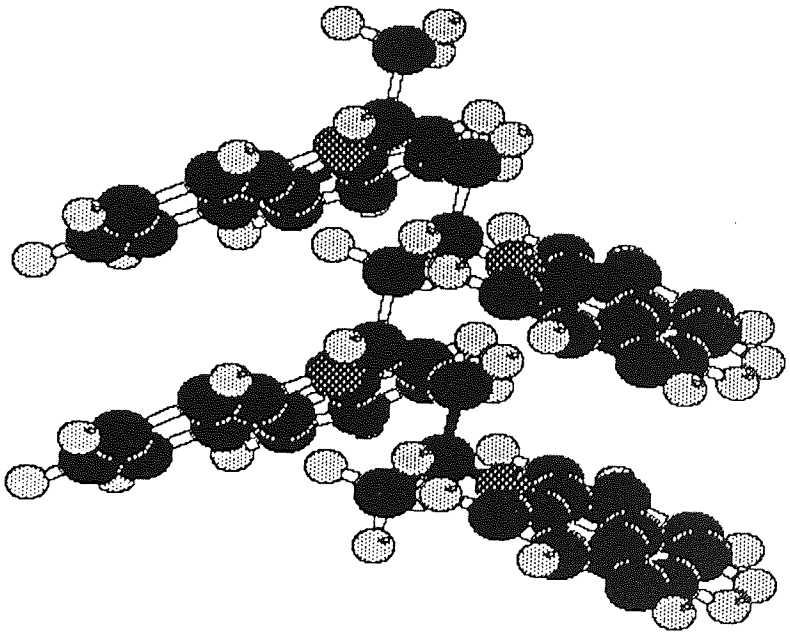

Longitudinal view

Figure 7.2 Representations of syndiotactic 2/1 helix of PVK (4 repeat units) in ball-and-stick form

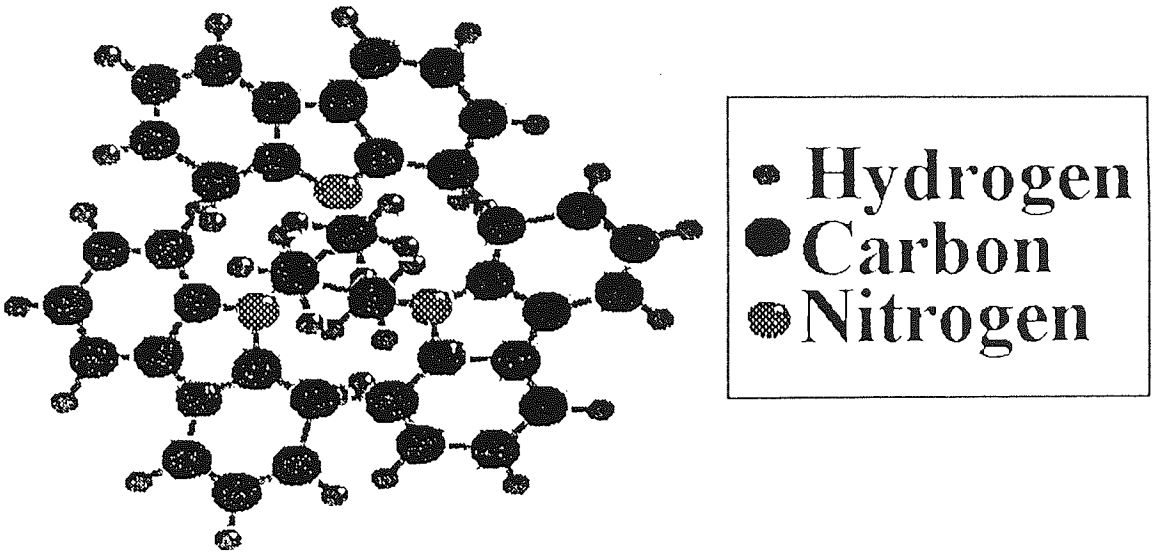

Transverse view of 3/1 helix of PVK

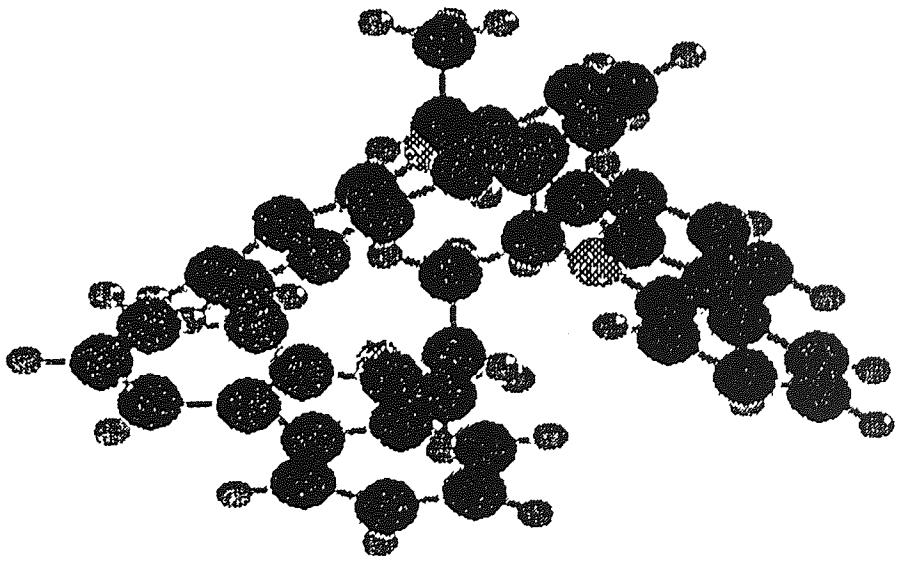

Longitudinal view of 3/1 helix of PVK

Figure 7.3 Representations of isotactic 3/1 helix of PVK (3 repeat units) in ball-and-stick form

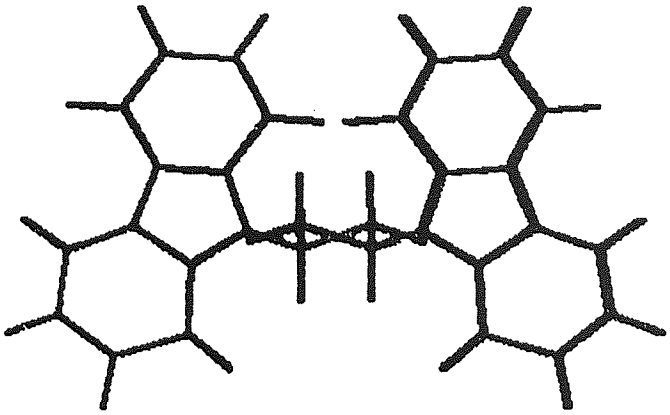

Transverse view of 2/1 helix of PVK

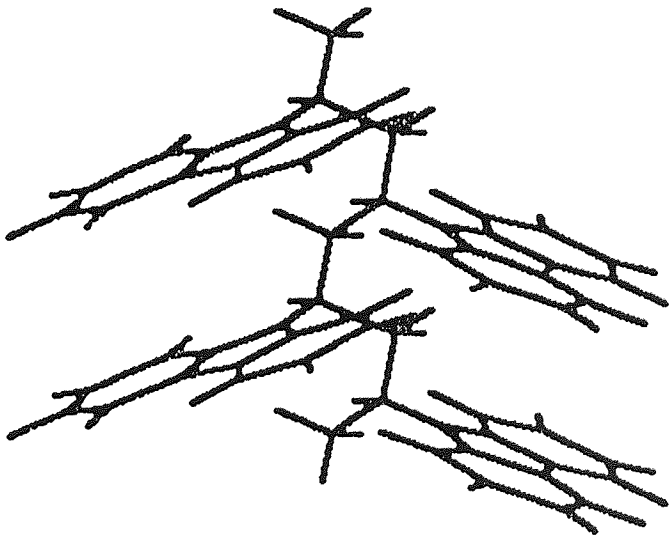

Longitudinal view of 2/1 helix of PVK

Figure 7.4 Represenations of syndiotactic 2/1 helices of PVK (4 repeat units) in thick line form

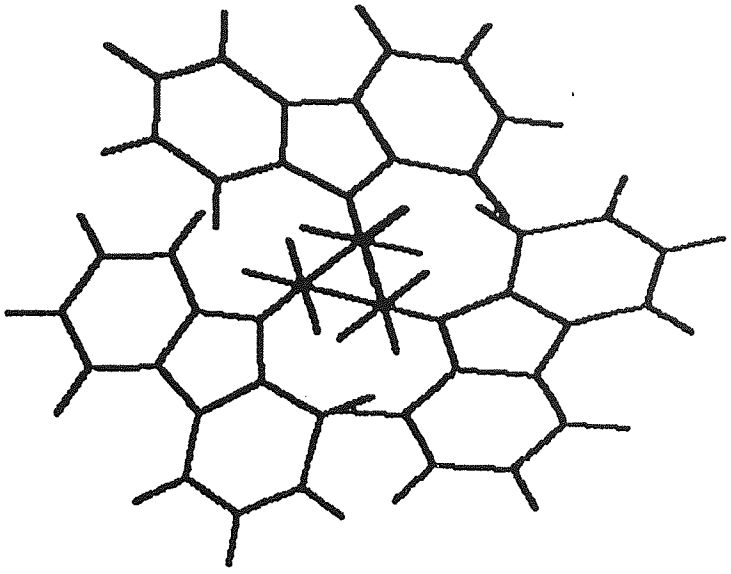

Transverse view of 3/1 helix of PVK

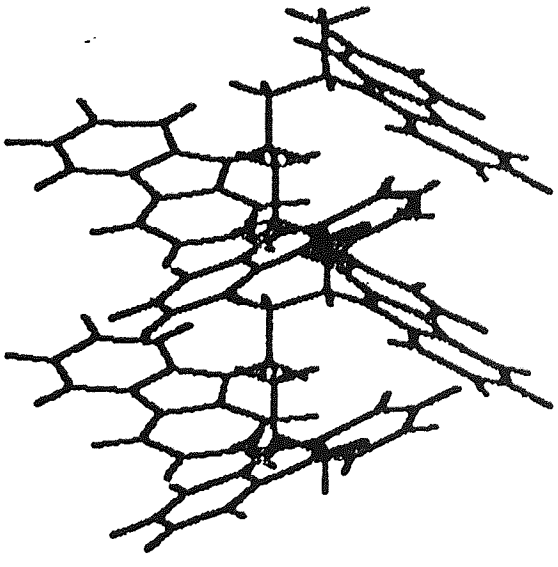

Longitudinal view of 3/1 helix of PVK

Figure 7.5 Represenations of isotactic 3/1 helices of PVK (3 repeat units) in thick line form

As discussed in earlier chapters in this thesis, it has been suggested that the syndiotactic chains of PVK may adopt 2/1 helices whereas the 3/1 conformation believed to be predominant in isotactic forms of PVK. Kimura et al[36] have suggested that intercarbazole group distances confines PVK to the isotactic 3/1 helix with TGTG sequences and that syndiotactic PVK adopts a 2/1 helix consisting of TGTG' sequences. In the present study, using the DTMM the bond rotational angles were set as suggested by these researchers and the final representation of models were produced. Tables 7.1 and 7.2 lists the DTMM data files for the 2/1 and 3/1 helices, respectively represented in figures 7.2 and 7.3 in ball-and-stick form. These figures display two views (transverse and longitudinal relative to the helix axis). For clarity these models are also represented in thick line configuration in figure 7.4 and 7.5. In isotactic chain of PVK it is clear that the all-trans conformation is not perferred because it extremely hindered and the molecule is forced to adopt less hindered conformations, like the helix. The situation for the syndiotactic form of PVK is not as clearly defined since the all-trans conformation does not appear to be sterically hindered. It seems feasible to assume that there is a greater range of conformations for syndiotactic PVK. A 4/1 helix is improbable in PVK, because of the bulkiness of the carbazole groups[36]. Study of models shows that if a PVK chain consists of 3/1 stereoblock array, the chain is rodlike and about 13.0Å in diameter and is nearly circular in cross section. However, the 2/1 helix is slightly elliptical, therefore, its smaller cross section diameter is 11.7Å and the larger diameter is 12.3Å.

Using DTMM the average distance (d) between i^{th} and $(i + 3)^{th}$ carbazole groups is calculated to be 6.10Å in 3/1 helices. The distance between i^{th} and $(i + 2)^{th}$ carbazole was calculated to be 4.33Å for the 2/1 helices (Figure 7.6).

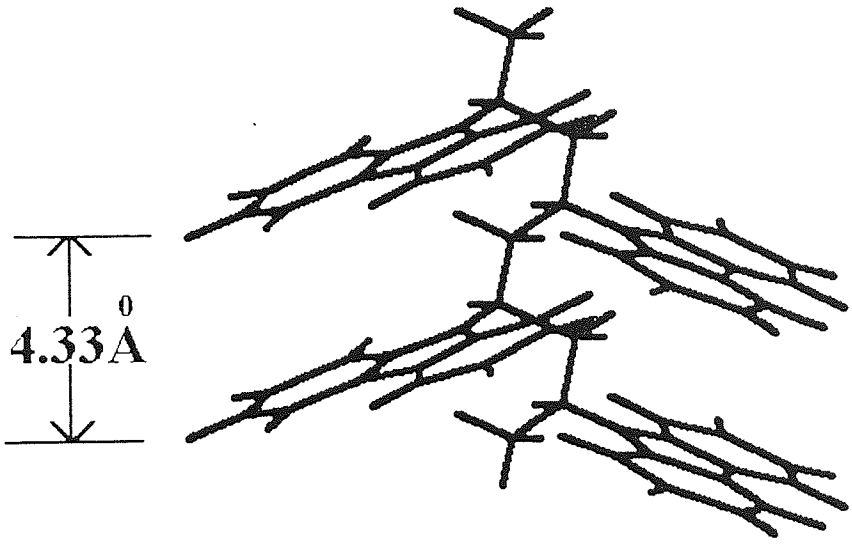

Longitudinal view of 2/1 helix of PVK

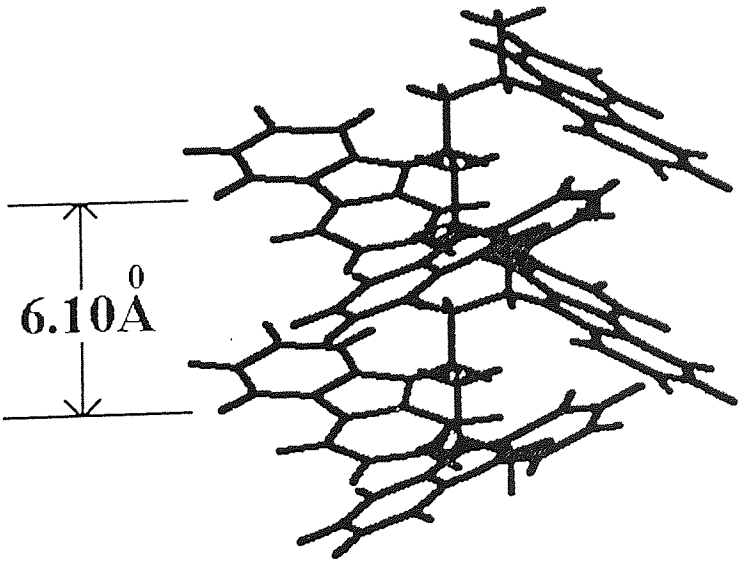

Longitudinal view of 3/1 helix of PVK

Figure 7.6 Pitch distance in 2/1 and 3/1 helices of PVK

It is interesting to note that the plane of the carbazole group and the helix axis are not normal to each other. The carbazole groups appear to be tilted and twisted with respect to the helix axis. In order to make the plane of carbazole groups normal to helix axis, in order to maximise d, it is necessary to rotate the carbazole group about the C-N bonds by 12 degrees in 3/1 helices and 9 degrees in the case of 2/1. Therefore, it is necessary to estimate accurately the distance (d) between the planes of carbazole groups in both helical forms. This can be calculated by using the constructions shown in figure 7.7.

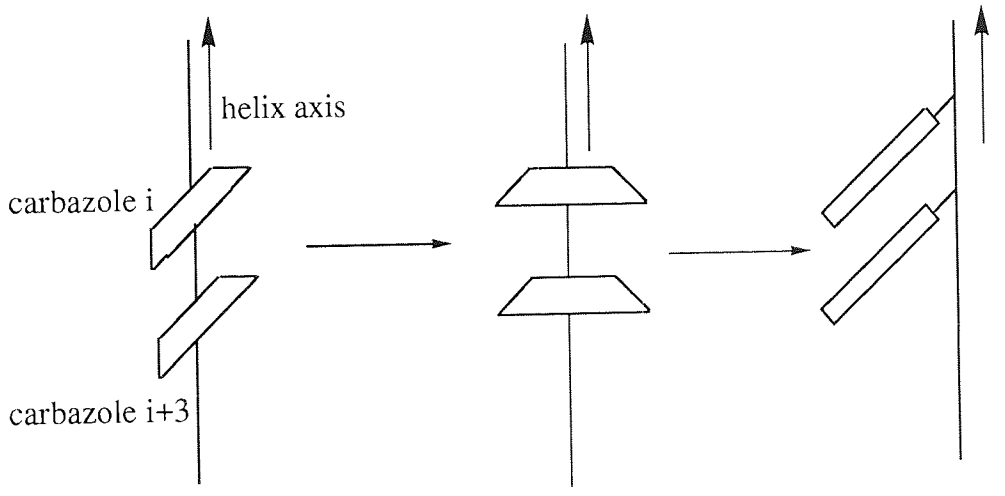

View (a)	View (b)	View (c)
This is the 3/1 helix formed from the all-trans conformation in which the plane of the carbazole groups is normal to the plane of backbone.	Carbazole groups are rotated by 12° about C-N bond to maximise the distance between planes of helical repeating carbazole groups.	Helix is rotated through 90° to give view c.

Figure 7.7 Representation of several views of carbazole groups i and i+3 in a 3/1 helix of isotactic PVK.

Figure 7.8 shows a detail construction of view (c) which is used to calculate the distance (dp) between the planes of carbazole groups i and i+3.

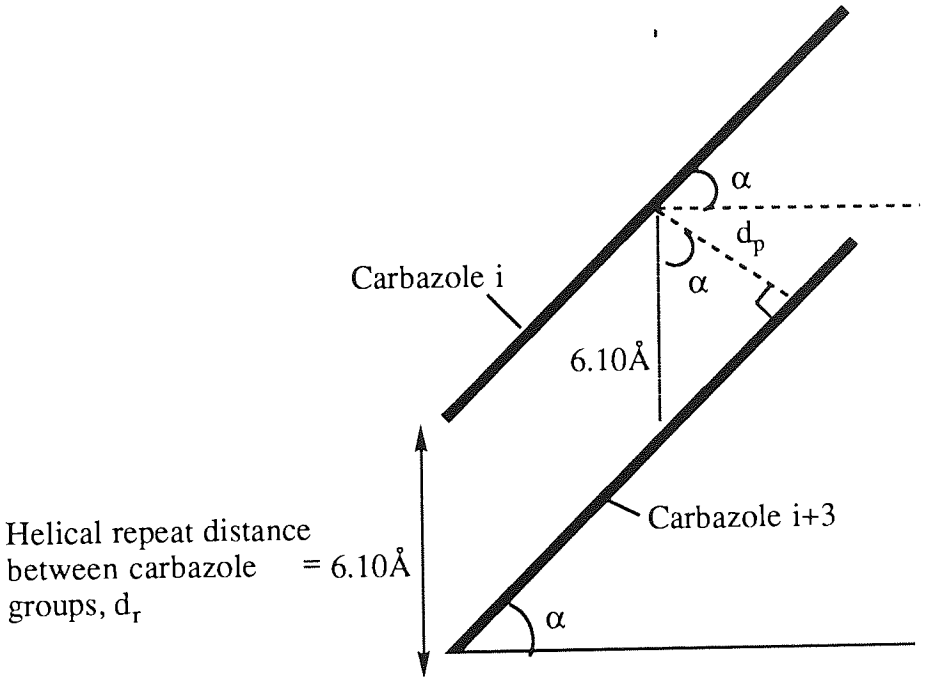

Figure 7.8 Construction of view (c)

From figure (7.8), $\cos \alpha = d_P / d_r = d_p / 6.1$

$\alpha = 20^o$ (determined by DTMM)

Therefore, $d_p = 5.73$ Å

This value is slightly less than the average pitch distance (6.1Å) of the helix estimated by the DTMM.

If the dipole moment (μ) of carbazole is assumed to be 7.04×10^{-30}Cm[144] at room temperature, then the net dipole moment per helical repeat carbazole may be calculated as follows:

Dipole moment along the helix axis for three carbazole units of the complete pitch of the helix $= 3(\mu \cos 90^{o} - \alpha)$

$= 7.23 \times 10^{-30}$ Cm

Therefore, dipole moment per repeat unit is 2.41×10^{-30} Cm along the helical axis. Due to the cylindrical symmetry of the helix there is no net dipole moment normal to the axis of the helix.

For the 2/1 helix:

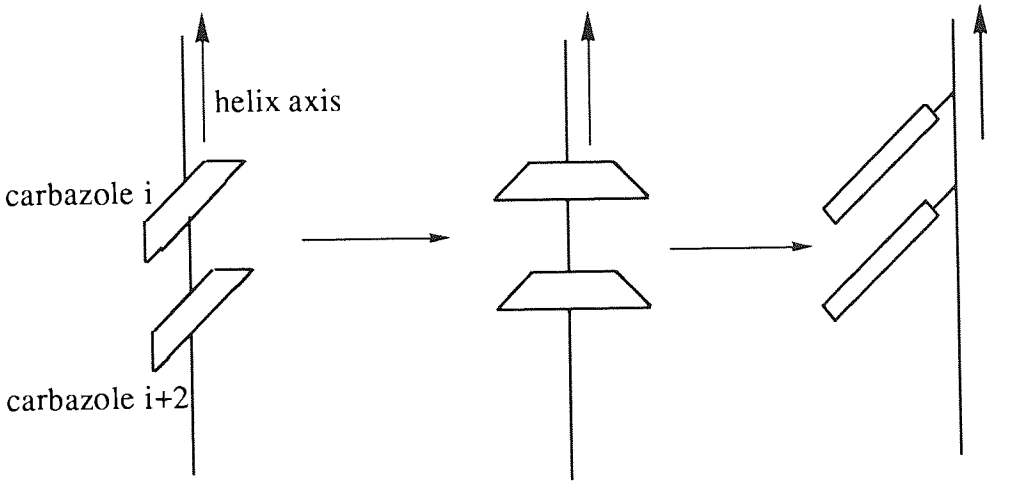

View (a)	View (b)	View (c)
This is the 2/1 helix formed from the all-trans conformation in which the plane of the carbazole groups is normal to the plane of backbone.	Carbazole groups are rotated by 9° at C-N bond to maximise the distance between planes of helical repeating carbazole groups.	Helix is rotated through 90° to give view c.

Figure 7.9 Representation of several views of carbazole groups i and i+2 in a 2/1 helix of syndiotactic PVK.

Figure 7.10 shows a detail construction of view (c) which is used to calculate the distance (d_p) between the planes of carbazole groups i and i+2.

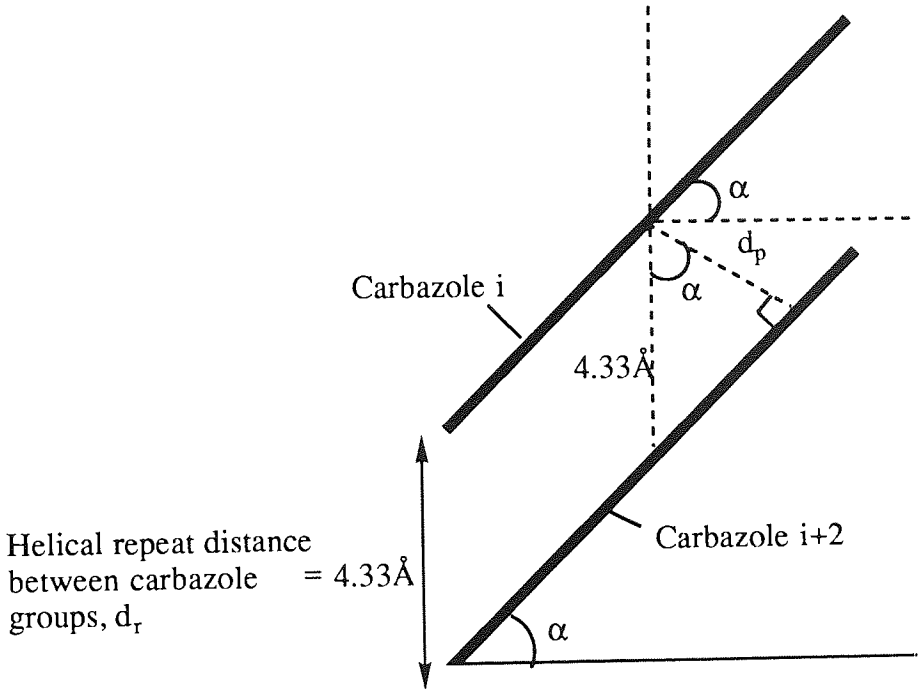

Figure 7.10 Construction of view (c)

From figure (7.10), $\cos \alpha = d_p / d_r = d_p / 4.33$

$\alpha = 28^o$ (determined by DTMM)

Therefore, $d_p = 3.82$ Å

Dipole moment parallel to helical axis for 2 repeat units = $2(\mu \cos 90^o - \alpha)$

$=2(7.04 \times 10^{-30} \cos 62^o)$

$= 6.61 \times 10^{-30}$ Cm

Dipole moment perpendicular to helical axis for 2 repeat units = $2 (\cos 67.5^0 (\mu \cos 28^o))$

$= 2 \cos 67.5^0 (6.2 \times 10^{-30})$

$= 4.75 \times 10^{-30}$ Cm

The nett dipole moment is at an angle θ to the axis of the helix, and not parallel to axis of helix as in the case of isotactic 3/1 conformation. This angle is calculated as shown below:

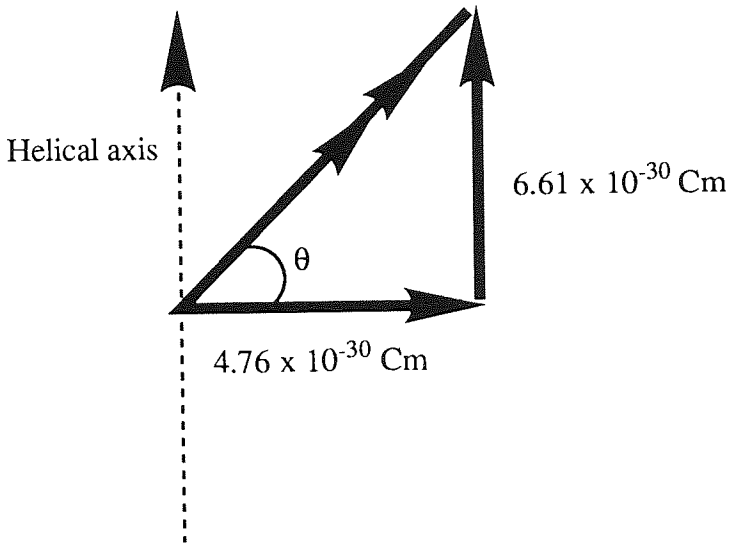

$$\tan\theta = \frac{6.61}{4.76} = 1.389$$

$$\theta = 54^{o}$$

Net dipole moment for a 2/1 pitch is 8.14×10^{-30} Cm or 4.1×10^{-30} Cm per repeat unit and is at an angle of 36^{o} with respect to axis of helix.

As mentioned in chapter 5, poly(N-vinylcarbazole) readily forms charge transfer complexes with molecules that are electron acceptors, such as, for example 2,4,7-trinitro-9-fluorenone. It was stated that the degree of complex formation and the thermal stability of complexes was strongly linked to the conformations of the PVK chains. It is important that the pitch distance in the helices is sufficiently large for the acceptor molecules to allow the formation of sandwich type complexes with suitable acceptor molecules.

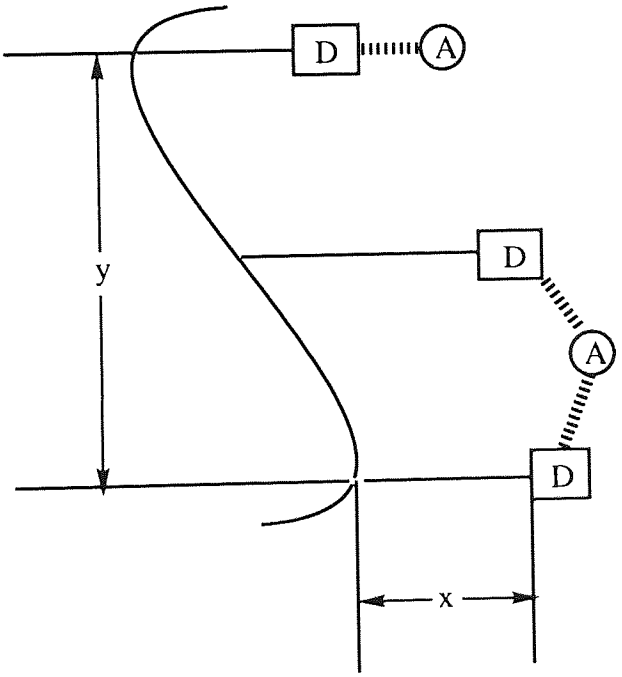

Figure 7.11 Schematic depiction of polymeric donor-acceptor interaction.
D : Donor group, (A) : Acceptor group

The effect of polymer type on complex formation is dependent on certain geometrical parameters, for example, the distances x and y (Figure 7.11) and van der Waal's radii of the molecules. Generally, if y is too large, x is too small and if the main chain is rigid, then the donor groups will be independent of each other. If x is too large, the donor groups are

seperated at too great a distance from each other. In these cases the 1:1 interaction, similar to that present in monomeric systems prodominates. The sandwich-like interaction, which requires an acceptor molecules to be located between two donor groups is more common when the distances x and y are only slightly bigger than the acceptor molecules.

The spectroscopic data in chapter 5 revealed that degree of complexation depended on the conformations of the PVK polymer chains. For sample F1, in which the chains were prodominately arranged in 2/1 helices, the equilibrium constants were smaller than obtained those for sample F2 which favours 3/1 helical conformations. It was concluded that this was due to the fact that 2/1 helix could not easily accommodate bulky TNF acceptor molecules between the pendant carbaozole groups and that this restriction results in lower degree of charge transfer formation. It was decided to use the DTMM to model TNF and to show how its van der Waals size relates to the pitch distances of PVK.

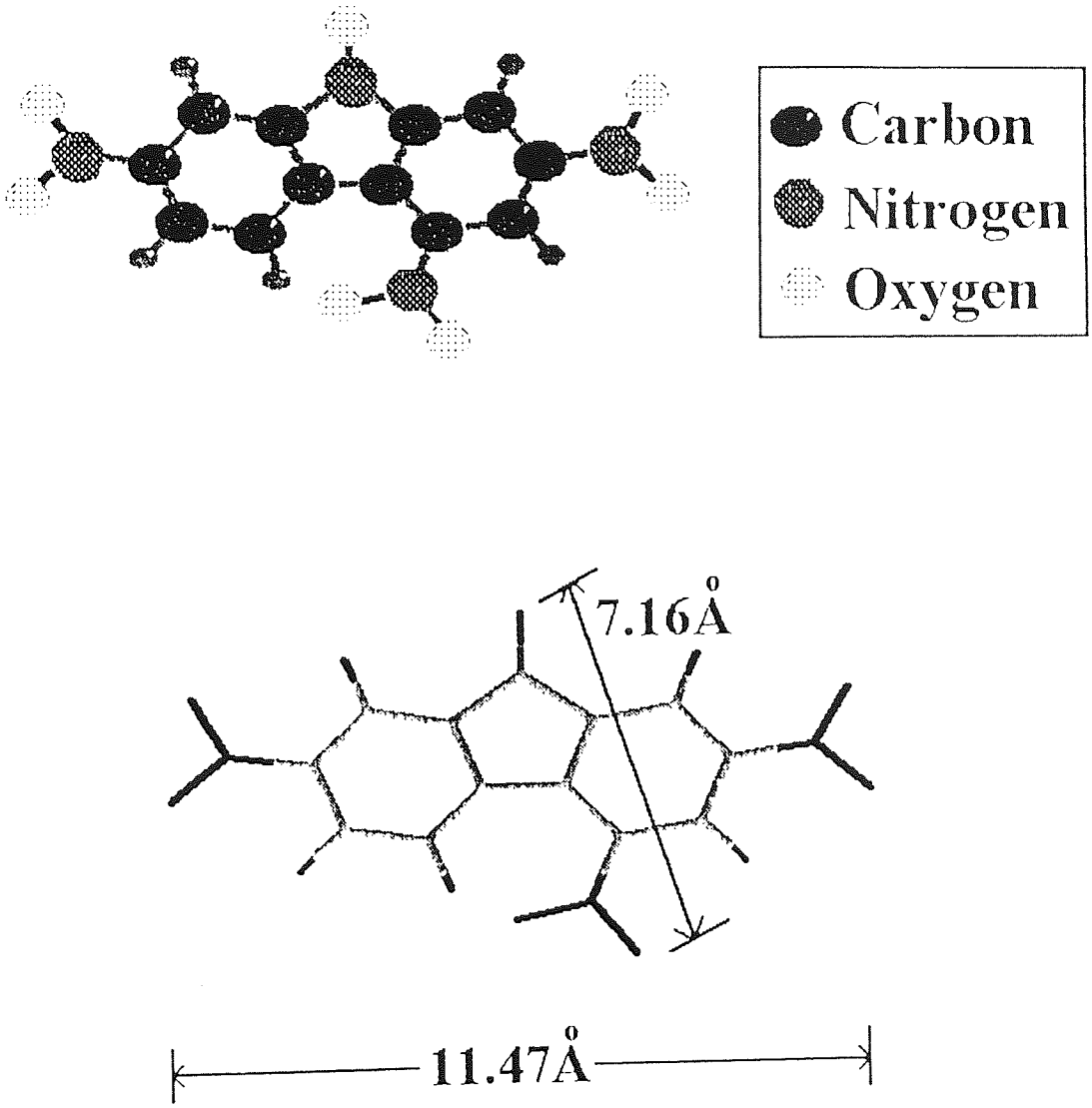

Figure 7.12 Representation of TNF in ball-and-stick and thick line forms

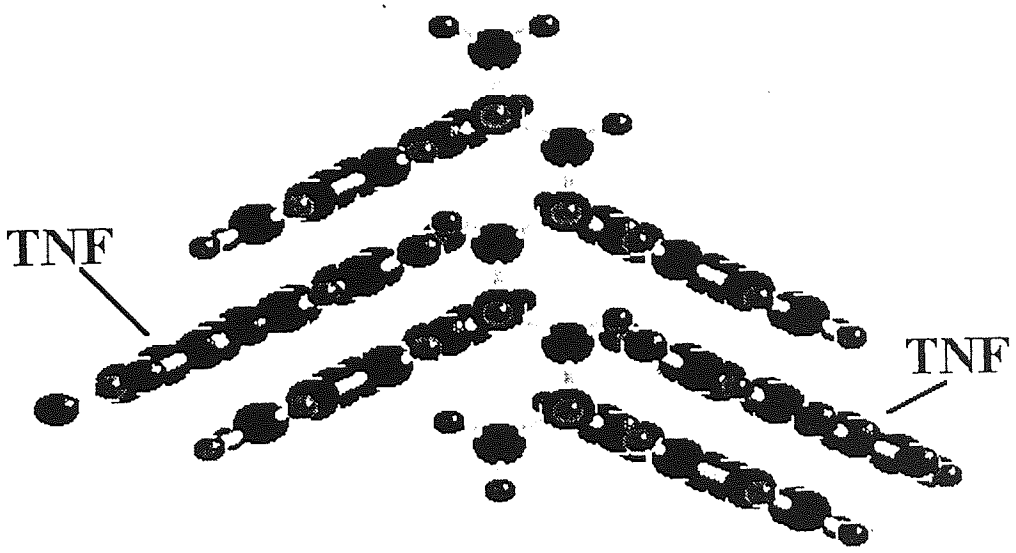

Figure 7.13 A simple representation of sandwich-type complex of PVK and TNF in ball-and-stick form

Figures 7.12 illustrates the ball-and-stick molecular model representation of 2,4,7-trinitro-9-fluorenone. From these figures the maximum dimension across the plane of 2,4,7-trinitro-9-fluorenone is estimated to be 11.47Å. A simple representation of complex between the PVK and TNF is shown in figure 7.13. From this figure it is clear that due to the steric hindrance of the carbazole groups, the TNF molecules does not lie totally between carbazole groups. This is because van der Waals interaction between backbone atoms of polymer and nitro groups of TNF prevents complete overlap with carbazole groups. The resultant overlap is as shown in figure 7.14:

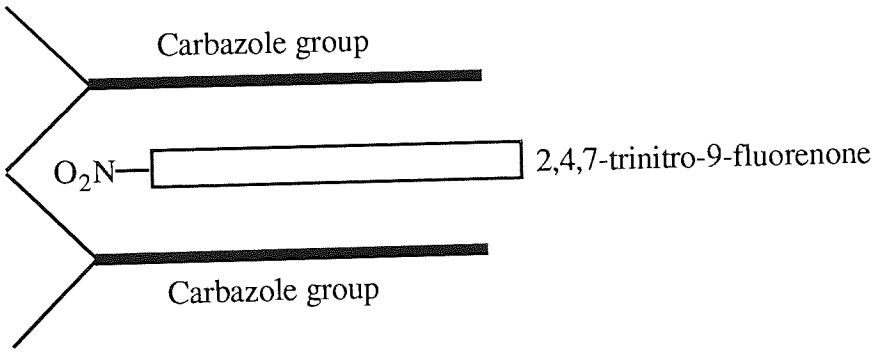

Figure 7.14 Side view of sandwich-type complex between carbazole and TNF

Although, a quick glance at figure 7.13 may reflect PVK favouring sandwich-type complex formation for both 3/1 and 2/1 helical forms, the van der Waals radii representation (figure 7.15 and 7.16) suggests that this type of complex formation is only possible with 3/1 helices. Firstly, the average pitch distance is 5.73Å is sufficient for the TNF molecules to accommodate itself between the i^{th} and $(i+3)^{th}$ carbazole groups. The ability of atoms of TNF to dove-tail with respect to those in the 3/1 helical forms of PVK may be the second reason. However, in the case of the 2/1 helix, the average pitch distance is only 3.82Å, hence it would be extremely difficult for TNF molecules to form sandwich-type complexes. Therefore, it is most likely that TNF will not form 1:1 complexes with TNF.

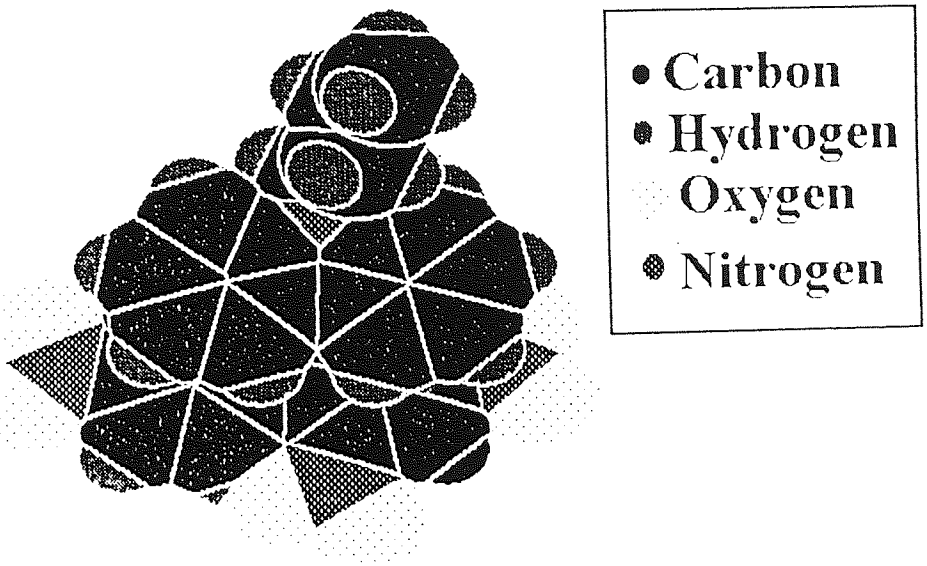

Transverse view of charge transfer complex between syndiotactic PVK(helical 2/1) and TNF

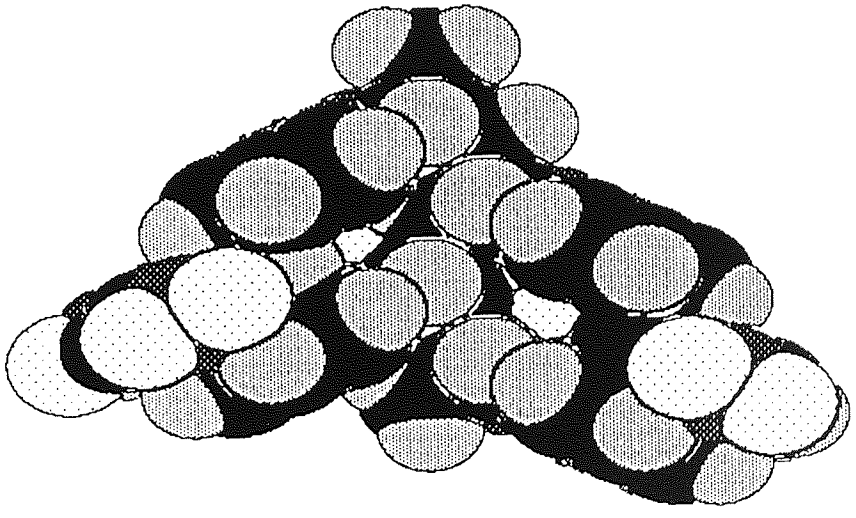

Longitudinal view of charge transfer complex between syndiotactic PVK(helical 2/1) and TNF

Figure 7.15 Space filled representation of sandwich-tpye complex of syndiotactic 2/1 helix of PVK (4 repeat units) and TNF

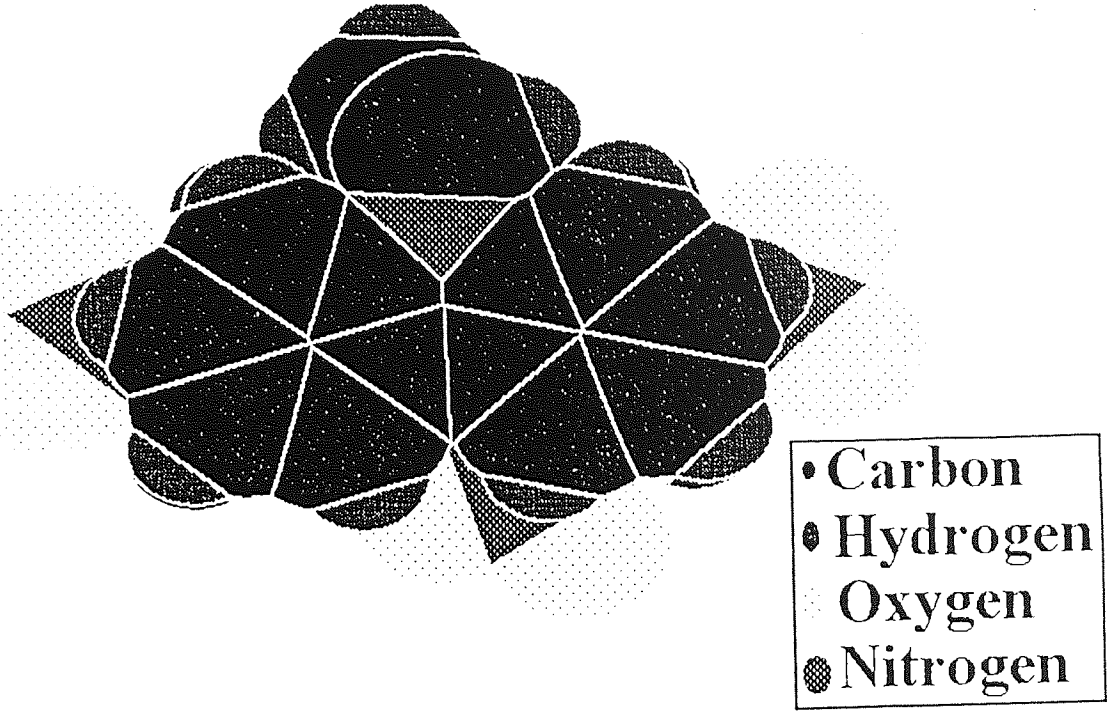

Transverse view of charge transfer complex between isotactic PVK (3/1 helix) and TNF

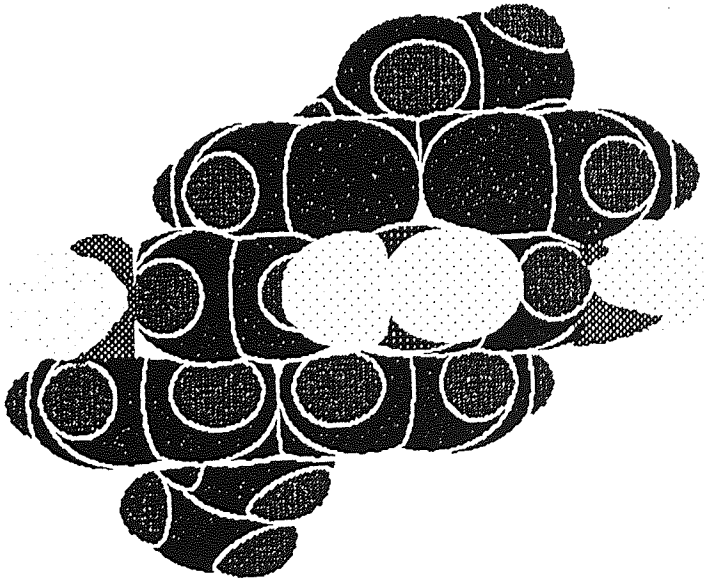

Longitudinal view of charge transfer complex between isotactic PVK(3/1helix) and TNF

Figure 7.16 Space filled representation of sandwich-tpye complex of isotactic 3/1 helix of PVK (6 repeat units) and TNF

Chapter Eight

Conclusions and Suggestions For Future Work

8.1 General conclusions

In this chapter the main conclusions of the preceding chapters are discussed and enlarged upon. Suggestions are also made for extending certain aspects of the research.

The synthetic work described in the earlier part of this thesis was concerned with the preparation of samples of poly(N-vinylcarbazole) (PVK) with different stereostructures. As far as the tacticity of poly(N-vinylcarbazole) is concerned, an improved correlation of tacticity and catalysts was made by using proton nuclear magnetic resonance spectroscopy and fully relaxed carbon-13 nuclear magnetic resonanace spectroscopy. Both techniques confirmed that the use of boron trifluoride etherate catalyst produced a polymer with the highest isotactic content while free radical (azo-bisisobutyronitrile) catalyst resulted in the lowest isotactic content.

The static dielectric studies of PVK in solution in either 1,4-dioxane or toluene revealed that the temperature coefficients of dipole moments of PVK samples were strongly related to the stereostructures and tacticity of the polymers. All the polymer types showed positive temperature coefficients that increased in magnitude as the isotactic content of the polymer decreased. These results support the view that PVK samples with high isotactic contents exist largely in 3/1 helical conformations and that the partial cancellation of the dipole moments per repeat unit is not the same as the partial cancellation of dipole moments in 2/1 helices.

The temperature coefficients of the dipole moments of PVK were larger when measured in toluene, compared to values obtained in 1,4-dioxane. This was discussed in terms of van der Waals interactions of solvents with the PVK chains. A "fall off" of the dipole moment for all the samples was noted when measured in toluene at high temperatures. However, experimental errors in the measurements of the dielectric permittivities and the apparent dilution of solutions at higher temperatures could contribute to this decrease. More detailed studies are necessary to correlate abnormalities in the dielectric behaviour with the use of higher boiling point solvents, such as xylene. This would enable a more extensive investigation into the effects of solvents on PVK molecules and their structures.

A spectrophotometric method by Weiser and Seki[125] involving the measurement of charge transfer bands was employed in determining the equilibrium constants of charge transfer complexes of poly(N-vinylcarbazole) and 2,4,7-trinitrofluorenone (TNF) in 1,4-dioxane. The data was used to calculate the concentration of complex moieties in the solutions which consisted of three components: free TNF, free PVK and PVK:TNF complex. The results indicated that there is a higher degree of complexation between TNF and polymer samples that consist largely of isotactic chains. A knowledge of the concentration of complex facilitated the calculation of the dielectric increments of the charge transfer complexes, which further enabled the determination of dipole moment of the complex moiety.

The temperture coefficient of the Kerr constant, is larger for the PVK sample which consist largely of syndiotactic chains than the sample in which the isotactic chains prodominates; behaviour also reflected by the dielectric data. The molar Kerr constants for PVK systems shows a high sensitivity to stereostructures of PVK. All the PVK polymer samples had a negative Kerr constant whereas that for ethylcarbazole is positive. The positive Kerr constant of N-ethylcarbazole implies that the molecular dipole moment of N-ethylcarbazole is parallel to the maximum polarizability. However, since PVK is believed to exist as a series of

straight rigid helical sections in which the axes of maximum polarizability of the carbazole side groups are approximately perpendicular to the chain axis, it follows that the maximum axis of polarizability of PVK is normal to the helix axis. The three parallel components add up in a cummulative manner. The perpendicular components of three consecutive repeat units in a 3/1 helix cancel to zero. The situation is different for a 2/1 helix. The parallel components adds cummulatively, but the perpendicular components of two consecutive repeat units do not quite cancel to zero, hence there is also a small cummulative perpendicular dipole moment. This means that, for the 2/1 helix the overall molecular dipole moment is not parallel to the axis of the helix but is not greater than 54^{o} - hence molar Kerr constants are still negative.

All PVK : TNF complexes had solution molar Kerr constants that were smaller than the solution Kerr constants of the pure (undoped) polymers. This was only possible if the complex formation was accompanied by changes in the optical anisotropy and dipole moments compared to that of the pure polymer. It was concluded that the dipole moment contribution to the Kerr constants was less significant than the anisotropy contribution.

8.2 Suggestions for future work

The synthetic work should obviously be continued in an attempt to improve the percentage isotactic content. The dielectric and electro-optic Kerr effect of highly rich isotactic sample would be of obvious interest.

Expansion of the project to include the measurement of photoconductivity, would be of great interest.

The "fall off" in the dielectric behaviour observed at higher temperature in PVK solutions in toluene, should be investigated with the use of higher boiling point solvents, such as xylene. This would also enable a more extensive investigation into the effects of solvents on PVK molecules and their structures.

The electro-optic work could be extended to measure depolarisation ratios of polymer samples which, together with dielectric and Kerr effect results, could be used to calculate the anisotropy of polarisability of the pure polymer and of polymer : TNF complexes.

Since the solutions of PVK:TNF complexes are coloured, it should be possible to measure electric dichroism in order to obtain information about the relative direction of the transition moments and the helix axis of PVK. This would enable the structure of PVK : TNF complexes to be fine-tuned.

Various polymer chains with known isotactic sequences could be simulated using computerised Monte Carlo techniques and derived theoretical dipole moments could then be compared with those determined experimentally.

References

1. DeBaeve E.C. and Anderson C.A., 'Moisture Studies on Ozone-Resisting and Type RH-RW Rubber Insulation', *Trans American Institute of Electrical Engineers , Power Apparatus*, **3**, 1746-1751, 1954.

2. Blodgatt R.B. and Fisher R.G., 'Present Status of the Corona and Heat Resistant Cable Insulation Based on Ethylene-Propylene Rubber', *Trans American Institute of Electrical Engineers - Power Apparatus and Systems,* 1129-1143, 1968.

3. Babbit R.O, 'The Vanderbilt Rubber Handbook', R.T. Vanderbilt Co. Norwalk, Communication, 1978.

4. Skotheim T., 'Handbook of Conducting Polymers', Marcel Dekker, New York, 1986.

5. Hoffer D., 'Int. conf. Recent Advances in Polyimides and Other High Performance Polymers', Reno, Nevada, USA, 1987.

6. Chin G.Y., 'Second Int. conf., Passive Components', Paris, France, 1987.

7. Mittal K.L., Polyimides, Plenum Press, New York 1984.

8. Bessonov M.I., Koton M.M., Kudryatsev V.V. and Lains L.A., 'Polyimides Thermally Stable Polymers', Consultant Bureau, New York, 1987.

9 Korshak V.V., Vinogradova S.V. and Vygodskii Y.S., 'Cardo Polymers', *J. Macromol Sci. Rev. Macromol .*, **C11(1)**, 45-142, 1974.

10. Reppe W. and Keyssner E, Ger. Pat., 618-619, 120(Sep.,1935).

11. Beller H., Christ R.E. and Wureth F., British Pat., 641, 437(Aug. 9, 1950).

12. Hoegel H., Sus O., and Neugebaner W., German Pat., 1,068,115,1957.

13. Hatano H., and Tanikawa K., 'Recent Developments In Polymeric Photoconductors', *Prog. Org. Coat.*, **6**, 65-104, 1978.

14. Froix M.F., Williams D.J. and O'Godde A.O., 'N.M.R. Relaxation-time Studies of Poly(N- vinylcarbazole) and Sorbed-Oxygen Effect', *J. Appl. Physc.*, **41**, 4166-4172, 1975.

15. Ferrasis J., Cowan D.O. Walatka V. and Perlstein J.H., 'Electron Transfer In a New Highly Conducting Donor-acceptor Complex', *J. Am. Chem. Soc.*, **95(3)**, 948-949, 1973.

16. McCullough R.D., Kok G.B., Lerstrup K.A. and Cowan D.O., 'Tetratellurafulvalene'*J. Am. Chem. Soc.*, **109**, 4115-4116, 1987.

17. Feast W.J., 'Synthesis and Properties of Some Congugated Conductive Polymers, Polymers',*Chem. Ind.*, **8**, 263-268, 1985.

18. Schimmel T., Riess W., Gmeiner J., Denninger G., Schwoerer M., Naarmaan H. and Theophilou N, 'DC-Conductivity on a New Type of Highly Conducting Polyacetylene, n-$(CH)_x$', *Solid State Commun.*, **65**, 1311-1315, 1988.

19. MacDiarmid A.G., Chiang J.C., Nanayakkara L.D., and Wu w., 'Polyaniline: Interconversion of Metallic and Insulating Forms', *Mol. Cryst. Liq. Cryst.*, **121**, 173-180, 1985.

20. Andreatta A., Cao Y., Chiang J.C. Smith P. and Heeger A.J., 'High-Performance Fibres of Conducting Polymers', *Molecular crystals and liquid crystals* , **189**, 169-182, 1990.

21. Angelopoulos M., Asturias G.E., Ermer S.P., Ray A., Scherr E.M., MacDiarmid A.G. Akhtar M. and Epstein A.J.,'Polyaniline-Solutions, Films and Oxidation-state', *Mol. Cryst. Liq. Cryst.*, **160**, 151-163, 1988.

22. Wang L., Jing, X. and Wang F., 'Polytoludines with different degrees of oxidation and their doping with hydrogen chloride', *Synth. Met.*, **29(1)**, E363-E370, 1989.

23. Li S., Dong H., and Cao Y.'Synthesis and Characterisation of Soluble Polyaniline', *Synth. Met.*, **29**, No.1, E329, 1989.

24. Tokito S., Smith P. and Heeger A.J., 'Highly Conducting and Stiff Fibers of Poly(2- dimethoxy-*p* -phenylenevinylene) Prepared From Soluble Precursor Polymers', *Polymer*, **32**, 464-470, 1991.

25. Blythe A.R., 'Electrical Properties of Polymers', Cambridge University Press, 1979.

26. Taniguchi A., Kauda S., Kusabyashi T., Mikawa H., and Ito K., 'The Electrical Properties of the Poly(N-vinyl Carbazole)-Tetracyanoquinodimethane Charge Transfer Complex', *Bull Chem. Soc.*, Japan, **37**, 1386-1388, 1964.

27. Kuczkowski A., Dreger Z., Slupkoweki T., Jachym B., 'Electrical Conductivity of Poly(N- vinylcarbazole) : Tetracyanoquinodimethane Complexes', *J. Polymer* , **20**, 1161-1163, 1979.

28. Okamoto K.I., Yamada M., Itaya A., Kimura T. and Kusabayashi S., 'Polymerisation of N-Vinylcarbazole, N-Vinyl-5H-Benzo(b)Carbazole and N-Vinyl-7H-Benzo-(C)Carbazole', *Macromolecules*, **9**, 645, 1976.

29. Williams D.J. and Froix M.F., 'The Stereoregularity of Poly(N-vinylcarbazole) *Polymer Preparation*, **18**, 445-449, 1977.

30. Kawamura T. and Matsuzaki K., 'Carbon-13 Nuclear Magnetic Resonance Studies of poly(N-vinylcarbazole)*Makromol. Chem.*, **179**, 1003-1010, 1978.

31. Terrell D.R., Evers F., Smoorenburg H. and Van den Bogaerts, H.M., 'The Dependence of the Glass Transition Temperature of Poly(N-Vinylcarbazole) Upon Steric Microstructure and Molecular Weight' *J. Polym. Sci., Polym. Phys.*, **20**, 1933-1945, 1982.

32. Beevers M.S., Mumby S.J., 'Dielectric and Kerr effect Studies of Stereoregular Poly(N-Vinylcarbazole)', *Polymer Communications*, **25**, 173-175, 1984.

33. Froix M.F., Williams D.J. and Goedde A.O., 'Nuclear Magnetic Resonance Relaxation Time Studies of Photoconductive Polymers. Poly(N-ethyl-2-vinylcarbazole) and Poly(N-ethyl-3-vinylcarbazole)', *Macromolecules*, **9(1)**, 81, 1976.

34. Tsuchihashi N., Hataro M. and Sohma J., 'Carbon-13 and Proton Magnetic Resonance Studies of poly(N-vinylcarbazole)', *Makromol. Chem.*, **17**, 2739-2747, 1976.

35. Kawamura T., and Matsuzaki K., 'Carbon-13 Nuclear Magnetic Resonance Studies of Poly(N-vinylcarbazole)', *Makromol. Chem.*, **179**, 1003-1010, 1978.

36. Kimura A., Yoshimoto S., Akana Y., Hirata H., Kusabayashi S. and Mikawa H., Kasin N., 'Crystallinity of Poly(N-vinylcarbazole)',*J. Polym. Sci. Polym. Phys.*, **8**, 643-648, 1970.

37. Crystal R.C., 'The Crystalline Morphology of Poly(N-vinylcarbazole)', *Maromolcules* **4**, 379-384, 1971.

38. Griffiths C.H., 'Folded Chain Crystallization of Poly(N-vinylcarbazole)', *J. Polm. Sci. Polym. Phys.*, **13**, 1167-1176, 1975.

39. Terrel D.R., Evers F., Smoorenburg H., Bogaert H.M., 'The Dependence of the Glass Transition Temperature of Poly(N-Vinylcarbazole) Upon Steric Microstructure and Molecular Weight' *J. Polym. Sci. Polym.Phys.*, **20**, 1933-1945, 1982.

40. Le Fevre R.J.W., Dipole Moments, Methuen, 1953.

41. Mark J.E., 'The Use of Dipole Moments to Characterize Configurations of Chain Molecules', *Acc. Chem. Res.*, **7**, 218-225, 1974.

42. Marchal J., and Benoit H., 'Contribution of the Electric Moments in the Study of Polymer Chains in Solutions', *J. Chim. Phys. Physicochim. Biol..*, **52**, 818-825, 1955.

43. Marchal J., and Benoit H., 'Comparaison Between the Theoretical Results and the Determination of the Dimensions and the Average Electric Moments of the Polymer Chains', *J. Polym. Sci.*, **23**, 223-232, 1957.

44. Stockmayer W.H., 'Dielectric Dispersion in Solutions of Flexible Polymer', *Pure Appl. Chem.*, **15**, 539-554, 1967.

45. Nagai K. and Ishikawa T., Excluded Volume Effect on Dipole Moments of Polymer Chains', *Polymer J.*, **2(3)**, 416-421, 1971.

46. Doi M., 'Excluded-Volume Effect on Dipole Moment of Polar Macromolecules', *Polymer J.*, **3(2)**, 252-253, 1972.

47. Liao S.C. and Mark J.E., 'Effect of Excluded Volume on the Dipole Moments of Chain Molecules', *J.Chem.Phys.*, **59(7)**, 3825-3830, 1973.

48. Flory P.J., 'Statistical Mechanics of Chain Molecules', Interscience, New York, 1969.

49. Mark J.E., 'Dipole Moments of Dimethyl Siloxane Chains', *J.Chem., Phys.*, **49(3)**, 1398-1402, 1968.

50. Flory P.J., Crescenzi V. and Mark J.E., 'Configuration of the poly(dimethyl Siloxane) Chain III, Correlation of Theory and Experiment', *J.A.C.S.*, **86**, 146-152, 1964.

51. Yu, Cu. and Mark, J.E., 'Specific Solvent Effects in Swollen Polymer Networks', *Macromolecules*, **7(2)**, 229-232, 1974.

52. Le Fevre C.G., Le Fevre R.J.W. and Parkins G.M., 'Molecular Polarizability. The Specific Kerr Constants and Polarizations of Polystyrenes Dissolved in Carbon Tetrachloride', *J. Chem. Soc.*, **A**, 1468-1474, 1958.

53. Le Fevre C.G., Le Fevre R.J.W. and Parkins G.M., 'Molecular Polarizability. The Specific Kerr Constants and Polarizations of Vinyl Acetate and Various Polyvinyl Acetates Dissolved in Carbon Tetrachloride or Benzene', *J. Chem. Soc.*, **A**, 1814-1819, 1960.

54. Le Fevre R.J.W. and Sundaram K.M.S., 'Molecular Polarizability. Molar Kerr Constants and Dipole Moments of Vinyl Chloride and Six Polyvinyl Chloride as Solutes in Dioxan'*J. Chem. Soc.*, **A**, 1494-1502, 1962.

55. Le Fevre R.J.W. and Sundaram K.M.S., 'Molecular Polarizability. Molar Kerr Constants and Dipole Moments of Vinyl Bromide and Six Polyvinyl Bromides as Solutes in Dioxan', *J. Chem. Soc.*, **A**, 4003-4008, 1962.

56. Le Fevre R.J.W. and Sundaram K.M.S., 'Molecular Polarizability. Molar Kerr Constants of Methyl-Methacrylate and its polymer', *J. Chem.Soc.*, **A**, 1880-1887, 1963.

57. Le Fevre R.J.W. and Sundaram K.M.S., 'Molecular Polarizability. The Molar Kerr Constants, Dipole Moments, etc., of Isoprene, Polyisoprene and Some Related Hydrocarbons', **A**, *J. Chem.Soc.*, 3547-3554, 1963.

58. Le Fevre R.J.W. and Sundaram K.M.S., 'Molecular Polarizability. The Molar Kerr Constants and Apparent Dipole Moments of Cyclopentadiene and Some of its Polymers', *J. Chem.Soc.*, **A**, 3518-3523, 1964.

59. Saiz E., Suter U.M., and Flory P.J., 'Optical Anisotropies of Para-Halogenated Polystyrene and Related Molecules',*J.C.S.*, Faraday II, **73**, 1538-1552, 1977.

60. Tonelli A.E., 'Possible Characterisation of Homopolymer Configuration and Copolymer Sequence Distribution by Comparison of Measured and Calculated Kerr Constants', *Macromolecules*, **10**, 153-157, 1977.

61. Khanarian G., Schilling F.C., Cais R.E. and Tonelli A.E., 'Kerr Effect and Dielectric Study of Poly(Oxyethylene Glycols)', *Macromolecules*, **16**, 287-291, 1983.

62. Le Fevre C.G. and Le Fevre R.J.W., 'Molecular Polarizability. The Measurement of Molecular of Molecular Kerr Constants in Solution', *J.C.S.*, 4041-4051, 1953.

63. Frederiq E. and Honssier C., 'Electric Dichroism and Electric Birefringence', Clarendon Press, Oxford, 1973.

64. O'Konski C.T. and Farinato R.S., Jennings B.R., editor, 'Electro-optic and Dielectrics of Macromolecules and Colloids', 133-142, Plenum Press, New York, 1979.

65. Beevers M.S., Khanarian G. and Moore W.J., Jennings B.R., editor, 'Electro-optics and Dielectrics of Macromolecules and Colloids', 269-275, Plenum Press, New York, 1979.

66. Beevers M.S., Khanarian G., 'Measurement of Kerr Constants of Conducting Liquids', *Aust. J. Chem.*, **32**, 263-269, 1979.

67. Beevers M.S., 'The Electro-Optical Kerr Effect in Solutions of Nematogen N-(p-Methoxybenzylidene)-p-n-butylaniline', *Mol. Cryst. Liq. Cryst.*, **31**, 333-348, 1975.

68. Davies M., Moutran R., Price A.H., Beevers M.S. and Williams G., 'Dielectric and Optical Studies of Nematogen 4, 4'-n-Heptyl-Cynanobiphenyl', *J. Chem.S.*, Faraday II, **72**, 1447-1458, 1972.

69. Beevers M.S. and Williams G., 'Electro-Optical Kerr Effect in Solutions of Benzylidene Aniline and its Derivatives', *J. Chem.Soc.*, Faraday II, **72**, 2171-2177, 1976.

70. Beevers M.S. Garrington D.C. and Williams G., 'Dielectric and Dynamic Kerr Effect Studies of Poly(n-Butyl Isocyanate) and Poly(n-Octyl Isocyanate) in Solution', *Polymer J.*, **18**, 540-546, 1977.

71. Beevers M.S., Elliot D.A. and Williams G., 'Studies of Cholesteryl Oleyl Carbonate in its Isotropic and Homeotropic States Using Optical Rotation, Kerr Effect and Light Scattering', *Mol. Liq. Cryst.*, **80**, 135-156, 1982.

72. Bovey F.A., 'The Stereochemical Configuration of Vinyl Polymers and Its Observation By Nuclear Magnetic Resonance', *Accounts Chem. Res.*, **1**, 175-185, 1968.

73. Bovey F.A., 'Polymer Nuclear Magnetic Resonance Spectroscopy. VI. Methylmethacrylate-Styrene and Methylmethacrylate- α -Methylstyrene Copolymers', *J. Polym. Sci.*, **62**, 197-209, 1962.

74. Heatley F. and Bovey F.A., Polymer Nuclear Magnetic Resonanace Spectroscopy. XIV. The Nuclear Magnetic Resonance Spectrum of Poly(isopropyl acrylate)', *Macromolecules*, **1**, 301-308, 1968.

75. Heller J., Tiezen D.O. and D.B. Parkinson, 'Polymerisation of N-vinylcarbazole with Zeigler Type Catalyst Systems', *Macromolecules*, Part A, **1**, 125-138, 1963.

76. Yoshimoto S., Akana Y., Kimura A., Hirata H., Kusabyashi S. and Mikawa H., 'The Nuclear Magnetic Resonance Spectrum of Poly(N-vinylcarbazole)', *Chem. Comm.*, 987, 1969.

77. Williams D.J., 'Nuclear Magnetic Resonance Studies of Poly(N-vinylcarbazole)', *Maromolecules*, **3**, 620, 1970.

78. Tsuuchihashi N., Hatano M. and Sohma J., 'Carbon-13 and Proton Magnetic Resonance Studies of Poly(N-Vinylcabazole)', *Makromol. Chem.*, **177**, 2739-2747, 1976.

79. Debye P., 'Polar Molecules', Chem. Catalog, New York, 1929.

80. Onsager L., 'Electric Dipole Moments of Molecules in Liquids', *J.A.C.S.*, **58**, 1486-1493, 1936.

81a. Guggenheim E.A., 'A Proposed Simplification in the Procedure for Computing Electric Dipole Moments', *Trans. Far. Soc.*, **45**, 714-720, 1949.

81b. Smith J.W., 'Some Developments of Guggenheim's Simplified Procedure For Computing Electric Dipole Moments' *Trans. Faraday Soc.*, **46**, 394-398, 1950.

82. Kerr J., 'A New Relation Between Electricity and Light Dielectrified Media Birefringent', *Phil. Mag.*, **50(4)**, 337-348, 1875.

83. Saiz E., Suter U.W., and Flory P.J., 'Possible Characterisation of Homopolymer Configuration and Copolymer Sequence Distribution by Comparison of Measured and Calculated Molar Kerr Constants', *J. Chem. Soc.*, Faraday Trans. II, **73**, 1538-1552,1977.

84. Buckingam A.D., 'Birefringence Resulting From the Application of an Intense Beam of Light to an Isotropic Medium' *Proc. Phys. Soc.*, **69B**, 344-349, 1956.

85. Paillitte M., 'Measurement of Optical Kerr Effect in Aqueous Solutions of Mineral Salts', *J.Chem Phys.*, **65**, 1629-1668, 1968.

86. Lalane J.R., Martin F.B. and Brothorel P., 'Dispersion of the Molecular Optical Anisotropy by Depolarized Rayleigh Scattering and Birefringence Induced By High Energy Laser Waves', *J. Colloid Intrerfac Sci.*, **39**, 601-610, 1972.

87. Ho P.P. and Alfano R.R.,'Optical Kerr Effect in Liquids', *Phys. Rev.*, **A20(5)**, 2170-2187, 1979.

88. Paillitte M., 'Measurement of Kerr Effect Induced by a Intense Bright Light',*C.R. Acad.Sci.*, **Ser.B**, 262, 264-267, 1966.

89. Ho P.P., Yu. W. and Alfano R.R., 'Relaxation of the Optical Kerr Effect of Anisotropic Molecules in Mixed Liquids', *Chem. Phys. Lett.*, **37**, 91-96, 1976.

90. Jennings B.R. and Coles H.J. 'Laser-Induced Orientation in Macromolecular Suspensions', *Nature*, **252**, 33-34, 1974.

91. Coles H.J., Jennings B.R., 'Laser-induced Birefringence in Pure Liquids', *Phil Mag.*, **32**, 1051-1061, 1975.

92. Yoshioka K., 'Field Strength Dependence of the Electric Birefringence of Rigid and Non-rigid Molecules', *J. Chem. Phys.*, **86**, 491-495, 1987.

93. Wegener W.A., Dowben R.M., Koester V.J., 'Time-dependent Birefriengence, Linear Dichroism and Optical Rotation Resulting From Rigid-Body Rotational Diffusion', *J. Chem. Phys.*, **70(2)**, 622-632, 1979.

94. Wegener W.A.,'Transient Electric Birefringence of Dilute Rigid Body Suspensions at Low Field Strengths', *J. Chem. Phys.*, **84**, 5989-6004, 1986.

95. Roitman D.B. and Zimm B.H.,'An Elastic Hinge Model for Dynamics of stiff Chains. 2. Transient electro-optical properties', *J. Chem. Phys.*, **81**, 6348-6355, 1984.

96. Roitman D.B., *J. Chem. Phys.*,'An Elastic Hinge Model for Dynamics of Stiff Chains. 3. Viscoelastic and Kerr-Effect Behaviour of Bent Molecules', **81**, 6356-6360, 1984.

97. Diaz F.G. and De La Torre J.G.,'Simulation of the Rotational Brownian Dynamics of a Simple, Segmentally Flexible Model - The Elastic Trumbbell', *J. Chem. Phys.*, **88**, 7698 - 8705, 1988.

98. Nagai K. and Ishikawa T., 'Excluded Volume Effect on Dipole Moments of Polymer Chains', *J. Chem. Phys.*, **2(3)**, 416-421, 1971.

99. Aroney M.J., 'The Electro-Optical Kerr Effect in Conformation Analysis', *Angew. Chem.*, **89(10)**, 725-736, 1977.

100. Jennings B.R., 'Electro-Optic Methods for Characterising Macromolecules', *Adv. Polym. Sci.*, **22**, 61-81, 1977.

101. Aroney M.J., Battaglia M., Ferfoglia R., Millar D. and Pierens R.K., *J. Chem. Soc.*, Faraday Trans. II, 'The Kerr Constant of Water and other Pure Liquids at 633nm', **72**, 724-726, 1976.

102. Lewis J.W. and Orttung W.H., 'The Kerr Effect of Carbon disulfide and other Organic Liquids in the Ultraviolet', *J. Phys. Chem.*, **82(6)**, 698-705, 1978.

103. Okamoto K., Yamada M., Itaya A., Kimura T. Kusabayashi S., 'Polymerisation of N-Vinylcarbazole, N-Vinyl-5H-Benzo(b)Carbazole and N-Vinyl-7H-Benzo-(C)Carbazole', *Macromolecules*, **9**, 645-649, 1976.

104. Mikawa H., Kasai K., Kusahoyashi S., Hirata H. and Kimura A., 'Crystallinity of Poly(N-Vinylcarbazole), *J. Polym. Sci.*, Pt A-2, **8**, 613-618, 1970.

105. Fox T.G. and Flory P.J., ' The Glass Temperature and Related Properties of Polystyrene. Influence of Molecular Weight', *J. Polym. Sci.*, **14**, 315-319, 1954.

106. Hatano M. and Kambara S., 'Infrared Spectra and Crystallinitity of Poly[3,3-bis-(chloromethyl)-oxacyclobutane]', *J. App. Polymer Sci.*, **6**, 232-239, 1962.

107. Airapetyants A.V., Voitenko R.M., Davidov B.E. and Krentsel B.A., 'Electrical Properties of Polymer Semiconductors' *Vysokomol.*, Soedin, **6**, 291-315, 1964.

108. Beck H. and Dorrer, U.S. Patent 2,215,537, 1940, Assigned to General Aniline and Film Corporation.

109. British Patent 914,418, 1963, Assigned to Montecatini Societa L'Industria Mineralia E. Chemica.

110. Griffiths C.H., 'Folded Chain Crystallization of Poly(N-vinylcarbazole)'*J. Polym. Sci.*, Phys. Edn., **13**, 1167-1176, 1975.

111. Fox T.G. Flory P.J., 'The Glass Temperature and Related Properties of Polystyrene. Influence of Molecular Weight', *J. Polym. Sci.*, **14**, 315-319, 1954.

112. Schouhorn H., 'Heterogeneous Nucleation of Polymer Melts on High Energy Surfaces. II. Effect of Substrate on Morphology and Wettability', *Macromolecules*, **1**, 145-151, 1968.

113. Fredericks R.J., Melvger A.J. and Dolegiewitz L.J., 'Morphological and Structural Changes in a Copolymer of Glycolide and Lactide Occurring as a Result of Hydrolysis', *J. Polym. Sci.*, Phys. Edn., 22, 57-66, 1984.

114. Debye P. and Bueche F., 'Electric Moments of Polar Polymers in Relation to Their Structure', *J. Chem. Phys.*, **19**, 589-594, 1951.

115. North A.M. and Phillips P.J., 'Dielectric Properties of Poly(N-vinylcarbazole) Solution', *Chem. Comm.*, **21**, 1340-1341, 1968.

116. North A.M. and Phillips P.J., 'Correlation of Dielectric and Viscoelastic Relaxation in Polymer Solutions', *J. British Polym.*, **1(2)**, 76-80, 1969.

117. Dev S.B., Lochhead R.Y. and North A.M.,'Dielectric and Viscoelastic Relaxation in Dilute Solutions of Some Non-Gaussian Chains', *Farraday Soc.*, **49**, 244-256, 1990.

118. Pochan J.M. Hinman D.F., Froix M.F. and Nash R.W., 'Dielectric Relaxation Studies of Poly(N-vinylcarbazole) and Poly(3-Chloro-N-VinylCarbazole) Including the Effects of Sorbed Oxygen', *Polymer Preprints, A.C.S.*, Div.Polym. Chem., 570-575, 1975.

119. Froix M.F., Williams D.J., Pochan J.M. and Geodde A.O., 'Anomalous Relaxation in Carbazole Polymers', Polymer Preprints, *A.C.S.*, Div. *Polym. Chem.*, 576-582, 1975.

120. Pochan J.M. Hinman D.F. and Nash R.W., 'Dielectric Relaxation Studies of Poly(N-vinylcarbazole) and Poly(3-chloro-N-vinylcarbazole) Including the Effects of Sorbed Oxygen', *J. Appl. Phys.*, **46(10)**, 4115-4119, 1975.

121. Beevers M.S., Mumby S.J., 'Dielectric and Kerr effect Studies of Stereoregular Poly(N-Vinylcarbazole)', *Polymer Communications*, **25**, 173-175, 1984.

122. Riande E., Barrales-Rianda J.M., Molina M.S. and Saiz E.,'Dipole Moments of Poly(N-vinylcarbazole)', *Macromolecules*, **17**, 2728-2731, 1984.

123. Vincent V.M. and Wright J.D., 'Photoconductivity and Crystal Structure of Organic Molecular Complexes,' *J. Chem. Soc.*, Faraday Trans., **70(1)**, 58-71, 1974.

124. Kuckowski A., Slupkowski T. and Jachym B., 'Photoelectric Properties of the Charge-Transfer Complexes of Poly(N-vinylcarbazole) with Tetracyanoquinodimethane,' *J. Eur. Poly.*, **19**, 25-28, 1983.

125. Agarwal S.K., Hemmadi S.S. and Pathak N.L.,'Electrophotographic Characteristics of Pure and Sensitized poly(N-vinylcarbazole)', *Polymer.*, **20**, 867-871, 1982.

126. Pochan J.M. and Gibson H.W.,'Chemical Bound Sensitizers: Dye Sensitization of poly(N-vinylcarbazole) via Sulfonation and Ion Exchange', *J. Polym. Sci.*, Polym. Phys Ed., **20,** 2059-2067, 1982.

127. Balabanov E.M., Bukin Yu. L., Lokmane E., Dregeris J., Rumyantsev B.M., Semenova L.A. and Titov V.V., 'Study of the Electrophotographic Sensitivity and Photoconductivity of Poly(N-vinylcarbazole) and Poly(N-epoxypropylcarbazole) Films Doped with Some Derivatives of Naphthoquinone', *Chem. Abstr.*, **94**, 22853Y, 1981.

128. Balabanov E.M., Bukin Yu. L., Lokmane E., Dregeris J., Rumyantsev B.M., Semenova L.A., Titov V.V., Freimanis J. and Yudina, G.I., 'Study of the Electrophotographic Sensitivity and Photoconductivity of Poly(N-vinylcarbazole) and Poly(N-epoxypropylcarbazole) Films Doped with Some Derivatives of Naphthoquinone',*Vysokomol.*, Soedin, Ser., **A22**, 2545-2552, 1980.

129. Hasegawa S., Kawaguchi T., Shoda M. and Uekawa J., 'Photoconductive Properties of Poly(N-vinylcarbazole) Chemisorbed Natural Dye',*Chem. Abstr.*, **93**, 17723f, 1980.

130. Terrell D.R. and Evers F., German Offen., DE 3, 032, 425, 1982.

131. Seanor D.A., 'Electrical Properties of Polymers', Jenkins A.D. ed., North Holland, Amsterdam, 1972.

132. Tazuke S., and Matsuyama Y., 'Donor Acceptor Interactions in Polymeric Systems', *Makromol. Chem.*, **176**, 3167-3178, 1975.

133. Penwell R.C., Ganguly B.N. and Smith T.W.J., Poly(N-vinylcarbazole): 'A Selective Review of its Polymerisation, Structure, Properties, and Electrical Characteristics', *Polym. Sci., Macromol., Rev.*, **13**, 63, 1978.

133a. Weiser G., Seki H., 'Charge transfer complex formation of trinitrofluorenone with polyvinylcarbazole and ethylcarbazole', IBM Journal of Research and Development, **16(6)**, 598-603, 1972.

134. Aroney M.J., 'The Electro-Optical Kerr Effect in Conformation Analysis, *Angew. Chem.*, **89(10)**, 725-736, 1977.

135. Le Fevre R.J.W., Radford D.A., Ritchie G.L.D. and Stiles R.J., 'The Conformations of Some Weak Complexes of Benzene', *J. Chem. Soc.*, **B**, 148-156, 1968.

136. Hopkins P.A., Le Fevre R.J.W., L. Radom and Ritchie G.L.D., 'Molecular Polarizability. Association of Some Aromatic Aldehyde and Ketones With Benzene', *J. Chem. Soc.*, **B**, 574-576, 1971.

137. Beevers M.S., 'The Electro-Optical Kerr Effect in Solutions of the Nematogen N-(p-Methoxybenzylidene)-p-n-butylaniline', *Mol. Crys., Liq. Cryst.*, **31**, 333, 1975.

138. Gentle I.R. and Ritchie G.L.D.,'Second Hyperpolarizabilities and Static and Optical Frequency Polarizability Anisotropies of Benzene', *J. Phys. Chem.*, **93**, 7740-7744, 1989.

139. Aroney M.J., Le Fevre R.J.W., Parkins G.M., 'Molecular Polarizability. The Molar Kerr Constants and Dipole Moments of Six Polyethylene Glycols as Solutes in Benzene', *J. Chem. Soc.*, 2890-2895, 1960.

140. Le Fevre R.J.W., and Sundaram K.M.S., 'Molecular Polarizability. Molar Kerr Constants of Methyl-methacrylate and Its Polymer', *J. Chem., Soc.*, 1880-1887, 1963.

141. Le Fevre R.J.W., and Sundaram K.M.S., 'Molecular Polarizability. The Molar Kerr Constant, Dipole Moments etc., of Methyl acrylate and Five of Its Polymers', *J. Chem., Soc.*, 3188-3193, 1963.

142. Tonelli A.E., 'Possible Characterization of Homopolymer Configuration and Copolymer Sequences Distribution by Comparison of Measured and Calculated Molar Kerr Constants', *Macromolecules*, **10**, 153-157, 1977.

143. Saiz E., Suter U.W. and Flory P.J., 'Optical Anisotropies of para-Halogenated Polystyrenes and Related Molecules', *J. Chem., Soc.*, Faraday Trans.II, **73**, 1538-1552, 1977.

144. Mumby S.J., Experimental and Theoretical Investigations of the Dielectric and Electro-optic Properties of Polycarbazoles and Polysiloxanes' PhD Thesis, University of Aston In Birmingham, 1983.

145. Volkenstein M.V., 'Configurational Statistics of Polymer Chains', English Translation, Interscience, New York, 1963.

146. Sundararajan P.R.,'Conformational Aspects of Poly(N-vinylcarbazole)', *Macromolecules*, **13**, 512-517, 1980.

Appendix 1

Light scattering data of molecular weights and radii of gyration of PVK samples F1, F2 and F3 (synthesised with different catalysts) determined in 1,4-dioxane.

Sample	Cell /mm	Concentration (mg/ml)	Refractive index	dn / dc	Molecular weight (M_W)	Radii of gyration (Å/10^2)
F1	21	2.5	1.4242	0.1840	$1.5x10^5$	3.57
		5	1.4242	0.2300	$9.59x10^4$	3.57
		10	1.4242	0.2760	$6.66x10^4$	3.57
F2	21	2.5	1.4242	0.1840	$3.91x10^6$	7.40
		5	1.4242	0.2300	$2.50x10^6$	7.40
		10	1.4242	0.2760	$1.74x10^5$	7.40
F3	21	2.5	1.4242	0.1840	$3.28x10^5$	4.50
		5	1.4242	0.2300	$2.10x10^5$	4.50
		10	1.4242	0.2760	$2.00x10^4$	4.50

Light scattering data of molecular weights and radii of gyration of PVK samples F1, F2 and F3 (synthesised with different catalysts) determined in toluene.

Sample	Cell /mm	Concentration (mg/ml)	Refractive index	dn/dc	Molecular weight (M_W)	Radii of gyration ($Å/10^2$)
LS1	21	2.5 5 10	1.4242	0.2300	$3.59x10^4$	1.69
LS2	21	2.5 5 10	1.4242	0.2300	$1.14x10^6$	3.89
LS3	21	2.5 5 10	1.4242	0.2760	$2.74x10^5$	3.28

Appendix 2

Carbon-13 inversely gated decoupled nuclear magnetic resonanace spectrum for sample F1 (initiated with azo-bisisobutyronitrile at 343K) was obtained by using the following spectrometer settings:

Settings of (Bruker 300 MHz) N.M.R. Spectrometer	
Spectrometer Frequency	75.466 MHz
Offset	25269.698 Hz
Sampling Interval	32768
Total Data (FID)	32768
Spectral Width	16666.667 Hz
Data Resolution	1.017
Pulse Width	4.6
Spin Lattice Relaxation (T1)	11.126 Sec.
Acquisition time	0.983 μSec.
Receiver Gain	200
Number of Scans	6256
Temperature	303 K
Filter Width	20900
Offset To Decoupler	5000 Hz

Carbon-13 inversely gated decoupled nuclear magnetic resonanace spectrum for sample F2 (initiated with boron trifluoride etherate 298K) was obtained by using the following spectrometer settings:

Settings of (Bruker 300 MHz) N.M.R. Spectrometer	
Spectrometer Frequency	75.466MHz
Offset	28532.698Hz
Sampling Interval	32768
Total Data (FID)	32768
Spectral Width	17857.143Hz
Data Resolution	1.000
Pulse Width	4.9
Spin Lattice Relaxation (T1)	11.126
Acquisition time	0.916 μSec
Receiver Gain	200
Number of Scans	3608
Temperature	383K
Filter Width	22400
Offset To Decoupler	4800Hz

Appendix 3

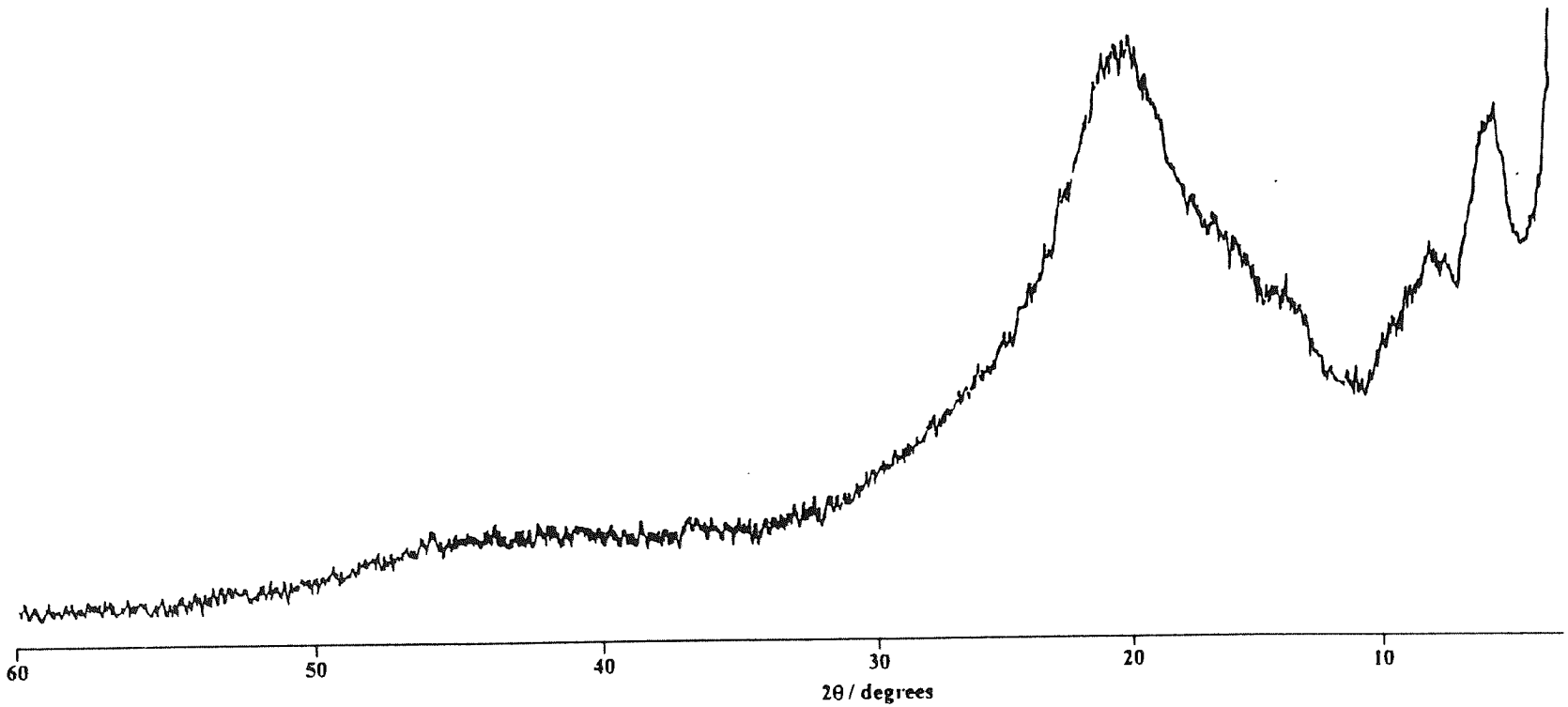

X-ray diffraction curve of PVK sample F1 (before heat treament)

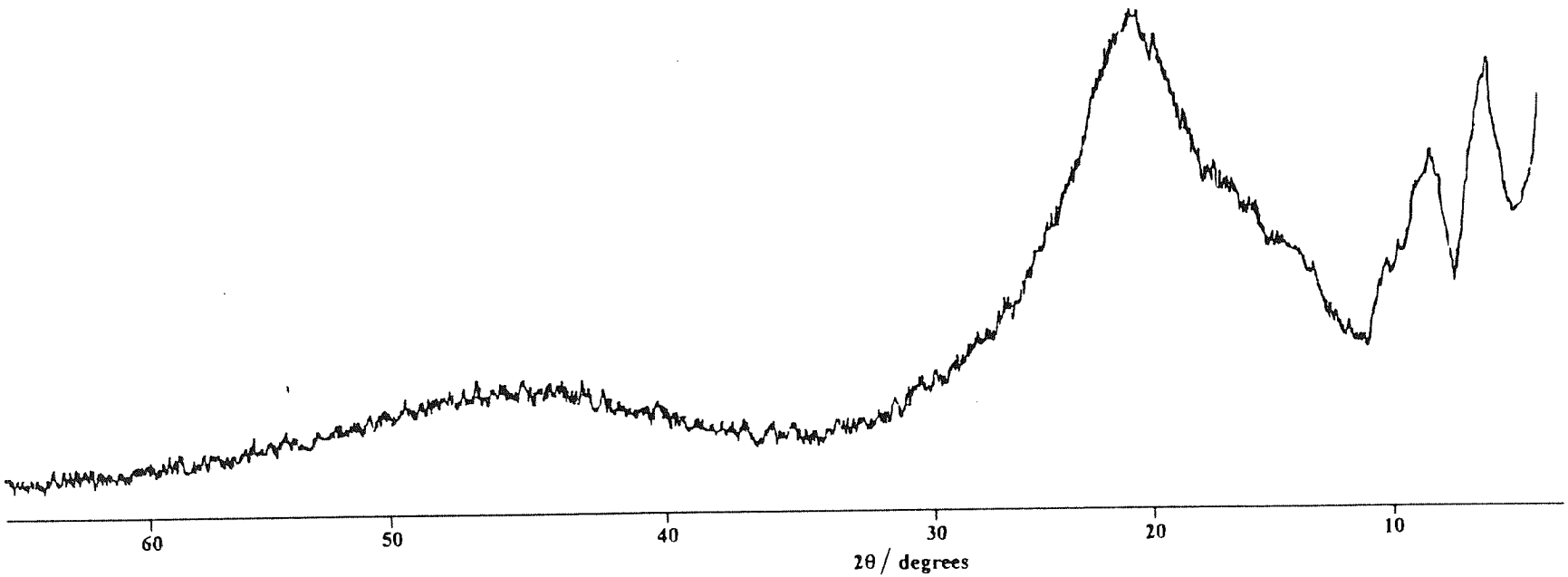

X-ray diffraction curve of PVK sample F1 (after heat treatmeant at 300 ^{o}C for 30 minutes)

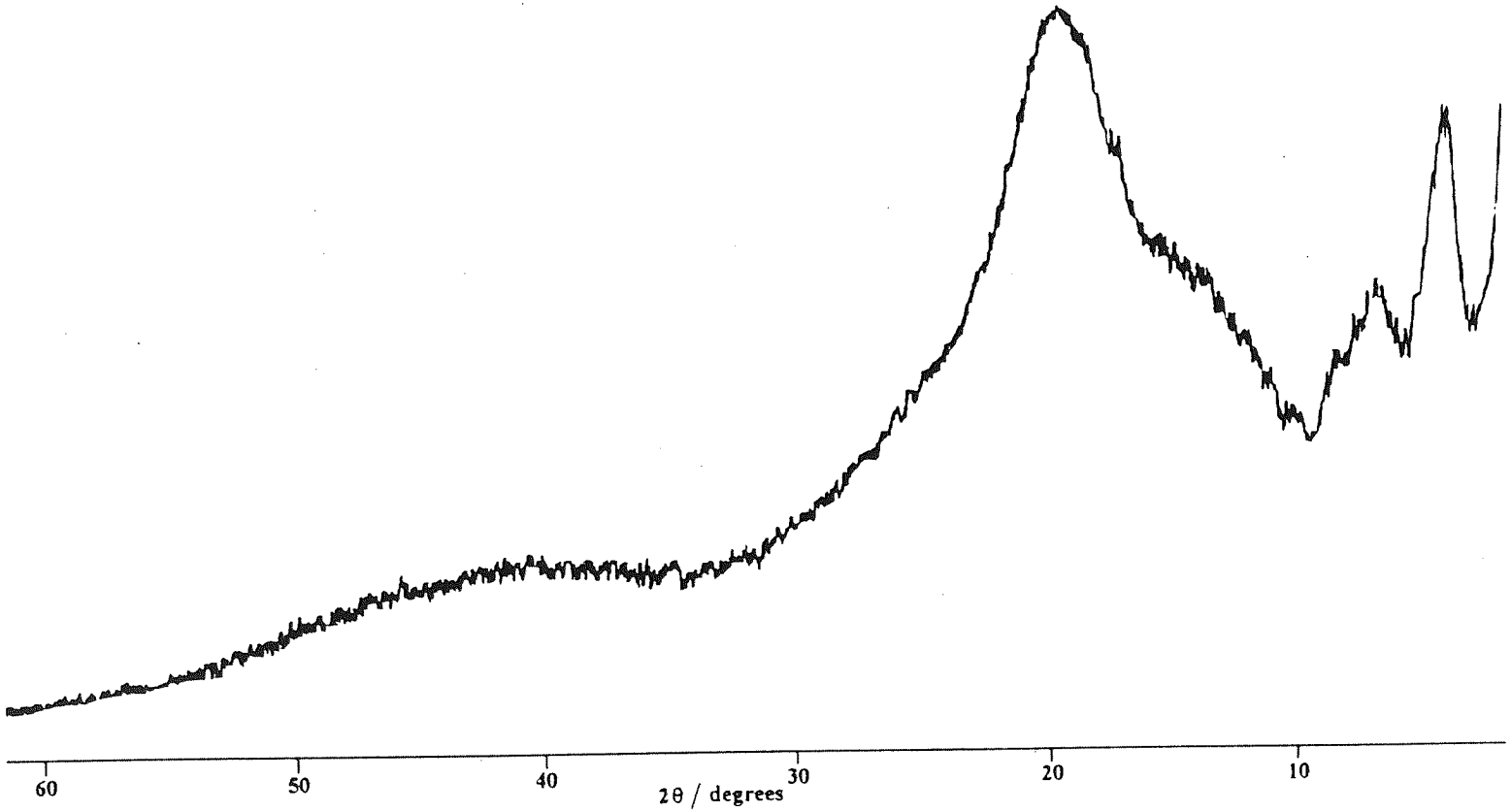

X-ray diffraction curve of PVK sample F2 (before heat treatment)

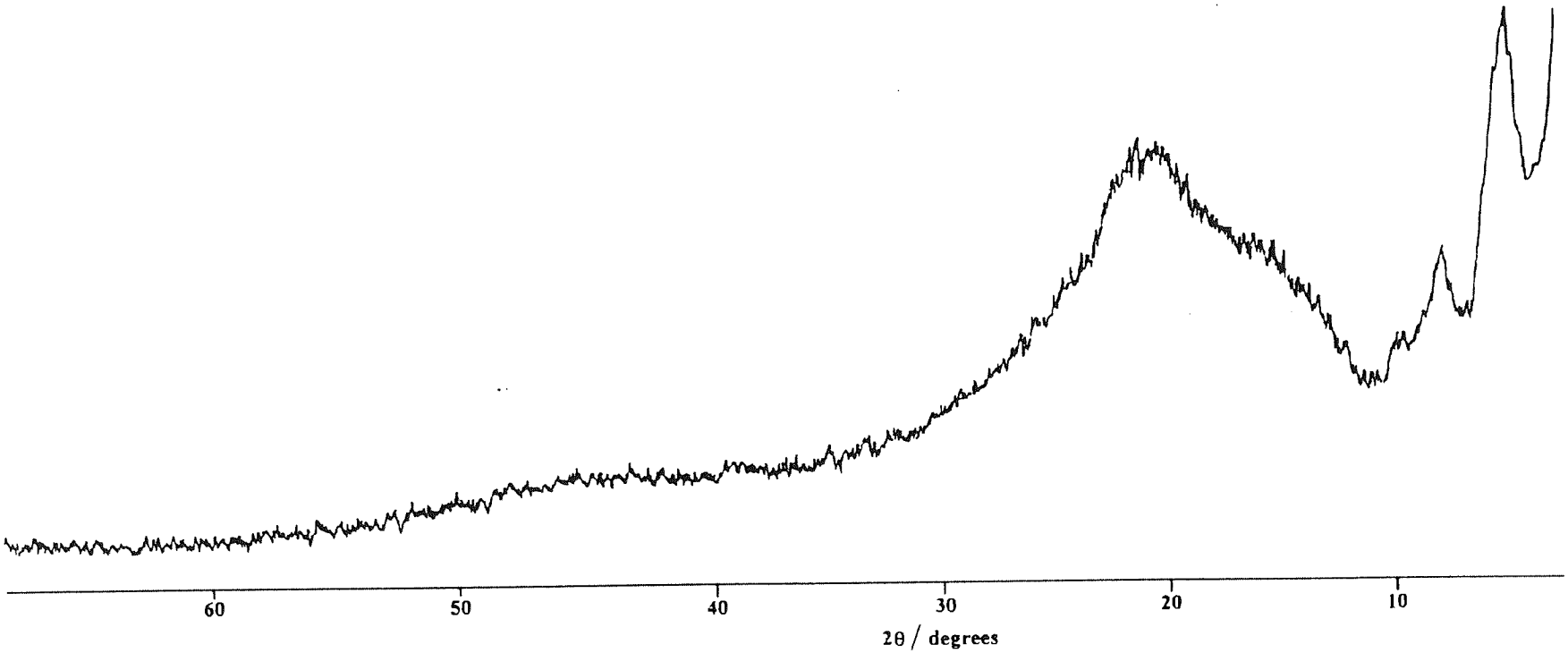

X-ray diffraction curve of PVK sample F2 (after heat treatment at 300 ^{0}C for 30 minutes)

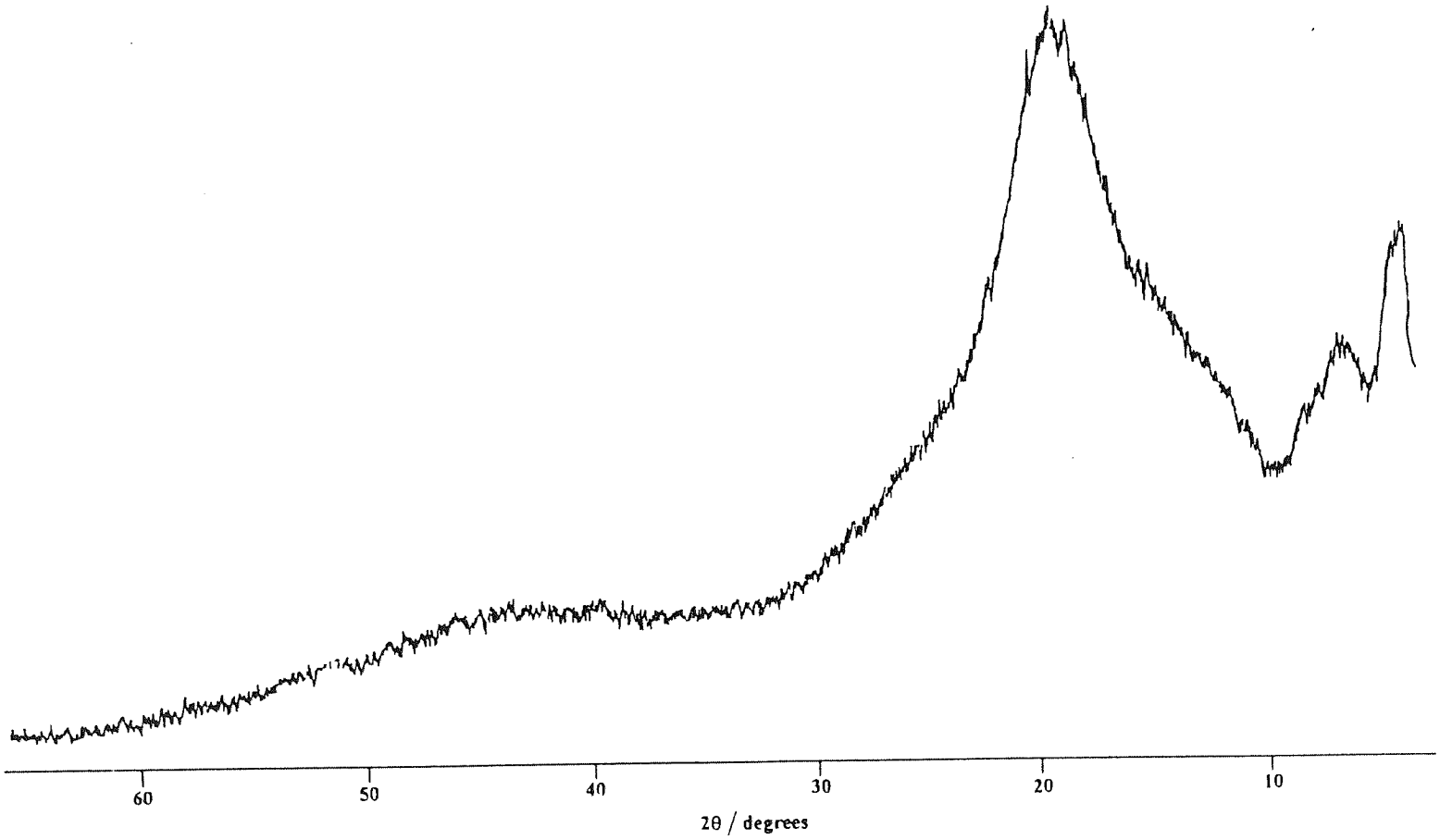

X-ray diffraction curve of PVK sample F3 (before heat treatment)

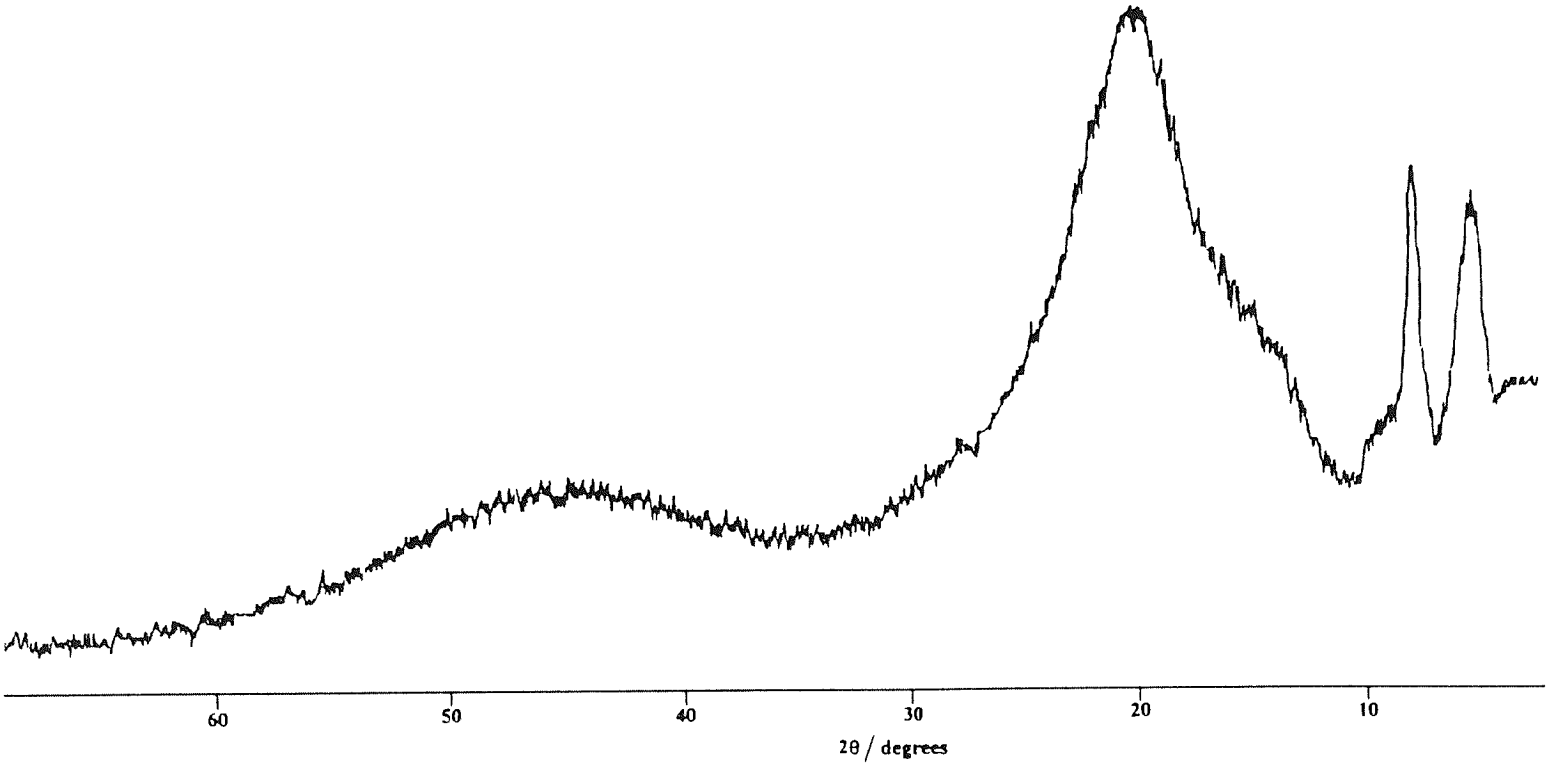

X-ray diffraction curve of PVK sample F3 (after heat treatment at 300 °C for 30 minutes)

Appendix 4

COMPUTER PROGRAM

This program was written using Quick Basic on an Apple Macintosh. The program evaluates the concentration values of PVK : TNF complex moeity [c] by manipulating the visible spectroscopic data (see Chapter 5). The program requires the input of equilibrium constants K_e and initial concentrations of acceptor (a_o) and donor (d_o).

```
10 INPUT " Input value of initial concentration of acceptor ";ao
20 INPUT " Input value of initial concentration of donor  ";do
30 LET c=1
40 INPUT " input value of equilibrium concentration";Ke
50 :
60 a=ao*do
70 b=-ao+do+1/Ke
80 :
90 chk = (b^2-4*a*c)
100 IF chk < 0 THEN GOTO 160
110 x1 = (-b+(b^2 - 4*a*c)^.5)/(2*a)
120 x2 = (-b-(b^2-4*a*c)^.5)/(2*a)
130 :
140 PRINT "values of concentration of complex moeity = ";x1,x2
150 END
160 PRINT " Insolvable solutions "
170 END
```

Appendix 5

Initial concentration of TNF (mol cm^{-3})	Temperature (K)	ε_{12}
1.65×10^{-5}	298	2.2682
3.20×10^{-5}		2.2899
4.80×10^{-5}		2.2974
6.35×10^{-5}		2.3123
1.65×10^{-5}	308	2.2560
3.20×10^{-5}		2.2756
4.80×10^{-5}		2.2902
6.35×10^{-5}		2.3029
1.65×10^{-5}	318	2.2150
3.20×10^{-5}		2.2387
4.80×10^{-5}		2.2474
6.35×10^{-5}		2.2614
1.65×10^{-5}	328	2.1962
3.20×10^{-5}		2.2153
4.80×10^{-5}		2.2264
6.35×10^{-5}		2.2384
1.65×10^{-5}	338	2.1685
3.20×10^{-5}		2.1891
4.80×10^{-5}		2.2009
6.35×10^{-5}		2.2101

Table A5.1 Dielectric permittivity of solutions of TNF in 1,4-dioxane at various temperatures.

Initial concentration of TNF (mol cm^{-3}) (**NEK=1.04×10^{-4}** mol cm^{-3})	**Temperature** (K)	ε_{12}
1.65×10^{-5}	298	2.3048
3.20×10^{-5}		2.3096
4.80×10^{-5}		2.3173
6.35×10^{-5}		2.3266
1.65×10^{-5}	308	2.2932
3.20×10^{-5}		2.2999
4.80×10^{-5}		2.3061
6.35×10^{-5}		2.3168
1.65×10^{-5}	318	2.2581
3.20×10^{-5}		2.2651
4.80×10^{-5}		2.2727
6.35×10^{-5}		2.2816
1.65×10^{-5}	328	2.2393
3.20×10^{-5}		2.2437
4.80×10^{-5}		2.2526
6.35×10^{-5}		2.2596
1.65×10^{-5}	338	2.2144
3.20×10^{-5}		2.2209
4.80×10^{-5}		2.2299
6.35×10^{-5}		2.2358

Table A5.2 Dielectric permittivity of solutions of NEK : TNF (complex + free TNF + free NEK) in 1,4-dioxane at various temperature.

Initial concentration of TNF (mol cm^{-3}) (**F1=1.04x10^{-4}** mol cm-3)	**Temperature** (K)	ε_{12}
1.65 x10^{-5}	298	2.2396
3.20 x10^{-5}		2.2490
4.80 x10^{-5}		2.2518
6.35 x10^{-5}		2.2684
1.65 x10^{-5}	308	2.2225
3.20 x10^{-5}		2.2395
4.80 x10^{-5}		2.2443
6.35 x10^{-5}		2.2587
1.65 x10^{-5}	318	2.2011
3.20 x10^{-5}		2.2097
4.80 x10^{-5}		2.2134
6.35 x10^{-5}		2.2272
1.65 x10^{-5}	328	2.1630
3.20 x10^{-5}		2.1774
4.80 x10^{-5}		2.1857
6.35 x10^{-5}		2.1863
1.65 x10^{-5}	338	2.1380
3.20 x10^{-5}		2.1534
4.80 x10^{-5}		2.1696
6.35 x10^{-5}		2.1863

Table A5.3 Dielectric permittivity of solutions of F1: TNF (complex + free TNF + free F1) in 1,4-dioxane at various temperatures.

Intial concentration of TNF (mol cm^{-3}) (F2 = 1.04×10^{-4} mol cm^{-3})	Temperature (K)	ε_{12}
1.65×10^{-5}	298	2.3135
3.20×10^{-5}		2.5939
4.80×10^{-5}		2.7488
6.35×10^{-5}		2.9945
1.65×10^{-5}	308	2.3050
3.20×10^{-5}		2.5633
4.80×10^{-5}		2.6872
6.35×10^{-5}		2.8755
1.65×10^{-5}	318	2.2733
3.20×10^{-5}		2.5168
4.80×10^{-5}		2.6599
6.35×10^{-5}		2.7982
1.65×10^{-5}	328	2.2529
3.20×10^{-5}		2.5032
4.80×10^{-5}		2.6298
6.35×10^{-5}		2.7452
1.65×10^{-5}	338	2.2347
3.20×10^{-5}		2.4948
4.80×10^{-5}		2.6089
6.35×10^{-5}		2.7035

Table A5.4 Dielectric permittivity of solutions of F2 : TNF (complex + free TNF + free F2) in 1,4-dioxane at various temperature.

As explained in chapter 5, equilibrium constants (K_c) of charge transfer complexes were determined by using optical density measurements from u.v. / visible spectra. All solutions of F1: TNF, F2 : TNF and N-ethylcarbazole : TNF had absorbance between 450 - 600nm. Spectrum of pure (uncomplexed) TNF and (uncomplexed) poly(N-vinylcarbazole) indicated that at 500nm there is virtually zero absorbance suggesting that all the absorbance was due to charge transfer and not due to uncomplexed species. The optical densities readings at 500nm are shown in the following table:

Temperature (K)	Optical Density at 500nm				
	F1 : TNF 2% : 0.25%	F1 : TNF 2% : 0.5%	F1 : TNF 2% : 1.0%	F1 : TNF 2% : 1.5%	F1 : TNF 2% : 2.0%
298	0.09	0.13	0.23	0.30	0.46
308	0.09	0.13	0.22	0.28	0.38
318	0.10	0.14	0.22	0.29	0.38
328	0.10	0.14	0.22	0.28	0.37
338	0.10	0.12	0.20	0.26	0.37
	F2 : TNF 2% : 0.25%	F2 : TNF 2% : 0.5%	F2 : TNF 2% : 1.0%	F2 : TNF 2% : 1.5%	F2 : TNF 2% : 2.0%
298	0.11	0.15	0.22	0.29	0.38
308	0.08	0.12	0.19	0.26	0.34
318	0.08	0.14	0.21	0.32	0.38
328	0.10	0.14	0.20	0.26	0.36
338	0.09	0.12	0.18	0.24	0.31
	NEK: TNF 2% : 0.25%	NEK : TNF 2% : 0.5%	NEK : TNF 2% : 1.0%	NEK : TNF 2% : 1.5%	NEK : TNF 2% : 2.0%
298	-	0.38	0.75	1.15	1.46
308	-	0.50	0.67	1.04	1.32
318	-	0.45	0.61	0.95	1.26
328	-	0.41	0.56	0.88	1.18
338	-	0.43	0.53	0.86	1.20

Table A5.5 Optical density at 500nm for various solutions of PVK TNF at different temperatures.

According to equation 5.11 (in chapter 5), a plot of y = ln (optical density) against x = 1/T should give a straight line plot that has a gradient of $\frac{-\Delta H}{R}$ and an intercept of $[\Delta S/R + \ln (a_0\, d_0\, \varepsilon\, l)]$ where:

H = enthalpy of complex formation

ΔG = Gibbs free energy

R = gas constant

a_0 = intial concentration of acceptor

d_0 = initial concentration of donor

ε = extinction coefficient

l = cell pathlength (2mm)

A typical graph of ln (optical density) against 1/ temperature is shown below:

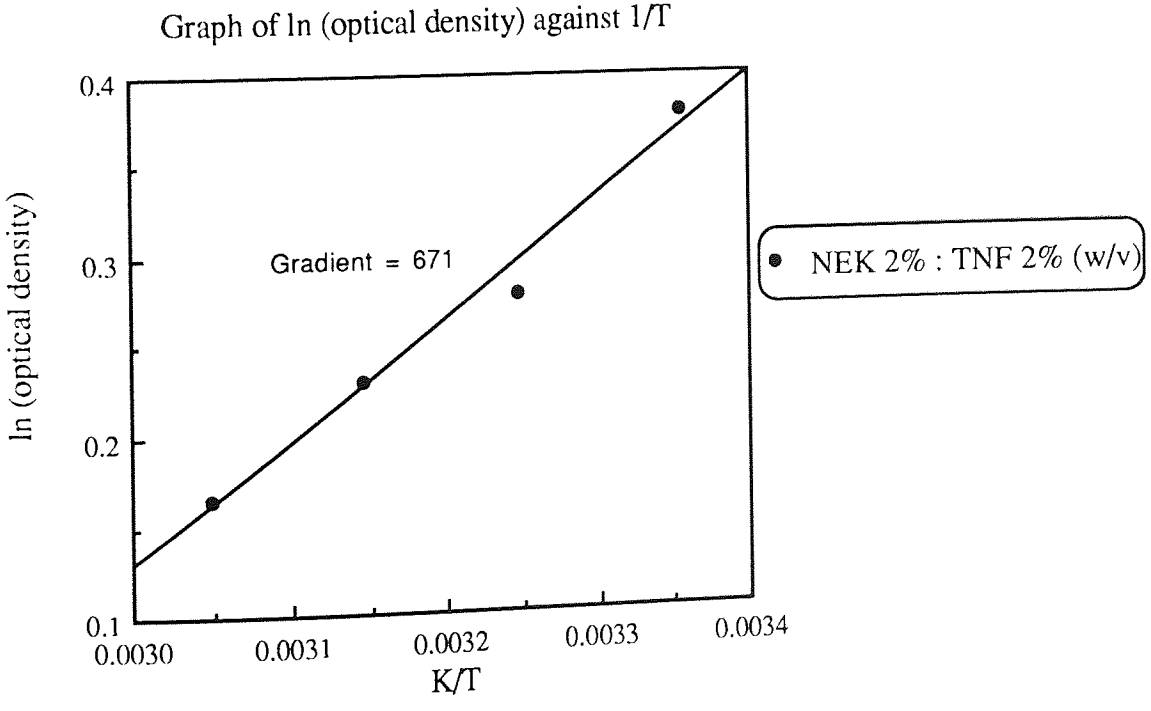

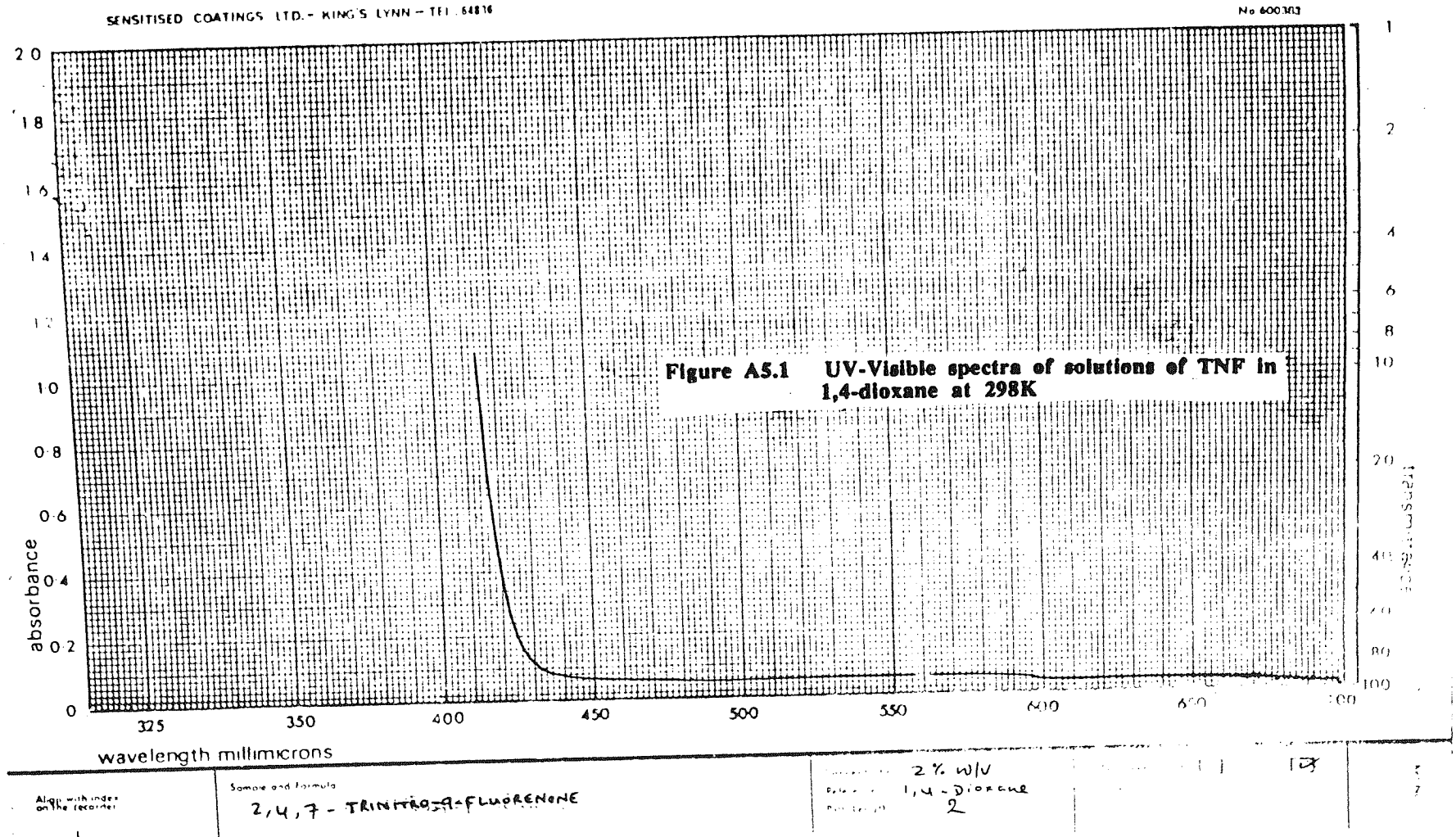

Figure A5.1 UV-Visible spectra of solutions of TNF in 1,4-dioxane at 298K

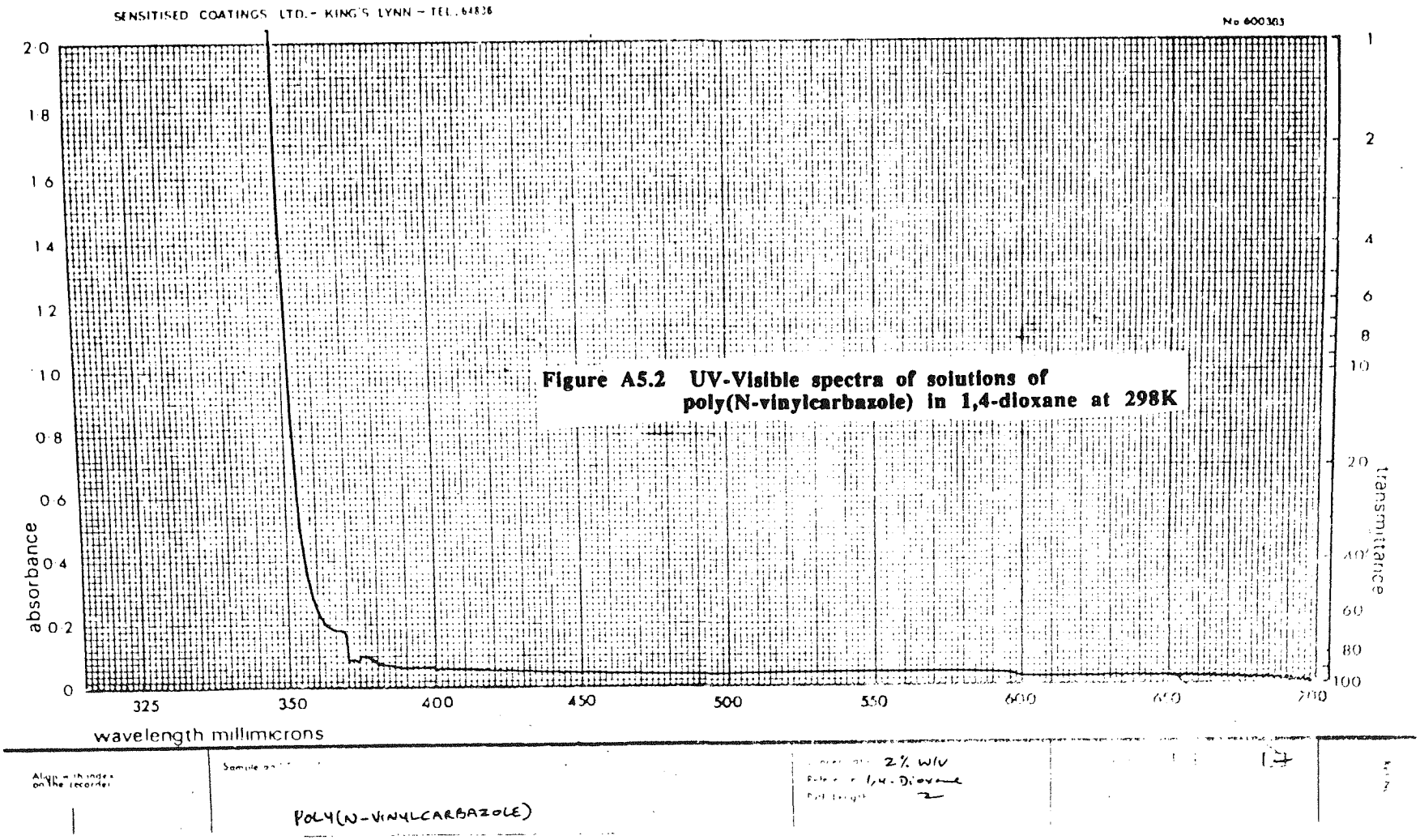

Figure A5.2 UV-Visible spectra of solutions of poly(N-vinylcarbazole) in 1,4-dioxane at 298K

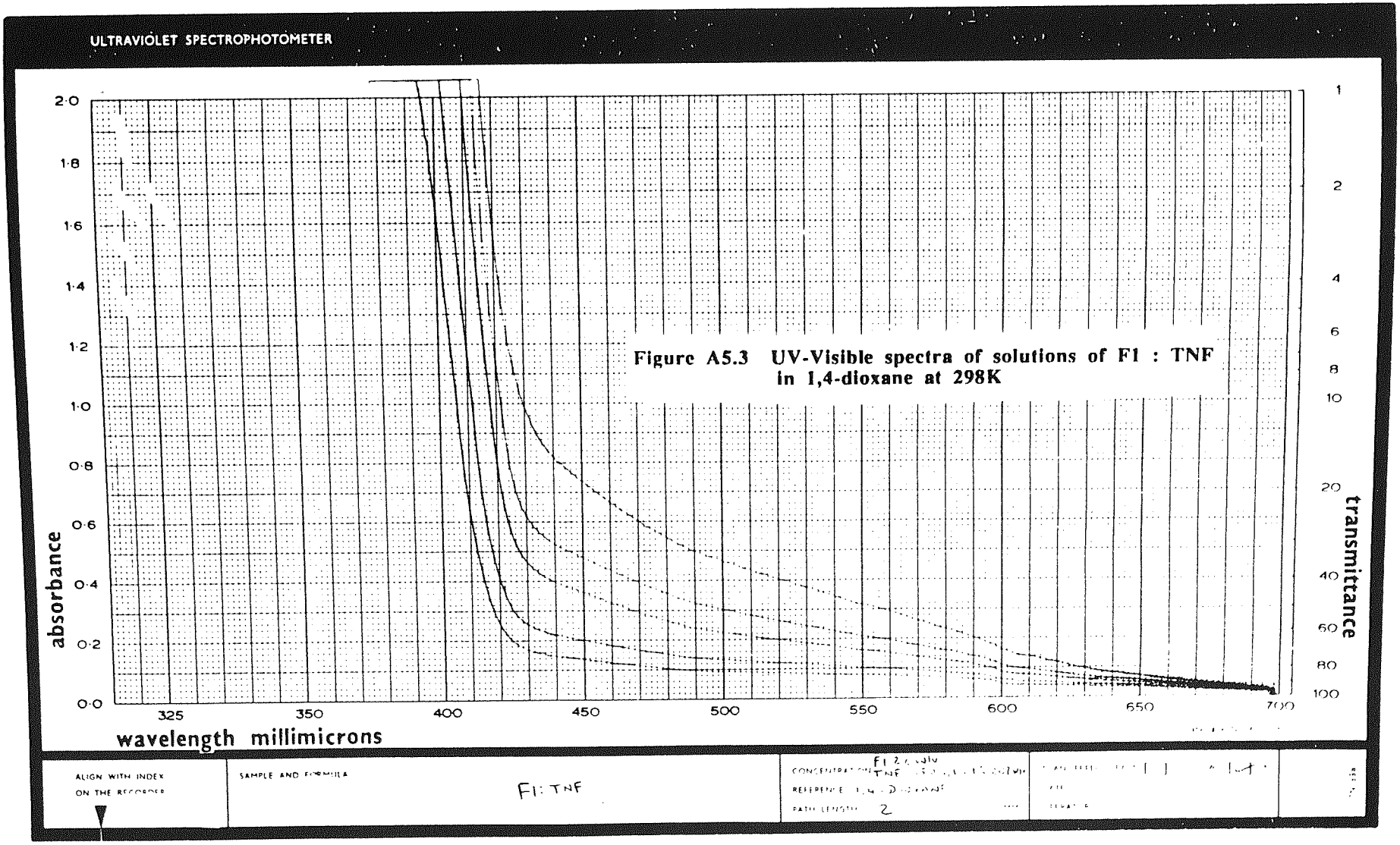

Figure A5.3 UV-Visible spectra of solutions of F1 : TNF in 1,4-dioxane at 298K

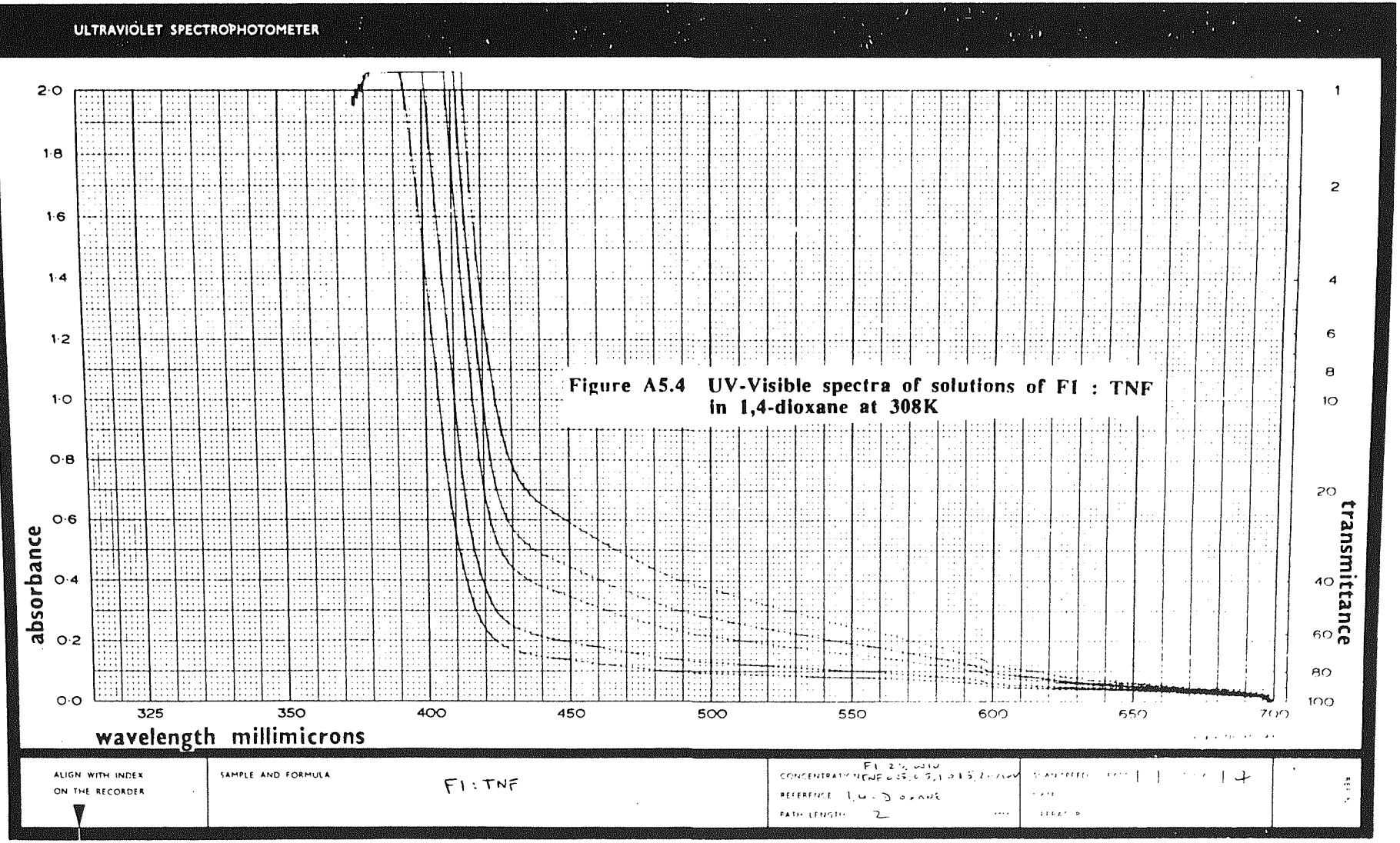

Figure A5.4 UV-Visible spectra of solutions of F1 : TNF in 1,4-dioxane at 308K

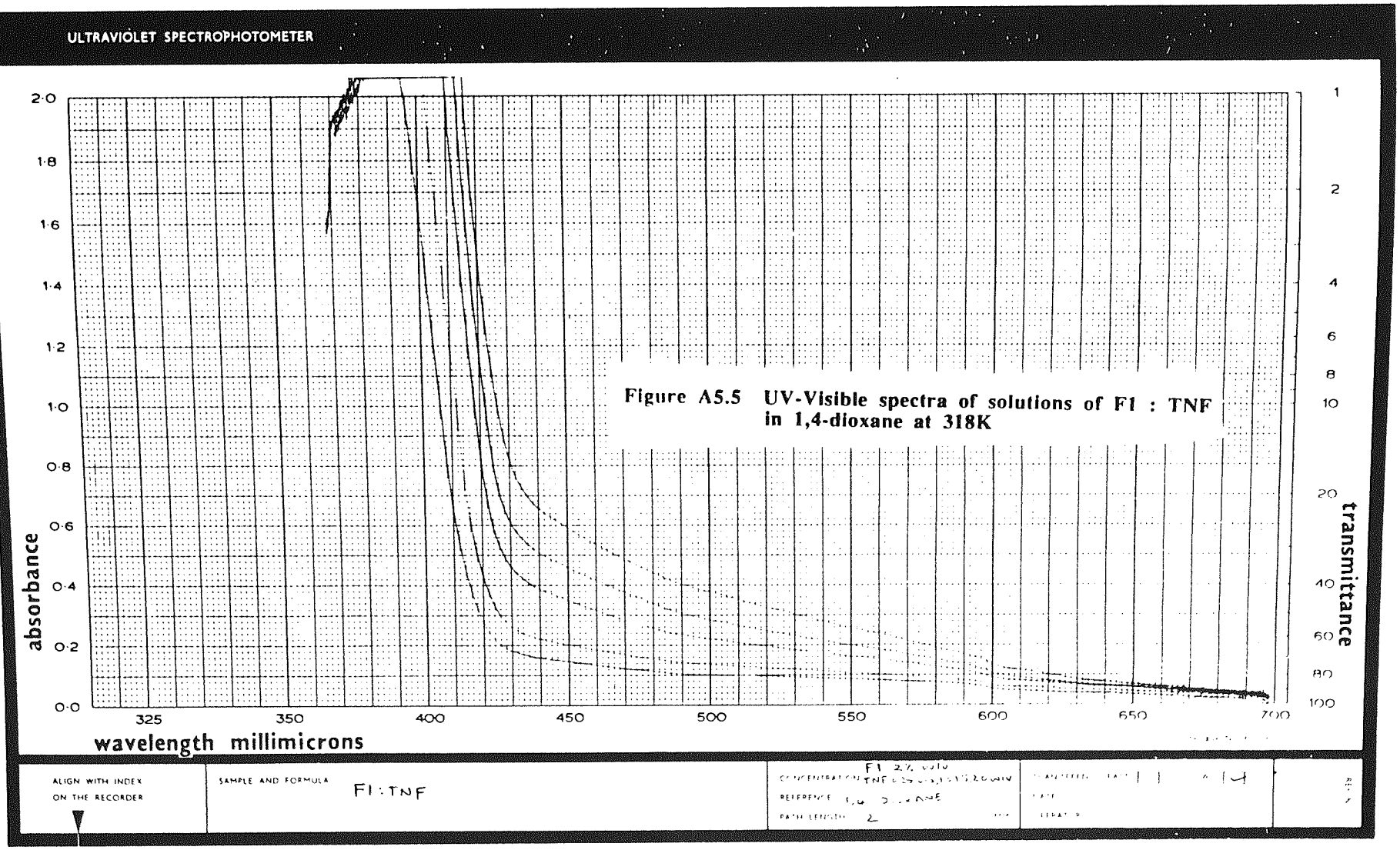

Figure A5.5 UV-Visible spectra of solutions of F1 : TNF in 1,4-dioxane at 318K

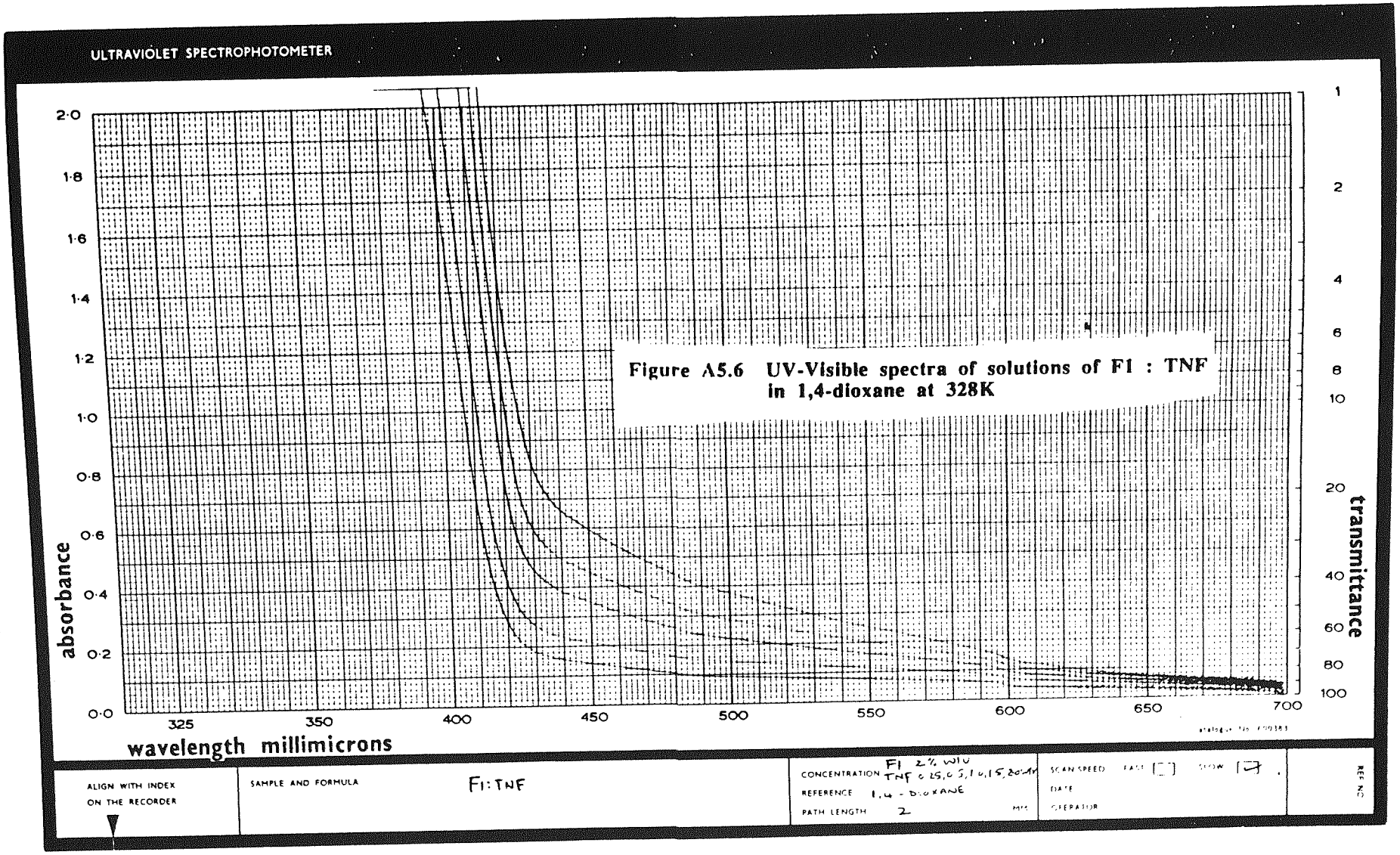

Figure A5.6 UV-Visible spectra of solutions of F1 : TNF in 1,4-dioxane at 328K

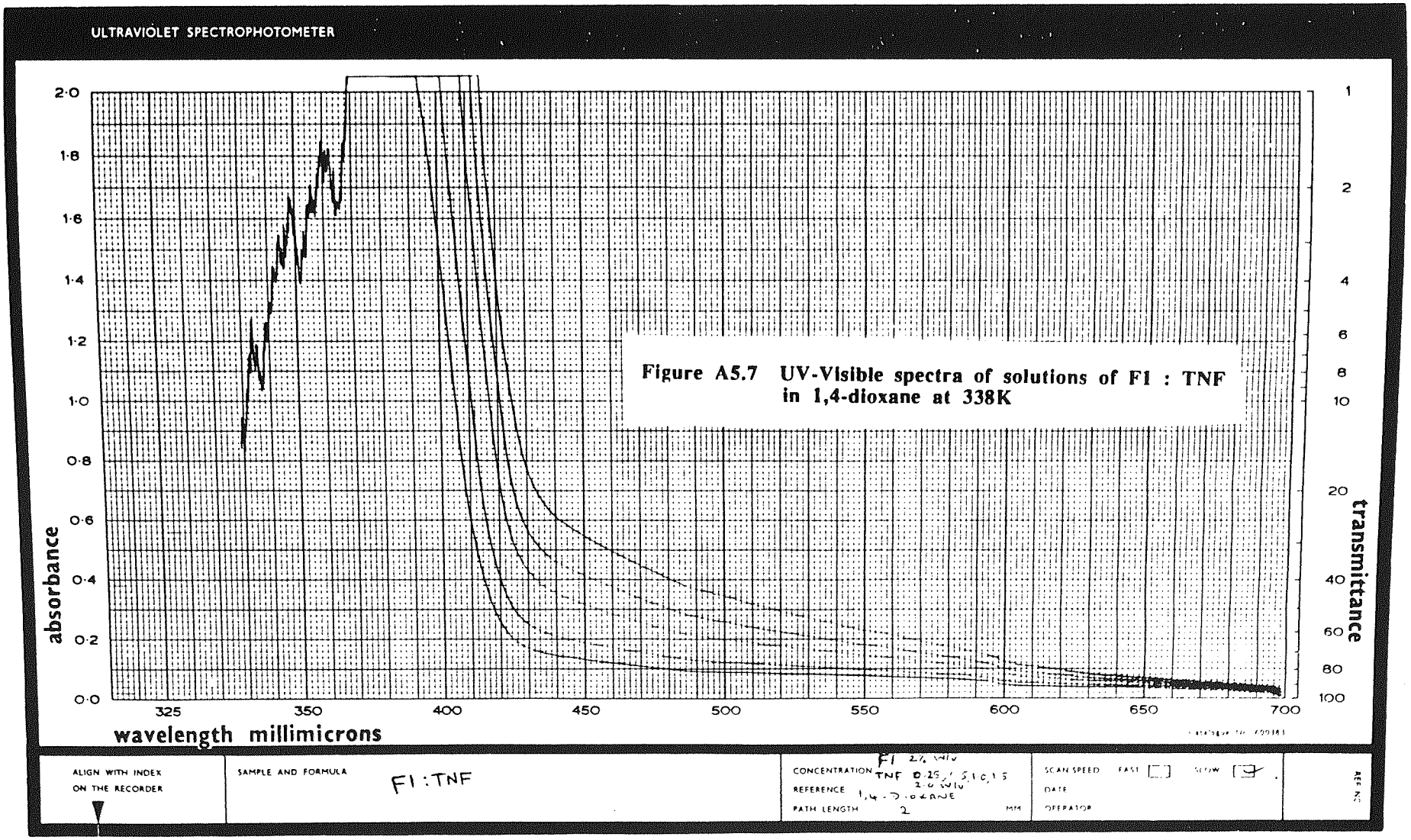

Figure A5.7 UV-Visible spectra of solutions of F1 : TNF in 1,4-dioxane at 338K

Appendix 6

List of Supporting Publications

(1) "Temperature coefficients of dipole moment of poly(N-vinylcarbazole) and its complexes with 2,4,7-trinitro-9-fluorenone", M Fiaz and M S Beevers, Proceedings of Third International Symposium on Advanced Materials, 20-24 September, 1993, Islamabad, Pakistan, in print.